Technische Universität München

Fakultät Wissenschaftszentrum Weihenstephan
für Ernährung, Landnutzung und Umwelt

Lehrstuhl für Biotechnologie der Nutztiere

Generation of a Porcine Model for Atherosclerosis

Benedikt Johannes Baumer, M.Sc. (Univ.)

Vollständiger Abdruck der von der Fakultät Wissenschaftszentrum Weihenstephan für Ernährung, Landnutzung und Umwelt der Technischen Universität München zur Erlangung des akademischen Grades eines Doktors der Naturwissenschaften (Dr. rer. nat.) genehmigten Dissertation.

Vorsitzender:	Univ.-Prof. Dr. Martin Klingenspor
Prüfer der Dissertation:	
	1. Univ.-Prof. Angelika Schnieke, Ph.D.
	2. Univ.-Prof. Dr. Eckhard Wolf

Diese Dissertation wurde am 29.12.2015 bei der Technischen Universität München eingereicht und durch die Fakultät Wissenschaftszentrum Weihenstephan für Ernährung, Landnutzung und Umwelt am 13.07.2016 angenommen.

"Der Mensch ist so alt wie seine Gefäße."

Rudolf Virchow (1821–1902),
Deutscher Arzt und Gründer
der modernen Pathologie

Danksagung

Prof. Angelika Schnieke danke ich für die Vergabe des herzspezifischen Promotionsthemas, die Möglichkeit der Durchführung dieser Arbeit an ihrem Lehrstuhl für Biotechnologie der Nutztiere, sowie für ihr großes Verständnis und Entgegenkommen.

Prof. Dr. Eckhard Wolf danke ich dafür, meine Arbeit sehr spontan als Zweitprüfer zu bewerten.

Prof. Dr. Martin Klingenspor danke ich für die Übernahme des Prüfungsvorsitzes und die Bereitstellung des Piccolo Analysers zur Erhebung der Cholesterinwerte aus Schweineblut.

Mein besonderer Dank gilt Dr. Tatiana Flisikowska für ihre fürsorgliche und ermutigende Betreuung meiner Arbeit.

Bei Dr. Krzysztof Flisikowski bedanke ich mich für die Unterstützung während den Fütterungsstudien und bei Konrad Fischer und Steffen Löbnitz für ihre Mithilfe im Umgang mit den Schweinen.

Weiterhin bedanke ich mich bei Dr. Benjamin Schade für die Präparation der Aorten aus Schweinen.

Von ganzem Herzen möchte ich mich bei allen Kolleginnen und Kollegen für die familiäre Atmosphäre und unvergessliche Zeit am Lehrstuhl, sowie die vielen daraus entstandenen Freundschaften bedanken:

Marlene Edlinger, meiner "Laborehefrau", für die angenehme Zusammenarbeit im Labor, die tiefreichenden Gespräche und die vielen Ausflüge außerhalb des Arbeitsalltags.

Anja Saalfrank, meiner "Laborschwester", für ihre zahlreichen Anregungen und Ratschläge und den atemberaubenden Urlaub in Island mit Besuch bei unserem Freund Tobias Richter.

Peggy "Inga" Müller-Fliedner, meiner "Laborverehrerin", für ihre motivierenden Umarmungen, den stetigen Sprachkurs und die Beratung in Modefragen.

Außerdem danke ich Barbara "Bärbel Bob" Bauer, Angela Zaruba, Margret Bahnweg, Kristina Mosandl, Sulith Christan, Simone Kraner-Scheiber und Erica Schulze für ihre unermüdliche Hilfsbereitschaft und die langjährige Begleitung meiner Lehrstuhlzeit.

Besonderer Dank gilt meinen Eltern und Geschwistern für ihr Verständnis und ihre Unterstützung.

Abstract

Atherosclerosis is a chronic disease characterised by pathological hardening and narrowing of the arterial vasculature. Plaques arise at susceptible sites of the vascular wall, protrude into the vessel lumen and cause acute thromboses triggering myocardial infarction and stroke, the leading causes of death worldwide. Atherosclerosis is a multifactorial disease and is affected by both lifestyle and genetic predisposition.

Animal models have been generated for preventive, diagnostic and therapeutic medicine, but fail to replicate all stages of the human atherosclerosis. Mouse models differ from humans in anatomy and physiology and exhibit natural resistance to the disease. Atherosclerosis impairs the aortic root but not the coronary arteries and does not generate plaque rupture and life-threatening thrombosis. In this regard, pigs have numerous advantages. The porcine cardiovascular system features a human-like size, anatomy, blood perfusion, physiology and platelet coagulation. Pigs spontaneously develop atherosclerosis in the coronary arteries and reveal thrombotic plaque rupture.

The aim of this work was the generation of a porcine model with accelerated and human-like atherosclerosis including vulnerable coronary plaques. For this purpose, the genes apolipoprotein E (APOE) and low-density lipoprotein receptor (LDLR) were to be disrupted by gene targeting. For visual indication of atherosclerosis, the reporter gene enhanced green fluorescent protein (EGFP) driven by the cell-specific porcine fractalkine receptor (CX3CR1) promoter was to be placed at the endogenous ROSA26 locus. In coronary artery disease (CAD) patients, CX3CR1 expression is known to be upregulated in monocytes differentiating into macrophages during atherogenesis.

Apolipoprotein E is an anti-atherogenic protein and modulates the lipoprotein metabolism and immune response. It mediates the clearance of lipoproteins from blood circulation by binding to hepatic LDL receptors and not only decelerates, but also regresses atherosclerosis. In addition, ApoE inhibits platelet aggregation and defends against risk factor hypertension. LDL receptor is a cell surface receptor and mediates the clearance of low-density lipoprotein (LDL) particles. Functional disruption of LDLR elevates plasma

LDL and causes atherosclerosis. Fractalkine receptor is also located at the cell surface and is involved in inflammatory responses. During coronary artery disease, its expression is upregulated and present in both early and advanced atherosclerotic plaques.

Gene inactivations and transgene placement were successfully established in porcine mesenchymal stem cells (MSCs) and cell clones were used for pig generation by somatic cell nuclear transfer (SCNT). A healthy offspring was born in line with LDLR and CX3CR1 project and analysed at genotypic and phenotypic level. Although incorrect LDL receptor gene targeting was ascertained, a cocos oil feeding study verified a direct correlation between plasma cholesterol level, CX3CR1 expression and coronary artery disease for the first time in pigs. Functional evidence of the reporter cassette CX3CR1-EGFP was already provided by cell-specific EGFP expression, but need for definite validation by EGFP upregulation during diet-induced atherosclerosis.

Zusammenfassung

Arteriosklerose ist eine chronische Erkrankung, die durch pathologische Verhärtung und Einengung der arteriellen Blutgefäße charakterisiert ist. Plaques entstehen an anfälligen Stellen der Arterienwand, weiten sich in das Gefäßlumen aus und verursachen akute Thrombosen, die die weltweit führenden Todesursachen Myokardinfarkt und Schlaganfall auslösen. Arteriosklerose ist eine multifaktorielle Erkrankung und wird sowohl durch den Lebensstil also auch durch genetische Prädisposition beeinflusst.

Tiermodelle wurden für die präventive, diagnostische und therapeutische Medizin generiert, scheitern aber daran, alle Stadien der menschlichen Arteriosklerose nachzubilden. Mausmodelle unterscheiden sich zur menschlichen Anatomie und Physiologie und weisen eine natürliche Resistenz gegen die Erkrankung auf. Arteriosklerose schädigt die Aortenwurzel nicht aber die Koronararterien und verursacht keine Plaqueruptur und lebensbedrohlichen Thrombosen. Diesbezüglich besitzen Schweine zahlreiche Vorteile. Das kardiovaskuläre System des Schweins zeichnet sich durch seine menschenähnliche Größe, Anatomie, Blutperfusion, Physiologie und Koagulation von Blutplättchen aus. Schweine entwickeln Arteriosklerose spontan in den Koronararterien und zeigen thrombotische Plaqueruptur.

Das Ziel dieser Arbeit war die Generierung eines Schweinemodells mit beschleunigter und menschenähnlicher Arteriosklerose inklusive verwundbarer Koronarplaques. Hierfür waren die Gene Apolipoprotein E (APOE) und Rezeptor für Lipoproteine niederer Dichte (low-density lipoprotein receptor: LDLR) durch Gen-Targeting zu unterbrechen. Für die visuelle Indikation der Arteriosklerose war das durch den zellspezifischen Fraktalkinrezeptor (CX3CR1)-Promoter des Schweins angetriebene Reportergen verstärktes grün fluoreszierendes Protein (enhanced green fluorescent protein: EGFP) in den endogenen ROSA26-Lokus einzubringen. In Patienten mit koronarer Arterienkrankheit wird die Expression von CX3CR1 bekannterweise in Monozyten hochreguliert, die während der Atherogenese zu Makrophagen ausdifferenzieren.

Das Apolipoprotein E ist ein anti-atherogenes Protein und moduliert den Lipoprotein-

metabolismus und die Immunantwort. Durch Bindung an den LDL-Rezeptor der Leber vermittelt es die Beseitigung von Lipoproteinen aus der Blutzirkulation und verlangsamt nicht nur, sondern bildet die Arteriosklerose auch zurück. Zusätzlich hemmt ApoE die Aggregation von Blutblättchen und schützt vor dem Risikofaktor Bluthochdruck. Der LDL-Rezeptor ist ein Rezeptor auf der Oberfläche von Zellen und vermittelt die Beseitigung von LDL (low-density lipoprotein: Lipoproteine niederer Dichte)-Partikeln. Die funktionale Unterbrechung von LDLR erhöht das LDL im Plasma und verursacht Arteriosklerose. Der Fraktalkinrezeptor befindet sich ebenfalls auf der Zelloberfläche und ist an Entzündungsreaktionen beteiligt. Während der koronaren Arterienkrankheit ist dessen Expression hochreguliert und sowohl in frühen als auch fortgeschrittenen atherosklerotischen Plaques vorhanden.

Die Geninaktivierungen und die Transgeneinbringung wurden erfolgreich in mesenchymalen Stammzellen (mesenchymal stem cells: MSCs) des Schweins etabliert und die Zellklone für die Generierung von Schweinen durch somatischen Zellkerntransfer (somatic cell nuclear transfer: SCNT) verwendet. Im Rahmen des LDLR- und des CX3CR1-Projektes wurden gesunde Nachkommen geboren und genotypisch und phänotypisch analysiert. Obwohl ein inkorrektes Gen-Targeting des LDL-Rezeptors festgestellt wurde, wies eine Kokosölfütterungsstudie zum ersten Mal einen direkten Zusammenhang zwischen Plasmacholesterinspiegel, CX3CR1-Expression und koronarer Arterienkrankheit in Schweinen nach. Ein funktionaler Beweis der Reporterkassette CX3CR1-EGFP wurde bereits durch eine zellspezifische EGFP-Expression erbracht, bedarf aber einer endgültigen Bestätigung durch die Hochregulierung von EGFP während einer ernährungsinduzierten Arteriosklerose.

Contents

List of Abbreviations

24(S)-OH-C	24(S)-hydroxycholesterol
27-OH-C	27-hydroxycholesterol
α1,3GT	α1,3-galactosyltransferase
Aβ	β-amyloid peptide
ABCA1	ATP-binding cassette transporter A1
ABCG1	ATP-binding cassette transporter G1
ACAT	Acyl-coenzyme A: cholesterol acyltransferase
ACS	Acute coronary syndrome
AD	Alzheimer's disease
AIDS	Acquired immunodeficiency syndrome
APC	Adenomatous polyposis coli
Apo	Apolipoprotein
Arg	Arginine
BAC	Bacterial artificial chromosome
BMI	Body mass index
BS	Blasticidin S resistance gene
C	Cholesterol
CABG	Coronary artery bypass grafting
CAD	Coronary artery disease
cAMP	Cyclic adenosine monophosphate
CCN	CAGGS Cherry nuclear localisation signal
CCR	CC-chemokine receptor
CCRL	CC-chemokine receptor-like
CD	Cluster of differentiation
CDF	Chemokine domain of function
cDNA	Complementary deoxyribonucleic acid
CETP	Cholesteryl ester transfer protein

CFTR	Cystic fibrosis transmembrane conductance receptor
CHD	Coronary heart disease
CMP-Neu5Ac	CMP-N-acetylneuraminic acid
CNS	Central nervous system
CRP	C-reactive protein
CSF	Cerebrospinal fluid
CSFL	Cerebrospinal fluid lipoprotein
CVD	Cardiovascular disease
CX3CL1	Fractalkine
CX3CR1	Fractalkine receptor
Cys	Cysteine
D	Dilution
DMSO	Dimethyl sulphoxide
DNA	Deoxyribonucleic acid
DSB	Double strand break
E	Exon
EC	Esterified cholesterol
ECM	Extra-cellular matrix
EGF	Epidermal growth factor
EGFP	Enhanced green fluorescent protein
EL	Endothelial lipase
ES	Embryonic stem
FA	Fatty acid
FBS	Foetal bovine serum
FCC	Free cholesterol complex
FGF-2	Fibroblast growth factor 2
FH	Familial hypercholesterolemia
FKN	Fractalkine
G-	Guanosine triphosphate-binding-
GAPDH	Glyceraldehyde 3-phosphate dehydrogenase
GHR	Growth hormone receptor
GWA	Genome wide association
HA	Homology arm
HDL	High-density lipoprotein
HDR	Homology-directed repair
HFHC	High fat, high cholesterol diet
HIF	Hypoxia-inducible factor
HIV	Human immunodeficiency virus
HL	Hepatic lipase
HMG CoA reductase	3-hydroxy-3-methylglutaryl coenzyme A reductase

HR	Homologous recombination
HRE	Hypoxia-response element
HSPG	Heparan sulphate proteoglycan
ICAM	Inter-cellular adhesion molecule
ID	Identity
IDL	Intermediate-density lipoprotein
IL-6	Interleukin-6
Il2rg	X-linked interleukin-2 receptor gamma
IMT	Intima media thickness
indel	Insertion and deletion
iPSC	Induced pluripotent stem cell
IRES	Internal ribosome entry site
KRAS	Kirsten rat sarcoma viral oncogene homologue
LCAT	Lecithin: cholesterol acyltransferase
LDL	Low-density lipoprotein
LDLR	Low-density lipoprotein receptor
LINE	Long interspersed nuclear element
LOS	Large offspring syndrome
LOX-1	Lectin-like oxidised low-density lipoprotein receptor-1
Lp(a)	Lipoprotein(a)
LPL	Lipoprotein lipase
LRP	Low-density lipoprotein receptor-related protein
LRP1	Low-density lipoprotein receptor-related protein 1
M	Marker
MCP	Monocyte chemotactic protein
MMP	Matrix metalloproteinase
MRI	Magnetic resonance imaging
mRNA	Messenger ribonucleic acid
MSC	Mesenchymal stem cell
neo	Neomycin resistance gene
NFT	Neuro-fibrillary tangle
NHEJ	Non-homologous end-joining
NK	Natural killer
NLS	Nuclear localisation signal
NO	Nitric oxide
NPC	Niemann-Pick type C
ORF	Open reading frame
P	Passage
pADMSC	Porcine adipose tissue-derived mesenchymal stem cell
PBMC	Peripheral blood mononuclear cell

PCR	Polymerase chain reaction
PCSK9	Proprotein convertase subtilisin/kexin type 9
pEF	Porcine ear fibroblast
PGK	Phosphoglycerate kinase
PKC	Porcine kidney cell
pKDNF	Porcine kidney fibroblast
PL	Phospholipid
PLTP	Phospholipid transfer protein
PTCA	Percutaneous transluminal coronary angioplasty
PNS	Positive negative selection
qRT-PCR	Real time quantitative polymerase chain reaction
QTL	Quantitative trait locus
RA	Retinoic acid
RAG	Recombination-activating genes
ROS	Reactive oxygen species
RPL	Recurrent pregnancy loss
RSV	Respiratory syncytial virus
RT-PCR	Reverse transcriptase polymerase chain reaction
SA	Splice acceptor
SCNT	Somatic cell nuclear transfer
SDSA	Synthesis-dependent strand annealing
SINE	Short interspersed nuclear element
SNP	Single nucleotide polymorphism
SR-B1	Scavenger receptor class B type 1
SREBP	Sterol regulatory element-binding protein
STEMI	ST-elevation myocardial infarction
SV	Screening vector
T1/2	Transcription activator-like effector nuclease 1/2
Ta	Annealing temperature
TALEN	Transcription activator-like effector nuclease
TBP	TATA-binding protein
TG	Triglycerides
Th	T-helper
TRE	Tetracycline/tetracycline responsive element
TV	Targeting vector
UTR	Untranslated region
VEGF	Vascular endothelial growth factor
VLDL	Very low-density lipoprotein
WT	Wild-type

List of Figures

List of Tables

CHAPTER 1

Introduction

1.1 Atherosclerosis

Atherosclerosis is a chronic and multifactorial disease of the arterial wall triggered by accumulation and modification of excess lipids with an accompanied inflammation at susceptible sites. Development of plaques and rupture-prone vulnerable plaques ultimately causes advanced stenosis or acute thrombosis responsible for cardiovascular diseases (CVDs) including coronary heart, cerebrovascular and peripheral arterial disease, also deep vein thrombosis and pulmonary embolism. Globally, CVDs are the leading cause of death, predicted to increase in future. In 2008, estimated 17.3 million people representing 30% of all deaths worldwide died from these [6], of which 7.3 million from coronary heart and 6.2 million from cerebrovascular disease [7]. These deaths will raise 23.3 million by 2030 [8]. Between 2010 and 2030 the real total direct medical costs for American cardiovascular care are projected to rise from 273 billion $ to 818 billion $, whereas additional real indirect costs from 172 billion $ to 276 billion $ [9].

1.1.1 Cholesterol homeostasis

Cholesterol is an steroid lipid essential for fluidity and permeability of cell membranes [10], membrane signaling and trafficking [11] and myelination of the central nervous system (CNS) [12]. Cholesterol and its derivatives are precursors for biosynthesis of bile acid [13], steroid hormones [14], oxysterols [15] and vitamin D [16]. The basal metabolic net flux of cholesterol through the body is about 10mg/day/kg [17]. Cholesterol is primarily synthesised by the liver [18] utilising at least 20 enzymes [19] and additionally absorbed by the intestine (approximately 23% of absorbable total cholesterol). Hepatic cholesterol is stored as esterified cholesterol or is eliminated from the body as cholesterol and bile

acid by the secretion into bile [20].

However, the transport and redistribution among intestine, liver and peripheral tissues is effected by plasma lipoproteins [21]. Plasma lipoproteins facilitate the transport of the water-insoluble lipids cholesterol and triglycerides through aqueous blood circulation and feature an amphipathic surface monolayer of phospholipids, cholesterol and apolipoproteins surrounding a lipid core of metabolic triglycerides and esterified cholesterol [22]. The plasma lipoproteins are characterised by different physical and chemical properties [23].

Since blood-brain barrier prevents uptake of cholesterol from plasma lipoproteins during late fetal and post-natal development [17], the brain representing the most cholesterol-rich organ (approximately 25% of body total cholesterol) [24] has its own cholesterol metabolism with low cholesterol net flux of only about 0.14mg/day/kg (see figure 1.1) [17]. It features high cholesterol synthesis and turnover rates only during peri- and early post-natal myelination, cellular ApoE-associated cholesterol transport via cerebrospinal fluid lipoproteins (CSFLs) and very limited cholesterol net efflux from CNS into circulation (reviewed in [17, 1]). The CSFL exhibit a bigger size than plasma high-density lipoprotein (HDL) and an intermediate-density of low-density lipoprotein (LDL) and HDL [25]. They are associated particularly with ApoE, redistribute lipids and regulate cellular cholesterol homeostasis in the brain. Here, cholesterol is primarily secreted by astrocytes and microglial cells [1]. Adult neurons sufficiently take up exogenous cholesterol from circumjacent cells [26], but during maturation they depend on astrocytes [27]. However, neurons can also synthesise cholesterol [28] and lipoproteins [29]. Main cholesterol seems to efflux from neurons, astrocytes and microglial cells via ATP-binding cassette transporter A1 (ABCA1) and ATP-binding cassette transporter G1 (ABCG1) and is transferred to both discoidal and spherical ApoE-associated lipoprotein particles [30]. Cellular uptake of ApoE-associated cholesterol is mainly mediated by LDL receptor and LDL receptor-related protein 1 (LRP1) expressed by neurons, astrocytes and microglial cells [1]. Cholesterol does not accumulate in the CNS and access cholesterol is exported from cells into cerebrospinal fluid (CSF) by an ApoE-dependent shedding pathway (1–2mg/day) [25]. The cholesterol flux through the blood-brain barrier occurs via exchange of oxysterols between brain CSFL and plasma LDL [1] shuttling between membranes and lipoproteins [31]. The 24(S)-hydroxycholesterol is primarily synthesised in the brain [32] and exported via blood-brain barrier (6–7mg/day) [33]. 27-hydroxycholesterol is also synthesised in the brain [34], but net flux occurs into the brain (5mg/day) [35] dependent of integrity of blood-brain barrier [36].

However, ApoE-associated cholesterol can bind to ApoE receptors (LDL receptor related proteins) and interfere with developmental and functional signaling in the nervous system [37]. Nevertheless, high cholesterol concentrations are required for synaptic transmission and plasticity [38]. Cholesterol also regulates embryonic hedgehog signaling [39]. Thus, embryonic cholesterol metabolism contributes to CNS development [40]. Conversely, defects in brain cholesterol metabolism result in structural and functional diseases of central

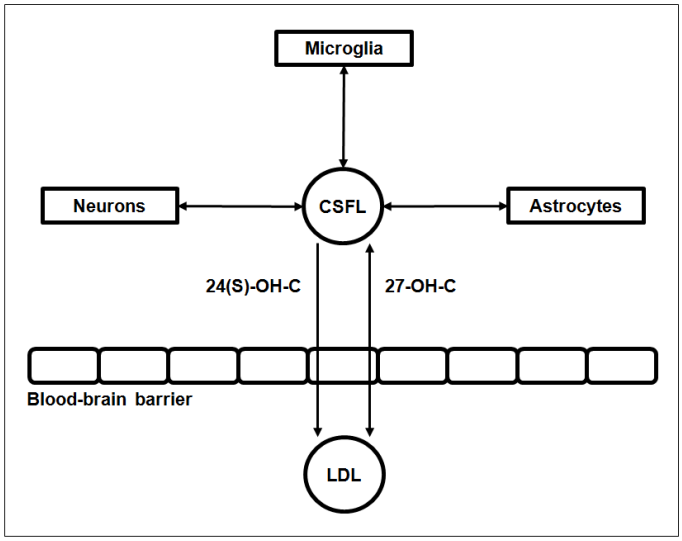

Figure 1.1: Brain cholesterol homeostasis: Cholesterol flux between neurons, microglial cells (microglia) and astrocytes via cerebrospinal fluid lipoproteins (CSFLs) and through blood-brain barrier as 24(S)-hydroxycholesterol [24(S)-OH-C] and 27-hydroxycholesterol (27-OH-C) between CSFL and low-density lipoprotein (LDL). Adapted from [1].

nervous system like Smith-Lemli-Opitz syndrome, Niemann-Pick type C (NPC) disease, Huntington's disease and Alzheimer's disease (reviewed in [1]).

Physiologic cholesterol concentration in cells is tightly regulated by biosynthesis and endocytotic and secretory pathways. Free cholesterol is detoxified and stored as cytosolic lipid droplets by esterification and remobilised by hydrolysis (reviewed in [41]). The cholesterol biosynthesis is controlled by proteolytic cleavage of membrane-bound transcription factors activating enzyme-encoding genes for synthesis of cholesterol and fatty acids. Here, active domains of the sterol regulatory element-binding proteins (SREBPs) are cleaved sequentially from golgi apparatus membrane and enhance transcription, whereas accumulation of sterol inhibits the transport of SREBPs from endoplasmic reticulum to golgi apparatus and thus its transcription-activating cleavage (reviewed in [42, 43]) declining all enzymes for cholesterol biosynthesis [44, 45]. Accordingly, SREBPs also regulate transcription of the LDL receptor gene primarily mediating cholesterol uptake from ApoB-containing lipoproteins [43, 46]. However, endocytosis of LDL cholesterol was shown to occur clathrin-mediated [47] and caveolin-mediated [48] or via macropinocytosis [49] and macrophage phagocytosis [50]. The secretion of free cholesterol via HDL is mediated by four pathways, the aqueous diffusion, scavenger receptor class B type 1 (SR-B1), ABCG1 and ABCA1 [51]. However, the secretion of esterified cholesterol from hepatocytes and enterocytes occurs via ApoB-containing lipoproteins very low-density lipoprotein (VLDL) and chylomicrons. Alternatively, cholesterol efflux from cells can also occur via 27-hydroxycholesterol [52] and via shedding of small vesicles from the cell surface [53, 54]. The transport of cholesterol between cell compartments and plasma membrane is effected

by both intra-cellular vesicles and diffusible carrier proteins (reviewed in [55, 56]) with different transport pathways for cholesterol derived from LDL and acetylated LDL [57].

1.1.2 Lipoprotein metabolism

The plasma lipoprotein metabolism involves three independent and inter-connected pathways, the transport of exogenous dietary lipids/cholesterol (C) from intestine to liver by chylomicrons and chylomicron remnants, the transport of endogenous hepatic lipids/cholesterol from liver to peripheral tissues by very low-density lipoprotein (VLDL), intermediate-density lipoprotein (IDL) and low-density lipoprotein (LDL) and the reverse cholesterol transport from peripheral cells including macrophages back to liver by high-density lipoprotein (HDL) (see figure 1.2) [58]. Here, the lipoprotein classes VLDL, IDL, LDL and HDL reveal further subclasses with different sizes and densities [59] differently associated with coronary artery disease (CAD) [60]. However, almost the total cholesterol is transported by the three lipoprotein classes VLDL, LDL and HDL [58]. For this, cholesterol is esterified and assembled into the hydrophobic triglyceride core of lipoproteins solubilised by a surface monolayer of phospholipids, cholesterol and apolipoproteins [61]. In the human lipoprotein metabolism, the lipoprotein-associated apolipoproteins B-48, B-100, E and A-I have outstanding function.

In the exogenous pathway, ApoB-48 provides structural integrity for synthesis of chylomicrons and thus is essential for absorption of dietary lipids and fat-soluble vitamins from intestine. After secretion into circulation, most triglycerides are hydrolised by lipoprotein lipase (LPL) becoming chylomicron ramnants [62]. Finally, hepatic uptake of these remnants is mediated by interaction of ApoE with LDL receptor, heparan sulphate proteoglycan (HSPG)/LDL receptor-related protein (LRP) complex or HSPG alone. Additionally, internalisation of HSPG-modified remnants can occur via LRP also dependent of ApoE (reviewed in [63]).

In the endogenous pathway, ApoB-100 is necessary for hepatic synthesis and secretion of VLDL in circulation [62]. LPL hydrolyses triglycerides (TGs) and probably induces conformational change of ApoE enabling effective LDL receptor binding [64]. However, half of the VLDL is reabsorbed by the liver via LDL receptor interaction [65], the other half is further hydrolysed and become IDL. Hepatic lipase (HL) finally generates LDL [66]. Only few IDL particles are removed from circulation by binding of ApoE to hepatic LDL receptor [58]. LDL particles mainly are absorbed by interaction of ApoB-100 with LDL receptor, although there is an additional receptor-independent pathway [67]. In total, one half of the plasma LDL is removed by the liver, the other half by peripheral tissue [68]. Additionally, lipoprotein(a) [Lp(a)] can be formed after covalent binding of apolipoprotein(a) [Apo(a)] to ApoB-100 within an cholesterol-rich LDL particle. Apo(a) is believed to be synthesised in liver [69].

In the reverse cholesterol transport, ApoA-I is involved in all steps including formation of nascent HDL particles, HDL remodeling and HDL delivery to the liver. Here, structural

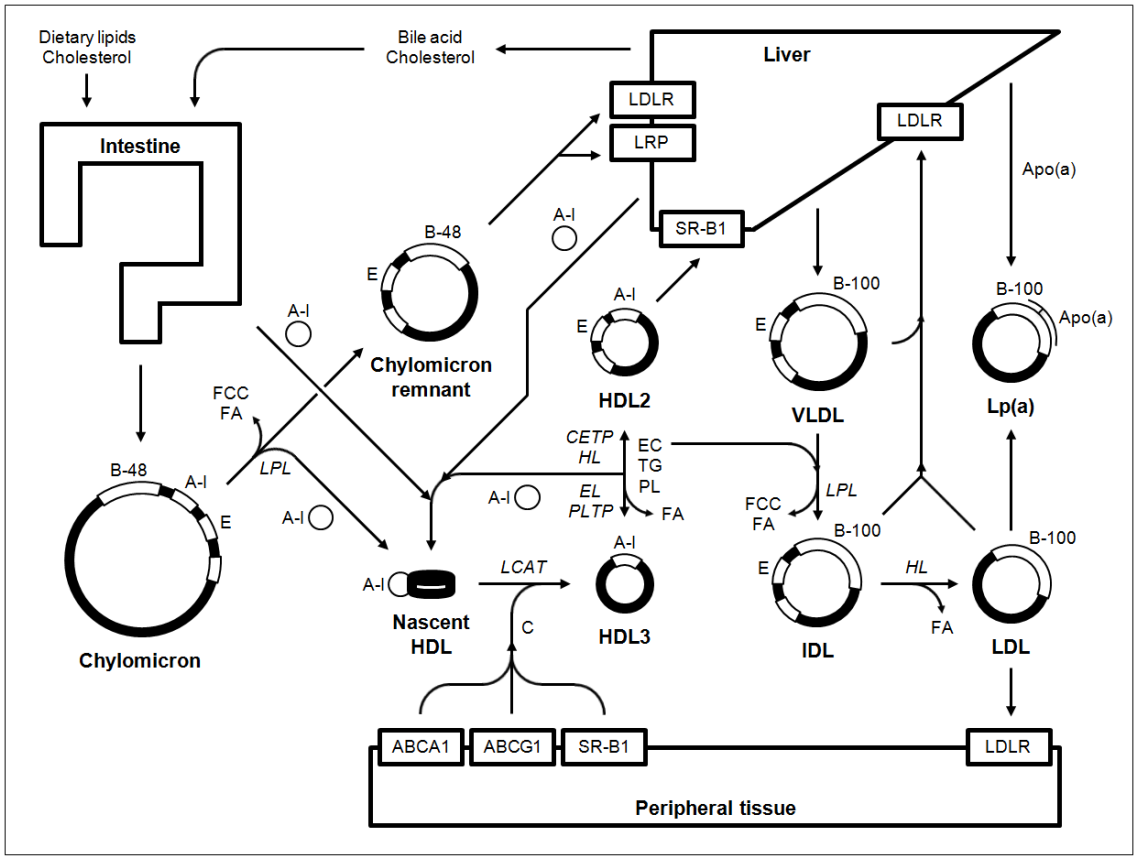

Figure 1.2: Plasma lipoprotein metabolism between intestine, liver and peripheral tissue featuring lipoproteins with important apolipoproteins, lipid transfer proteins and lipid-modifying enzymes with their respective artefacts, receptors for lipoprotein uptake and cholesterol (C) efflux transporters. Lipoproteins: chylomicron, chylomicron remnant, very low-density lipoprotein (VLDL), intermediate-density lipoprotein (IDL), low-density lipoprotein (LDL), lipoprotein(a) [Lp(a)], nascent high-density lipoprotein (HDL), HDL3, HDL2. Apolipoproteins (Apos): A-I: ApoA-I; B-48: ApoB-48, B-100: ApoB-100; E: ApoE and Apo(a): apolipoprotein(a). Lipid transfer proteins and lipid-modifying enzymes (italic type): LPL: lipoprotein lipase; HL: hepatic lipase; EL: endothelial lipase; LCAT: lecithin: cholesterol acyltransferase; CETP: cholesteryl ester transfer protein; PLTP phospholipid transfer protein. Artefacts: FA: fatty acid; FCC: free cholesterol complex; EC: esterified cholesterol; TG: triglyceride; PL: phospholipid. Receptors: LDLR: low-density lipoprotein receptor; LRP: low-density lipoprotein receptor-related protein; SR-B1: scavenger receptor class B type 1. Cholesterol efflux transporters: SR-B1; ABCG1: ATP-binding cassette transporter G1; ABCA1: ATP-binding cassette transporter A1. Adapted from [2].

heterogeneity reveals a wide variety of HDL particles with different subclasses and subpopulations (reviewed in [51]). ApoA-I is synthesised and secreted by liver and intestine [70]. Initial intra- and peri-cellular lipidation of newly synthesised and exogenous lipid-free ApoA-I occurs dependent and independent of ATP-binding cassette transporter A1 (ABCA1) [71]. However, ApoA-I lipidation by ABCA1 allows for a more efficient assembly of nascent HDL particles and increases their availability for cholesterol efflux [72] generating mature HDL particles (HDL3 and following HDL2) [73]. Cholesterol efflux from cells to plasma occurs in four pathways, the aqueous diffusion, scavenger receptor class B type 1 (SR-B1), ATP-binding cassette transporter G1 (ABCG1) and ABCA1. In the plasma, the HDL is remodeled by lipid transfer proteins and lipid-modifying enzymes effecting conversions of nascent discoidal and mature spherical HDL particles. The plasma factors hepatic lipase and endothelial lipase (EL) release fatty acids (FAs) from HDL and lecithin: cholesterol acyltransferase (LCAT) esterifies HDL-associated cholesterol. The cholesteryl ester transfer protein (CETP) and phospholipid transfer protein (PLTP) transport esterified cholesterol (EC), TGs and phospholipids (PLs) among lipoproteins (reviewed in [51]). Here, ApoA-I activates LCAT [74] which is a critical enzyme in HDL metabolism [75] and is essential for the conversion of discoidal to spherical HDL particles [76]. Remodeling is also effected by free cholesterol complexes (FCC) (surface remnants) of triglyceride-rich lipoproteins generated by LPL [77]. During remodeling, ApoA-I determines the thermodynamic stability of HDL and is often released for further formation of nascent HDL [78]. Finally, hepatic SR-B1 receptors selectively bind HDL particles and following esterified and free cholesterol diffuse into the cell membrane [79]. In total, one half of esterified cholesterol of mature spherical HDL is delivered via HDL particles the other half via VLDL, IDL and LDL particles [58].

1.1.3 Lipoproteins and atherosclerosis

Defects in lipoprotein metabolism due to impaired binding of cholesterol-enriched lipoproteins to their specific cell surface receptors result in type III hyperlipoproteinemia (ApoE-related) and familial hypercholesterolemia (LDL receptor-related) provoking atherosclerosis (reviewed in [21]). Here, especially high levels of large VLDL are more likely associated with extensive coronary artery disease (CAD) [60]. In contrast, number of LDL particles is an independent risk factor and more significantly associated with coronary heart disease (CHD) than LDL particle size [80]. Nevertheless, the small LDL5, one of seven distinct LDL particle sizes [81], is detected as the most electronegative LDL fraction and induces platelet activation and aggregation via the lectin-like oxidised low-density lipoprotein receptor-1 (LOX-1) possibly triggering ST-elevation myocardial infarction (STEMI) [82]. Lipoprotein(a) [Apo(a)] is related to premature cardiovascular disease (CVD) independent of LDL levels. It has pro-inflammatory, pro-thrombotic and anti-fibrinolytic properties and accelerates atherogenesis (reviewed in [69]).

HDL is an independent protective factor for CAD [83]. Beside the reverse choles-

terol transport, HDL has several additional athero-protective properties. It exhibits anti-inflammatory, anti-infectious, anti-apoptotic, anti-thrombotic, anti-oxidative, pro-vasodilatory and pro-fibrinolytic function (reviewed in [84, 85]). However, small and dense HDL3 particles protect LDL against oxidative stress more powerful than large and light HDL2 particles [86]. Oxidised plasma LDL is likely a predictive marker for future atherosclerotic events [87] since its removal from circulation was shown to reduce atherosclerosis and almost completely prevent atherosclerotic progression in a mouse model [88]. Nevertheless, high levels of HDL3 particles are more likely associated with CHD [89] and myocardial infarction [90] since smaller HDL particles bind weaker to scavenger receptor class B type 1 (SR-B1) [91] and deliver less cholesterol than bigger HDL particles [92]. However, chronic and acute inflammation causes structural and functional changes of HDL particles provoking pro-inflammatory and reducing anti-oxidative properties [84]. Oxidation of HDL-associated ApoA-I inhibits ATP-binding cassette transporter A1 (ABCA1)-dependent cholesterol efflux [93] and the generation of stable nascent and mature HDL particles [94]. Triglyceride-rich HDL particles are unstable [95] and reveal diminished capacity in esterified cholesterol delivery via SR-B1 in reverse cholesterol transport [96]. Oxidised HDL inhibits fibrinolysis [97]. Thus, dysfunctional HDL loses anti-atherogenic properties and contributes to CAD [84].

1.1.4 Macroscopic development of atherosclerosis

The pathology of atherosclerosis can be described simplified as sequential development of histologic plaque classes responsible for sudden coronary deaths (see figure 1.3), which can be applied to choose an adequate imaging method, diagnosis, prognosis and therapy of plaques. The histologic plaque characteristics are inflammation (reviewed in [98]), calcification (reviewed in [99]), necrotic core [100], fibrous cap [101], neovascularisation (reviewed in [102]) and intra-plaque hemorrhages (reviewed in [103]). The pathogenesis ranges from non-atherosclerotic intimal lesions, intimal xanthoma and thickening to progressive atherosclerotic lesions, fibrous cap atheroma, pathologic intimal thickening, thin fibrous cap atheroma and fibrocalcific plaque. Here, only the three plaques fibrous cap atheroma, pathologic intimal thickening and thin fibrous cap atheroma are associated with thrombosis, fibrous cap atheroma and pathological intimal thickening by erosion of endothelium, thin fibrous cap atheroma by rupture of fibrous cap or protrusion of calcified nodule into arterial lumen. The fourth fibrocalcific plaque is not associated with thrombosis and causes sudden coronary death due to lethal arrhythmia triggered by myocardial ischemia at 75% cross-sectional luminal narrowing [3]. However, such a severe stenosis is not required for acute or healed thrombosis [104], but can be progressed by healed plaque rupture [105]. In 61% of sudden coronary death patients, silent and not acute plaque ruptures were detected indicating cyclic thrombosis and healing [105] and 44% of thrombotic sudden coronary death patients revealed erosions without plaque rupture and less often inflammatory cells indicating occlusive thrombosis without rupture and

inflammation [104].

Fatty streak formation already begins in fetal aortas [106]. Following fatty streaks (intimal xanthoma) and also raised lesions (fibrous plaques) occur in arterial segments of thoracic aorta, abdominal aorta and right coronary artery at 15 years of age with rapidly increasing prevalence and extend till 34 years of age. This indicates development of fibrous plaques from fatty streaks. In total, the aortas are favoured for higher prevalence of atherosclerotic lesions, the right coronary artery for higher proportion of raised lesions [107]. Most of the intimal xanthoma regress spontaneously since distribution of fatty streaks in childhood differ from lesions in young adults [108]. However, specific shear stress conditions at branch points of major conduit arteries (bifurcations) promote development of advanced plaques and their transformation into rupture-prone vulnerable plaques (reviewed in [109]). In contrast to extensive distribution of fatty streaks and raised lesions in young adults, thin cap fibroatheroma and ruptured plaques are highly limited and located at proximal portions of major coronary arteries [110]. About 60% of sudden coronary deaths are caused by thrombosis, of which 55–60% due to plaque rupture, 30–35% due to plaque erosion and only 2–7% due to calcified nodule [100]. Plaque erosion is etiologic for 20–25% of myocardial infarctions [111]. In 40% of sudden coronary deaths, no acute thrombosis was diagnosed with 25% healed myocardial infarctions and total occlusions and 15% severe luminal narrowing of coronary artery [100].

Gradual development of atherosclerotic lesions is independent of sex and geographic ethnic group related risk range. Fatty steaks appear in almost all aortas of all groups at an age of ten years and in almost every coronary artery at 20–30 years of age. Raised lesions were detected in several coronary arteries of each group younger than 20 years with increasing prevalence and extend [112]. However, there are sex and ethnic risk related differences in rate and extend of atherosclerotic lesions. Fatty streaks in white subjects are less frequent than in black subjects [107]. Within right coronary arteries, high risk group develops more rapid raised lesions [112] and women less raised lesions than men [107]. Calcification of coronary arteries differs quantitatively within ethnic groups in the absence of coronary risk factors [113], correlates with age of sudden coronary death patients [100] and shows a delay of ten years in women compared to men with compensation at the eight decade [114]. Plaque rupture responsible for 55–60% of thrombotic sudden coronary deaths seems to appear only in post-menopausal women older than 50 years. When younger than 50 years, acute coronary thrombosis is mainly caused by plaque erosion. For men, plaque rupture was observed at all ages [100]. The incidence of sudden coronary death of women lags 20 years behind men [115]. Post-menopausal administration of estrogen was shown to have an athero-protective effect in women since it decreases the progression of intima media thickness (IMT) by increasing HDL and decreasing LDL cholesterol [116].

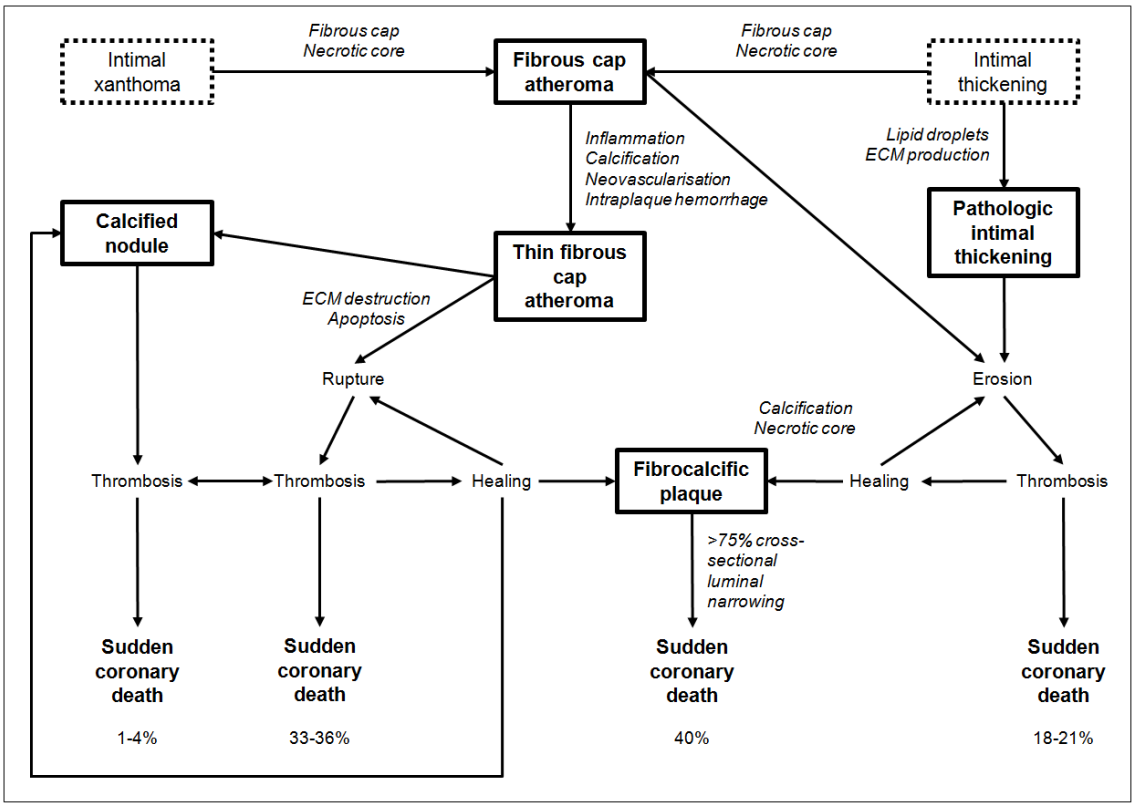

Figure 1.3: Sequential development of major histologic plaque classes with calculated probabilities of revealing sudden coronary death events. Italic type describes respective characteristic changes. Dotted boxes indicate possible regression, lined boxes irreversible progression. Adapted from [3].

1.1.5 Microscopic development of atherosclerosis

Serial development of grossly visible plaques during atherosclerosis is raised by continuous and increasingly complex histological processes and changes in the arterial wall. Development of early fatty streaks begins with infiltration of excess LDL in the intima [117] influenced by arterial wall permeability and plasma LDL concentrations (reviewed in [118]). Lipoproteins are retained by artery wall proteoglycans [119] by their ionic interaction to ApoB-100 [120]. Within extra-cellular matrix of arterial intima, extensive proteolytic, phospholipolytic and oxidative modifications of LDL particles and hydrolysis of containing cholesteryl esters lead to the formation of lipid vesicles and membranous material (reviewed in [121]). Here, the oxidised phospholipids initiate and propagate chronic inflammation and inhibit acute inflammation thus causing a mononuclear-cell-specific response with activated endothelium monocyte adhesion (reviewed in [122]). Endothelial cell activation preferentially take place at arterial segments revealing specific shear stress conditions [123]. By binding to lectin-like oxidized low-density lipoprotein receptor-1 (LOX-1), the oxidised LDL also contributes to activation of endothelial cells, macrophages, smooth muscle cells and platelets promoting endothelial dysfunction and formation and progression of atherosclerotic plaques (reviewed in[124]). Platelets adhere to the endothelium [125] and get activated [126] contributing to sub-endothelial recruitment of monocytes [127]. Different monocyte subsets responsive to innate and acquired immunity invade arterial intima and differentiate into macrophages revealing different properties in plaque formation (reviewed in [128]). Macrophages take up sub-endothelial lipid particles and droplets by endocytosis dependent or independent of scavenger receptor [50] and transform into foam cells [129]. Here, the scavenger receptors mediate innate pattern recognition and clearance of pathogenic host molecules and particles [130] like oxidised LDL [131]. Resident intimal dendritic cells also express scavenger receptor [130] and become foam cells [132]. Innate immune recognition also occurs by Toll-like receptors and induces inflammatory signaling pathways [133]. However, expression of Toll-like receptors is present in atherosclerotic plaques [134] and modified LDL activates the macrophage Toll-like receptor [135]. Thus, macrophages modulate the immune response by production of pro- and anti-inflammatory cytokines controlling the progression of atherosclerosis [136], activate T-cells by presentation of antigens [137] and promote migration of smooth muscle cells contributing to intimal growth and vessel wall remodeling [138]. Vascular inflammation finally features a wide spectrum of immune cells like macrophages, T-cells (CD4, CD8, $\gamma\delta$), T-helper cells (Th1, Th2, Th3), B-cells, NK-cells, mast cells and dendritic cells [139]. Mast cells crucially contribute to plaque progression and destabilization [140]. Smooth muscle cells express adhesion molecules promoting further migration of monocytes and lymphocytes in the vascular intima and suppress their apoptosis. They also generate inflammatory cytokines for immune response and by modifying the production of extra-cellular matrix (ECM) proteins they can influence the content of lipids and proliferation of immune cells.

Furthermore, smooth muscle cells exhibit receptors for lipid uptake and can become foam cells (reviewed in [141]).

These processes contribute to the development of a fibrous cap arising the early fibroatheroma. Necrosis and apoptosis of foam cells forms a lipid core, the necrotic core and debris triggers further inflammation [142]. There is evidence that monocytes and macrophages also regulate calcification of the vascular wall via osteoblast-like cells [143]. Additionally, macrophages synergistically enhance inflammation by induction of cyclic angiogenesis and recruitment of immune cells and thus induce intra-plaque hemorrhages [144]. The immune response in the atherosclerotic plaque can be further potentised by inflamed visceral adipose tissue. Systemic release of pro-inflammatory cytokines like interleukin-6 (IL-6) causes hepatic acute phase reaction [145] with the release of positive acute phase proteins like C-reactive protein (CRP) [146]. However, IL-6 is associated with visceral adipose tissue and CPR to increased body mass index (BMI) [147]. IL-6 contributes to atherosclerosis (reviewed in [148]) and oxidised LDL was shown not only to activate several innate immune receptors, but also bind to CRP inducing the classic complement pathway and receptor mediated phagocytosis [135].

Prone to rupture thin-cap fibroatheroma develop when fibrous cap is degraded. Matrix metalloproteinases (MMPs) are expressed and regulated in all cells of the arterial wall promoting vascular repair. Mediated by soluble cytokines and cell-cell interactions during inflammation MMPs are progressively upregulated in smooth muscle cells and macrophages and are activated in a multistep cascade. This contributes to matrix destruction (reviewed in [138]). Endothelial cells, smooth muscle cells and macrophages also express cathepsin cysteine proteases involved in lipid metabolism and ECM remodeling. In the progression of atherosclerosis, they are differentially expressed and contribute to macrophage foam cell formation and ECM degradation (reviewed in [149]). Thus, both classes of proteases provoke plaque rupture. In parallel, atherogenic LDL concentrations promote platelet aggregation by decreasing availability of endothelial nitric oxide (NO) and changing the platelet surface. Thereby, thrombogenicity of blood and plaque is increased contributing to thrombosis after plaque rupture (reviewed in [150]. Additionally, oxidised LDL binding to LOX-1 amongst others induce apoptosis of endothelial and smooth muscle cells thus contributing to atherosclerotic plaque rupture [124]. However, mechanical stress finally ruptures the plaque and the luminal regorged necrotic core activates the coagulation cascade causing coronary thrombosis and myocardial infarction [151].

1.1.6 Risk factors and prevention of atherosclerosis

Acute myocardial infarction is significantly associated with risk factors. The worldwide case-control study INTERHEART revealed nine risk factors and their population attributable risks collectively accounting for 94% of myocardial infarctions in women, 90% in men, respectively. Association of smoking, abnormal lipids, hypertension, diabetes, abdominal obesity, psychosocial factors, lack of daily fruit and vegetable consumption, al-

cohol consumption and irregular physical activity were noted for both sexes, all ages and all regions of the world. A healthy lifestyle with daily consumption of fruits and vegetables, regular physical activity and non-smoking was suggested to reduce the risk of acute myocardial infarction by more than three-quarters [152]. Hypertension was estimated to reduce life expectancy by 3.2 and 4.2 years and diabetes by 8.6 and 4.6 years for women and men, respectively. By contrast, physical activity, consumption of nuts, vegetarian diet and medium body mass index were proposed to gain life expectancy by 8.7 for women and 10.8 years for men [153]. For men, changes in lifestyle during early elderly years including physical activity, non-smoking and adjustment of blood pressure and weight not only accounted for an increased life span but also for significantly better physical and mental function [154].

However, there is evidence for a molecular link of sedentary lifestyle, systemic inflammation and chronic diseases like atherosclerosis [155]. Additionally, daily moderate-intensity exercise of only 15min was shown to be sufficient for 14% mortality reduction and three year extension of life expectancy. Every additional 15min of exercise further reduced mortality by 4%. These effects were demonstrated also for cardiovascular disease patients [156]. In patients with stable coronary artery disease (CAD), regular exercise training compared to percutaneous transluminal coronary angioplasty (PTCA) following stenting or coronary artery bypass grafting (CABG) even revealed a significantly higher event-free survival rate, exercise capacity, cost efficiency [157] and reduction of inflammation [158]. Physical activity at vigorous intensity seems to exhibit a more cardioprotective effect (reviewed in [159]). For CABG patients, aerobic interval training compared to continuous moderate exercise revealed a superior long-term exercise capacity [160] decreasing the annual mortality of coronary heart disease patients [161]. Moreover, high-intensity interval training was also able to reduce restenosis of coronary segments with both implanted bare metal and drug eluting stents and to enhance the endothelial function [162].

Nevertheless, preventive daily drug administration at an age of 55 years was also estimated to gain on average about 11–12 years of life free from acute cardiovascular disease events. Simultaneous reduction of cardiovascular risk factors LDL cholesterol, blood pressure, serum homocysteine and platelet function by only one polypill should reduce ischemic heart disease by 88% and stroke by 80%. Though, adverse effects would occur in 8–15% of people [163].

1.2 Apolipoprotein E

Apolipoprotein E (APOE) is a polymorphic and multifunctional gene modulating the lipoprotein metabolism, triglyceride homeostasis, immune response, inflammation, adrenal function and central nervous system (CNS) physiology [164, 165]. ApoE was first described as a structural component of triglyceride-rich plasma lipoproteins [166] inducible by high cholesterol diet [167]. ApoE is expressed by hepatic and extra-hepatic tissues [168] in

a tissue-specific manner [169] and its plasma concentration is extensively regulated on transcriptional, post-transcriptional and post-expressional level (reviewed in [170]). There are three major isoforms of ApoE, namely apolipoprotein E2, E3 and E4, whereas E3 is considered as parent isoform with its variants E2 and E4 [171]. ApoE2 is associated with type III hyperlipoproteinemia [167] and end-stage renal disease [172], whereas ApoE4 with both cardiovascular disease [173] as well as neuropathological disorders like Alzheimer disease [174, 175], infectious diseases like acquired immunodeficiency syndrome (AIDS) [176], also cancer [177], CNS ischemia [178], poor outcome after traumatic brain injury [179], obstructive sleep apnea [180] and recurrent pregnancy loss (RPL) [181]. Both isoforms are associated with type 2 diabetes [182]. These findings are attributed to structural and functional abnormalities of ApoE isoforms on cellular and molecular level.

1.2.1 Gene and protein

The human APOE gene is located on chromosome 19 (19:44905754–44909393) in a gene cluster containing the apolipoproteins E, C-I, C-I pseudogene, C-II and C-IV [183], spans 3640bp and contains four exons. There are five transcript splice variants and four protein coding transcripts. The primary translation product consists of 317 amino acids including a signal peptide of 18 amino acids for directing the nascent protein into endoplasmic reticulum [184]. The post-translational modifications in the golgi apparatus include O-linked glycosylation with addition of sialic acid carbohydrates prior to secretion [185]. The secreted protein is 299 amino acids long and features two functional domains separated by a hinge-region [186, 187]. The amino-terminal domain exhibit a bundle of four amphipathic anti-parallel α-helices [188] featuring binding affinity to LDL receptor [189] and scavenger receptor class B type 1 (SR-B1) [190] both essentially enhanced by lipidation, LDL receptor-related protein (LRP) [191] and heparan sulphate proteoglycan (HSPG) [192]. The carboxy-terminal domain exhibit an amphipathic α-helical conformation with coiled-coil structure for lipoprotein binding [193, 194] and additionally features sites for apolipoprotein self association only without lipidation [191] and HSPG binding [195]. The domain also promotes the secretion of triglycerides from VLDL [196] and anti-oxidant activity [197] protecting against LDL oxidation [86, 198].

1.2.2 Anti-atherogenic functions

ApoE is a highly anti-atherogenic protein involved in almost every step of atherogenesis by modulating lipoprotein metabolism and immune response. ApoE in the plasma is associated with the major lipoprotein classes chylomicrons, chylomicron remnants, VLDLs as well as HDLs [199] and is capable to regress atherosclerosis even at low expression [200, 201] and independently on lowering plasma cholesterol levels [200]. In the endogenous and exogenous cholesterol pathway, it mediates both high affinity binding and plasma lipoprotein recycling via LDL receptor and LDL receptor-related protein (LRP) [167].

ApoE also affects both the production and assembly of VLDL as well as the production and secretion of VLDL triglycerides [196, 202] and ApoE preferentially associates to larger and triglyceride-rich lipoproteins after lipoprotein secretion [203]. It is also capable to restrict VLDL lipolysis [204]. In the reverse cholesterol transport, ApoE [205, 206, 207] and even its expression [208] stimulate cellular cholesterol efflux and binds to the SR-B1 receptor [190] for cholesterol diffusion into cell membrane [79]. Furthermore, ApoE activates lipid transfer proteins and lipid-modifying enzymes important in lipoprotein metabolism like cholesteryl ester transfer protein (CETP) [209], lecithin: cholesterol acyltransferase (LCAT) [210] and hepatic lipase [211].

Independent of plasma levels, ApoE within the arterial wall suppresses atherosclerosis [212, 213, 214, 215, 216, 217] evidencing its role in immune response [218, 219]. Here, ApoE inhibits endothelial cell proliferation [220], platelet aggregation [221], T-lymphocyte activation [219, 222, 223, 224, 225] and proliferation [226, 227] and also smooth muscle cell (SMC) migration and proliferation [228, 229]. Additionally, ApoE has anti-oxidant activity [198] reducing LDL oxidation [86] and stimulates release of endothelial nitric oxide [230] featuring vasculoprotective functions (reviewed in [231]). Here, it defends against risk factor hypertension [232].

1.2.3 Polymorphisms and functional differences in atherosclerosis

The humans feature several ApoE isoforms (reviewed in [170]). The most frequent are ApoE2, E3 and E4, whereas E3 is seen as the parent form and E2 and E4 its variants. They are derived from the three alleles $\epsilon 2$, $\epsilon 3$ and $\epsilon 4$ [171]. Consequently, the three alleles reveal six genotypes with an order of decreasing frequencies in European Caucasian populations of $\epsilon 3/3$, $\epsilon 3/4$, $\epsilon 2/3$, $\epsilon 4/4$, $\epsilon 2/4$, $\epsilon 2/2$ [233]. The allelic isoforms differ from each other by Cysteine/Arginine substitutions at codons 130 and 176 due to T/C single nucleotide polymorphisms (SNPs) [234]. Worldwide the frequencies of allelic ApoE4 isoform in populations vary from 0–49% generally increasing with high-latitude cold environments [235]. In European Caucasian populations, the homozygous ApoE4 phenotype ranges from ∼1–11% [233] and carriers of ApoE4 phenotype (genotypes $\epsilon 4/4$ and $\epsilon 2/4$) have an up to 6.4 years shorter life expectancy [177] mainly resulting from structural and functional abnormalities of the variant isoforms ApoE4 [236, 237], which additionally exhibit a decreased anti-oxidant activity effecting cytotoxicity [198].

The three isoforms of ApoE exhibit different chemical and thermal stabilities [238, 239] and their two domains unfold independently [239]. The three isoforms [238] as well as their amino-terminal domains [238, 239] show the same order of increasing stabilities of ApoE4, E3, E2 and feature almost the same differences in thermal stabilities. Here, the isoforms E3 and E2 feature interactions of both terminal domains destabilising their amino-terminal domain. The amino-terminal domains of the isoforms E3 and E4 unfold with stable intermediates, whereas the isoform E2 domain in a two-state mechanism [238]. Consequently, only the isoforms E3 and E4 are partially unfolded *in vivo* [238] contributing

to different biological functions like binding to LDL receptor and lipoprotein (reviewed in [237]).

A functional consequence is a highly reduced LDL receptor binding affinity of ApoE2 compared to ApoE3 and ApoE4 ($\leq$2%) [240] due to change of conformation by alteration of a salt bridge and due to reduction of positive potential of the amino-terminal receptor binding region [241, 188]. Thus, ApoE2 delays the clearance of chylomicron remnants and VLDL [242] resulting in type III hyperlipoproteinemia [167, 243]. Nevertheless, ApoE2 can still utilise particle clearance via heparan sulphate proteoglycan (HSPG)/LDL receptor-related protein (LRP) complex or HSPG alone [244, 63], whereas ApoE2 binds more efficient to LRP than to LDL receptor [167]. Additionally, ApoE2 is also capable to upregulate the expression of hepatic LDL receptors [43, 46]. However, in the absence of type III hyperlipoproteinemia ApoE2 seems to be the most advantageous isoform preventing cardiovascular disease [167].

In contrast, lipid-free and phospholipid-bound ApoE4 reveals a closer inter-domain distance than ApoE3, which increases when bound to triglyceride-rich particles [245]. Here, a salt bridge-mediated amino acid side chain reorientation causes domain interaction [246] and a less organised structure of the carboxy-terminal lipid binding region changing its lipoprotein binding preference. ApoE4 features a higher lipid affinity than ApoE3 and E2 and preferentially binds to triglyceride-rich VLDL, whereas ApoE3 and E2 associate to phospholipid-rich HDL [247]. Thus, ApoE4 accelerates the clearance of chylomicron remnants and VLDL [242, 248] and thereby downregulates the expression of hepatic LDL receptors [43, 46]. Additionally, these particles compete for LDL receptors [236]. Finally, increased plasma LDL results in a 42% higher risk of cardiovascular disease [173].

Beside the endogenous and exogenous cholesterol pathway, the ApoE isoforms also affect the reverse cholesterol transport of macrophages. ApoE2 reveals the most efficient cholesterol efflux protecting from intra-cellular cholesterol accumulation. In contrast, ApoE4 shows an increased cholesterol uptake and accumulation [249] likely due to impaired ApoE4 recycling [250] promoting foam cell formation [129].

In addition to lipoprotein metabolism, ApoE isoforms influence cholesterol homeostasis with an inverse correlation of absorption and synthesis. Adults carrying E4 phenotype exhibit increased cholesterol absorption and decreased cholesterol synthesis, whereas E2 carriers a decreased absorption and increased synthesis [251]. Young children with ApoE4 also absorb cholesterol more effectively than young E3 children, but feature no compensatory reduction of cholesterol synthesis [252].

Finally, the isoforms exhibit different expression levels [233, 253] and reveal different concentrations and compositions of plasma lipoproteins [167, 253]. Compared to ApoE3, the variant E2 is associated with increased levels of ApoE, triglycerides and VLDL and decreased levels of ApoB, HDL, LDL and total cholesterol. Contrary, ApoE4 is associated with increased levels of ApoB, VLDL, HDL, LDL and total cholesterol and decreased levels of ApoE and triglycerides [167]. The increased expression of ApoE2 isoform likely delays

VLDL removal by inducing the VLDL triglyceride production and by reducing lipoprotein lipase-mediated VLDL lipolysis thereby contributing to hypertriglyceridemia [254].

1.3 Low-density lipoprotein receptor

The low-density lipoprotein receptor (LDLR) is a cell surface receptor utilising the cellular uptake of LDL particles (VLDL and LDL) from blood circulation [255]. The LDL receptor is subject to continuous recycling into and out of the cell. After binding LDL particles, the LDL-LDL receptor complex is internalised, dissociates in endosomes due to low-pH environment and LDL receptor can either recycled back to the cell surface or degraded in lysosomes [256, 257]. Thereby, cholesterol is internalised, which intra-cellular concentration regulates the transcription of LDL receptor gene [43, 46]. In patients with the semi-dominant disease familial hypercholesterolemia (FH) up to 1741 mutations (substitutions, deletions, insertions, duplications and inversions) of LDL receptor gene were detected so far (www.ucl.ac.uk/ldlr/). These patients exhibit decreased clearance of LDL [61] and increased synthesis of LDL [258] and of relatively small VLDL [259] and suffer from elevated blood cholesterol and early myocardial infarctions [260]. Only elevated LDL without other risk factors can trigger human atherosclerosis [261, 262, 263]. In addition, polymorphisms of the LDL receptor have been associated with obesity [264].

1.3.1 Gene and protein

The human LDL receptor gene is located on chromosome 19 (19:11089362–11133816) [265]. The encoding gene comprises 44.5kb (44455bp) and features 18 exons. There are 14 transcript splice variants and eight protein coding transcripts. The primary translation product exhibit 860 amino acids containing a 21 amino acid signal peptide for translocation of the nascent protein into endoplasmic reticulum [266]. Differing from vectorial folding of multi-domain proteins from amino-terminus to the carboxy-terminus, the folding of newly synthesised LDL receptor proteins in the endoplasmic reticulum occurs post-translationally in collapsed non-reactive intermediates. Here, rapidly folded structures feature non-native inter-domain disulphide bonds isomerising with time into the native intra-domain state [267]. The folding is further characterised by the incorporation of stabilising calcium ions and is assisted by chaperones and folding enzymes [268]. Post-transcriptional modifications in the endoplasmic reticulum-golgi apparatus complex comprise N-linked glycosylation and O-linked glycosylation with sialic acid carbohydrates [269, 270]. The exons function as independent modules and correlate with distinct protein domains [271] shared with different LDL receptor family members [268]. The mature LDL receptor is 839 amino acids long and features five functionally defined protein regions (reviewed in [268]). The amino-terminal ligand binding region consists of seven LDL receptor class A repeats [266] revealing six conserved cysteine residues, which form three disulphide bonds [272, 273, 274] and stabilise the two-loop repeat conformations

[275, 276, 277, 278, 279]. The repeats 2–7 and epidermal growth factor (EGF) repeat A are essential for LDL binding via ApoB-100, whereas repeat 5 mediates interaction with VLDL via ApoE [280, 281, 282]. However, calcium is required for lipoprotein binding [283]. The EGF precursor homology region comprises three EGF repeats (A, B, C), which also reveal six conserved cysteine residues allowing for disulphide bonds and a β-propeller structure between repeat B and C [284, 285]. This region promotes the acid-dependent release of lipoproteins from LDL receptors in endosomes [280, 286, 287]. The O-linked glycan region features several acceptors for O-linked glycosylation, which seems to impair neither the binding and internalisation of lipoproteins nor the recycling and degradation of LDL receptor [288], whereas O-linked glycosylation in the first and second domain effects binding and internalisation of lipoproteins and degradation of LDL receptor [289]. O-linked glycosylation of the O-linked glycan domain likely reduces unspecific extra-cellular proteolysis and intra-cellular domain release [290, 291]. The trans-membrane domain is lipophilic and anchors the LDL receptor in plasma membrane [268]. The carboxy-terminal cytosolic domain facilitates the basolateral targeting of LDL receptor into membrane bilayer [292] and the clathrin-mediated endocytosis of lipoproteins [280, 293]. Therefore, the binding of modular adapter proteins to the cytosolic domain regulates the clustering of LDL receptor into clathrin-coated pits [294, 295, 296]. The domain was also shown to interact with a protein implicated in internalisation and intra-cellular trafficking of the LDL receptor [297, 298].

1.3.2 Pathway, regulation and anti-atherogenic function

Initially LDL binds with high affinity to LDL receptors [299] and is internalised by receptor-mediated endocytosis utilising clathrin-coated pits and vesicles [300]. In endosomal low-pH environment, LDL receptor dissociates from its ligand LDL and is recycled back to the cell surface or degraded in lysosomes [256, 257]. LDL is hydrolysed in lysosomes by lysosomal enzymes [301, 302] and the LDL-derived cholesterol decreases 3-hydroxy-3-methylglutaryl coenzyme A reductase (HMG CoA reductase) activity [303, 304, 305] a rate-limiting enzyme in cholesterol synthesis [19]. Here, the LDL cholesterol suppresses the transcription of HMG CoA reductase gene [43, 46] and also accelerates the degradation of HMG CoA reductase in endoplasmic reticulum [306]. Additionally, LDL-derived cholesterol decreases LDL receptor activity [307] by suppressing its gene transcription [43, 46]. Finally, LDL cholesterol activates acyl-coenzyme A: cholesterol acyltransferase (ACAT), which esterifies cholesterol for cytoplasmic droplet storage [308, 307].

The transcriptional regulation of LDL receptor and all enzymes in cholesterol synthesis including HMG CoA reductase is controlled by active domains of the sterol regulatory element-binding proteins (SREBPs), which are cleaved proteolytically from golgi apparatus membrane and subsequently act as transcription factors. When sterols accumulate, the transport of SREBPs from endoplasmic reticulum to golgi apparatus is suppressed and thereby transcription-activating cleavage [42, 44, 46, 43, 45]. This end-product feedback

regulation prevents from cellular cholesterol accumulation by both decreased cholesterol uptake [309] and cholesterol synthesis [303, 304, 305].

In total, the anti-atherogenic function of the LDL receptor is the regulation of cellular cholesterol metabolism including uptake of lipoprotein particles VLDL and LDL from blood circulation as well as synthesis and storage of cholesterol [61, 255]. Furthermore, the LDL receptor seems to inhibit an additional synthesis pathway of LDL [258] and the production of relatively small VLDL [259].

1.3.3 Mutations and familial hypercholesterolemia

Mutations in the LDL receptor gene most commonly cause semi-dominant familial hypercholesterolemia (FH) [310]. This disease disrupts the cellular cholesterol metabolism and is characterised by elevated plasma LDL and cholesterol [271] and xanthomas (LDL cholesterol-rose yellowish papules of the skin) [311]. Elevated LDL in the absence of any risk factors can produce human atherosclerosis [261, 262, 263] and cause early myocardial infarctions [260]. Here, patients with two variant alleles of the LDL receptor gene (FH homozygotes) are affected more severely than patients with only one variant allele (FH heterozygotes) [311]. FH heterozygous exhibit a 2-fold increase in number of LDL particles with myocardial infarctions at an age of 30 years, FH homozygotes a 6–10-fold increase with infarctions already in early childhood, respectively. FH heterozygotes amount to about one in 500 individuals worldwide, FH homozygotes to one in one million individuals [263].

Up to now, 1741 mutations of the LDL receptor gene were revealed comprising substitutions, deletions, insertions, duplications and inversions with the highest proportion of substitutions (73.5%) (www.ucl.ac.uk/ldlr/). Most of the reported variants are predicted to be pathogenic (79%) [310] and there are 19 polymorphisms revealing no phenotypic effect. Sequence variants arise in all exons and most frequently concern exon 4 (19.5%) (www.ucl.ac.uk/ldlr/). With 381bp it is the largest exon coding for critical class A repeats 3–5 within the ligand binding region [281, 282, 266]. Traditionally, the mutations were graduated into five classes disrupting physiological functions of the LDL receptor at different levels [271, 312]. Class 1 mutations generate no protein by disrupting the synthesis or the secretory pathway. Class 2 mutations block or reduce the protein transport from endoplasmic reticulum to golgi apparatus due to impaired receptor folding. Class 3 mutations produce surface-bound proteins, which are defective in LDL binding and class 4 mutations inhibit LDL-LDL receptor complex internalisation via clathrin-coated pits. Class 5 mutations prevent LDL receptor recycling from endosomes back to the cell surface resulting in degradation in lysosomes. Recently, a class 6 mutation were added, which targets the LDL receptor to the apical instead to the basolateral side of the membrane bilayer [292]. These mutations result in reduced receptor-mediated endocytosis of LDL particles.

1.4 Fractalkine receptor

Fractalkine receptor (CX3CR1) is a cell surface receptor mediating critical physiological functions by binding its ligand fractalkine, a chemokine which exists both in a soluble and membrane-bound form [313]. Fractalkine/CX3CR1 signaling regulates microglia- and complement-mediated synaptic remodeling during central nervous system (CNS) development [314] and microglia-mediated adult neurogenesis influencing cognitive function [315]. It also modulates pancreatic β cell function and insulin secretion [316] and cardiovascular responses like blood pressure and heart rate [317].

Additionally, the signaling regulates critical physiological events during innate and adaptive inflammatory responses [318, 319, 320, 321]. It is relevant in coronary artery disease [322, 319, 320, 323], vasculitis and vasculopathy [324], cardiac allograft rejection [325], lung disease [326], liver injury [327], kidney disease [328, 329, 330, 331] and injury [332, 333], sepsis [334], cancer [335, 336, 337, 338], chronic pain and inflammation [339, 340, 341], neuropathological disorders like Alzheimer disease [342, 343], organ-specific auto-immune disorders like atopic dermatitis [344] and multiple sclerosis [345], systemic auto-immune disorders like rheumatoid arthritis [346, 347], systemic sclerosis [348], osteoarthritis [349] and Wegener's granulomatosis [350] and controls human immunodeficiency virus (HIV) infection [318].

Polymorphisms of CX3CR1 even increase the risk of ischemic cerebrovascular disease [351, 352, 353], internal carotid artery occlusive disease [354], restenosis after coronary stenting [355], pulmonary arterial hypertension [356], obesity [357], infectious liver fibrosis [358] and post-transplant liver rejection [359], end-stage renal disease [360], psoriasis [361], cancer [362, 363], arthritis [364] and infectious diseases like severe respiratory syncytial virus (RSV) bronchiolitis [365].

However, there are also polymorphisms of CX3CR1 associated with a reduced risk of atherosclerosis [351], coronary artery disease (CAD) [351, 366], carotid artery stenosis [367], coal workers' pneumoconiosis [368], tumor infiltration with increased cancer survival [369], chronic tonsillitis [370] and recurrent headaches [371].

These associations illustrate that fractalkine/CX3CR1 signaling represents a potential target for future treatment especially of inflammatory diseases, cancer and pain [372, 373].

1.4.1 Gene and protein

The human fractalkine receptor (CX3CR1) gene is located on chromosome 3 (3:39263494–39281735) in a CC-chemokine receptor (CCR) gene cluster containing the six genes CCR1, CCR3, CCRL2, CCR5, CCR2 and CCXCR1 [374]. The gene spans 18.2kb (18240bp) and features six exons. There are seven transcript splice variants and five protein coding transcripts revealing the two isoforms a and b. The mature transcripts are generated by alternative splicing of one out of five exons featuring distinct functional promoter regions with an universal exon containing the complete open reading frame (ORF) and coding for the

355 amino acid long isoform b. Thereby, one of the transcripts features an translated exon elongating the ORF and encoding the 387 amino acid long isoform a. In human peripheral blood mononuclear cells (PBMCs), four transcripts were identified at different expression levels and two promoters were found to reveal constitutive activity in a cell-specific manner [375, 376]. Transcription of the human CX3CR1 was detected in endothelial cells [377], monocytes [378, 379], dendritic cells [380], granulocytes [379], mast cells [381], T-lymphocytes [382, 321], natural killer cells [379], platelets [383] and in neurons, microglial cells and astrocytes [384, 385]. CX3CR1 shapes a guanosintriphosphate-binding (G)-protein-coupled, 7-transmembrane receptor [379], whose amino-terminal domain is able to bind the highly flexible and variable chemokine domain of function (CDF) of fractalkine [386]. The receptor is able to mediate cell migration dependent of G-protein activation and signal transduction [379] and cell adhesion even independent of G-protein signaling [387].

1.4.2 Upregulation, distribution and atherosclerosis

Coronary artery disease (CAD) patients exhibit both expression upregulation of fractalkine receptor (CX3CR1) in peripheral blood mononuclear cells (PBMCs) [319, 320] and increased plasma levels of soluble fractalkine (CX3CL1) [320]. CX3CR1 and CX3CL1 is expressed in all stages of atherosclerotic carotid artery plaques including intra-plaque microvessels and are collocated in endothelial cells, macrophages and smooth muscle cells. Here, CX3CL1 is detected especially within deeper layers of the vessel wall. In advanced plaques, CX3CL1 is enriched in the plaque core, whereas less distinctive in the fibrous cap [322]. In atherosclerotic coronary arteries, the expression of CX3CR1 and CX3CL1 is detected in macrophages, foam cells and smooth muscle cells, both expressions colocalise specifically and are present throughout the whole vessel, in endothelium, intima, media and adventitia, whereas absent in normal coronary arteries [323]. In coronary artery disease patients with unstable angina pectoris (plaque rupture), the plasma levels of CX3CR1 and soluble CX3CL1 are even higher than in patients with stable angina pectoris and thus associated to plaque rupture [388, 320]. In contrast, atherosclerosis was reduced in murine models by suppressing the CX3CR1 and CX3CL1 expression [389], pharmacological inhibition of CX3CR1 [390] or gene knockout of CX3CR1 [391, 392].

1.4.3 Atherogenic functions

The expression of fractalkine receptor (CX3CR1) by platelets [383], endothelial cells [377], monocytes [319] differentiating into expressing macrophages [128, 393] as well as smooth muscle cells [394] is crucial for the progression of atherosclerosis. CX3CR1 binds its sole ligand CX3CL1, a chemokine which exists both in a soluble and membrane-bound form [313] with chemoattractant and adhesive function [395]. The soluble form is generated by metalloproteinase-mediated specific cleavage of the membrane-bound form [396, 397, 398].

The CX3CL1/CX3CR1 signaling mediates chemotaxis and adhesion of immune cells and vascular cells, pro-inflammatory cytotoxicity as well as anti-apoptosis and cell proliferation during early stage of atherosclerosis and apoptosis in the progressive stage (reviewed in [395]).

During atherosclerosis the plasma level of soluble fractalkine (CX3CL1) is increased [320] and thereby upregulates inter-cellular adhesion molecule (ICAM)-1 in endothelial cells in a dose-dependent manner [377]. This mediates fractalkine-dependent platelet adhesion to activated endothelium independent of CX3CR1 [126] and also enhances monocyte adhesion to endothelial cells in a dose-dependent manner [399, 400]. CX3CR1 can also induce fractalkine-dependent endothelial cell migration [401] possibly contributing to stenosis of atherosclerotic vessels or restenosis of grafted vessels [395]). Subsequently, endothelial expressed membrane-bound CX3CL1 activates platelets via CX3CR1 [126, 383] contributing to sub-endothelial recruitment of monocytes [127].

In monocytes, the expression of CX3CR1 can be induced by monocyte chemotactic protein (MCP)-1 [402] and angiotensin II [403], a vasoconstrictive and pro-inflammatory agent generating oxidative stress and being relevant in atherogenesis [404]. Thereby, CX3CR1 mediates fractalkine-dependent leukocyte adhesion and migration [379]. Soluble CX3CL1 antagonises MCP-1 and suppresses the transendothelial migration of monocytes [405]. However, leukocyte adhesion to the vascular endothelium can occur integrin-dependently via soluble CX3CL1, and also integrin-independently via membrane-bound CX3CL1 [400], which contribute to leukocyte capture under physiological shear stress conditions [406, 407]. For capturing leukocytes under high shear stress conditions, platelet activation with subsequent P-selectin secretion is strictly required. Both the soluble and the membrane-bound CX3CL1 is capable to induce P-selectin expression and its secretion via platelet degranulation [408]. Circulating leukocytes contain peripheral blood monocytes, which can be sub-divided into three subsets, a classical (90–95%: $CD14^{high}$ $CD16^{-}$ $CX3CR1^{low}$), intermediate ($CD14^{high}$ $CD16^{+}$ $CX3CR1^{high}$) and non-classical population (5–10%: $CD14^{low}$ $CD16^{high}$ $CX3CR1^{high}$) [409, 410] developing gradually from classical via intermediate into non-classical monocytes [411]. Here, the low expression of CX3CR1 determines the recruitment to inflamed tissue, whereas high expression the CX3CR1-dependent recruitment to non-inflamed tissue [412]. However, in atherosclerotic plaques the oxidised LDL is capable to induce specific differentiation of monocytes with increased expression of CX3CR1, which predominantly mediates adhesive property to coronary smooth muscle cells [393] and thus promote survival [413] and accumulation of monocytes/macrophage within the vascular wall [414, 393]. However, in the advanced plaque the expression of CX3CL1 decreases [415] impairing cell survival and monocyte homeostasis [413].

Furthermore, CX3CR1 expression of smooth muscle cells mediates their migration to a subset of CX3CL1-expressing mononuclear cells in coronary artery plaques [394] and additionally induces their cell-cell adhesion and proliferation [416]. The cross-talk be-

tween smooth muscle cells and monocytes potentiates their inflammatory response [417]. However, metalloproteinase-mediated shedding of soluble CX3CL1 from vascular smooth muscle cells counter-regulates the fractalkine-mediated adhesion of monocytes promoting monocyte recruitment [396]. CX3CR1 also regulates fractalkine-dependent anti-apoptosis and proliferation of coronary artery smooth muscle cells [418] due to predominant expression of CX3CL1 in early lesions [415] likely contributing to destabilisation of advanced plaques containing rare smooth muscle cells in the fibrous cap [100]. After vascular injury, CX3CR1-expressing bone marrow mononuclear cells differentiate in the vessel wall and contribute to smooth muscle cells within atherosclerotic plaques [419]. These progenitor cells also contribute to the formation of plaque microvessels [420].

Beside cell adhesion and migration, CX3CL1/CX3CR1 signaling can activate several signal transduction pathways, which regulate the function of cytokines and CX3CL1 [377, 416, 421, 422, 405]. It also has a cytotoxic effect by activating T lymphocytes [321] and natural killer cells, which induce endothelial cell injury [423].

Ultimately, monocytes and macrophages are important for formation [424], maintenance [425], neovascularisation [420] and instability of atherosclerotic plaques [100]. Here, angiogenesis is triggered by endothelial cells via fractalkine-induced activation of CX3CR1 [426].

1.4.4 Polymorphisms and atherosclerosis

In the human CX3CR1 gene, two disease-related and non-synonymous single nucleotide polymorphisms (SNPs) V249I and T280M were detected. They are located within the coding region of the sixth and seventh transmembrane-domain of the receptor [427]. The T280M polymorphism is non-conservative due to an exchange of a polar for a non-polar side chain revealing major effects on protein structure and function [428]. However, both SNPs are highly linked to each other revealing three predominant and an extremely rare haplotype [351]. The Valine/Isoleucine substitution at codon 249 by G/A SNP probably is a prerequisite for Threonine/Methionine substitution at codon 280 by C/T SNP [351, 366, 429, 428]. Within pooled Caucasian and Asian populations, the frequencies of the revealing haplotypes $V_{249}T_{280}$, $I_{249}T_{280}$, $I_{249}M_{280}$ and $V_{249}M_{280}$ are 72.2%, 10.5%, 17.2% and 0.06%, respectively [351].

The haplotype $I_{249}M_{280}$ exhibits a reduced risk of atherosclerosis and coronary artery disease (CAD) already in the heterozygous state [351, 366] but an elevated risk of ischemic cerebrovascular disease in the homozygous state [351, 353]. Thereby, it features decreased binding affinity to labeled and soluble CX3CL1 as well as a reduced density of CX3CR1 compared to the wild-type haplotype $V_{249}T_{280}$ with I_{249}-mediated reduced receptor expression [428]. In contrast, the haplotype $I_{249}M_{280}$ showed an increased I_{249}-mediated cell adhesion to membrane-bound FKN [430]. However, both SNPs are related to abnormal receptor functionality. Furthermore, the M_{280} allele exhibits decreased CX3CL1 binding kinetics and impairs inflammatory leukocyte chemotaxis, leukocyte-endothelial cell adhe-

sion and G-protein signaling-mediated leukocyte transmigration into the vessel wall [429].

The I_{249} allele in the heterozygous state also reduces the risk of atherosclerosis and CAD [351, 427] and without the protective effect of M_{280} allele, I_{249} is also associated with elevated risk of acute coronary syndrome (ACS) during CAD [431] and restenosis after stent implantation [355]. However, the I_{249} allele in both the heterozygous and the homozygous state promotes survival of acute myocardial infarction and decreases T-cell recruitment into infarct related artery [432]. At heterozygosity, the allele decreases the total number of CX3CL1 binding sites about ∼40% with reduced receptor expression and ligand binding affinity [427], whereas the homozygous M_{280} allele about ∼85% [428].

Finally, the polymorphisms combined genotypes VITM and IITM also decreases the risk of atherosclerosis [351].

1.5 Animal models for atherosclerosis

Animal models are a useful tool for understanding biological processes of the human atherosclerosis and for simultaneous evaluation of therapeutic methods. This will allow for an early diagnosis of atherosclerosis, forecast of progression and treatment of pathologies. However, there is no perfect model, which replicates all developmental stages of the human atherosclerosis including arising atherothrombotic diseases. Moreover, genetic and environmental factors significantly influence the development of the cardiovascular pathophysiology in a synergistic manner making it almost impossible to address a particular disease complication to one experimental model. Nevertheless, there are several animal models for atherosclerosis [433, 434] and cardiovascular diseases [435] including rabbit, mouse, rat, hamster, guinea pig, pigeon, quail, chick, dog, cat, pig and non-human primate, each with their specific advantages and disadvantages in the human atherosclerosis research (reviewed in [433, 434, 435]). In these animals, the manipulation of the atherogenic process is limited and commonly induced by cholesterol feeding and mechanical endothelial injury. However, they often differ from the human in cholesterol homeostasis, lipoprotein metabolism and arterial vessel hemodynamics determining total plasma cholesterol, plasma lipoprotein profile, systemic and site-specific athero-susceptibility of arteries as well as plaque morphology.

1.5.1 Mouse models for atherosclerosis

The mouse is the predominant model for understanding the underlying immunologic molecular and cellular mechanisms in atherosclerosis and for evaluation of new and existing therapeutic drugs against risk factors like hypercholesterolemia, hypertriglyceridemia, hypertension, and inflammation [436]. They feature relatively low costs of purchase, maintenance and study-related compounds and furthermore easy breeding due to their short reproductive cycle and large litter size. The mouse offers a well-known genome, defined genetics and ease of genetic manipulation [433, 434, 435] allowing for multiple

gene modification by random and targeted transgenesis, gene knockout as well as temporal and tissue specific conditional knockout [433]. Current mouse models for a diet-induced atherosclerosis feature gene knockouts and transgenes, which genetically modify the lipoprotein metabolism and are additionally exposed to risk factors like hypertension and diabetes [435]. The JAX mice database provides 239 mouse models for atherosclerosis research (www.jax.org) including humanised transgene strains bearing ApoE2 [437], mutant ApoE3Leiden [438, 439], CETP [440], ApoA-I [441] and ApoB-100 [442] as well as knockout strains deficient in ApoA-I [443], ApoE [444, 445] and LDL receptor (LDLR) [446, 447]. However, the most common atherosclerosis models are the ApoE$^{-/-}$ mice and the LDLR$^{-/-}$ mice, also present in a double-deficient state [448, 449]. Furthermore, there are many inbred mouse strains with diverging susceptibility to atherosclerosis [450] due to genetic differences effecting the endothelial response in the arterial wall [451, 452] and the angle of aortic arch curvature [453]. Crossing these inbred strains with genetically modified models which rapidly develop atherosclerotic plaques allows for an advanced determining of pro- and anti-atherogenic genes by quantitative trait loci (QTL) linkage analysis [454, 455, 456, 457]. Cross-species comparison of these data with genome wide association (GWA) studies in humans further improves identification of candidate genes and variants [458]. Moreover, mice are also suitable for non-invasive magnetic resonance imaging (MRI) and in combination with novel emerging contrast agents they even enable to serially monitor individual plaque progression at the molecular and cellular level [459]. By the transplantation of donor bone marrow into irradiated and bone marrow deficient recipients, the atherogenic influence of monocytes and cells of the adaptive immune system as well as their response to chemokines and cytokines can be evaluated [213, 214, 216]. Adoptive transfer of specific immune cells into immune deficient hosts even allows for a more individual elucidation [425, 460]. Tissue specific Cre recombinase/loxP-mediated gene inactivation [461, 462, 463], tetracycline/tetracycline responsive element (TRE)-mediated temporal gene induction [464] and adeno-associated virus-mediated gene expression in liver [465] are further strategies to establish the function of genes on atherogenesis.

However, mice do not lend themselves to frequent blood sampling and to dissection of small- and medium-sized blood vessels [433, 434]. Wild-type mice distinguish significantly from human in immune system [466] and carry about 70% of the total plasma cholesterol in HDL particles [434, 467], which protects against atherosclerosis by promoting cholesterol efflux and reverse cholesterol transport [468]. Besides, there is only a single isoform of ApoE in the mouse [433] in contrast to two additional major isoforms in the human [171], which are associated with type III hyperlipoproteinemia [167] and a 42% higher risk of cardiovascular disease (CVD) [173]. Additionally, they lack the cholesteryl ester transfer protein (CETP) [433, 434], a potential therapeutic athero-protective target promoting atherogenic dyslipidemia with small and dense HDL and LDL particles when triglyceride levels are increased [469]. Especially, these particles are associated with coronary heart disease (CHD) [89, 80] and myocardial infarction in human [90]. Furthermore, a substan-

tial fraction of the liver-secreted VLDL features apolipoprotein B-48 [470] instead of B-100 in humans [471] and in addition to LDL receptor these lipoproteins were efficiently cleared by LDL receptor-related protein (LRP) [446]. In general, mice are not susceptible to atherosclerosis and do not develop lesions spontaneously. They are also highly resistant to diet-induced atherosclerosis and reveal genetic background-dependent susceptibility to disease induction [450] and variations in the efficiency of dietary cholesterol absorption [472]. By feeding a semi-synthetic diet (high fat, high cholesterol) for five weeks, indeed all ten analysed inbred strains developed increased and varying levels of total plasma cholesterol with decreased and less varying levels of plasma triglycerides. However, after ten weeks only two strains and after 14 weeks five strains showed formation of early lesions (fatty streaks) with reproducibility for the most susceptible strain. Within this strain, plasma total cholesterol increased from 112–134$\frac{mg}{dL}$ to 282–350$\frac{mg}{dL}$ [450] with reduced HDL and elevated VLDL and LDL cholesterol. Here, the lower cholesterol-carrying capacity of HDL is due to a smaller HDL particle size [473]. This diet generated no fat accumulation and gallstone formation [473] and the arisen lesions comprised intra-cellular fat and several layers of foam cells invading the vessel media without fibrous cap formation. Importantly, there was almost no correlation between plasma cholesterol levels and susceptibility to lesion formation [450]. Compared to human, the mouse models indeed features high similarity in genetics and histology of lesion development, but extremely rarely generate the most feared human complications plaque rupture [474, 475, 476] and thrombosis [474, 475, 477]. There are also no plaques with thick fibrous caps [475, 477, 478, 444] and only small lamellae (arrangement of plain muscle fibers) and vasa vasorum (blood vessel network within the vessel wall) in the vessel media [433]. Furthermore, lesions do not develop predominantly in coronary arteries [479] but in the aortic root [476]. Whether the mouse reflects a precise model for the human disease is under discussion [480].

1.5.2 Pig models for coronary atherosclerosis

The pig already serves for decades as a human biomedical model. Pigs feature similarities in size, physiology, organ development and disease progression. Besides, their long life expectancy allowing for time studies they enable repeated collection of peripheral tissue samples and imaging of vessels and organs by diagnostic standard procedures. The large litter size, availability of cloning in combination with knockout and transgene technologies as well as high homology of sequence and chromosome constitution provide for genomic analysis like comparative quantitative trait loci (QTL) linkage analysis. Additionally, well-defined cell lines representing different tissues allow for proteomic and toxicological analysis (reviewed in [481]).

Of particular importance is that porcine coronary arteries respond to balloon angioplasty-induced arterial media injury with human-like restenotic neointimal thickening featuring smooth muscle cell proliferation [482], which is proportional to coronary artery injury [483]. To reduce this adverse effect in percutaneous transluminal coronary angioplasty (PTCA)

patients [484, 485], the injury-response relationship of the porcine coronary restenosis model was used to quantify the effects of preventive restenosis treatment by drug administration [486, 487, 488, 489] and by drug-eluting stents [490]. In contrast to bare metal stents, which predominantly generate restenosis and need revascularisation, the drug-eluting stents rather delay coronary arterial healing and cause late stent thrombosis [491]. Since endothelial coverage ratio of stent struts is the best predictor for late stent thrombosis [492], the first post-operative time point for preclinical evaluation of stent performance should be at ∼28 days within the recommended follow-up interval of six month [493, 494].

A further development of the coronary restenosis model was the porcine heat-injury restenosis model by using thermal balloon angioplasty [495, 496]. Contrary, this model generates true stenotic lesions after 28 days and thus is suitable for evaluation of bioabsorbable and bifurcation stents, coronary artery imaging without stent-related artifacts, and complex minimal-invasive (percutaneous) coronary interventions [495]. However, since balloon angioplasty and stent implantation do not generate coronary total occlusions, several porcine chronic total occlusion models have been developed to improve recanalisation treatments either pharmacologically or invasively (reviewed in [497]). Implantation of a bioabsorbable polymer construct into porcine coronary artery was shown to generate a human-like chronic total occlusion after 28 days. The occurring thrombo-fibrotic occlusion featured microvascular channels, dense collagen as well as elastic tissue [498].

A more clinically relevant model for evaluation of diagnostic and therapeutic procedures would be a porcine atherosclerosis model of vulnerable plaque. The porcine cardiovascular system features human-like size, anatomy, perfusion distribution of blood flow, physiology [499, 500, 501, 502] influencing cardiac function [499, 503] as well as platelet coagulation [504]. Likewise, pigs only insufficiently develop coronary collateral vessels after femoral artery ligation [505] as well as coronary artery occlusion, which highly variably respond to vasodilatators [506]. Additionally, they feature a human-like lipoprotein profile [434] with similar characteristics [507, 508], natural atherogenic mutations of apolipoproteins [509, 510, 511] and the LDL receptor [512, 513, 514]. In contrast to the human with its three major isoforms of ApoE [171], the pig seems to bear only the ApoE4 isoform [5], which is associated with a 42% higher risk of cardiovascular disease [173]. Advanced in years, pigs spontaneously develop atherosclerosis [515, 516], which can be accelerated by high levels of dietary fats and cholesterol [517, 5, 518, 519, 520]. Furthermore, dietary fats are capable to increase blood coagulation and thrombus formation [521]. Finally, in Belgian pigs even myocardial infarctions can be induced by stress [522]. Although pigs, like mice, lack the cholesteryl ester transfer protein (CETP), they are considered to bridge the gap between small animal models and human clinical trials [523].

Generally, atherosclerosis is promoted at vascular branches, bifurcations and bends where physiological flow separations and flow disturbances generate hemodynamic shear stress characteristics regulating pro-atherogenic endothelial responses and functions (re-

viewed in [524]). Respectively, in the pig atherosclerosis of the major coronary arteries is promoted synergistically by low endothelial shear stress and excessive expansive vascular remodeling [525] with adventitial neovascularisation [526]. Functional investigations of the porcine aortic vasculature revealed increased protein permeability associated with ultrastructural changes of endothelium and vascular intima at athero-susceptible sites [527]. The athero-susceptible proximal regions of porcine coronary arteries reveal distinct endothelial transcript profiles triggering endoplasmic reticulum (ER) stress and accumulation of reactive oxygen species (ROS) [528].

Hypercholesterolemic pigs fed a supplemented lard diet (high fat, moderate cholesterol) exhibit circulating cholesterol-enriched blood monocytes with both increased acyl-coenzyme A: cholesterol acyltransferase (ACAT) activity and lipid biosynthesis [529], which were recruited exclusively into the aorta by chemotactic factors of the athero-susceptible site [530]. These monocytes adhere to the endothelium and subsequently transform into macrophage foam cells contributing to the development of fatty streak lesions [531]. The foam cells of this lesion state are capable to migrate back into the blood stream and induce endothelial damage [532]. In the progress of lesion development, smooth muscle cells proliferate within the coronary intima [533]. Lesions arise at coronary arteries, thoracic aorta and carotid arteries and develop to human-like complex unstable atherosclerotic plaques predominantly at coronary arteries associated with an site-specific early increase in inflammatory gene expression and with a late upregulation of plaque destabilising genes [534]. Since a porcine model of carotid atherosclerosis revealed distal embolisms associated with vulnerable carotid plaques, the pig is assumed the most promising animal to resemble human plaque instability and thrombotic rupture [535].

The progression and histology of advanced coronary lesions with human-like features is dependent of the swine breed, plasma cholesterol levels, their exposure time and addition of pro-atherogenic factors like vascular injury and diabetes (reviewed in [536]). Hypercholesterolemia and atherosclerosis is often induced by highly modified diets containing 1–4% pure cholesterol and sodium cholate. These substances are not common in human diets and the latter potentially is toxic and even counterproductive [537]. Moreover, these diets are ∼40 times more expensive than regular pig diets [523].

Current porcine models with accelerated atherosclerosis (reviewed in [538]) are the induced diabetic/hypercholesterolemic pig model [539], the inherited hyper-LDL cholesterolemia pig model [540, 512, 513, 514, 541, 509, 510, 511], proprotein convertase subtilisin/kexin type 9 (PCSK9) gain of function mutant pig model [542] and the metabolic disease pig model [543, 544]. However, beside their advantages, these porcine atherosclerosis models exhibit relative disadvantages (reviewed in [538, 536]). The induced diabetic/hypercholesterolemic pig model is expensive in husbandry and reveals highly variable lesion sizes and locations, develop hypoglycaemic coma and are prone to infections and gastroparesis [536]. The inherited hyper-LDL cholesterolemia pig model features a long induction period for atherosclerosis and a considerable phenotypic variability in

plasma cholesterol level and disease development due to its broad heterogeneous genetic background [540, 513]. The PCSK9 gain of function mutation reduces the hepatic LDL receptor level and impairs plasma LDL clearance causing severe hypercholesterolemia with spontaneous and progressing atherosclerosis [542]. Since the mutant PCSK9 transgene is ∼500-fold overexpressed in liver, these pigs are not suited for treatments increasing hepatic LDL receptor levels or reducing PCSK9 activity [523]. Finally, the metabolic disease pig model generates extensive and diffuse atherosclerosis covering proximal, intermediate as well as distal segments of coronary arteries [545, 546] complicating the preclinical evaluation of novel stents by increased peri-stent (adjacent to the stent) coronary artery disease [545]. Additionally, the latter two are commercially limited available [538].

Thus, a large animal model without disadvantages of the current porcine models but with an accelerated and human-like atherosclerosis including vulnerable coronary plaques is increasingly important. The $LDLR^{-/-}$ pig would address the disadvantages and allow for a cost-efficient and rapid preclinical validation of innovative diagnostic and therapeutic technologies for the treatment of human coronary artery disease (CAD). Compared to wild-type animals, the $LDLR^{+/-}$ pig would be susceptible to diet-induced atherosclerosis and enable therapeutic modification of LDL receptor expression attenuating or accelerating the progression of atherosclerosis [523].

1.5.3 Generation of gene targeted pigs by somatic cell nuclear transfer

Somatic cell nuclear transfer (SCNT) is a cloning method, in which a donor nucleus is transferred into the cytoplasm of a unfertilised and enucleated oocyte. The efficiency of generating life offspring is limited to 1–3% and is determined by nuclear remodeling (change in chromatin architecture) and the resulting nuclear reprogramming (change in gene transcription profile). It is recommended that unfertilised oocytes mature *in vivo* and are isolated from sexually mature animals since they best supply factors remodeling the transferred nucleus. In contrast, the donor nucleus should be isolated from less differentiated cells, since it is more plastic and more susceptible to remove transcription affecting proteins (reviewed in [547]). Insufficient remodeling and reprogramming of the nucleus cause an aberrant gene expression and result in abnormal development of the placenta [548, 549] and the fetus [550]. This symptomatic is referred as large offspring syndrome (LOS), which provokes a continuum of phenotypes (reviewed in [547]). The porcine SCNT can be accompanied with underdeveloped placenta, high post-natal mortality, stillbirth, small litter size as well as low litter weight and average birth weight [551]. A further characteristic of the abnormal fetal development is the large tongue.

However, pigs were successfully cloned using fibroblasts as donors for SCNT [552, 553, 554, 555, 556, 557]. Based on this fact, several gene targeted pigs were generated featuring targeted disruption of α1,3-galactosyltransferase (α1,3GT) [558, 559, 560, 561, 562, 563, 564, 565, 566, 567], cystic fibrosis transmembrane conductance receptor (CFTR) [568, 569, 570, 571, 572], J-region gene segment of the heavy chain locus [573], immunoglob-

ulin kappa light chain locus [574], breast cancer associated gene 1 (BRCA1) [575, 576], X-linked interleukin-2 receptor gamma (Il2rg) chain gene [577], low-density lipoprotein receptor (LDLR) [523, 578, 579], sialoadhesin gene [580], CMP-Neu5Ac hydroxylase [581], recombination-activating genes 1 and 2 (RAG1, RAG2) [582] and growth hormone receptor (GHR) [583].

SCNT was also performed with less differentiated mesenchymal stem cells (MSCs) hypothesised to increase cloning efficiency. Compared to fibroblasts these cells doubled the embryo blastocyst development [584] and were successfully used to generate gene targeted live pigs with both a latent mutant $p53^{R167H}$ [585] and $Kras^{G12D}$ [586], a mutant adenomatous polyposis coli (APC^{1311}) [587] and a transgenic ROSA26 allele [588]. Primary porcine kidney cells (PKCs) revealed a comparable increase in blastocyst rate after SCNT and exhibited higher proliferation rates than porcine fetal fibroblasts [589]. Furthermore, porcine liver-derived cells were shown to be suitable for SCNT [590, 558]. Additionally, pigs were also cloned from induced pluripotent stem cells (iPSCs) [591]. Unfortunately, validated porcine embryonic cell lines have not been established to date [592].

1.6 Aim of this work

The aim of this work was the generation of a porcine model for atherosclerosis. For acceleration and worsening of pathogenesis, the two genes apolipoprotein E (APOE) and LDL receptor (LDLR) were to be disrupted by gene targeting. For cell imaging during atherogenesis, the reporter gene enhanced green fluorescent protein (EGFP) driven by the cell-specific porcine fractalkine receptor (CX3CR1) promoter was to be placed at ROSA26 genomic locus. Gene knockouts and transgene placement should be established by gene targeting strategies based on homologous recombination of promoter-trap vectors. For this, gene targeting was primarily to be optimised or alternatively be mediated by transcription activator-like effector nucleases (TALENs) in combination with donor plasmids inducing double strand breaks (DSBs) and subsequent homology-directed repair (HDR). All transfections were to be performed in porcine adipose tissue-derived mesenchymal stem cells (pADMSCs) proven to efficiently produce healthy offspring after somatic cell nuclear transfer (SCNT). The transfected cells were to be analysed genotypically. To evaluate the predisposition of atherosclerosis-related diseases and complications, the used cells additionally should be screened for single nucleotide polymorphisms and mutations within the three genes APOE, LDLR and CX3CR1. If possible, the cloned animals were to be validated genotypically and furthermore be analysed phenotypically.

CHAPTER 2

Material

2.1 Equipment

Balances	
Analytical balance 440-33N	Kern, Balingen-Frommen, GER
Analytical balance APX-1502	Denver Instruments, Göttingen, GER
Analytical balance EMB 2200-2	Kern, Balingen-Frommen, GER
Analytical balance PI-214	Denver Instruments, Goettingen, GER
Blood chemistry analyser	
Piccolo Xpress Chemistry Analyser	Abaxis Europe, Darmstadt, GER
Centrifuges	
Centrifuge 5810	Eppendorf, Hamburg, GER
Laboratory clinical centrifuge 3-16	Sigma, Osterode am Harz, GER
Laboratory micro centrifuge 1-15	Sigma, Osterode am Harz, GER
Micro centrifuge Mikro 200	Hettich, Tuttlingen, GER
Micro centrifuge Minispin	Eppendorf, Hamburg, GER
Mini centrifuge GMC-060	LMS, Tokyo, JPN
Refrigerated laboratory centrifuge 4K15C	Sigma, Osterode am Harz, GER
Refrigerated laboratory mini centrifuge 1-15K	Sigma, Osterode am Harz, GER
Savant DNA110 SpeedVac Concentrator	Thermo Fisher Scientific, Dreieich, GER
Cooling devices	
Freezer (-20°C)	Liebherr, Ochsenhausen, GER
Freezer Thermo Forma (-80°C)	Thermo Electron, Karlsruhe, GER
Freezing container Mr. Frosty	Nalgene, Rochester (NY), USA

Fridge (4°C)	Siemens, München, GER
Iceflaker	Eurfrigor, Villa Cortese (MI), ITA
Water bath RMS6	Lauda-Brinkmann, Delran (NJ), USA
Counting devices	
Automated cell counter Invitrogen Countess	Life Technologies, Darmstadt, GER
Counting chamber Neubauer	Hecht-Assistent, Sondheim/Rhön, GER
Electrophoresis devices	
Maxi gel system Perfect Blue 41-2325	Peqlab, Erlangen, GER
Midi gel system Perfect Blue 40-2314N	Peqlab, Erlangen, GER
Mini gel system Perfect Blue 40-0708	Peqlab, Erlangen, GER
Mini gel system Perfect Blue 40-1214	Peqlab, Erlangen, GER
Submarine gel system Classic CSSU2020	Thermo Electron, Karlsruhe, GER
Submarine gel system Primo CSSU78	Thermo Electron, Karlsruhe, GER
Electroporator	
Multiporator	Eppendorf, Hamburg, GER
Gel documentation devices	
Digital graphic printer UP-D895MD	Sony Europe Limited, Berlin, GER
Gel imaging system GeneGenius	Syngene Europe, Cambridge, UK
UV-transilluminator NU72KM	Benda, Wiesloch, GER
Heating device	
Aluminium hot plate stirrer ARE	VELP Scientifica, Usmate (MB), ITA
Heating block VLM 2Q	Gefran, Seligenstadt, GER
Hybrisisation oven Hybaid Shake 'n' Stack	Thermo Fisher Scientific, Dreieich, GER
Incubator BD 240	Binder, Tuttlingen, GER
Microwave MDA	MHA, Barsbüttel, GER
Incubators	
Forma Orbital Shaker 420	Thermo Electron, Karlsruhe, GER
Forma Series II Water Jacketed CO_2 Incubator (N_2)	Thermo Electron, Karlsruhe, GER
Forma Steri-Cycle CO_2 Incubator	Thermo Electron, Karlsruhe, GER
Incubator BD 115	Binder, Tuttlingen, GER
X-ray clip cassette CVE-blank	Rego X-Ray, Augsburg, GER
Laminar airflow cabinet	
HERAsafe HSP	Heraeus Instruments, München, GER
Luminometer	
Glomax 20/20 Luminometer	Promega, Mannheim, GER
Microscopes	
Axiovert 25	Zeiss, Oberkochen, GER
Axiovert 40 CFL	Zeiss, Oberkochen, GER
Axiovert 200M	Zeiss, Oberkochen, GER

PCR devices	
Applied Biosystems 7500 Fast Real-Time PCR System	Life Technologies, Darmstadt, GER
Thermal Cycler DNA Engine Dyad PTC 220	Bio-Rad Laboratories, München, GER
Photometers	
BioPhotometer 6131	Eppendorf, Hamburg, GER
NanoDrop Lite Spectrophotometer	Thermo Fisher Scientific, Dreieich, GER
pH meter	
Cyberscan pH 510	Eutech Instruments, SIN
Pipettes	
Pipette M10	Sartorius, Göttingen, GER
Pipetus Reddot	Hirschmann, Eberstadt, GER
Rainin Pipet-Lite LTS (2, 20, 200, 1000μl)	Mettler Toledo, Giessen, GER
Rainin Pipet-Lite LTS (8 channels, 20–200μl)	Mettler Toledo, Giessen, GER
Pipetman P20, P200, P1000	Gilson, Bad Camberg, GER
Power supplies	
Owl EC-105	Thermo Fisher Scientific, Dreieich, GER
PowerPac 300	Bio-Rad Laboratories, München, GER
Shaker and vortex mixer	
Minishaker MS2	IKA Werke, Staufen, GER
Unitwist 3-D rocker shaker	Uniequip, Planegg, GER
Vortex-Genie 2	Scientific Industries, New York, USA
Vortex Mixer Classic	VELP Scientifica, Usmate (MB), ITA
Water baths	
Thermolab shaking water bath 1086	GFL, Burgwedel, GER
Water bath T	Lauda-Brinkmann, Delran (NJ), USA
Water bath WB 14	Memmert, Schwabach, GER

2.2 Consumables

0.45μm sterile filters	Brand, Wertheim, GER
0.5, 1.5, 2.0ml microcentrifuge tubes	Brand, Wertheim, GER
1, 2, 5, 10, 25ml plastic stripettes	Corning, New York, USA
10cm Petri dishes	Brand, Wertheim, GER
14ml round-bottom tubes	Becton Dickinson, Heidelberg, GER
15, 50ml centrifuge tubes	Corning, New York, USA
150mm cell culture dishes	Corning, New York, USA
2, 20, 200, 1000μl filter pipette tips	Fisher Scientific, Schwerte, GER

2, 20, 200, 1000μl filter pipette tips	Mettler Toledo, Giessen, GER
2, 20, 200, 1000μl pipette tips	Brand, Wertheim, GER
2, 20, 200, 1000μl pipette tips	Mettler Toledo, Giessen, GER
2ml cryogenic vials	Corning, New York, USA
20ml syringes	Becton Dickinson, Heidelberg, GER
50, 100, 1000, 2000ml graduated cylinders	Brand, Wertheim, GER
6, 12, 24 well cell culture plates	Corning, New York, USA
Applied Biosystems Optical adhesive covers	Life Technologies, Darmstadt, GER
Applied Biosystems Fast optical 96 well reaction plates	Life Technologies, Darmstadt, GER
EDTA monovettes	Sarstedt, Nümbrecht, GER
Electroporation cuvettes (2, 4mm)	Peqlab, Erlangen, GER
Filter paper	Bio-Rad Laboratories, München, GER
Invitrogen Countess cell counting chamber slides	Life Technologies, Darmstadt, GER
Laboratory glassware	Marienfeld, Lauda-Königshofen, GER
Lithium-heparin monovettes	Sarstedt, Nümbrecht, GER
Positively charged nylon membrane Amersham Hybond-N+	GE Healthcare Europe, Freiburg, GER
T25, T75, T150 cell culture flasks	Corning, New York, USA
UV cuvettes	Eppendorf, Hamburg, GER
X-ray film	Agfa HealthCare, Bonn, GER

2.3 Chemicals and solutions

Acetic acid	AppliChem, Darmstadt, GER
Acetone	Sigma-Aldrich, Steinheim, GER
Accutase	Sigma, Steinheim, GER
Agarose	Sigma, Steinheim, GER
Agarose LE	Genaxxon Bioscience, Ulm, GER
Ambion Trizol reagent	Life Technologies, Darmstadt, GER
Amphotericin B	Sigma, Steinheim, GER
Ampicillin	Carl Roth, Karlsruhe, GER
β-mercapto ethanol	Sigma, Steinheim, GER
Blasticidin S	InvivoGen Europe, Toulouse, FRA
Blocking reagent	Roche Diagnostics, Mannheim, GER
Boric acid	Sigma, Steinheim, GER
Bromphenol blue	Sigma-Aldrich, Steinheim, GER
Cell culture grade H_2O	PAA, Pasching, AUT
Chloramphenicol	Sigma, Steinheim, GER

Chlorophorm	Sigma, Steinheim, GER
Chlorophorm	AppliChem, Darmstadt, GER
Collagenase I	Serva, Heidelberg, GER
Complete RPMI	Sigma, Steinheim, GER
Cyclic AMP (Dibutyryladenosine cyclic monophosphate)	Sigma, Steinheim, GER
Developer solution	Calbe Chemie, Calbe, GER
Difco LB Agar	Becton Dickinson, Heidelberg, GER
Difco LB Base, Miller	Becton Dickinson, Heidelberg, GER
DIG easy Hyb buffer	Roche Diagnostics, Mannheim, GER
DMEM (Dulbecco's Modified Eagle Medium) high glucose	Sigma, Steinheim, GER
DMSO (Dimethyl sulphoxide)	AppliChem, Darmstadt, GER
EDTA (Ethylenediaminetetraacetic acid)	Sigma, Steinheim, GER
Ethanol absolute	Riedel-de-Haen, Seelze, GER
Ethanol absolute	AppliChem, Darmstadt, GER
Ethidium bromide solution ($10\frac{mg}{ml}$)	Sigma, Steinheim, GER
FCS (Foetal calf serum)	PAA, Pasching, AUT
FGF-2 (Fibroblast growth factor 2)	PromoCell, Heidelberg, GER
Fixer solution	Calbe Chemie, Calbe, GER
Formaldehyde	Sigma, Steinheim, GER
G418 (Geneticin)	PAA, Pasching, AUT
Gibco Advanced DMEM (Dulbecco's Modified Eagle Medium)	Life Technologies, Darmstadt, GER
Gibco GlutaMAX	Life Technologies, Darmstadt, GER
Glacial acetic acid	Fluka, Seelze, GER
Glycerol	Carl Roth, Karlsruhe, GER
Glycerol	AppliChem, Darmstadt, GER
HBSS (Hank's Balanced Salt Solution)	BioChrom, Berlin, GER
Hydrochloric acid	J.T.Baker, Deventer, NED
Igepal CA-630	Sigma, Steinheim, GER
Invitrogen Trypan blue solution	Life Technologies, Darmstadt, GER
Isopropanol	Carl Roth, Karlsruhe, GER
Isopropanol	AppliChem, Darmstadt, GER
Kanamycin	Omni Life Science, East Taunton (MA), USA
LSM 1077 (Lymphocyte separation medium $1.077\frac{g}{l}$)	PAA, Pasching, AUT
Magnesium chloride	Merck Millipore, Darmstadt, GER
Maleic acid	Carl Roth, Karlsruhe, GER

Non-essential amino acids	Sigma, Steinheim, GER
PBS (Phosphate buffered saline)	Sigma, Steinheim, GER
Penicillin/Streptomycin	Sigma, Steinheim, GER
Phenol-chlorophorm-isoamyl alcohol (25:24:1)	Sigma, Steinheim, GER
Phenol-chlorophorm-isoamyl alcohol (25:24:1)	AppliChem, Darmstadt, GER
Potassium chloride	Merck Millipore, Darmstadt, GER
Refined cocos oil	Vandemoortele Lipids, Dresden, GER
Retinoic acid (All-trans-retinoic acid)	Sigma, Steinheim, GER
Saline-sodium citrate buffer	Sigma, Steinheim, GER
SDS (Sodium dodecyl sulphate)	Sigma, Steinheim, GER
Silicone grease	GE Bayer Silicones, Erkrath, GER
Sodium acetate	Carl Roth, Karlsruhe, GER
Sodium acetate	AppliChem, Darmstadt, GER
Sodium chloride	AppliChem, Darmstadt, GER
Sodium hydroxide pellets	Sigma, Steinheim, GER
Sodium pyruvate	PAA, Pasching, AUT
Sucrose	Sigma, Steinheim, GER
Sudan IV	Sigma, Steinheim, GER
Tris	AppliChem, Darmstadt, GER
Trizma base	Sigma, Steinheim, GER
Trizma hydrochloride	Sigma, Steinheim, GER
Tween 20	Sigma, Steinheim, GER
Trypsin	PAA, Pasching, AUT

2.4 Custom solutions and buffers

Bacteria culture	
LB-agar	4% (w/v) Difco LB Agar
LB-medium	2.5% (w/v) Difco LB Base, Miller
Cell culture	
Complete RPMI-10/20 medium	Complete RPMI, 10%/20% FCS, 100$\frac{U}{ml}$ Penicillin, 100$\frac{\mu g}{ml}$ Streptomycin, 2.5$\frac{\mu g}{ml}$ Amphotericin B)
Expression upregulation medium	MSC medium; 1.0mM cyclic AMP, 1.0μM retinoic acid (filtered)
Freezing medium	20% MSC medium, 70% FCS; 10% DMSO (filtered)
HEK medium	DMEM high glucose, 10% FCS; 2.0mM Gibco GlutaMAX, 0.1mM non-essential amino acids (filtered)

KDNF medium	DMEM high glucose, 10% FCS; 2.0mM Gibco GlutaMAX, 0.1mM non-essential amino acids, 1mM sodium pyruvate (filtered)
Low TE buffer	10mM Tris, 0.1mM EDTA
MSC medium	Gibco Advanced DMEM, 10% FCS, $5\frac{\mu g}{ml}$ FGF-2; 2.0mM Gibco GlutaMAX, 0.1mM non-essential amino acids, 50μM β-mercapto ethanol (filtered)
Starvation medium	Gibco Advanced DMEM, 0.5% FCS, $5\frac{\mu g}{ml}$ FGF-2; 2.0mM Gibco GlutaMAX, 0.1mM non-essential amino acids, 50μM β-mercapto ethanol (filtered)
Gel electrophoresis	
100bp ladder	$\frac{1}{6}$ volume 100bp DNA ladder, $\frac{1}{3}$ volume 5×loading dye
10×TBE buffer	0.9M Trizma base, 0.2M EDTA, 0.9M boric acid
1kb ladder	$\frac{1}{6}$ volume 1kb DNA ladder, $\frac{1}{3}$ volume 5×loading dye
50×TAE buffer	1.0M Trizma base, 50mM EDTA, 2.0M glacial acetic acid (pH 8.0)
5×loading dye	50% (v/v) glycerol, 0.2M EDTA, tip of spatula bromphenol blue
Low MW ladder	$\frac{1}{6}$ volume Low Molecular Weight DNA ladder, $\frac{1}{3}$ volume 5×loading dye
Genomic DNA isolation	
Igepal lysis buffer	50mM potassium chloride, 1.5mM magnesium chloride, 10mM Trizma hydrochloride (pH 8.0), 0,5% (v/v) Igepal CA-630, 0.5% (v/v) Tween 20
Lysis buffer	80mM Trizma hydrochloride (pH 7.4), 0.8% SDS, 170mM EDTA, 170mM sodium chloride
Plasmid DNA isolation	
Lysis solution II	0.2M sodium hydroxide, 1% (w/v) SDS
Neutralisation solution III	3.0M sodium acetate (pH 4.8)
Resuspension solution I	5mM sucrose, 10mM EDTA, 25mM Tris (pH 8.0)
Southern blot	
20×SSC buffer	3.0M sodium chloride, 0.3M sodium citrate, adjust to pH 7.0 with 1.0M hydrochloric acid
Blocking solution	1% (v/v) blocking reagent in maleic acid buffer
Denaturation buffer	0.5M sodium hydroxide, 1.5M sodium chloride
Depurination buffer	250mM hydrochloric acid
Detection buffer	0.1M Trizma hydrochloride (pH 9.5), 0.1M sodium chloride

High-stringency buffer	0.1×SSC, 0.1% (w/v) SDS
Low-stringency buffer	2×SSC, 0.1% (w/v) SDS
Maleic acid buffer	0.1M maleic acid, 0.15M sodium chloride, adjust to pH 7.5 with sodium hydroxide
Neutralisation buffer	0.5M Trizma hydrochloride (pH 7.5), 1.5M sodium chloride
Southern blot ladder	$\frac{1}{6}$ volume gel loading dye, blue (6×), $\frac{1}{16}$ volume DNA Molecular Weight Marker VII, DIG-labeled
Washing buffer	0.003% (v/v) Tween 20 in maleic acid buffer
Staining	
Decolorising solution	80% ethanol
Sudan IV staining solution	50% acetone, 35% ethanol, 5g Sudan IV

2.5 Enzymes, kits and molecular markers

Enzymes	
Anti-Dig-AP-Fab-Fragment	Roche Diagnostics, Mannheim, GER
CDP Star	Roche Diagnostics, Mannheim, GER
CIP	New England Biolabs, Frankfurt, GER
Deoxynucleotide (dNTP) Solution Mix (10mM each nt)	New England Biolabs, Frankfurt, GER
Digoxigenin-11-dUTP	Roche Diagnostics, Mannheim, GER
DNA Polymerase I, Large (Klenow) Fragment	New England Biolabs, Frankfurt, GER
Proteinase K	Sigma-Aldrich, Hamburg, GER
Restriction endonucleases	New England Biolabs, Frankfurt, GER
RNase	Sigma-Aldrich, Hamburg, GER
T4 DNA ligase	New England Biolabs, Frankfurt, GER
Kits	
Ambion TURBO DNA-free Kit	Life Technologies, Darmstadt, GER
Applied Biosystems SYBR Green PCR Master Mix	Life Technologies, Darmstadt, GER
CloneJET PCR Cloning Kit	Thermo Scientific, Schwerte, GER
GenElute Mammalian Genomic DNA Miniprep Kit	Sigma-Aldrich, Hamburg, GER
GoTaq Hot Start Polymerase	Promega, Mannheim, GER
Herculase II Fusion Enzyme with dNTPs Combo	Agilent Technologies, Böblingen, GER
High Pure RNA Isolation Kit	Roche Diagnostics, Mannheim, GER
innuPREP RNA Mini Kit	Analytic Jena, Jena, GER

Invitrogen SuperScript III One-Step RT-PCR System with Platinum Taq DNA Polymerase	Life Technologies, Darmstadt, GER
Invitrogen SuperScript III Reverse Transcriptase	Life Technologies, Darmstadt, GER
Nanofectin Kit	PAA, Pasching, AUT
NucleoBond Xtra Midi Kit	Macherey-Nagel, Düren, GER
PCR Extender System	5Prime, Hilden, GER
pGEM-T Easy Vector System	Promega, Mannheim, GER
Piccolo Xpress Lipid Panel Plus	Abaxis Europe, Darmstadt, GER
QIAamp RNA Blood Mini Kit	Qiagen, Hilden, GER
Stemfect RNA Transfection Kit	Stemgent, Cambridge (MA), USA
SurePrep RNA/DNA/Protein Purification Kit	Fisher Scientific, Schwerte, GER
Wizard SV Gel and PCR Clean-Up System	Promega, Mannheim, GER
Molecular markers	
1bk DNA ladder	New England Biolabs, Frankfurt, GER
100bp DNA ladder	New England Biolabs, Frankfurt, GER
DNA Molecular Weight Marker VII, DIG-labeled	Roche Diagnostics, Mannheim, GER
Gel loading dye, blue (6×)	New England Biolabs, Frankfurt, GER
Low Molecular Weight DNA ladder	New England Biolabs, Frankfurt, GER
RiboRuler High Range RNA Ladder	Thermo Scientific, Schwerte, GER
RNA loading dye (2×)	New England Biolabs, Frankfurt, GER

2.6 Bacteria, Cells, DNA and RNA

BAC DNA	
BAC CH242-142P24 (LDLR, duroc breed)	Children's Hospital Ookland Research Institute (CHORI), Oakland (CA), USA
BAC CH242-480J10 (APOE, duroc breed)	Children's Hospital Ookland Research Institute (CHORI), Oakland (CA), USA
Bacteria	
E. coli K12 ER2925 (Dam^-, Dcm^-)	New England Biolabs, Frankfurt, GER
Invitrogen ElectroMAX DH10B Cells (E. coli)	Life Technologies, Darmstadt, GER
Cells	
Human embryonic kidney (HEK293) cells	Chair of Nutrition and Immunology, Freising, GER

Porcine adipose tissue-derived mesenchymal stem cells (pADMSCs)	Isolated from German Landrace
Genomic DNA	
Porcine genomic DNA	Isolated from German Landrace
Porcine genomic DNA of fetus #4	Shun Li, Chair of Livestock Biotechnology, Freising, GER
RNA	
Porcine adipose tissue-derived mesenchymal stem cells (pADMSCs)-derived RNA	Isolated from German Landrace
Porcine brain tissue-derived RNA	Isolated from German Landrace
Porcine ear tissue-derived RNA	Isolated from German Landrace
Porcine ear fibroblast-derived RNA	Isolated from German Landrace
Porcine kidney fibroblasts-derived RNA	Isolated from German Landrace
Porcine kidney tissue-derived RNA	Isolated from German Landrace
Porcine lung tissue-derived RNA	Isolated from German Landrace

2.7 Cloned plasmids

ApoE project	
ApoE Donor IRES (Neo)	
ApoE Donor PGK (Neo)	
ApoE Donor IRES CCN (Neo)	
ApoE Donor PGK CCN (Neo)	
ApoE reporter	German Research Center for Environmental
pCMVTALENLucDuplirep	Health, Helmholtz Zentrum München, GER
ApoE reporter + TALEN	
ApoE SV (IRES Neo)	
ApoE SV IRES (Neo)	
ApoE SV PGK (Neo)	
ApoE TV1 (IRES Neo)	
ApoE TV2 (IRES Neo)	
ApoE TV3 (IRES Neo)	
ApoE TV4 (IRES Neo CCN)	
loxIRESBSpolyAlox	Marlene Edlinger, Chair of Livestock Biotechnology, Freising, GER
psiCHECK 2	
psiCHECK 2 (pSL1180 + psiCHECK XhoI$^-$)	Tatiana Flisikowska, Chair of Livestock Biotechnology, Freising, GER

pSLCAGGSCherryNLSfor	Tatiana Flisikowska, Chair of Livestock Biotechnology, Freising, GER
pSLIRESneo	
SsApoE TAL1/2	German Research Center for Environmental Health, Helmholtz Zentrum München, GER
CX3CR1 project	
CX3CR1 TV (SA BS)	
CX3CR1 TV2 (SA Neo)	
pGFP EGFP1	
psiCheckCX3CR1	
pSL1180SAneopA	Erica Schulze, Chair of Livestock Biotechnology, Freising, GER
Rosa26TomGFP	Shun Li, Chair of Livestock Biotechnology, Freising, GER
LDLR project	
LDLR SV (IRES BS)	
LDLR SV2 (IRES Neo)	
LDLR TV (IRES BS)	
LDLR TV2 (IRES Neo)	

2.8 Primers

APOE primers	
ApoE F1	CTGTCTGACCAAGTGCAGGA (20)
ApoE F4	CATCCTCATTGCACAAATCG (20)
ApoE F13	TCCTCTACTTGGCCTGTGCT (20)
ApoE F17	GGCTTGGATCTAGTGTTTCTG (21)
ApoE mut F1	CAGGCGCGCCTGTCCAAGGAG (21)
ApoE mut R1	CAATCGGCCCTGCTCCACCAG (21)
ApoE R1	CACCTCGCTGCGGTAGAG (18)
ApoE R4	AGCTGCTCACGCATCTCAT (19)
ApoE recSA R	TCCAAGCTCACGTTCTTCCT (20)
ApoE TAL endo R1	TCCTGCACTTGGTCAGACAG (20)
ApoE TAL targ F1	GGAAGAACGTGAGCTTGGAG (20)
ApoE TAL targ R1	TCGTCCTGCAGTTCATTCAG (20)
ApoE TALEN F1	TGTCTGACCAAGTGCAGGAG (20)
ApoE TALEN F2	AGCGTGCACGGAGCACACAA (20)
ApoE TALEN R1	ACCAAGAGGGCAGCTAAGG (19)
ApoE TALEN R2	CCCAGACCCCCAAGAGTTGGC (21)
ApoE targ F2	GTTACTGGGTGAGAGACACCTCTT (24)

ApoE targ F3	AAAGGATCTGCTCGGGAAAT (20)
ApoE targ R2	GGCGGATCCATAACTTCGTATAAT (24)
cMyc F	GGCTTTCTCTGACTCGCTGT (20)
cMyc R	GCGACAGGGAAAAGTGTCTC (20)
FokI F	CACCTGGGCGGATCTCGCAA (20)
FokI R	GCACGGCGCCATTGCAGTTT (20)
GAPDH F	TCCCACGGCACAGTCAA (17)
GAPDH R	GCAGGTCAGGTCCACAACC (19)
Kras F	CATTTCGGACTGGGAGCTA (19)
Kras R	TCCTGAGCCTGTTTTGTGTC (20)
pHPRT F1	GTGATAGATCCATTCCTATGACTGTAGA (28)
pHPRT R1	TGAGAGATCATCTCCACCAATTACTT (26)
CX3CR1 primers	
CD14 F1	GCGGTTAAAGGAGCCACAG (19)
CD14 R1	TCGTCTATTTGGCAGGGCTC (20)
CMVpA R	GGACAAACCACAACTAGAATGC (23)
CX3CR1 endo R1	GTTTGCACAGGAAACCCAAG (20)
CX3CR1 LR F1	CTAGGCTCCCAGGTTTGTGA (20)
CX3CR1 poly F1	TCATGTGGACACTGCTTTCC (20)
CX3CR1 poly R1	GGGTTGCTTTGGAGTATTGG (20)
CX3CR1 PR F1	GGGGAACTCCTCCTCTGTTC (20)
CX3CR1 PR R1	GGAGGGAACTTCTGGATGTG (20)
CX3CR1 RT F1	TAGAGTCTTCGCAGGACAGG (20)
CX3CR1 RT R1	CCAGACACTGAGGCTGATGA (20)
CX3CR1 qPCR R1	CACGATGTCTCCCATGTCAC (20)
CX3CR1 seq F1	ATGCTTCTGATTTGGTGGCC (20)
CX3CR1 seq R1	AGGTTTTGTCTCTCTGCCAAA (21)
CX3CR1 targ F1	TCTGCTGCCTCCTTTTCCTA (20)
CX3CR1 targ R1	GAAAGACCGCGAAGAGTTTG (20)
EGFP qPCR F1	CTTCTTCAAGTCCGCCATGC (20)
EGFP qPCR R1	TCCTTGAAGTCGATGCCCTT (20)
TBP F	AACAGTTCAGTAGTTATGAGCCAGA (25)
TBP R	AGATGTTCTCAAACGCTTCG (20)
LDLR primers	
BS probe F	ATGGCCAAGCCTTTGTCTC (19)
BS probe R	TAGCCCTCCCACACATAACC (20)
CMAH KV2r	CTTCACGACATTCAACAGACCTT (23)
LDLR E3 R1	AGCCATTCTCGCAGTCCTG (19)
LDLR endo F2	TTACCAAGCCTGACGTGTCC (20)
LDLR endo F4	CCATCTACTTCCTACCTCAGTTCAA (25)

LDLR F2	GGCTGCTATTGGGCACTACT (20)
LDLR F3	TTGGACCAGGCATTAGATCC (20)
LDLR F4	AATTCCCTATGTGGCAGGTG (20)
LDLR F5	TGAGTCTTGGAGGTGTGACG (20)
LDLR F8	GCAGTAGCTCCGATTCAACC (20)
LDLR F9 (AflIII)	GGGCTTAAGCAGGCTTCCCTCATTCTT (27)
LDLR I5 F1	GACGTGCTCCCAAGATGAGT (20)
LDLR I5 F2	TGAAAGAGCAACGGCTACAA (20)
LDLR I5 F3	TGGCCACGTGTAGTTAGTGG (20)
LDLR I5 R1	TGAGCACTGGAACTCGTCAG (20)
LDLR I5 R2	CAGGGCCATAGCAGTGAAAT (20)
LDLR I5 R3	TCGACAGAACATTGTAAATCGAC (23)
LDLR mut F1	GTGGATCCCTGTGCAAACTC (20)
LDLR qPCR F1	AGCAACAACCCCTGCTCA (18)
LDLR qPCR R1	TGAGCACTGGAACTCGTCAG (20)
LDLR R2	TAGGCCAGCGGCTACTACTC (20)
LDLR R3	CACAAAGGGAACTCCGAAGA (20)
LDLR R4	CTGGGTCTGGTCAGGTGTG (19)
LDLR R5	CGTCAGACTTGTCCTTGCAG (20)
LDLR R6	CCTGTTTTTGCTTTGTTTTGC (21)
LDLR R7	CAGGGCCATAGCAGTGAAAT (20)
LDLR RT F1	GAGGCTGGAAGCATGAAGTC (20)
LDLR RT R1	TGGGGATGCTGTTGATTGTA (20)
LDLR seq F1	AAACACAAAAACACAAAAGGATTCT (25)
LDLR site1 F1	ATCACAAACGGCATGATGAA (20)
LDLR site1 R1	GCGTGTTACGGTGAAAACCT (20)
LDLR site2 F2	CGGGATCAAAAACGTATGCT (20)
LDLR site2 R2	CAATGCCTGCCGTATATCCT (20)
LDLR TALEN F1	AGGAACTCAATCCTCCACGA (20)
LDLR TALEN F2	AGGGGAGCTCGCTACTCACT (20)
LDLR TALEN R1	AATACCTTCTCCGCCCACAT (20)
LDLR TALEN R2	CATGCCTTCCCATCTGAAAC (20)
LDLR targ F1	ATTGCATCGCATTGTCTGAG (20)
LDLR targ F2	GCATTGTCTGAGTAGGTGTCATTCT (25)
LDLR targ R1	TGTTTTGGGGCCATGTCTAT (20)
LDLR targ R2	AGAATCCTTTTGTGTTTTTGTGTTT (25)
LDLR targ2 F1	ATATATAGGGCCCGGAATTGTTGT (24)
Sp6 R	TATTTAGGTGACACTATAG (19)
T7 F	TAATACGACTCACTATAGG (19)
targBS R	ACATTGACACCAGTGAAGATGC (22)

All custom and random hexamer primers were derived from *Eurofins Genomics, Ebersberg, GER* as "unmodified DNA oligos" with salt free purification and 0.01μmol synthesis scale.

2.9 Databases and software

Databases	
CENSOR Repeat Screening	https://www.ebi.ac.uk/Tools/so/censor/
ClustalW2 Multiple Sequence Alignment	https://www.ebi.ac.uk/Tools/msa/clustalw2/
Ensemble Genome Browser	www.ensemble.org
ExPASy Translate Tool	web.expasy.org/translate/
GeneCards Human Gene Compendium	www.genecards.org
NCBI BLAST	blast.ncbi.nlm.nih.gov/Blast.cgi
NCBI Primer-BLAST	blast.ncbi.nlm.nih.gov/tools/primer-blast/
NEBcutter2	tools.neb.com/NEBcutter2/index.php
NEB Enzyme Finder	https://www.neb.com/tools-and-resources/interactive-tool/enzyme-finder
Primer3web	primer3.ut.ee
Search for promoters and functional motifs	linux1.softberry.com/berry.phtml?topic=index&group=programs&subgroup=promoter
Software	
Applied Biosystems 7500 Software	Life Technologies, Darmstadt, GER
Axiovision	Zeiss, Oberkochen, GER
Excel	Microsoft Deutschland, Unterschleissheim, GER
FinchTV	Geospiza, Seattle (WA), USA
GeneSnap	Syngene Europe, Cambridge, UK
ImageJ	National Institutes of Health, Bethesda (MD), USA
StatPlus	AnalystSoft, Alexandria (VA), USA
Vector NTI	Life Technologies, Darmstadt, GER

CHAPTER 3

Methods

3.1 Bacteria culture

Preferably, bacteria were cultured at 37°C and handling was carried out in laminar airflow cabinet. Exclusively for generation of DNA to be digested with Dam- or Dcm-sensitive restriction enzyme *E. coli K12 ER2925 (New England Biolabs)* were used.

3.1.1 Transformation of bacteria

For transformation of electro-competent bacteria (*E. coli* DH10B and ER2925) by electroporation, 2mm cuvettes, electroporator batch and ligation reactions were pre-cooled on ice. 50μl DH10B suspension were thawed on ice and 2–3μl ligation reaction were added. Suspension was directly transferred into cuvette. Electrodes were dried and cuvette was gently tapped to remove possibly air bubbles in suspension. Transformation was initialised by pulsing at 2500V for 5ms. Immediately, bacteria suspension was transferred into 1ml pre-warmed and antibiotic free LB-medium and recovered for 30–60min in orbital shaker. Subsequently, 20 and 200μl were plated on LB-agar plates containing respective antibiotics (100$\frac{\mu g}{ml}$ Ampicillin, 30$\frac{\mu g}{ml}$ Kanamycin).

3.1.2 Cultivation of bacteria

Bacteria (*E. coli* DH10B and ER2925) were either cultured as suspension in LB-medium or as colonies on LB-agar plates. For positive selection of bacteria containing low-copy BAC or high-copy plasmid, respective antibiotics (100μg/ml Ampicillin, 12.5μg/ml Chloramphenicol or 30$\frac{\mu g}{ml}$ Kanamycin) were used. Bacteria with BAC were initially streaked from LB-agar stab culture to single colonies. Transformed bacteria with high-copy plasmid were plated in volumes of 20 and 200μl on agar plates. For miniprep, single bacteria clones

from agar plate were picked into 5ml LB-medium. For midiprep of high-copy plasmid, either 1ml bacteria pre-culture or 50μl of glycerol stock were inoculated into 150ml LB-medium. For low-copy BAC, 500ml LB-medium were inoculated. Over night incubation of agar plates was performed in incubator, suspension cultures in orbital shaker at 230rpm, respectively. Low-copy BAC suspension cultures were incubated at 32°C for 24h.

3.1.3 Cryo-preservation of bacteria

For long-term storage of bacteria, 500μl of suspension culture in LB-medium was mixed rapidly with 500μl of sterile absolute glycerol and stored at -80°C.

3.2 Cell culture

Generally, eukaryotic cells were cultured in 37°C, 5% CO_2 humidified incubator. Cells were checked daily under microscope and only handled in laminar airflow cabinet using sterile material and filtered pipette tips. Respective media (HEK medium, MSC medium, KDNF medium, complete RPMI-10/20 media, expression upregulation medium) and Accutase were always pre-warmed at 37°C. Medium change was performed every second day and reaching 80% confluence cells were washed with PBS at RT and passaged with Accutase. Centrifugation steps were carried out at 320×g for 5min. Prior to clone picking and DNA isolation, certain cell clones were checked for expression of negative selectable marker (mCherry) under fluorescence microscope. Cell clones with positive expression were discarded.

3.2.1 Isolation of porcine cells

Cells were isolated with PBS and media treated with antibiotics and antimycotics (100$\frac{U}{ml}$ Penicillin, 100$\frac{\mu g}{ml}$ Streptomycin and 2.5$\frac{\mu g}{ml}$ Amphotericin B) and were obtained from Landrace pigs either from fat (pADMSCs) or kidney tissue (pKDNFs). For this, pure tissue was washed successively in 80% ethanol and twice in PBS. Tissue was cut into small pieces and digested in 10ml of medium containing 1$\frac{mg}{ml}$ Collagenase I on warm heating magnetic stirrer for 45min. Cell suspension was filtered through a mesh and added to an equal volume of respective medium. After centrifugation, pellet was resuspended in medium and plated on T150 flasks. The next three days medium was changed daily. On fourth day antibiotics and antimycotics were discontinued and cells were washed with pure PBS for further expansion. Additionally, cells were screened for absence of mycoplasmae by PCR.

3.2.2 Antibiotic killing curve

For determination of optimal working concentration of antibiotics, a killing curve of porcine cells visualising their antibiotic sensitivity was performed. Previously, cells were cultured

in 6 wells reaching ∼80% confluence. Subsequently medium supplemented with increasing amounts of appropriate antibiotics were plated on cells. Following concentration ranges were used: 0–1000$\frac{\mu g}{ml}$ for G418 and 0–15$\frac{\mu g}{ml}$ for BS. Cells were cultured for ∼10 days with daily medium change in the first three days. Cells were examined every day for visual toxicity and optimal dose of antibiotic was ascertained. This was the minimal antibiotic concentration, at which cells died off completely after exposure time.

3.2.3 Cryo-preservation of eukaryotic cells

For long-term storage, cells were detached with Accutase. After adding equal volume of medium, cell suspension was centrifuged. Pellet was resuspended in freezing medium and separated in volumes of 1ml aliquots to cryogenic vials. Typically cell concentrations of $1 \times 10^5 - 3 \times 10^5$ cells were chosen. Initially, vials were frozen in freezing device Mr. Frosty to -80°C and finally transferred into -196°C liquid nitrogen.

3.2.4 Thawing of eukaryotic cells

Cells were thawed in 37°C water bath and transferred in 10ml medium. After centrifugation, pellet was resuspended in medium and typically plated on 6 well plate or T25 flask.

3.2.5 Determination of cell concentrations

Cell concentrations were determined either automated by *Invitrogen Countess (Life Technologies)* or manually with the use of Neubauer counting chamber according to manufacturer's instructions. After detaching by Accutase and adding respective medium, 10μl of cell suspension were mixed with an equal volume of *Invitrogen Trypan blue solution (Life Technologies)*. Subsequently, 10μl of stained cell suspension were plated in respective counting chamber. Manual calculus was carried out with the following equation: $C_{cells} = \varnothing N_{cells/grosssquare} \times \frac{10^4}{ml}$.

3.2.6 Transfection of eukaryotic cells by electroporation

For transfection by electroporation, early passage pADMSCs were detached from substrate with Accutase and an equal volume of medium was added. Cell concentration was determined and the calculated volume of cell suspension containing 1×10^6 cells was centrifuged. Pellet was resuspended in 400μl of hypo-osmolar electroporation buffer and mixed gently with 10μg of linearised targeting vector. For co-transfection, 10μg of linearised donor plasmid and additional 2.5μg of each TALEN plasmid were applied. The mixture was transferred into 4mm electroporation cuvette, pulsed at 1200V for 85μs and left at RT for 10min. Subsequently, cell suspension was transferred into two T25 flasks and cultured for two days with daily medium change. Alternatively cells were cultured at 30°C for three days to increase target cleavage by TALENs (cold shock).

3.2.7 Transfection of eukaryotic cells by nanofection

Prior to β-Galactosidase reporter gene assay, HEK293 cells were co-transfected in triplicates by *Nanofectin Kit (PAA)* according to manufacturer's instructions. To increase efficiency of nanofection, cells were cultured in 12 wells with only 1ml medium and transfected with up to 1.8μg plasmid DNA (600ng of each plasmid DNA). 24h after co-transfection additional 1ml medium was added and after 48h reporter gene assay was performed.

For co-transfection of early passage pADMSCs with mRNA in combination with DNA, the *Stemfect RNA Transfection Kit (Stemgent)* was used according to manufacturer's instructions. Differing thereof, assay was scaled down to 12 wells. 1–2h prior to transfection, medium was aspirated and 1ml medium was added to the cells. Amounts of transfection buffer and RNA transfection reagent were decreased to 25μl and 2μl, respectively. To reduce cytotoxicity, finally 400ng of donor plasmid DNA and 200ng of each TALEN mRNA were used to form the transfection complex for 20min. Detailed amounts of all experiments are referred in table 4.3. After 24h, medium was changed and cells were cultured for one more day.

3.2.8 Selection of transfected porcine cells

Transfected cells were detached from T25 flasks and 12 well plate (electroporation and nanofection) by using Accutase. After adding equal volume of medium, cells were split to 150mm cell culture dishes and selected positively in medium supplemented with respective antibiotics ($600\frac{\mu g}{ml}$ G418 for neomycin and $10\frac{\mu g}{ml}$ BS for blasticidin S resistance gene). Typically, 5–6 cell culture dishes were used for electroporation experiment, 2–3 for nanofection experiment. Cell cultivation was kept for $\sim$10 days until single cell clones have developed and non-transfected cells on control plate have died off completely.

To pick single cell clones, medium was aspired and cells were washed gently with PBS. Cloning rings were dipped into silicone grease and placed over single cell clones. A few drops of Accutase were filled into the cloning rings and incubated at 37°C for 2–3min. After adding equal amount of medium, cells were detached by pipetting up and down and transferred into 24 well plates. Successively, single cell clones were expanded on 12 well and 6 well plates.

3.2.9 Serum starvation of porcine cells and nuclear transfer

Prior to nuclear transfer, cells were synchronised in G0/G1 phase by serum starvation. For this, up to three homogeneous gene targeted cell clones were pooled and plated on 12 wells in different amounts ($1 \times 10^3, 5 \times 10^3, 1 \times 10^4$ and 5×10^4 cells). After 24h, cells were washed twice with PBS and cultured in 1ml starvation medium. For animal cloning, 48h later nuclear transfer, after further 24h embryo transfer was carried out by *Chair for Molecular Animal Breeding and Biotechnology (LMU, München, GER).*

3.2.10 Gene expression upregulation experiment

To examine upregulation of apolipoprotein E gene expression different amounts of pADMSCs ($5 \times 10^3, 1 \times 10^4$, 5×10^4 and 1×10^5 cells) were plated on 6 wells and cultured with expression upregulation medium for up to 96h. For relative quantification of gene expression by real time quantitative polymerase chain reaction (section 3.4.4), total RNA was isolated every 24h from 6 well with the use of Trizol as described in section 3.4.1. Control pADMSCs were cultured in MSC medium.

3.2.11 Isolation of porcine monocytes/macrophages

Monocytes and macrophages for hypoxia assay were prepared from whole mononuclear cells isolated from peripheral blood by Ficoll density gradient centrifugation. Whole blood samples were collected with monovettes containing anti-coagulant Lithium-Heparin. 5ml of heparinised blood were diluted with an equal volume of PBS and layered carefully over 3ml of LSM 1077. Subsequently, centrifugation at 18–20°C was performed at 900×g for 30min without brake. After removing the upper layer containing plasma and platelets, the mononuclear cell layer was transferred in new 15ml centrifuge tube. Mononuclear cells were washed successively with ∼3-fold volume of HBSS at 400×g for 10min until most of residual platelets were removed. Alternatively, portions of 2×10^7 cells were resuspended in 2ml of HBSS and layered slowly over 6ml of FCS for centrifugation at 400×g for 5min. For purification of monocytes/macrophages from mononuclear cell population, the pure cell pellets were resuspended in complete RPMI-10 medium and centrifuged at 300×g for 10min. Cells were resuspended in complete RPMI-20 medium to a final concentration of $2 \times 10^6 \frac{cells}{ml}$ and ≤50ml cell suspension were plated on T150 flask. After horizontal incubation of 1–2h, non-adherent lymphocytes were aspirated and adherent monocytes/macrophages were successively rinsed and incubated with complete RPMI-10 medium.

3.2.12 Hypoxia assay

For induction of hypoxia, porcine cells were plated on 6 wells in different amounts ($5 \times 10^3, 1 \times 10^4$, 5×10^4 and 1×10^5 cells) and cultured in a 37°C, 5% CO_2, 1% O_2 humidified incubator. After 48h, cells were compared to respective controls cultured in 21% O_2 under fluorescence microscope for EGFP expression. To quantify gene expressions, total RNA was isolated from cells and qRT-PCR was performed as described in sections 3.4.1 and 3.4.5.

3.3 DNA techniques

Generally, genomic DNA and BAC DNA were stored at 4°C, tissue samples and cell pellets for DNA isolation at -20°C, respectively. DNA fragments for ligation or precipitation were

immediately processed and all reactions were carried out with cell culture grade H_2O.

3.3.1 Polymerase chain reaction

Qualitative amplification of specific DNA sequences was achieved by polymerases featuring high performance diversity. Standard PCR was performed with *GoTaq Hot Start Polymerase (Promega)*.

Generally, DNA for cloning and sequencing was amplified by *PCR Extender System (5Prime)* featuring high extension rate and high proof-reading assisted fidelity. To reduce template DNA damage, the elongation temperature was reduced to 68°C.

For positive screening of single cell clones, 5μl supernatant of Igepal isolation were applied. Especially, for positive screening of LDL receptor targeted cell clones the *Herculase II Fusion Enzyme with dNTPs Combo (Agilent Technologies)* was used. PCR was set up with a final DMSO content of 4% and denaturation temperature of 98°C.

Typically, all kits were performed according to manufacturer's instructions. Table 3.1 refers the used kits, annealing temperatures, primer pairs and PCR product sizes of all PCRs related to the respective result sections.

For validation of PCR products and internal detection of single nucleotide polymorphisms and mutations, restriction enzyme digestion was conducted consistent with common terms in section 3.3.13.

3.3.2 Generation of probe for Southern blot

Experimental probes for Southern blot were generated by labeling PCR using *GoTaq Hot Start Polymerase (Promega)* according to manufacturer's instructions. Probe labeling was carried out in 50μl reaction supplemented with additional 3μl of *Digoxigenin-11-dUTP (Roche Diagnostics)*. To evaluate labeling efficiency, 5μl of labeled and unlabeled PCR product were each run on agarose gel as referred in section 3.3.6. Compared to unlabeled version, the probe should appear significantly longer due to greater molecular weight and slower migration. Efficiently labeled PCR product was purified consistent with section 3.3.7. Primer pair and appropriate annealing temperature are given in table 3.1.

3.3.3 Southern blot

For specific detection of DNA sequence in DNA samples, Southern blot was performed. Therefore, 10μg of genomic DNA were digested with respective restriction enzyme ($5\frac{U}{\mu g}$) for 5h as described commonly in section 3.3.13. Volume was adjusted to $\leq$70μl, supplemented with 5×loading dye and loaded on ethidium bromide free 0.8% 1×TAE agarose gel (150ml). Additionally, 6μl 1kb ladder and 12μl Southern blot ladder were loaded. Agarose gel was run at 100V for 10min, subsequently at 30V over night.

After ∼17h, agarose gel containing 1kb ladder was cut out and stained in ethidium bromide bath for ≥15min. By using a ruler, propagation of 1kb ladder was controlled

Section	Kits	Ta (v/v_{DMSO})	Primer pair	Product sizes
4.1.1	*PCR Extender System*	64°C	ApoE_mut_F1 ApoE_mut_R1	303bp
4.1.5	*GoTaq Hot Start Polymerase*	64°C	ApoE_TAL_targ_F1 ApoE_TAL_targ_R1	2112bp (1827bp) 2059bp (1774pb)
4.1.5	*GoTaq Hot Start Polymerase*	64°C	ApoE_TAL_targ_F1 ApoE_TAL_endo_R1	1305bp
4.1.5	*GoTaq Hot Start Polymerase*	64°C	ApoE_TALEN_F2 ApoE_TALEN_R2	2349pb ≤522bp
4.1.5	*GoTaq Hot Start Polymerase*	57°C	FokI_F FokI_R	313bp
4.2.1	*PCR Extender System*	58°C	LDLR_mut_F1 LDLR_R5	676bp
4.2.4	*Herculase II Fusion Enzyme*	61°C (4%)	LDLR_endo_F4 LDLR_targ_R2	1701bp
4.2.4	*Herculase II Fusion Enzyme*	61°C (4%)	LDLR_targ_F2 LDLR_targ_R2	1832bp (2126bp)
4.2.9	*GoTaq Hot Start Polymerase*	60°C	LDLR_F5 LDLR_R5	1438bp
4.2.9	*GoTaq Hot Start Polymerase*	60°C	LDLR_F5 CMAH_KV2r	1556bp
4.2.9	*GoTaq Hot Start Polymerase* *Digoxigenin-11-dUTP*	58°C	BS_probe_F BS_probe_R	399bp
4.2.9	*PCR Extender System*	62°C	LDLR_I5_F1 LDLR_I5_R1	unknown
4.3.1	*PCR Extender System*	57°C	CX3CR1_poly_F1 CX3CR1_poly_R1	554bp
4.3.4	*PCR Extender System*	61°C	CX3CR1_targ_F1 CX3CR1_endo_R1	3206bp
4.3.4	*PCR Extender System*	65°C	CX3CR1_targ_F1 CX3CR1_targ_R1	2616bp
4.3.6	*GoTaq Hot Start Polymerase*	62°C	CX3CR1_LR_F1 EGFP_qPCR_R1	664bp
4.3.6	*PCR Extender System*	60°C	CX3CR1_LR_F1 CMVpA_R	1210bp

Table 3.1: Overview of PCRs related to the respective result sections with the used kits, annealing temperatures (Ta) and DMSO content (v/v_{DMSO}), primer pairs and PCR product sizes.

by gel imaging system. At sufficient separation of bands amounting the expected DNA fragment, frames and one edge (check mark) of agarose gel were cut. Subsequently, agarose gel was shaken successively in depurination, denaturation and neutralisation buffer for 2×15min, respectively with H_2O washing steps in between. After incubation in 20×SSC buffer for 10min, blot was assembled. For this, a pan containing 2l of 20×SSC buffer was bridged by tissues allowing soaking of blotting buffer. Successively, moisten filter paper (20×SSC), prepared agarose gel, nylon membrane and dry filter paper were put on top of each other without air bubbles. To avoid evapuration of blotting buffer, tissue around the assembled blot was isolated by wrapping film. Finally, a deck of paper towels was placed on blot and weighted by a bottle of water (∼5kg). After 5h, soaked paper towels were exchanged and blotting was arranged over night.

1.5h prior to blot disassembly, soaked paper towels were renewed once again. Finally, agarose gel and nylon membrane were separated. To confirm DNA transfer to nylon membrane, the complete agarose gel was stained with ethidium bromide as already described and checked by gel imaging system. After successful blotting of DNA, the nylon membrane was further treated with 2×SSC buffer for 10min, rinsed with H_2O and baked at 120°C for 30min. Nylon membrane was transferred into hybridisation bottle and prehybridised with DIG easy Hyb buffer in rotation oven at 45°C for 3h without air bubbles. Prior to hybridisation, appropriate volume of probe was diluted in 50μl H_2O and denatured at 95°C for 5min. After chilling on ice, probe was added to unused DIG easy Hyb buffer for a final concentration of $3\frac{\mu l}{ml}$. Alternatively, already used probe in DIG easy buffer was denatured at 68°C for 15min and chilled on ice. Hybridisation was carried out in rotation oven at 45°C over night.

After ∼17h, hybridisation buffer with probe was stored at -20°for re-use. Successively, nylon membrane in hybridisation bottle was treated with low-stringency buffer at RT and high-stringency buffer at 68°C for 2, 15 and 10min, for 2×15min, respectively. Subsequently, nylon membrane was transferred to a dish and shaken firstly in washing buffer for 2×2min. Then nylon membrane was blocked by blocking solution for 1h. For antibody hybridisation, primary sheep antibody *Anti-Dig-AP-Fab-Fragment (Roche Diagnostics)* was centrifuged at 14000×g for 5min and mixed with blocking solution for a dilution of 1:10000. Then hybridisation was carried out for 30min. Prior to film development, nylon membrane was shaken in washing buffer for 2×15min and equilibrated with detection buffer for 3min. After dripping, nylon membrane was placed on foil and 1:100 dilution of *CDP Star (Roche Diagnostics)* in detection buffer was dropped. Then foil was sealed without air bubbles. In dark room, X-ray film and welded membrane were placed on top of each other and put into X-ray clip cassette at 37°C for adequate exposure time of ∼1.5h. Finally, X-ray film was developed in dark room by developer solution. After washing with H_2O, X-ray film was fixed by fixer solution, again washed and dried.

3.3.4 Analytical isolation of genomic DNA from cells and tissues

For positive screening of single cell clones, genomic DNA was isolated using Igepal method. Sufficient portion of cells were detached by Trypsin ($\sim\frac{1}{6}$ 24 well for ApoE, $\frac{1}{2}$ 24 well for LDLR and CX3CR1 project) and centrifuged at 14000×g at 4°C for 10min. Supernatant was aspired thoroughly and cell pellet was resuspended in 50μl of Igepal lysis buffer containing 0.2–0.4$\frac{\mu g}{\mu l}$ Proteinase K by vortexing. Successively, incubation at 60°C for ≥1.5h and at 95°C for 15min was performed. After centrifugation at 14000×g for 15min, 5μl of supernatant were used for respective screening PCR.

For genotyping of porcine gene isoforms and positive screening of cell pools and newborn piglets, pure genomic DNA was isolated using *GenElute Mammalian Genomic DNA Miniprep Kit (Sigma-Aldrich)* according to manufacturer's instructions. Typically, single cell clones on 150mm cell culture dishes were detached simultaneously by Accutase and cells were split for two columns. Genomic DNA of piglets was isolated from ear tissue.

3.3.5 Preparative isolation of genomic DNA from cells and tissues

For DNA isolation in a big scale, phenol chlorophorm method was carried out. For this, piece of tissue was cut into smaller fragments (without hairs) and suspended in 500μl of lysis buffer and 20μl of Proteinase K (20$\frac{mg}{ml}$ stock). For lysis, suspension was shaken at 55°C over night. Alternatively, lysis was performed from frozen cell pellet. The next day 5μl of RNase (20$\frac{mg}{ml}$ stock) were added. After incubation at RT for 5min, lysate was supplemented with 500μl of phenol-chlorophorm-isoamyl alcohol (25:24:1) and shaken rapidly by hand. After further incubation at RT for 10min, the mixture was centrifuged at 14000×g for 10min. Subsequently, upper aqueous phase was transferred in new 2ml microcentrifuge tube and 500μl of chlorophorm were added for rapid shaking by hand. After centrifugation at 14000×g for 10min, again aqueous upper phase was transferred in 1.5ml microcentrifuge tube. Then $\frac{1}{20}$ volume of 3M sodium acetate and 0.7 volume of isopropanol were added and mixture was shaken gently by hand until DNA precipitated. DNA was pelleted by centrifugation at 14000×g for 10min and washed with 500μl of 70% ethanol by further centrifugation at 14000×g for 5min. Alternatively, precipitated DNA was fished out the solution by using a pipette tip and transferred in new 1.5ml microcentrifuge tube containing 70% ethanol for centrifugation at 14000×g for 10min. Pellet was air-dried and resolved in ≥100μl H_2O at 4°C over night. Additionally, pellet was vortexed briefly and incubated at 55°C for 1–2h. Quality and concentration of 500ng isolated DNA was verified by agarose gel electrophoresis as described in section 3.3.6.

3.3.6 Analytical and preparative agarose gel electrophoresis

Analytical gel electrophoresis was performed to determine quality and confirm concentration measurement of genomic DNA and linearised plasmid DNA for gene targeting, respectively, and to validate length of PCR products and DNA fragments. However,

preparative gel electrophoresis was adopted to purify PCR products and DNA fragments. Typically, 1.0% 1×TBE agarose gel for analytical and 1.0% 1×TAE agarose gel for preparative purpose was used. Agarose gels were supplemented with $0.6\frac{ng}{ml}$ ethidium bromide. Samples were supplemented with 5×loading dye and loaded with 5μl respective DNA ladder (100bp, 1kb) on agarose gel. Electric tension and current time were adopted to expected DNA length and used agarose gel size. Typically, 120V for ∼1.5h were used for medium size agarose gel (100ml). To avoid antidromic migration of ethidium bromide band, 6–12μl ethidium bromide were supplemented to running buffer. DNA was visualised by gel imaging system.

3.3.7 Isolation of DNA from agarose gel and PCR

For extraction of pure DNA from preparative agarose gel or PCR, the *Wizard SV Gel and PCR Clean-Up System (Promega)* was performed according to manufacturer's instructions. Prior to isolation from agarose gel, DNA of expected length was cut out using UV transilluminator at wavelength of $\lambda = 312nm$. Differing from protocol, elution step was performed typically twice with 30μl H_2O at 65°C. To validate efficient purification, DNA concentration was determined as referred in section 3.3.8.

3.3.8 Determination of DNA concentrations

Concentration and purity of DNA was ascertained by photometer. To measure DNA withing a linear range, dilutions of 1:35 were typically used. Absorptions at wavelengths of $\lambda = 230nm$, $\lambda = 260nm$ and $\lambda = 280nm$ were detected and concentration of DNA was calculated by using the following equation: $c_{dsDNA} = OD_{260} \times 50\frac{ng}{\mu l}$. Purity of DNA was determined by calculation of ratios $OD_{260} : OD_{280}$ and $OD_{260} : OD_{230}$. Values of ≥1.8 appointed absence of contaminations.

Alternatively, 1μl of DNA was measured by *Nanodrop Lite Spectrophotometer (Thermo Fisher Scientific)*.

3.3.9 Sequencing of DNA

For custom DNA sequencing in tube format, purified PCR and RT-PCR products and plasmid DNA were sent to *Eurofins Genomics, Ebersberg, GER* following the sample submission guide. Typically, DNA samples were adjusted to recommended concentrations and premixed with primers.

3.3.10 Ligation of DNA

Subcloning of PCR products with single 3'-terminal adenines was carried out with *pGEM-T Easy Vector System (Promega)* following manufacturer's instructions. Therefore, both sides of the linearised vector exhibit 3'-single thymidine overhangs for easy TA-cloning.

DNA fragments with 5'- or 3'-overhangs due to restriction digest were subcloned with *CloneJET PCR Cloning Kit (Thermo Scientific)* according to manufacturer's sticky-end cloning protocol featuring successive blunting (remove of 3'- and fill-in of 5'-overhangs) and ligation reaction. For both kits, typically a insert:vector molar ratio of 3:1 was adjusted using the following equation: $\frac{ngofvector \times kbsizeofinsert}{kbsizeofvector} \times \frac{3}{1} = ngofinsert.$ For cloning of short DNA, molar ratio was increased. Prior to transformation of bacteria, the ligation reaction was incubated at RT for ≥1h. To receive the maximum number of transformants, incubation was performed at 16°C over night, 4°C over week end, respectively.

For ligation of two DNA fragments after restriction digest, DNA fragment comprising the vector backbone with resistance gene was considered as vector, the other as insert, respectively. Ligation reaction was set up with 1μl of *T4 DNA ligase (New England Biolabs)* in a reaction volume of ≥10μl according to manufacturer's instructions. For cloning of long DNA, amount of vector was increased approaching copy number of vector used in the kits.

3.3.11 Analytical isolation of plasmid DNA

For positive screening of transformed bacteria by restriction digest, plasmid DNA was isolated using mini preparation method. 2ml of over night bacteria suspension culture were centrifuged at 14000×g for 1min. Pelleted bacteria were vortexed in 100μl of resuspension solution I and lysed by adding 200μl of lysis solution II. After incubation at RT for 3min, 150μl of neutralisation solution III were added for further incubation of ∼30min on ice. Bacteria debris was pelleted at 14000×g for 5min and supernatant was transferred in 2ml microcentrifuge tube. After adding 1ml of 95% ethanol, the DNA was precipitated and subsequently centrifuged for 14000×g for 15min. Successively, washing steps with 80% and again 95% ethanol were carried out by centrifugation at 14000×g for 5min. Finally, DNA pellet was dried and resolved in 50μl H_2O containing 20$\frac{ng}{ml}$ RNase by pipetting up and down.

3.3.12 Preparative isolation of plasmid and BAC DNA

Big scale isolation of plasmid and BAC DNA from bacteria was carried out with the use of *NucleoBond Xtra Midi Kit (Macherey-Nagel)* following manufacturer's instructions. Plasmid DNA was purified corresponding to high-copy protocol, BAC DNA to low-copy protocol, respectively. Differing thereof, the recommended volume of over night suspension culture was not determined by measurement of OD_{600}. Instead always 150ml for plasmid DNA and 500ml for BAC DNA were used. To increase yield of DNA, elution buffer was preheated at 55°C and DNA pellet was resolved in 150μl H_2O at 4°C over night or at 55°C for 1–2h. Additionally, pellet was vortexed briefly.

3.3.13 Restriction enzyme digestion in DNA cloning

Analytical digestion of plasmid DNA was performed for positive screening of transformed bacteria and verifying of plasmid structure and restriction sites for cloning. However, preparative digestion of plasmid DNA was carried out for generation of DNA fragments prior to ligation. Digestions were prepared with $3\frac{U}{\mu g}$ of respective restriction enzymes (*New England Biolabs*) as recommended by manufacturer considering following equation: $V_{enzyme} = \frac{1}{10} \times V_{tot}$. Typical incubation time was 1.5h.

For analytical digestion, typically either 1μl of plasmid DNA from mini preparation or 1μg of plasmid DNA from midi preparation were used. Generally, analytical digestion for plasmid structure validation was performed from midi preparation in triplicate with different restriction enzymes.

For preparative digestions, 7μg of plasmid DNA from midi preparation was used. In order to generate compatible ends for ligation, DNA fragments were blunted (remove of 3'- and fill-in of 5'-overhangs) with *DNA Polymerase I, Large (Klenow) Fragment (New England Biolabs)* according to manufacturer's instructions. Additionally, DNA fragment comprising the vector backbone with resistance gene was dephosphorylated with *CIP (New England Biolabs)* to avoid religation following manufacturer's protocol. When buffer was not compatible to restriction enzymes in double digestion, plasmid DNA was digested sequentially. Prior to blunting, dephosphorylation and sequential digestion DNA fragments were purified like PCR products as described in section 3.3.7. Heat inactivation was only performed after blunting reaction.

3.3.14 Preparation of plasmid DNA for gene targeting

Prior to transfection, 40μg of targeting vector and donor plasmid, respectively were linearised consistent with common terms in section 3.3.13. For precipitation and purification, either NaCl ethanol or phenol chlorophorm method was carried out. Generally, DNA pellet was treated in laminar airflow cabinet. To verify quality and concentration, 50 and 100ng of linearised plasmid DNA were loaded for agarose gel electrophoresis as referred in section 3.3.6.

For NaCl ethanol method, digestion was supplemented with $\frac{1}{10}$ volume of 3M NaCl and two volumes of 100% ethanol at -20°C and was shaken gently by hand until DNA precipitated. For maximal precipitation, mixture was chilled at -20°C over night or at -80°C for 2h. Subsequently, DNA was centrifuged at 14000×g for 10min. Pellet was further washed twice with 1ml of 70% ethanol by centrifugation at 14000×g for 10min, air-dried and resuspended in 140μl of sterile low TE buffer at 4°C over night.

To get rid of RNases, especially for co-transfection using DNA in combination with mRNA, the phenol chlorophorm method was performed. After restriction digest, an equal volume of phenol-chlorophorm-isoamyl alcohol (25:24:1) was added for rapid shaking by hand. After incubation for 10min at RT, mixture was centrifuged at 14000×g for 10min

and upper aqueous phase was transferred in new 1.5ml microcentrifuge tube. Then an equal volume of chlorophorm was added for further rapid shaking and centrifugation at 14000×g for 10min. Aqueous upper phase again was pipetted in new 1.5ml microcentrifuge tube and supplemented with $\frac{1}{20}$ volume of 3M sodium acetate and two volumes of chilled 100% ethanol (-20°C). Mixture was shaken gently by hand until DNA precipitated and stored at either -20°C over night or at -80°C for 2h. DNA was centrifuged at 14000×g for 10min and pellet was washed twice with 1ml of 70% ethanol by centrifugation at 14000×g for 5min. After air-drying, DNA pellet was resuspended in 140μl of sterile low TE buffer at 4°C over night.

3.3.15 β-Galactosidase reporter gene assay

For quantification of β-Galactosidase activity in HEK293 cells, *β-Gal Reporter Gene Assay (Roche Diagnostics)* was used according to manufacturer's instructions. Cells were cultured in 12 wells and lysed in 700μl of lysis reagent per well. Subsequent centrifugation was performed at RT and quantification by *Glomax 20/20 Luminometer (Promega)* was carried out in triplicates.

3.4 RNA techniques

Generally, RNA working was conducted in laminar airflow cabinet with filtered pipette tips on ice. Centrifugation steps were performed in cooling centrifuge at 4°C. All solutions were pre-cooled on ice. Only nuclease-free H_2O was used and RNA, tissue samples and cell pellet for RNA isolation were stored at -80°C.

3.4.1 Isolation of total RNA

RNA isolation from cultured cells was carried out with *Ambion Trizol reagent (Life Technologies)* typically from 6 well plates. Medium was aspirated and 1ml Trizol reagent was added. After incubation of 5min, cell lysis was controlled under microscope. Subsequently, cell lysate was transferred in 2ml microcentrifuge tube. For RNA isolation in a big scale, lysis was performed from frozen cell pellet (-80°C). After adding 200μl chloroform, cell lysate was shaken rapidly by hand, incubated for 2–3min and centrifuged at 14000×g for 15min. Upper aqueous phase was transferred in 1.5ml microcentrifuge tube and 500μl of -20°C isopropanol were added. After mixing, precipitate was incubated at RT for 10min and centrifuged at 14000×g for 10min. Pellet was washed and vortexed in 1ml of 75% ethanol. After centrifugation at 7500×g for 5min, pellet was air-dried and resolved in 50μl H_2O at 55°C for 10min.

Alternatively, RNA from cells was isolated using *High Pure RNA Isolation Kit (Roche Diagnostics)* and *SurePrep RNA/DNA/Protein Purification Kit (Fisher Scientific)* according to manufacturer's instructions.

For isolation of RNA from tissues, *SpeedMill PLUS homogeniser (Analytik Jena)* and *innuPREP RNA Mini Kit (Analytik Jena)* were used according to manufacturer's instructions. Prior to homogenisation of $2 \times 20sec$, sample holder and 0.5ml lysis tubes containing 2.4–2.8mm ceramic beads were pre-cooled at -20°C.

For isolation of RNA from porcine whole blood, *QIAamp RNA Blood Mini Kit (Qiagen)* was carried out according to manufacturer's instructions. Blood samples were collected with monovettes containing anti-coagulant EDTA and isolation protocol was performed with volumes of 1ml whole blood.

Subsequently, contaminating DNA was removed by use of *Ambion TURBO DNA-free Kit (Life Technologies)*. Differing from manufacturer's instructions, the DNase incubation and inactivation time was reduced to 10min and 2min, respectively.

3.4.2 Determination of total RNA concentrations

RNA concentration and purity was determined by standard photometer. Being withing linear measurement range RNA dilutions of 1:35 were typically used. Absorptions at wavelengths of $\lambda = 230nm$, $\lambda = 260nm$ and $\lambda = 280nm$ were measured and concentration of RNA was calculated by using the following equation: $c_{ssRNA} = OD_{260} \times 40\frac{ng}{\mu l}$. Purity of RNA was ascertained by calculation of ratios $OD_{260} : OD_{280}$ and $OD_{260} : OD_{230}$. Values of $\geq$2.0 appointed absence of contaminations.

Alternatively, 1μl of RNA was measured by *Nanodrop Lite Spectrophotometer (Thermo Fisher Scientific)*.

3.4.3 Determination of total RNA quality

RNA quality and concentration were verified by total RNA gel electrophoresis using 50ml gel. 2μl of *RiboRuler High Range RNA Ladder (Thermo Scientific)* and 400 or 500ng of RNA, respectively were mixed with *2×RNA loading dye (New England Biolabs)* and nuclease-free H_2O and incubated at 70°C for 10min. After cooling of 2–3min on ice, RNA was loaded on denaturing 0.8% TBE gel containing 0.3% formaldehyde. Gel electrophoresis was performed at 100V for 10min and at 70V for 30min, subsequently. RNA was visualised by gel imaging system. Integer RNA appeared with one 18S and one 28S band of double intensity.

3.4.4 Reverse transcriptase polymerase chain reaction

For semi-quantitative detection of gene expression, RT-PCR was carried out either as one-step or as two-step reaction. For one-step reaction, the kit *Invitrogen SuperScript III One-Step RT-PCR System with Platinum Taq DNA Polymerase (Life Technologies)* was used according to manufacturer's instructions.

For two-step reaction, 300ng of total RNA were transcribed initially with *ProtoScript M-MuLV Taq RT-PCR Kit (New England Biolabs)*, alternatively 400ng of total RNA with

Sections	Kits	Ta (D_{cDNA})	Primer pair	Product sizes
4.2.3	*SuperScript III One-Step RT-PCR System*	58°C	LDLR_RT_F1 LDLR_RT_R1	1331bp
4.2.3	*SuperScript III One-Step RT-PCR System*	58°C	LDLR_RT_F1 targBS_R	1401bp
4.2.3	*SuperScript III One-Step RT-PCR System*	58°C	LDLR_RT_F1 BS_R	1652bp
4.2.4	*SuperScript III One-Step RT-PCR System*	60°C	LDLR_RT_F1 targBS_R	1401bp
4.2.4 4.3.2	*SuperScript III One-Step RT-PCR System*	60°C	GAPDH_F GAPDH_R	536bp
4.2.6	*SuperScript III One-Step RT-PCR System*	59°C	LDLR_RT_F1 targBS_R	1401bp
4.2.6	*SuperScript III One-Step RT-PCR System*	59°C	LDLR_RT_F1 LDLR_R5	700bp
4.2.9	*SuperScript III Reverse Transcriptase* *GoTaq Hot Start Polymerase*	61°C (1:2.5)	LDLR_F5 targBS_R	1138bp
4.2.9	*SuperScript III Reverse Transcriptase* *GoTaq Hot Start Polymerase*	58°C (1:5)	LDLR_qPCR_F1 LDLR_E3_R1	223bp
4.3.2	*SuperScript III One-Step RT-PCR System*	60°C	CX3CR1_RT_F1 CX3CR1_RT_R1	541bp
4.3.7	*SuperScript III One-Step RT-PCR System*	60°C	CD14_F1 CD14_R1	156bp 236bp

Table 3.2: Overview of RT-PCRs related to the respective result sections with the used kits, annealing temperatures (Ta) and cDNA dilutions (D_{cDNA}), primer pairs and RT-PCR product sizes.

Invitrogen SuperScript III Reverse Transcriptase (Life Technologies) adding 30μl H_2O. Subsequently 1μl of 1:2,5–1:5 cDNA dilutions were set in PCR with *GoTaq Hot Start Polymerase (Promega)*. All kits were performed according to manufacturer's instructions. Table 3.2 refers the used kits, annealing temperatures, primer pairs and RT-PCR product sizes of all RT-PCRs related to the respective result sections.

3.4.5 Real time quantitative polymerase chain reaction

For relative quantification of gene expression, qRT-PCR was performed. In a first step, cDNA was synthesised from 300ng of total RNA by using *ProtoScript M-MuLV Taq RT-PCR Kit (New England Biolabs)*. Alternatively, $\leq$400ng of total RNA were transcribed by *Invitrogen SuperScript III Reverse Transcriptase (Life Technologies)* and diluted with 30μl H_2O. Finally, 1μl of 1:25 and 1:2.5 cDNA dilution, respectively was quantified in triplicate with *Applied Biosystems SYBR Green PCR Master Mix (Life Technologies)* using *Applied Biosystems 7500 Fast Real-Time PCR System (Life Technologies)*. Annealing and elongation temperature was 61°C and after each run melting curve was checked. Analysis of raw data was carried out as referred in *Applied Biosystems Guide to Performing Relative Quantification of Gene Expression Using Real-Time Quantitative PCR (Life Technolo-*

Sections	Kits	D_{cDNA}	Primer pair	Product size
4.1.3	*ProtoScript M-MuLV Taq RT-PCR Kit* *SYBR Green PCR Master Mix*	1:25	ApoE_F1 ApoE_R1	240bp
4.1.3	*ProtoScript M-MuLV Taq RT-PCR Kit* *SYBR Green PCR Master Mix*	1:25	GAPDH_F GAPDH_R	536bp
4.2.7 4.2.10 4.3.7	*SuperScript III Reverse Transcriptase* *SYBR Green PCR Master Mix*	1:2.5	CX3CR1_RT_F1 CX3CR1_qPCR_R1	160bp
4.2.7 4.2.10	*SuperScript III Reverse Transcriptase* *SYBR Green PCR Master Mix*	1:2.5	LDLR_qPCR_F1 LDLR_qPCR_R1	156bp
4.2.7 4.2.10	*SuperScript III Reverse Transcriptase* *SYBR Green PCR Master Mix*	1:2.5	TBP_F TBP_R	153bp
4.3.7	*SuperScript III Reverse Transcriptase* *SYBR Green PCR Master Mix*	1:2.5	CD14_F1 CD14_R1	156bp
4.3.7	*SuperScript III Reverse Transcriptase*	1:2.5	EGFP_qPCR_F1 EGFP_qPCR_R1	150bp
4.3.7	*SuperScript III Reverse Transcriptase*	1:2.5	TBP_F TBP_R	153bp

Table 3.3: Overview of qRT-PCRs related to the respective result sections with the used kits, cDNA dilutions (D_{cDNA}), primer pairs and qRT-PCR product sizes.

gies). All kits were performed according to manufacturer's instructions. Table 3.3 refers the used kits, cDNA dilutions, primer pairs and qRT-PCR product sizes of all qRT-PCRs related to the respective result sections.

3.5 Feeding study of pigs

To induce high blood cholesterol, German Landrace pigs (∼40kg) received ad libitum feeding supplemented with $250g/d/animal$ of *refined cocos oil (Vandemoortele Lipids)*. Cholesterol measurement was carried out directly before and during high-fat feeding as described in section 3.6.

3.6 Determination of blood cholesterol concentrations

Blood cholesterol was measured from whole blood by *Piccolo Xpress Chemistry Analyser (Abaxis)* using *Piccolo Xpress Lipid Panel Plus (Abaxis)*. Animals were sedated and fasting blood samples (8–12h) were collected by venipuncture with monovettes containing anti-coagulant Lithium-Heparin and volumes of 100–120μl were measured within 60min.

3.7 Sudan IV staining of pig aortas

For visualising of plaques, Sudan IV staining was performed. Porcine aortas were dissected by a veterinarian *(Tiergesundheitsdienst Bayern, Poing, GER)* and fixed in formalin.

Extraneous tissue from tunica adventitia was trimmed and abdominal aorta was opened longitudinally. Excessive formalin was drained under running water, vessel was covered with Sudan IV staining solution and shook periodically for 15min. To differentiate the stained tissue, the vessel was covered with Decolorising solution and shook for 5min. Subsequently, abdominal aorta was washed under running water for 1h and finally pinned on a tray for documentation.

CHAPTER 4

Results

4.1 Apolipoprotein E project

Apolipoprotein E (ApoE) is a highly anti-atherogenic protein involved in cholesterol homeostasis and immune response. ApoE is mostly synthesised by liver and to a smaller extend by extra-hepatic sources like macrophages influencing atherogenesis either systemic or local [169]. The gene expression is extensively regulated by activators and inhibitors (reviewed in [170]) and there are multiple redundant pathways of ApoE recycling [250, 593]. On the surface of circulating lipoproteins it mediates their hepatic clearance by high affinity binding to LDL receptor [167]. Independent of plasma levels, ApoE within the arterial wall decelerates [212, 213, 214, 215, 216, 217] and even regresses [200, 594, 201] atherosclerosis. Furthermore, it inhibits platelet aggregation [221] and defends against risk factor hypertension [232].

For generation of a porcine model for atherosclerosis with an accelerated and more severe pathogenesis (plaque rupture and thrombosis), at least one allele of the apolipoprotein E gene was to be knocked out functionally.

4.1.1 Genotyping of apolipoprotein E in different pig breeds

In human there are several isoforms of ApoE (reviewed in [170]), whereas the most frequent are E2, E3 and E4. They are derived from the three alleles $\epsilon 2$, $\epsilon 3$ and $\epsilon 4$ [171] revealing six genotypes with an order of decreasing frequencies in European Caucasian populations of $\epsilon 3/3$, $\epsilon 3/4$, $\epsilon 2/3$, $\epsilon 4/4$, $\epsilon 2/4$, $\epsilon 2/2$ [233]. Isoform ApoE3 is considered as parent form, whereas ApoE2 and E4 as its variants [171]. The allelic isoforms differ from each other by Cysteine/Arginine substitutions at codons 130 and 176 [234], in the pig at codons 129 and 175. The isoforms exhibit different expression levels [233, 253] and reveal different

HhaI fragment lengths [bp]	$\epsilon 2$ Cys_{129}/Cys_{175}	$\epsilon 3$ Cys_{129}/Arg_{175}	$\epsilon 4$ Arg_{129}/Arg_{175}
109	+	+	
90			+
66	+		
39		+	+
≤30	+	+	+

Table 4.1: Encoding of porcine ApoE isoforms by restriction enzyme digestion (*HhaI*) of 303bp PCR product: Fragment lengths (indicated by +) and appropriate allelic ApoE isoforms $\epsilon 2$, $\epsilon 3$ and $\epsilon 4$ with porcine amino acid positions of Cysteine (Cys) and Arginine (Arg).

concentrations and compositions of plasma lipoproteins [167, 253] and also different LDL receptor binding affinities [240]. ApoE2 is associated with type III hyperlipoproteinemia [167] and ApoE4 with a 42% higher risk of cardiovascular disease [173].

To determine the porcine ApoE isoforms and their distribution, in total 24 pigs of the three different breeds German Landrace, Goettingen Minipig and Schwäbisch Hall Domestic were screened. Genomic DNA was isolated from ear tissues. A sequence of 303bp covering crucial nucleotides for codons 129 and 175 was amplified by PCR with the primer pair ApoE_mut_F1/ApoE_mut_R1. PCR products were digested by restriction enzyme *HhaI* enabling restriction site polymorphims for Cysteine/Arginine substitutions at the respective codons (compare [234]). To validate Cysteine/Arginine distinction by restriction enzyme digestion, PCR product was sequenced and checked for nucleotide compliance at codons 129 and 175. Expected fragment lengths and appropriate allelic ApoE isoforms are referred in table 4.1.

Figure 4.1 shows restriction enzyme digestion of PCR product amplified from genomic DNA of porcine adipose tissue-derived mesenchymal stem cell (pADMSC) isolation 110111, which was later on used for gene targeting experiments. As referred in table 4.1, fragments of 90, 39 and ≤30bp indicated presence of $\epsilon 4$ alleles, homozygous ApoE4 phenotype, respectively. Also from the same sample, figure 4.2 and 4.3 show chromatograms with blue labeled nucleotides at codons 129 and 175 coding for Arginine. Homozygous ApoE4 phenotype was also detected by sequencing for pig #72 and sows #175 and #178.

The APOE genotyping revealed homozygous ApoE4 phenotype (two $\epsilon 4$ alleles) for all 27 pigs. This finding confirms published results showing the presence of only ApoE4 isoform in 128 pigs of eleven different pig breeds [5]. It differs from the human distribution, whose homozygous ApoE4 phenotype frequency ranges from ∼1–11% in different European Caucasian populations [233].

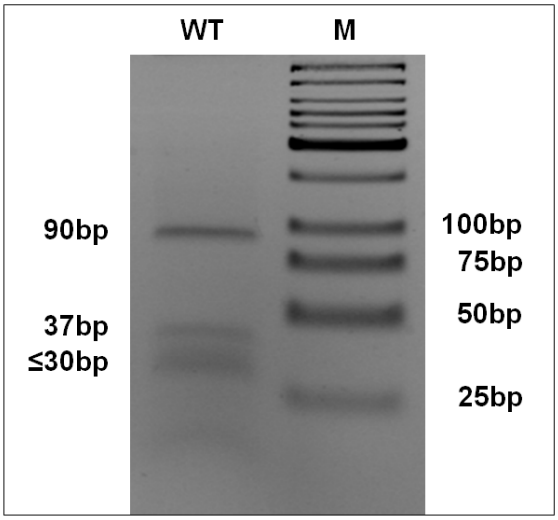

Figure 4.1: APOE genotyping by restriction enzyme digestion: WT: *HhaI* digestion of 303bp PCR product amplified from genomic DNA of pADMSCs 110111 revealing the three fragments of 90, 39 and ≤30bp indicative of homozygous $\epsilon 4$ allele, ApoE4; M: Low MW ladder.

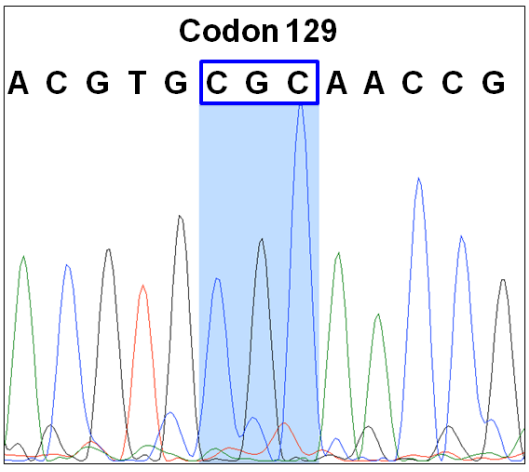

Figure 4.2: APOE genotyping by sequencing covering porcine codon 129 of pADMSCs 110111 (blue labeled): Nucleotides CGC coding for Arginine at respective site.

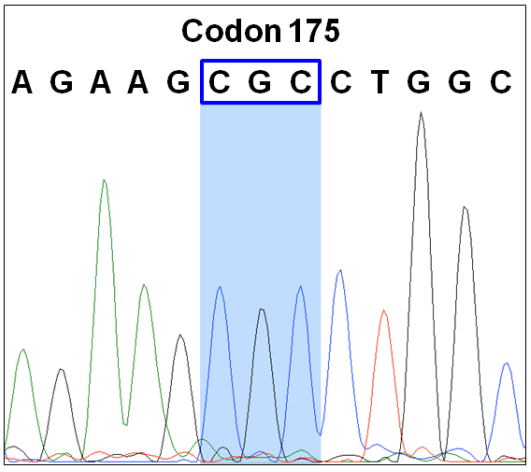

Figure 4.3: APOE genotyping by sequencing covering porcine codon 175 of pADMSCs 110111 (blue labeled): Nucleotides CGC coding for Arginine at respective site.

4.1.2 Conventional gene targeting strategy and targeting vectors

For functional knockout of porcine APOE gene, at first conventional gene targeting by homologous recombination was attempted. A promoter-trap vector was generated, which would replace the major coding region (exon 4) with a promoter-less selectable cassette (IRES neo) of 2.1kb. The initial targeting vector (ApoE TV1) featured a 2.5kb short and 9.7kb long homology arm. Further optimisation was required resulting in three additional targeting vectors (ApoE TV2, ApoE TV3 and ApoE TV4). The short homology arm was modified to remove a 0.9kb sequence within the first intron (ApoE TV2) containing an enhancer element [595], the long homology arm by removing 4.5kb repetitive sequences (ApoE TV3) and by addition of a 3.6kb negative selectable marker (CAGGS Cherry NLS) (ApoE TV4) for enrichment of targeting events against vector random integration (see figure 4.4) [596, 597]. Successful homologous recombination would result in a truncated protein of 63aa, compared to the full length protein of 318aa. This truncated protein should not be functional.

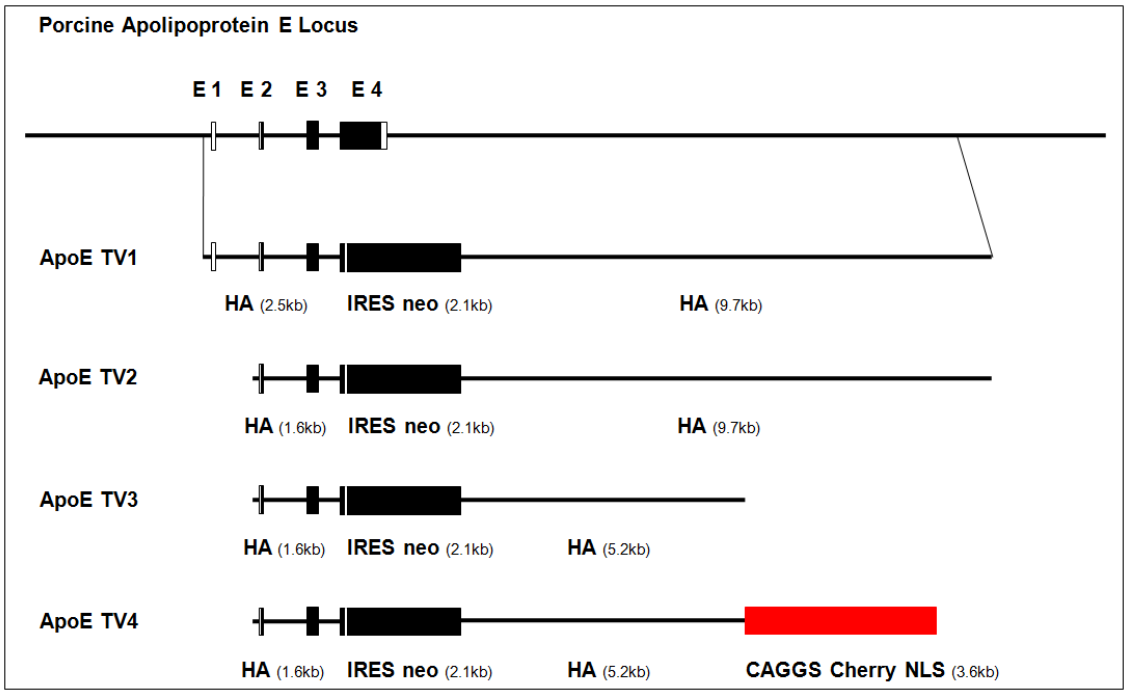

Figure 4.4: Conventional gene targeting strategy: Endogenous porcine APOE locus with its four exons (E1–E4) and the four targeting vectors ApoE TV1–ApoE TV4 containing promoter-less selectable cassette (IRES neo) of 2.1kb. Promoter-trap vectors differ in lengths of homology arms (HAs) and the negative selectable marker (CAGGS Cherry NLS) of 3.6kb (red labeled). Untranslated regions are labeled in white, coding regions in black. Respective sequence lengths of homology arms (2.5kb and 1.6kb for short and accordingly 9.7kb and 5.2kb for long HA) and integration site are indicated.

4.1.3 Gene targeting and apolipoprotein E expression upregulation

Conventional gene targeting of the porcine APOE gene was attempted with different promoter-trap vectors. The initial targeting vector was tried to be optimised by removal of an enhancer element and repetitive sequence elements, and by addition of a negative selectable marker (see section 4.1.2). Nevertheless, APOE gene targeting could not be achieved (for overview of transfections see table 4.2); screening details like polymerase, respective primer pairs, primer binding sites, annealing temperatures and PCR product sizes are not shown). A possible reason for the failure of the promoter-trap strategy could be a low expression of the APOE locus. Therefore, APOE expression was tried to be enhanced and to be validated by real time quantitative polymerase chain reaction (qRT-PCR). Increased transcription levels of the target gene were shown to directly enhance locus specific homologous recombination [598]. For this purpose, pADMSCs 170209 were treated with a synergistic combination of 1.0mM cyclic AMP and 1.0μM retinoic acid (expression upregulation medium) [599]. Since retinoic acid is a morphogenetic and teratogenic agent [599], cells were treated for only 24–96h prior to RNA isolation by Trizol. Subsequent relative quantification of gene expression by qRT-PCR was carried out using the primer pairs ApoE_F1/ApoE_R1 and GAPDH_F/GAPDH_R. Both primer pairs were designed over intron-exon borders amplifying a 240bp and 536bp qRT-PCR product, respectively. Cyclic AMP and retinoic acid treatment of pADMSCs was shown to consistently increase the APOE transcription compared to negative controls. Although the stimulatory effect follows a cell-specific manner [599], an up to ∼5-fold increase in APOE transcription was detected after 96h (see figure 4.5). Negative control at 0h could not be quantified. These findings allowed for cyclic AMP and retinoic acid treatment of pADMSCs three days before and during transfection with promoter-trap vector ApoE TV3. However, this treatment seemed to be harmful to the cells. Only eleven single cell clones could be obtained, which was under the average number of conventional gene targeting experiments. None of the cell clones was positive for gene targeting (see also table 4.2).

4.1.4 Transcription activator-like effector nuclease-mediated gene targeting strategy

Since APOE gene targeting could not be achieved by conventional promoter-trap strategy including several targeting vector modifications (for modifications see section 4.1.2, for transfections see table 4.2) and upregulation of the target gene transcription (see section 4.1.3) a second gene targeting strategy mediated by transcription activator-like effector nuclease (TALEN) was adopted. TALENs induce double strand breaks (DSBs) in the DNA [600], which can enhance homologous recombination (HR) [601] and stimulates subsequent introgression of linearised donor plasmids by homology-directed repair (HDR) [602]. DSBs should be induced either by TALEN expression constructs [603] or directly by TALEN mRNA [602, 578]. Target cleavage efficiency was tried to be enhanced by cold

Cell Isolation	Targeting Vector	Screenings	Positives
pADMSC 170209	ApoE TV1	47 mini pools	0
pADMSC 110111	ApoE TV1	5 pools	0
pADMSC 110111	ApoE TV2	61 clones, 129 mini pools, 4 pools	0
pADMSC 110111	ApoE TV3	146 clones, 3 pools	0
pADMSC 110111 (cAMP/RA)	ApoE TV3	11 clones	0
pADMSC 110111	ApoE TV4	84 clones	0

Table 4.2: Transfections for conventional gene targeting of APOE: Combinations of pADMSC isolations and different promoter-trap vectors with total number of screened mini cell pools, cell pools, single cell clones and their positive outcome. cAMP/RA: Cyclic AMP and retinoic acid treatment of cells.

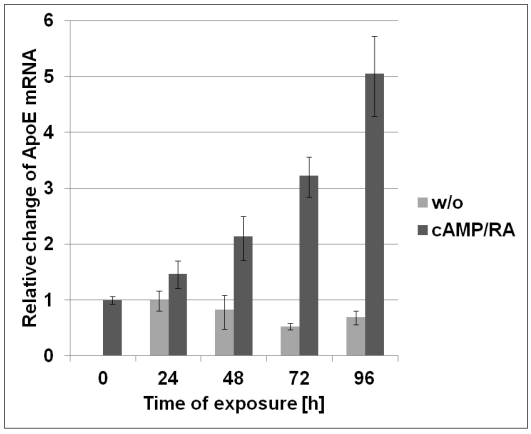

Figure 4.5: APOE expression upregulation: Relative change of ApoE mRNA over time of cyclic AMP and retinoic acid treatment (cAMP/RA) compared to control cells (w/o). Data were normalised to GAPDH expression. Respective standard deviations are indicated.

shock [578, 604, 605]. Two donor plasmids with selectable cassettes, one carrying PGK neo and the other IRES neo (promoter-trap strategy) of 1.8kb and 2.1kb flanked by short homology arms (HA) of 1.0kb and 1.1kb (ApoE Donor PGK and ApoE Donor IRES) provided for positive selection and for enrichment of homologous recombination against non-homologous end-joining (NHEJ). Additionally, to enrich targeting events against donor plasmid random integrations, a negative selectable marker [CAGGS Cherry NLS (CCN)] of 3.6kb was used (ApoE Donor PGK CCN and ApoE Donor IRES CCN) [596, 597]. To prevent repeated induction of DSB after plasmid introgression, the TALEN recognition site was omitted within the donor plasmids (see figure 4.6). Here, targeting of exon 3 should generate a truncated and non-functional protein of only 20aa.

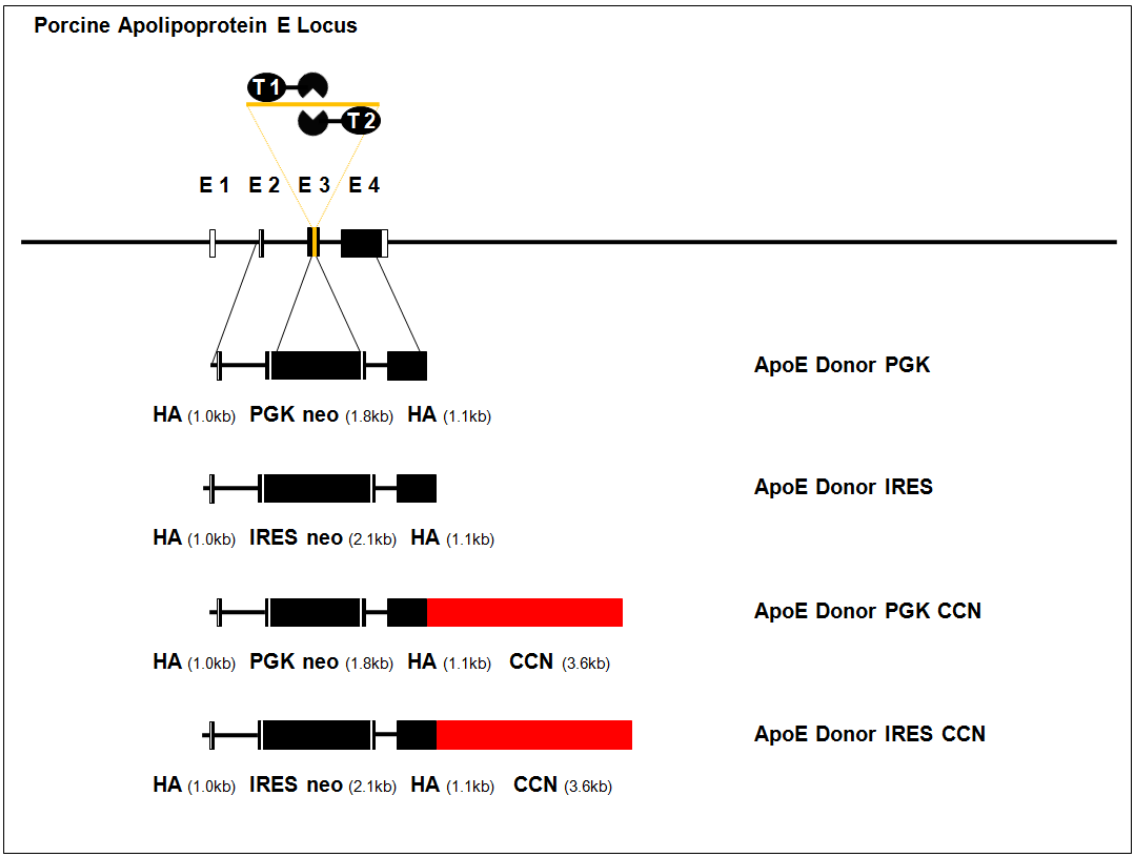

Figure 4.6: TALEN-mediated gene targeting strategy: Endogenous porcine APOE locus with its four exons (E1–E4), TALEN pair (T1 and T2) with respective recognition site within exon 3 (orange labeled) and the donor plasmids ApoE Donor PGK, ApoE Donor IRES, ApoE Donor PGK CCN and ApoE Donor IRES CCN featuring selectable cassettes (PGK neo and IRES neo) of 1.8kb and 2.1kb flanked by short HAs of 1.0kb and 1.1kb lacking TALEN recognition site and a optional negative selectable marker [CAGGS Cherry NLS (CCN)] of 3.6kb (red labeled). Untranslated regions are labeled in white, coding regions in black. Respective integration site is indicated.

4.1.5 Generation and genotype analysis of homozygous targeted porcine cells

For achievement of APOE gene targeting, pADMSCs were transfected with linearised donor plasmids ApoE Donor PGK and ApoE Donor IRES in combination with TALEN expression constructs or TALEN mRNA. After selection, cells were screened for homology-directed repair (HDR)-mediated donor plasmid introgression by PCR using the primer pair ApoE_TAL_targ_F1/ApoE_TAL_targ_R1. For ApoE Donor PGK introgression, a product size of 2112bp was expected, for positive control with screening vector ApoE SV PGK 1827bp. PCR products for ApoE Donor IRES introgression were 2059bp and 1774bp for screening vector ApoE SV IRES, respectively. To avoid false-positive results, the screening vectors lacked a distinguishable sequence of 285bp. Endogenous control PCR was conducted with the primer pair ApoE_TAL_targ_F1/ApoE_TAL_endo_R1 amplifying a PCR product of 1305bp. The forward primer ApoE_TAL_targ_F1 bound to an intron-sequence upstream of donor plasmid introgression, the reverse primer ApoE_TAL_targ_R1 within the selectable cassettes PGK neo and IRES neo. The endogenous reverse primer ApoE_TAL_endo_R1 was designed to detect wild-type (WT) allele excluding non-homologous end-joining (NHEJ)-affected allele and thus to bind within TALEN recognition site. All sequences, appropriate primers with their binding sites and expected PCR product sizes are given in figure 4.7.

The first transfection experiment with TALEN expression constructs and donor plasmid ApoE Donor PGK generated four targeted single cell clones, three of which were homozygous and one heterozygous. Appropriate screening PCR revealed expected PCR product sizes for WT endogenous control, screening vector (SV) positive control and analysed single cell clones. Water control was negative (see figure 4.8). For single cell clones 1, 2 and 5, only targeting PCR (see figure 4.8 A) was positive, whereas for single cell clone 4 both targeting PCR and endogenous PCR (see figure 4.8 B) at same intensity. Correctness of all targeting PCR products were further confirmed by sequencing.

Since targeting PCR could only detect gene targeting by homologous recombination (HR) and not by NHEJ, further investigation of homozygous targeted single cell clones was performed to distinguish between HR- or NHEJ-affected allele. Therefore, PCR was driven using the primer pair ApoE_TALEN_F2/ApoE_TALEN_R2 covering exon 3. For directed introgression of the donor plasmid, a PCR product of 2349pb was expected, for WT or NHEJ-affected allele $\leq$522bp, respectively. According to targeting PCR, all four clones (1-1–1-5) showed a 2349pb product indicating donor plasmid introgression and also the $\leq$522bp product. Water control was negative (see figure 4.9). Sequencing of the $\leq$522bp product revealed a WT allele, and thus an intact TALEN recognition site for all clones. However, this finding did not correspond to previous negative results of endogenous PCR. Here, the reverse primer should bind to TALEN recognition site and also detect the WT allele. Nevertheless, only for heterozygous clone 1-4 the 522bp band showed a correct stronger intensity than the 2349bp band, for homozygous clones 1-1, 1-2

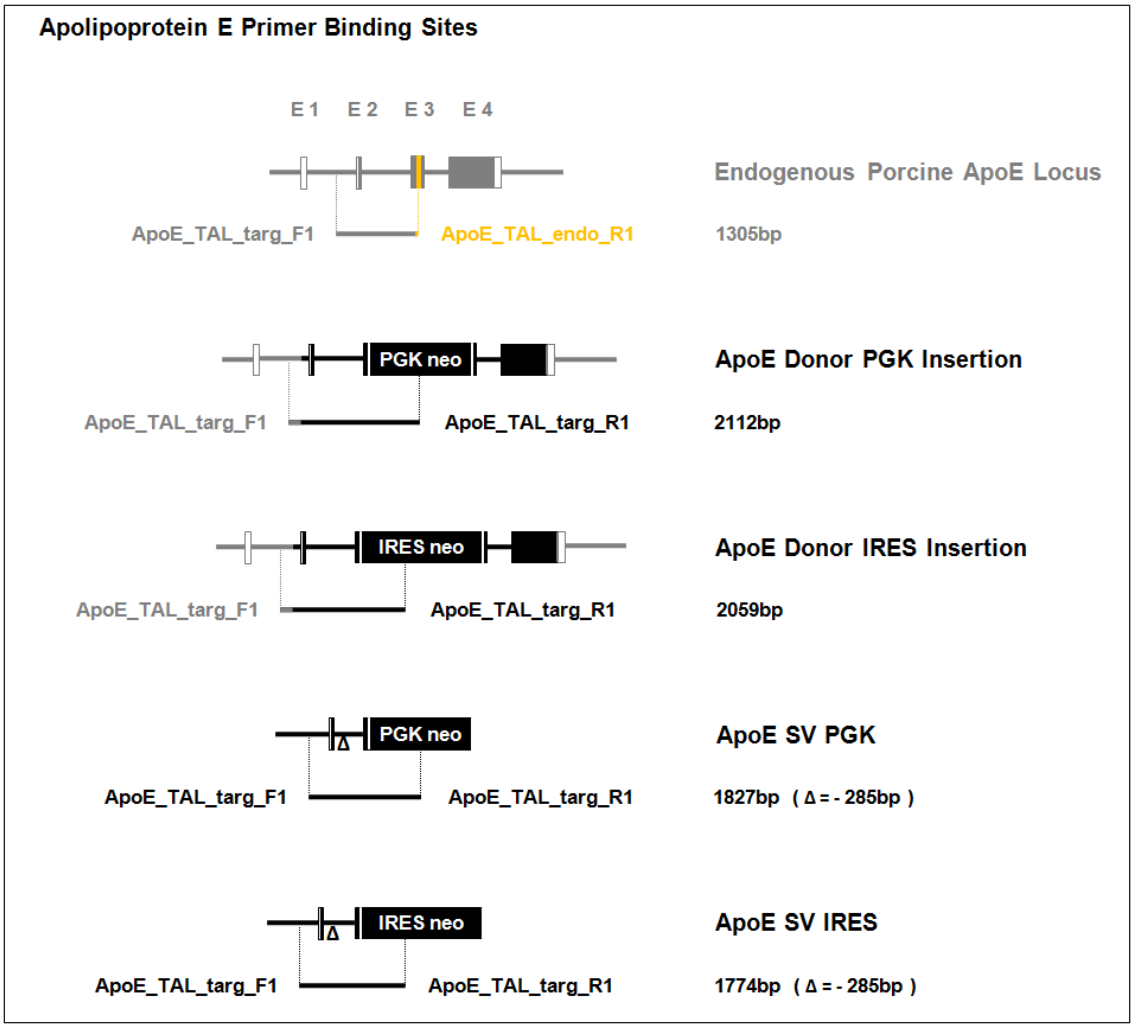

Figure 4.7: APOE primer binding sites of endogenous porcine gene locus and TALEN-mediated gene targeting with respective PCR products: Endogenous porcine APOE locus with its four exons (E1–E4) (gray labeled), TALEN recognition site within exon 3 (orange labeled) and the donor plasmid ApoE Donor PGK and ApoE Donor IRES introgressions (black labeled) featuring selectable cassettes (PGK neo and IRES neo). Untranslated regions are labeled in white, coding regions in gray/black. Screening vectors ApoE SV PGK and ApoE SV IRES featuring sequence deletion of 285bp (Δ). Primers, primer binding sites and respective PCR product sizes are indicated.

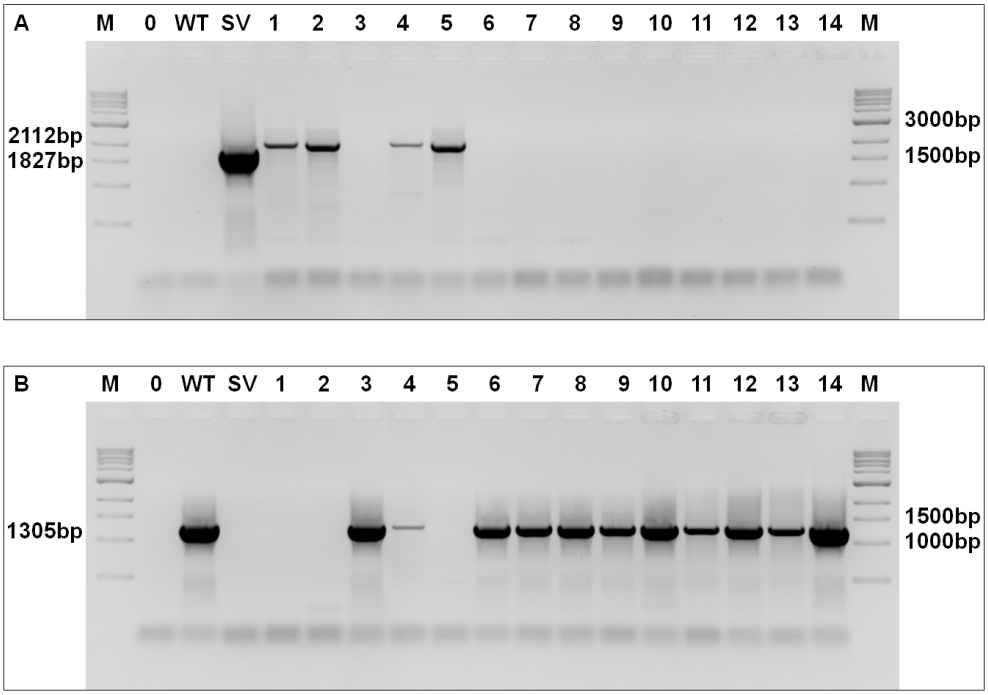

Figure 4.8: APOE screening PCR separated in targeting PCR (A) and endogenous PCR (B): PCR product of 2112bp for ApoE Donor PGK introgression, 1827bp for ApoE SV PGK positive control (SV) and 1305bp for wild-type endogenous control (WT). 1–14: Single cell clones; 0: Water negative control; M: 1kb ladder.

and 1-5 a weaker one. These results gave evidence for donor plasmid introgression at both alleles with subliminal overgrowing WT contamination of single cell clones.

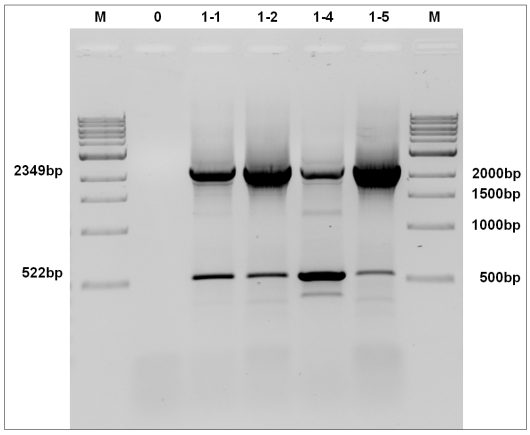

Figure 4.9: PCR covering APOE exon 3: PCR product of 2349pb for ApoE Donor PGK introgression, ≤522bp for wild-type or non-homologous end-joining (NHEJ)-affected allele. 1-1, 1-2, 1-4, 1-5: Single cell clones; 0: Water negative control; M: 1kb ladder.

To exclude random integration of TALEN expression constructs, all cell clones were further analysed by PCR. Here, the primer pair FokI_F/FokI_R were designed to detect FokI domain resulting in a 313bp PCR product. Only clone 1-5 was positive for FokI domain indicating random integration of TALEN expression construct.

Generally, due to high TALEN-mediated cytotoxicity, presumably induced by their frequent binding to genomic off-target sites [606], it was possible to produce and screen only a few cell clones. Additionally, positive clones could not be expanded sufficiently for further analysis. Only homozygous targeted clone 1-5 was used for two rounds of nuclear and embryo transfer, but no pregnancy could be established.

For generation of targeted cell clones, in total several varying transfection experiments were performed, but positive results from the first experiment were not reproducible. Table 4.3 shows all combinations of cell isolations and passages, donor plasmids and their amounts, TALEN expression constructs and TALEN mRNA amounts with total number of screened cell pools and single cell clones. For enhancement of target cleavage efficiency a cold shock was performed with a different pADMSC isolation (080812 P2) and for enrichment of targeting events against random integrations a donor plasmid with an additional negative selectable marker CAGGS Cherry NLS (CCN) was used (ApoE Donor PGK CCN). However, the cold shock experiment further decreased cell clone proliferation compared to normal culture conditions.

Nevertheless, it could be demonstrated that TALEN-mediated gene targeting is suitable to target difficult target genes like APOE, even homozygously and without random integration of TALEN expression construct. However, compared to conventional gene targeting experiments the TALEN-mediated gene targeting exhibited a high cytotoxicity.

pADMSCs	Donor	Donor DNA	TAL DNA	TAL RNA	Screenings	Positives
200212 P2	PGK	10μg	2.5μg each	/	9 pools	1
200212 P2	IRES	10μg	2.5μg each	/	9 pools	0
110111 P2	PGK	10μg	2.5μg each	/	30 clones	4
080812 P2 (30/37°C)	PGK CCN	10μg	2.5μg each	/	49 clones	0
110111 P3	PGK	800/1200ng	/	400ng each	2 pools	0
110111 P3	PGK	400/600ng	/	200ng each	2 pool 34 clones	0
110111 P4	PGK	10μg	2.5μg each	/	10 clones	0
110111 P5	PGK	400ng	/	200ng each	11 clones	0

Table 4.3: Transfections for TALEN-mediated gene targeting of APOE: Combinations of pADMSC isolations and passages (Ps), donor plasmids (PGK: ApoE Donor PGK, IRES: ApoE Donor IRES, PGK CCN: ApoE Donor PGK CCN) and amounts, TALEN expression constructs and TALEN mRNA amounts with total number of screened cell pools, single cell clones and their positive outcome. 30°C: Cold shock treatment of cells.

4.2 Low-density lipoprotein receptor project

The low-density lipoprotein receptor (LDLR) is a cell surface receptor mediating the clearance of LDL particles (VLDL and LDL) from blood circulation [255]. The gene transcription is regulated by intra-cellular cholesterol concentrations [43, 46]. After binding LDL particles, the LDL-LDLR complex gets internalised, dissociated and LDL receptor is recycled back to the cell surface [256, 257]. Up to now, 1741 mutations (substitutions, deletions, insertions, duplications and inversions) of LDL receptor gene have been found in patients suffering from familial hypercholesterolemia (FH) (www.ucl.ac.uk/ldlr/). These patients exhibit elevated blood cholesterol and early myocardial infarctions [260]. In humans, solely elevated LDL without other risk factors can cause atherosclerosis [261, 262, 263].

For acceleration of pathogenesis in a porcine model of atherosclerosis, at least one copy of the LDL receptor gene was to be disrupted.

4.2.1 Analysis of mutation associated with familial hypercholesterolemia in pigs

In human, more than 1700 mutations of the LDL receptor have been reported mostly associated with semi-dominant familial hypercholesterolemia (FH) (www.ucl.ac.uk/ldlr/) [310]. However, there was one mutation identified within the ligand binding domain of the LDL receptor contributing to recessive hypercholesterolemia in pigs [512, 514, 513]. The missense mutation (C→T) leads to amino acid substitution (Arg→Cys) at Arg_{115} and is also reported at the homologous Arg_{115} in human [607].

To screen for respective mutation, overall 24 pigs of the breeds German Landrace, Goettingen Minipig and Schwäbisch Hall Domestic were analysed. Genomic DNA was isolated

from ear tissues and PCR was performed with the primer pair LDLR_mut_F1/LDLR_R5 amplifying a product of 676bp. PCR products were digested by restriction enzyme *AciI* with the recognition site CCGC covering nucleotides CGC for Arg_{115}. To validate restriction enzyme digestion for detection of Arg→Cys substitution, PCR product was sequenced and checked for nucleotide compliance at respective codon. For wild-type (WT) allele fragments of 330bp, 239bp and 107bp were expected, for heterozygous mutated allele 437bp, 330bp, 239bp and 107bp, for homozygous 437bp and 239bp, respectively.

Since substitution of Arg_{115} is not a common polymorphism, as expected all analysed animals of the three breeds were negative for mutation. Additionally, pig #72 and sows #175 and #178 (German Landrace) used for animal breeding were also negatively screened for respective mutation by sequencing. For porcine adipose tissue-derived mesenchymal stem cells (pADMSCs) 110111, restriction enzyme digestion revealed no mutation.

4.2.2 Gene targeting strategy and targeting vector

Targeted disruption of porcine LDL receptor gene was attempted by conventional homologous recombination strategy. A promoter-trap vector comprising of a 1.9kb promoter-less selectable cassette (IRES BS) flanked by a 12.3kb long and a 1.6kb short homology arm was utilised to replace the major coding region of exon 4 (in total 16 exons), thus interrupting LDL receptor gene expression (see figure 4.10). The truncated protein featuring 120aa of 846aa is expected to be not functional.

4.2.3 Establishment of screening PCRs

Prior to targeting experiments, a protocol of screening PCR (endogenous PCR and targeting PCR) has to be established, which enables efficient screening of single cell clones. Towards this end, the screening vector LDLR SV was constructed, which was identical to the 3'-region of the targeted locus, except for a 294bp insertion. Due to this insertion, the 2126bp product of targeting control PCR product could be distinguished from the targeting PCR product of 1832bp avoiding false-positive results (see figure 4.10). However, establishment of screening PCR based on screening vector was problematic since several combinations of DNA polymerases and primer pairs provided either not the expected product, many additional unspecific product bands (ladder-like) or difficulties of reproducing positive results.

Nevertheless, after first transfection, gene targeting could be detected in two out of four cell pools and one out of 80 single cell clones. Due to the described problems with screening PCR, both the endogenous PCR and targeting PCR had been further optimised. For this purpose, the heterozygous targeted cell clone 1-16 was used, which was already verified by restriction enzyme digestion and by sequencing. For the final optimisation by temperature gradient, *Herculase II Fusion Enzyme with dNTPs Combo* and DMSO content of 4% were used with the endogenous primers LDLR_endo_F4 and LDLR_targ_R2

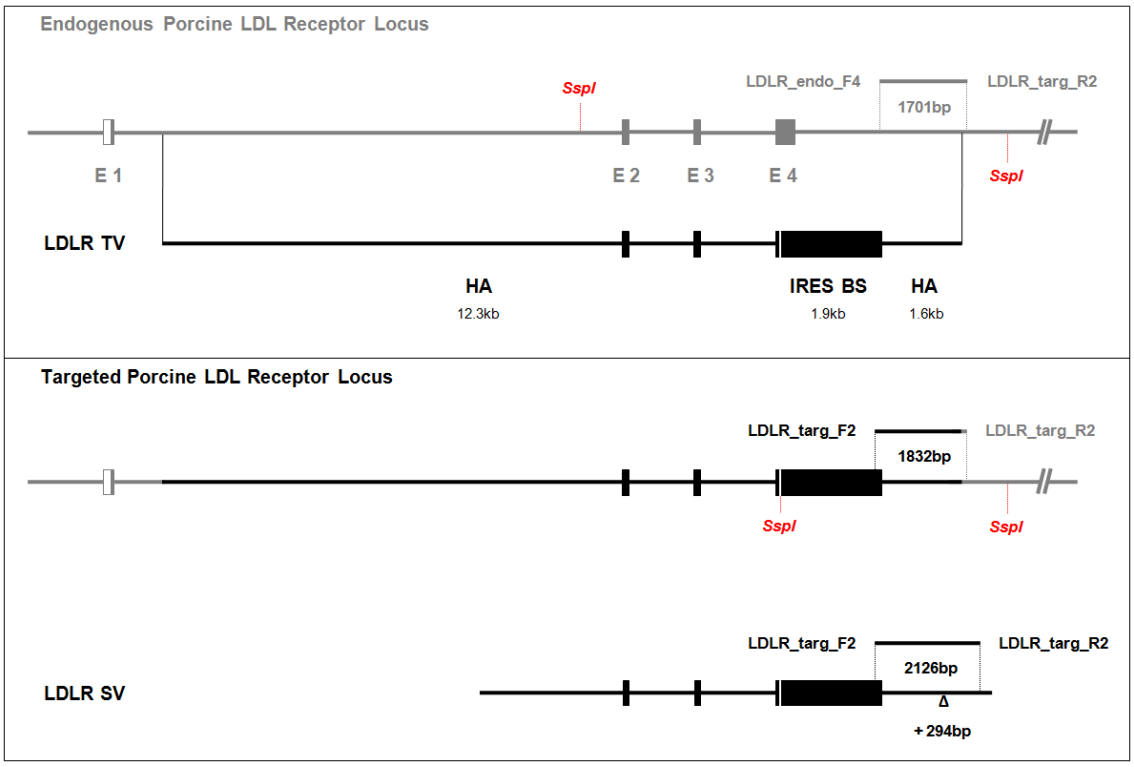

Figure 4.10: Gene targeting strategy and primer binding sites of endogenous and targeted porcine LDL receptor locus and screening vector LDLR SV with respective PCR products: Endogenous LDLR locus with the first four exons (E1–E4) (gray labeled) and LDLR TV with long and short homology arm of 12.3kb and 1.6kb and promoter-less selectable cassette (IRES BS) of 1.9kb (black labeled). Untranslated regions are labeled in white, coding regions in gray/black. Screening vector LDLR SV featuring sequence addition of 294bp (Δ). Integration site, respective primers, primer binding sites and PCR product sizes are indicated. *SspI*: restriction site for Southern blot (red indicated).

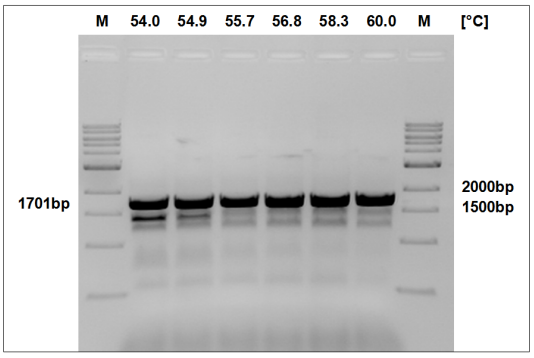

Figure 4.11: Temperature gradient for LDLR endogenous PCR: 1701bp PCR product amplified from heterozygous targeted cell clone 1-16 at indicated temperatures in °C. M: 1kb ladder.

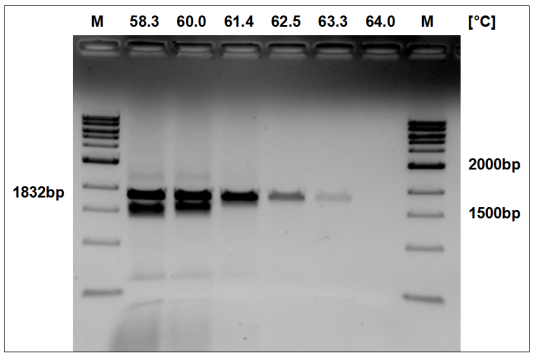

Figure 4.12: Temperature gradient for LDLR targeting PCR: 1832bp PCR product amplified from heterozygous targeted cell clone 1-16 at indicated temperatures in °C. M: 1kb ladder.

and the targeting primers LDLR_targ_F2 and LDLR_targ_R2 amplifying PCR products of 1701bp and 1832bp. The respective primer binding sites are described in section 4.2.4. For temperature gradient of endogenous PCR, 54.0–60.0°C were chosen, for targeting PCR 58.3–64.0°C.

Endogenous gradient PCR revealed a specific band with constant intensity and also continuous additional but weak unspecific bands of smaller products with highest intensity at 54.0/54.9°C (see figure 4.11). Targeting gradient PCR amplified a decreasing and finally disappearing specific band and exhibited also an additional smaller unspecific band with corresponding intensity at 58.3 and 60.0°C (see figure 4.12). Based on these results, an universal annealing temperature of 61°C was used for further screenings.

Targeting RT-PCR was also optimised based on the verified heterozygous targeted cell clone 1-16. For this purpose, different primer pairs were applied. Here, the forward primer LDLR_RT_F1 was used in combination with the three reverse primers LDLR_RT_R1, targBS_R and BS_R amplifying RT-PCR products of 1331bp, 1401bp and 1652bp, respectively, over intron-exon borders. The forward primer was designed to bind within exon 1 upstream of LDLR TV, the three reverse primers within IRES BS cassette. As expected, RT-PCR showed respective product sizes for cell clone 1-16 and negative water controls. For wild-type (WT) negative control, solely the primer pair LDLR_RT_F1/LDLR_RT_R1 amplified an additional strong product of expected size. Sequencing of targeting RT-PCR product derived from cell clone 1-16 only revealed LDLR mRNA of the WT allele indicating non-specificity of this primer pair (see figure 4.13). For further analysis, the primer pair LDLR_RT_F1/targBS_R was used and correctness of the respective targeting RT-PCR product was confirmed by sequencing. Further optimisation was tried by a temperature gradient, but intensity of the specific product band could not be increased (data

not shown).

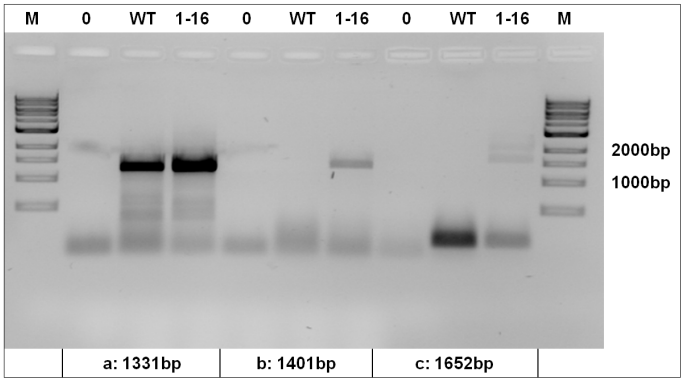

Figure 4.13: LDLR targeting RT-PCR: Products of 1331bp, 1401bp and 1652bp amplified by primer pairs LDLR_RT_F1/LDLR_RT_R1 (a), LDLR_RT_F1/targBS_R (b) and LDLR_RT_F1/BS_R (c). 0: Water negative control; WT: Wild-type negative control; 1-16: Heterozygous targeted cell clone 1-16; M: 1kb ladder.

4.2.4 Generation and genotype analysis of heterozygous targeted porcine cells

LDL receptor gene targeting in porcine cells was conducted by transfection of pADMSCs 110111 P2 with linearised targeting vector LDLR TV. After selection, single cell clones were analysed by screening PCR for homologous recombination (HR)-mediated LDLR TV integration. Endogenous PCR with the primers LDLR_endo_F4 and LDLR_targ_R2 amplified a 1701bp product, targeting PCR with the primers LDLR_targ_F2 and LDLR_targ_R2 a 1832bp product. Targeting positive control with LDLR SV carrying a distinguishable 294bp sequence addition for false-positive excision generated a PCR product of 2126bp. The forward primer LDLR_endo_F4 bound to an intron-sequence downstream of exon 4 replaced after HR-mediated targeting vector integration, the reverse primer LDLR_targ_R2 to an intron-sequence downstream of HR-mediated LDLR TV integration. The forward primer LDLR_targ_F2 bound to selectable cassette IRES BS. All sequences, appropriate primers with their binding sites and expected PCR product sizes are indicated in figure 4.10.

After the second transfection, 20 single cell clones were screened, of which five were positive for heterozygous LDL receptor gene targeting. Cell clones 2-2, 2-11 and the already existing cell clone 1-16 could be further expanded for nuclear transfer. Sufficient amounts of genomic DNA for further analysis like Southern blot could not be generated. Figures 4.14 and 4.15 only show a cutting of endogenous PCR and targeting PCR. Double positive results in screening PCR for clones 2-2 and 2-11 indicated their heterozygosity of LDL receptor alleles. Wild-type (WT) control was positive in endogenous PCR and screening vector (SV) control in targeting PCR. In each PCR, water controls were negative. Correctness of targeting PCR product for cell clones 1-16 and 2-2 was confirmed by sequencing.

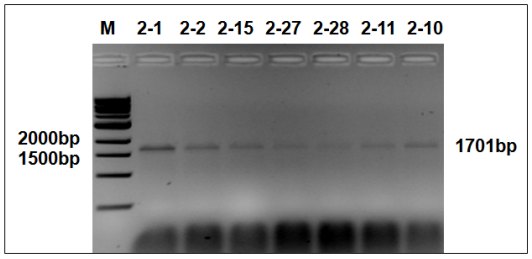

Figure 4.14: LDLR endogenous PCR: 1701bp product amplified from single cell clones 2-1, 2-2, 2-15, 2-27, 2-28, 2-11 and 2-10. M: 1kb ladder.

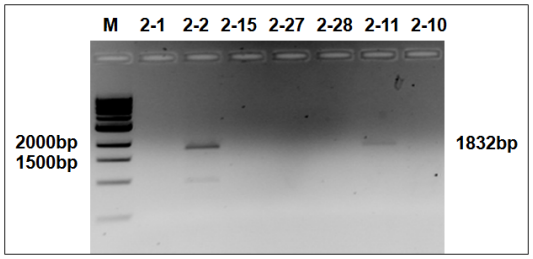

Figure 4.15: LDLR targeting PCR: 1832bp product amplified from single cell clones 2-2 and 2-11. 2-1, 2-15, 2-27, 2-28, 2-10: Single cell clones; M: 1kp ladder.

Single cell clones were further analysed for correctness of LDL receptor gene targeting. Therefore, expression was checked by one-step RT-PCR using the primers LDLR_RT_F1 and targBS_R. The forward primer LDLR_RT_F1 was designed to anneal within exon 1 upstream of HR-mediated LDLR TV integration and the reverse primer targBS_R within IRES BS cassette. Positive control was driven by the primer pair GAPDH_F/GAPDH_R. Both primer sets were designed over intron-exon borders to amplify RT-PCR products of 1401bp for LDL receptor gene targeting and of 536bp for GAPDH positive control.

Control RT-PCR (GAPDH) revealed the correct product sizes for WT positive control and the single cell clones 2-2 and 2-11, water control was negative (see figure 4.16). In contrast, LDL receptor targeting RT-PCR as expected was only positive for both clones (see figure 4.17) verifying allele heterozygosity already detected in screening PCR. Here, correctness of targeting RT-PCR product was confirmed by sequencing for the cell clones 1-16, 2-2 and 2-11.

4.2.5 Nuclear transfers, pregnancies and born animal

Generation of gene targeted animals was conducted by nuclear transfer followed by embryo transfer. For nuclear transfer, single cell clones 1-16, 2-2, 2-11 were pooled with cell clone types from unrelated experiments. Reconstituted embryos were transferred into a total of twelve sows establishing three pregnancies. Table 4.4 refers all trials of animal cloning with the used LDLR cell clones, established pregnancies and generated animal with genotype and identity (#). For LDL receptor project, one healthy piglet (#72) was born.

4.2.6 Genotype analysis of nuclear transfer animal #72

The LDL receptor genotype of the newborn piglet #72 was analysed by established screening PCR and RT-PCR. Screening PCR was performed as already described in section 4.2.4. As expected, endogenous PCR amplified a 1701bp product, whereas targeting PCR

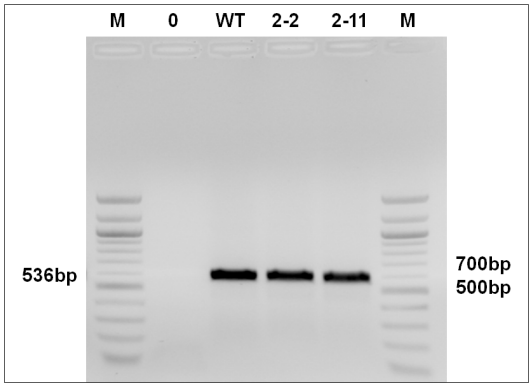

Figure 4.16: GAPDH control RT-PCR: 536bp product amplified from wild-type positive control (WT) and single cell clones 2-2 and 2-11. 0: Water negative control; M: 100bp ladder.

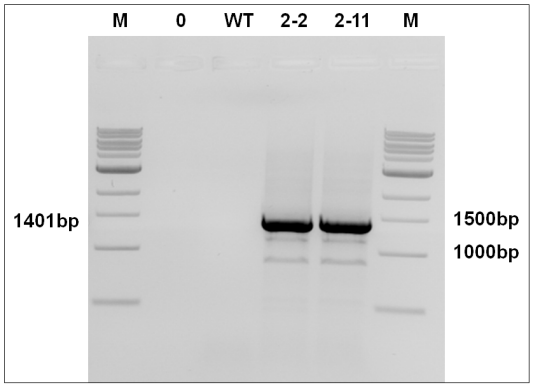

Figure 4.17: LDLR targeting RT-PCR: 1401bp product amplified from single cell clones 2-2 and 2-11. WT: Wild-type negative control; 0: Water negative control; M: 1kp ladder.

LDLR cell clones	Pregnancy	Animal (genotype, piglet ID)
1-16	+/-	0
1-16	-	0
1-16, 2-2, 2-11	-	0
1-16, 2-2, 2-11	-	0
1-16, 2-2, 2-11	-	0
1-16, 2-2, 2-11	-	0
1-16, 2-2, 2-11	+	1 piglet ($LDLR^{+/-}$, #72)
1-16, 2-2, 2-11	-	0
1-16, 2-2, 2-11	-	0
1-16, 2-2, 2-11	-	0
1-16, 2-2, 2-11	-	0
2-2, 2-11	+/-	0

Table 4.4: Nuclear transfers of LDL receptor project: Combinations of LDLR cell clones (1-16, 2-2, 2,11), establishment of pregnancy and generated animal with genotype and identity (ID in #). -: No pregnancy; +: Pregnancy; +/-: Termination of pregnancy; $^{+/-}$: Heterozygosity.

a 1832bp product and a distinguishable 2126bp product for screening vector (SV) positive control (Δ = +294bp). Endogenous PCR was positive for wild-type (WT) control and piglet #72, targeting PCR for SV control and piglet #72. For both, water control was negative (see figure 4.18). Correctness of targeting PCR product was confirmed by sequencing. These results indicated heterozygosity of LDL receptor targeted cell clones.

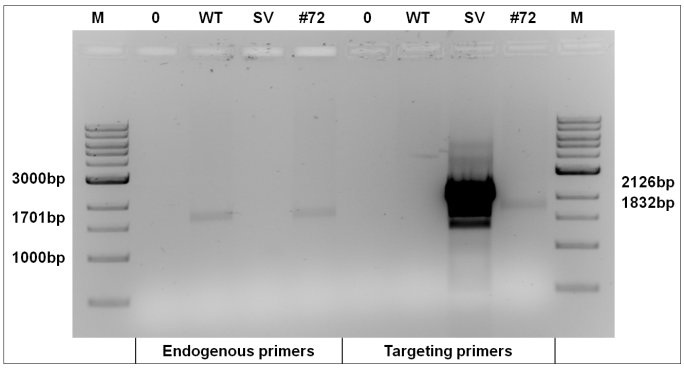

Figure 4.18: LDLR screening PCR for piglet #72: PCR product of 1701bp amplified by endogenous primers for wild-type positive control (WT) and piglet #72, products of 2126bp and 1832bp by targeting primers for screening vector positive control (SV) and piglet #72. 0: Water negative control; M: 1kb ladder.

To further verify the correctness of LDL receptor gene targeting, screening RT-PCR of piglet #72 was performed with the targeting primer pair LDLR_RT_F1/targBS_R. For endogenous control, primer pair LDLR_RT_F1/LDLR_R5 was used. Over intron-exon borders, the primer pairs amplified RT-PCR products of 1401bp for LDL receptor gene targeting and 700bp for endogenous control. The forward primer LDLR_RT_F1 annealed within exon 1 upstream of the homologous recombination (HR)-mediated LDLR TV integration, the reverse primer targBS_R within IRES BS cassette. The reverse primer LDLR_R5 for endogenous control bound to region of exon 4 substituted after HR-mediated LDLR TV integration. As expected, endogenous RT-PCR showed the 700bp product for WT positive control and for piglet #72 and targeting RT-PCR the 1401bp product for piglet #72. For both, water control was negative (see figure 4.19). These results again indicated allele heterozygosity for piglet #72. Targeting RT-PCR was repeated positively twice from different RNA isolations (ear tissue and isolated ear fibroblasts) and the correctness of the product was confirmed by sequencing. In contrast to the previous used GAPDH primers in section 4.2.4, the endogenous primers here generated weak bands of unspecific products for WT positive control and for piglet #72.

4.2.7 Phenotype analysis of nuclear transfer animal #72

For phenotypic examination of piglet #72, gene expression of LDL receptor (LDLR) in combination with fractalkine receptor (CX3CR1) was analysed quantitatively by real time quantitative polymerase chain reaction (qRT-RCR). In coronary artery disease (CAD) pa-

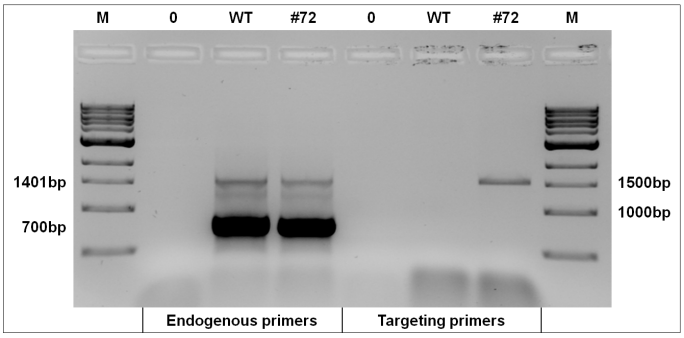

Figure 4.19: LDLR screening RT-PCR of piglet #72: RT-PCR product of 700bp generated by endogenous primers for wild-type positive control (WT) and piglet #72, correct product of 1401bp by targeting primers for piglet #72 (confirmed by sequencing). 0: Water negative control; M: 1kb ladder.

tients, the expression of CX3CR1 was found to be upregulated in peripheral blood mononuclear cells (PBMCs) [320], especially in the monocyte subpopulation [319]. These patients also exhibit a direct correlation between CX3CR1 expression and plasma LDL [320]. Relative quantification of both gene expressions on the one hand should verify heterozygous LDLR knockout and on the other hand possibly indicate parallel inflammatory processes during an early atherosclerosis. Since atherosclerosis already appears in fetal aortas and is highly increased by maternal hypercholesterolemia [106], sibling #74 was to be used as control. RNAs of piglet #72 and the age-matched control piglet #74 were isolated from ear tissue at one day and 222 days (∼7 month) after birth. Subsequent quantification of gene expression was performed with the primer pairs CX3CR1_RT_F1/CX3CR1_qPCR_R1, LDLR_qPCR_F1/LDLR_qPCR_R1, TBP_F/TBP_R amplifying qRT-PCR products of 160bp, 156bp and 153bp, respectively. All used primer pairs were designed over intron-exon borders. Expression of CX3CR1 and LDLR was normalised to TBP expression. Compared to control piglet #74 the newborn piglet #72 exhibited a ∼2.5-fold increase in CX3CR1 expression at a concurrent ∼0.5-fold decrease in LDLR expression. These data indicated inflammatory processes during possibly early atherosclerosis and correct gene targeting of one LDLR allele. After ∼7 month, the ∼0.5-fold decrease in LDLR expression was reproducible confirming heterozygous LDLR knockout. However, CX3CR1 expression was decreased at a level comparable to control pig #74 (see figure 4.20).

For phenotype analysis, also blood cholesterol concentrations of pig #72 were compared to sibling #73. Blood was collected 279 and 348 days after birth. According to normalisation of CX3CR1 expression after ∼7 month, pig #72 exhibited no elevated blood cholesterol values at both time points of measurement.

The increased CX3CR1 expression in combination with the decreased LDLR expression indicated a heterozygous LDLR knockout of pig #72 at phenotypic level. However, a direct correlation between increased CX3CR1 expression due to inflammation and elevated blood cholesterol triggering atherosclerosis could not be shown, also not an elevated blood

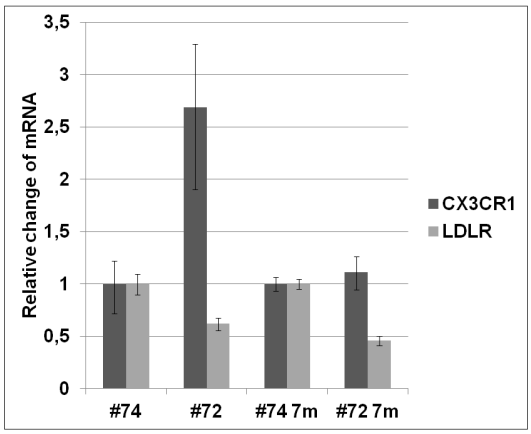

Figure 4.20: CX3CR1 and LDLR expression: Relative change of CX3CR1 and LDLR mRNA of piglets #74, #72 directly after birth and after ∼7 month (7m). Data were normalised to TBP expression. Respective standard deviations are indicated.

cholesterol due to heterozygous targeted LDLR. To induce an atherosclerotic phenotype, it was decided to mate pig #72 with two sows and conduct a cocos oil feeding study with a part of the offspring referred in table 4.5.

4.2.8 Breeding

After reaching sexual maturity, boar #72 (German Landrace) was mated at an age of 219 days with sow #175 (German Landrace) and at an age of 265 days with sow #178 (German Landrace). Sow #175 gave birth to 13 and sow #178 to five healthy piglets. Respective identities (#) and genders are given in table 4.5.

4.2.9 Genotype analysis of F1 generation animals revealing incorrect gene targeting

During cocos oil feeding study (see section 4.2.10), all 18 F1 generation piglets were analysed genotypically by PCR, RT-PCR and Southern blot. Due to screening PCR problems (endogenous PCR and targeting PCR), only homologous recombination (HR)-mediated LDLR TV integration could be verified by PCR using the primer pairs LDLR_F5/LDLR_R5 and LDLR_F5/CMAH_KV2r amplifying a 1438bp product for LDLR wild-type (WT) allele and 1556bp for HR-mediated LDLR TV integration. The forward primer LDLR_F5 bound to exon 3 (within LDLR TV), the reverse primer LDLR_R5 to exon 4 substituted after HR-mediated LDLR TV integration and the reverse primer CMAH_KV2r to IRES within IRES BS cassette. Pig #72 served as positive control for WT allele and HR-mediated LDLR TV integration, whereas both mothers, sow #175 and #178, as positive control for only WT allele. HR-mediated LDLR TV integration could be detected in animals #72, #201, #202, #203, #207, #210, #211, #212, #213, #222 and #224. PCR for WT allele

Sow ID	Piglet IDs	Genders	Genotypes
#175	#201	m	$LDLR^{+/-}$
	#202	m	$LDLR^{+/-}$
	#203	f	$LDLR^{+/-}$
	#204	m	WT
	#205	m	WT
	#206	f	WT
	#207	f	$LDLR^{+/-}$
	#208	f	WT
	#209	f	WT
	#210	f	$LDLR^{+/-}$
	#211	f	$LDLR^{+/-}$
	#212	f	$LDLR^{+/-}$
	#213	f	$LDLR^{+/-}$
#178	#221	m	WT
	#222	m	$LDLR^{+/-}$
	#223	m	WT
	#224	f	$LDLR^{+/-}$
	#225	f	WT

Table 4.5: Offspring of sows #175 and #178 with respective identities (ID in #), genders and genotypes. f: Female; m: Male; WT: Wild-type; $LDLR^{+/-}$: Heterozygous knockout of LDLR.

was positive for all screened animals. Water control was always negative. In total, ten piglets were positive for HR-mediated LDLR TV integration. Respective genotypes are referred in table 4.5.

For screening RT-PCR, several combinations of primer pairs with different polymerases in two-step reactions and also in one-step reaction were tried, but the results were negative and could not reproduce the previous positive results of LDL receptor gene targeting in various cell clones and pig #72 (see figures 4.13, 4.17 and 4.19) (data and screening details like polymerase, respective primer pairs, primer binding sites, annealing temperatures and RT-PCR product sizes not shown). Therefore, RT-PCR was retried as referred in section 4.2.4 for the three cell clones 1-16, 2-2 and 2-11 previously used for nuclear and embryo transfer generating pig #72. Cell clones were re-expanded and RNA was newly isolated. Here, GAPDH control RT-PCR was positive and showed the expected product sizes of 536bp for WT control and the three cell clones 1-16, 2-2 and 2-11. Water control was negative (see figure 4.21). Contrary of expectation, LDLR targeting RT-PCR revealed the positive product of 1401bp only for single cell clones 2-2 and 2-11, but no more for cell clone 1-16. Water and WT control were negative (see figure 4.22). These data indicated a contamination of cells, which have overgrown the correct targeted cells in the LDLR cell clone 1-16 and likely have generated pig #72.

To check the 3'-end structure of the HR-mediated LDLR TV integration, Southern blot

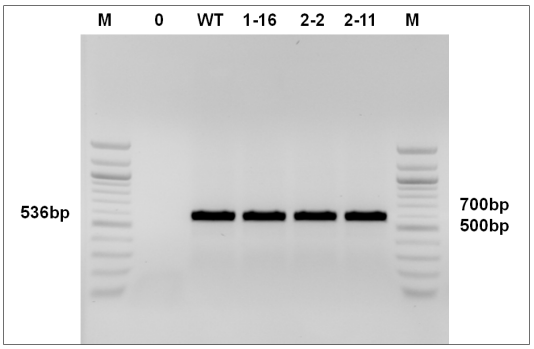

Figure 4.21: GAPDH control RT-PCR: 536bp product amplified from wild-type positive control (WT) and cell clones 1-16, 2-2 and 2-11 generating pig #72. 0: Water negative control; M: 100bp ladder.

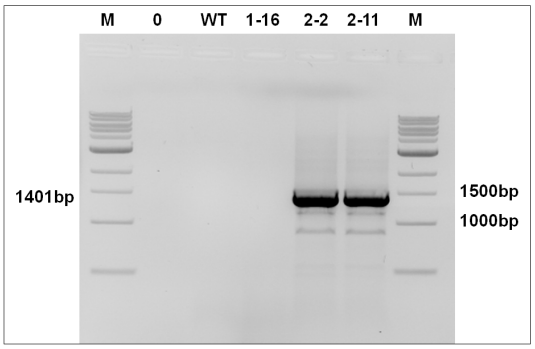

Figure 4.22: LDLR targeting RT-PCR: 1401bp product amplified from single cell clones 2-2 and 2-11 generating pig #72. 1-16: Cell clone 1-16; WT: Wild-type negative control; 0: Water negative control; M: 1kp ladder.

was performed. The BS probe of 399bp was generated by labeling PCR using the primer pair BS_probe_F/BS_probe_R. Genomic DNA of pig #72 and its genetically modified offspring #201, #202, #203, #207, #210, #211, #212, #213, #222 and #224 was digested by restriction enzyme *SspI-HF*. The *SspI* restriction sites were 775bp upstream of exon 2, within a sequence between partial exon 4 and IRES of LDLR TV and 823bp downstream of HR-mediated LDLR TV integration. Restriction sites are indicated in figure 4.10. For HR-mediated LDLR TV integration, a single fragment of 4372bp was expected. The endogenous fragment size was 7513bp. Genomic DNA of sows #175 and #178 served as WT negative controls. Southern blot for all screened animals revealed a single band of 7188bp differing from the expected fragment size of 4372bp. Both controls were negative. Southern blot for piglet #224 was repeated since restriction enzyme digestion failed. An additional band for piglet #203 could be result of incomplete restriction enzyme digestion (see figures 4.23 and 4.24).

To explain the structure of the received fragment, a high fidelity PCR was conducted with the primer pair LDLR_I5_F1/LDLR_I5_R1 ranging from exon 4 to exon 5 of LDLR and covering both *SspI* restriction sites. As expected, in addition to an endogenous PCR product of unknown length, high fidelity PCR generated an even longer product, which was subcloned with *CloneJET PCR Cloning Kit (Thermo Scientific)* and sequenced by primer walking. For continuous sequencing, the subcloned PCR product was digested by the restriction enzymes *EcoRI-HF* and *KpnI-HF* and fragments diverging from the known restriction digest pattern were further subcloned (primers and fragment sizes are not referred). The sequencing results revealed a duplication of the 1.9kb IRES BS cassette and the 1.6kb short homology arm with a 487bp deletion at the 5'-end of IRES (see figure 4.25).

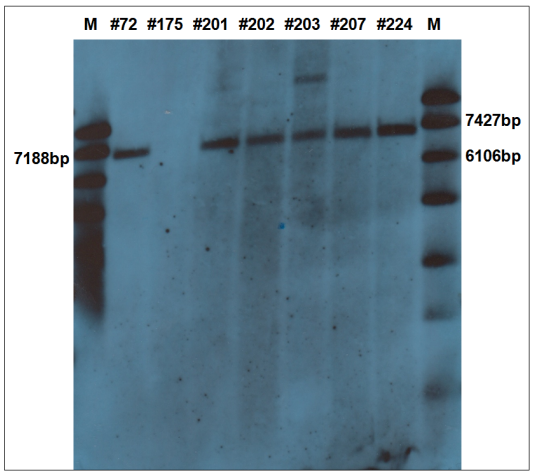

Figure 4.23: LDLR Southern blot utilising BS probe: 7188bp fragment for HR-mediated LDLR TV integration derived from *SspI-HF* restriction enzyme digestion of genomic DNA of pigs #72, #201, #202, #203, #207, #224. Genomic DNA of sow #175 served as wild-type negative control. M: Southern blot ladder.

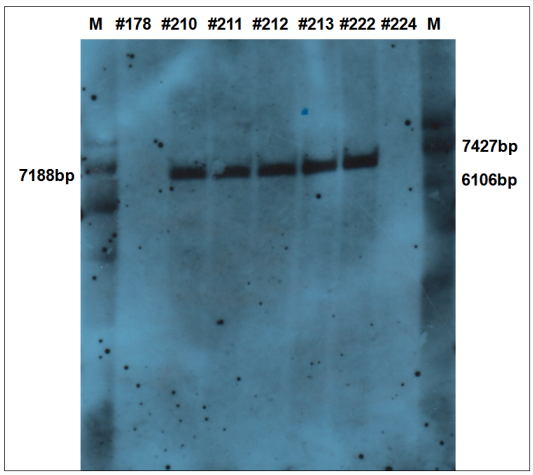

Figure 4.24: LDLR Southern blot utilising BS probe: 7188bp fragment for HR-mediated LDLR TV integration derived from *SspI-HF* restriction enzyme digestion of genomic DNA of pigs #210, #211, #212, #213, #222. Genomic DNA of sow #178 served as wild-type negative control, genomic DNA of pig #224 was undigested. M: Southern blot ladder.

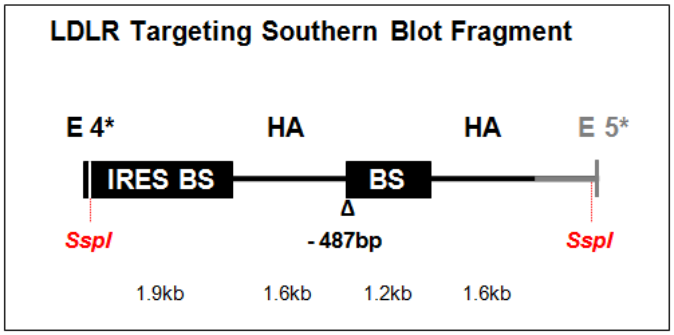

Figure 4.25: LDLR targeting Southern blot fragment elucidated by sequencing of high fidelity PCR product ranging from exon 4 to exon 5: Partial exon 4 (E4*) with duplication of IRES BS cassette (1.9kb) and short homology arm (1.6kb) featuring an 5'-end deletion of IRES ($\Delta = 487$bp) (black labeled) downstream of endogenous intron-sequence and partial exon 5 (E5*) (gray labeled). *SspI*: Restriction site for Southern blot (red indicated).

These data unfortunately indicated an incorrect LDL receptor gene targeting. On the one hand side, positive results of previous targeting RT-PCRs were not reproducible and thus could not verify correct 5'-end of HR-mediated LDLR TV integration and upstream presence of the endogenous LDLR promoter driving expression and thus splicing of endogenous exon 1 with exon 2 within LDLR TV. Nevertheless, expression of IRES BS cassette was demonstrated by two-step RT-PCR using the primer pair LDLR_F5/targBS_R annealing withing exon 3 and IRES BS cassette of the LDLR TV and amplifying a 1138bp product. Also, an exon duplication was detected by two-step RT-PCR. Here, the primer pair LDLR_qPCR_F1/LDLR_E3_R1 generated a 223bp RT-PCR product ranging from exon 4 to exon 3. The forward primer LDLR_qPCR_F1 annealed to exon 4 sequence substituted after HR-mediated LDLR TV integration. Correctness of the RT-PCR product was confirmed by sequencing indicating clustering of exons upstream of HR-mediated LDLR TV integration. However, structure upstream of HR-mediated LDLR TV integration could not be elucidated conclusively.

On the other hand, the 3'-end of HR-mediated LDLR TV integration could be verified by Southern blot in combination with sequencing of high fidelity PCR product covering the utilised restriction sites. Although sequencing of the high fidelity PCR product revealed a duplication of the IRES BS cassette and the short homology arm with 5'-end deletion of IRES, the expected presence of exon 5, 875bp downstream of HR-mediated LDLR TV integration was confirmed.

These data excluded a random insertion of LDLR TV and possibly indicated bidirectional homology arm elongation following ectopic vector integration at an adjacent or random position [608] with additional complex partial duplication of the targeting vector [609].

4.2.10 Phenotype analysis of F1 generation animals

For analysis of an atherosclerotic phenotype, animals of F1 generation were subjected to cocos oil feeding study. Before and during feeding a high-fat diet, gene expression of LDL receptor (LDLR) in combination with fractalkine receptor (CX3CR1) was analysed quantitatively and blood cholesterol was measured. After feeding study, abdominal aortas were examined for plaques.

Since upregulation of CX3CR1 expression was detected in peripheral blood mononuclear cells (PBMCs) [320] of coronary artery disease (CAD) patients, especially in the monocyte subpopulation [319], total RNA for real time quantitative polymerase chain reaction (qRT-PCR) was isolated from porcine whole blood. In patients, additionally a direct correlation of LDLR mRNA levels between mononuclear leukocytes and liver cells was demonstrated. Although a variation of 1–6 LDLR mRNA copies for both cell types were shown between individuals [610], whole blood was assumed to be a good source for quantification of LDLR expression in liver. For previous examination of the single piglet #72 (see section 4.2.7), total RNA was isolated from ear tissues since blood collection possibly can be dangerous

to animal life due to stress or sedation. Since ear tissue is taken regularly for animal genotyping after birth, both sources for total RNA isolation were compared to each other based on relative LDLR and CX3CR1 expression results. To exclude a disparate maternal influence over atherosclerosis already appearing in human fetal aortas and being highly increased by hypercholesterolemia of the mother [106], only siblings of one litter were examined.

For quantification of LDLR and CX3CR1 gene expression, RNAs of piglets #201–#213 were isolated from ear tissues one day after birth and from whole blood 85 and 90 days after birth. RNAs were transcribed and quantified as referred in section 4.2.7. Relative expression levels of LDLR and CX3CR1 were determined from ear tissue of 13 animals and from whole blood of eleven animals and are referred in figure 4.26 and 4.27. LDLR expression levels from ear tissues (1.1±0.6) showed a considerably higher variation than from whole blood (1.0±0.2). However, expression levels of CX3CR1 reached almost the same average for ear tissue (1.1±0.5) and whole blood (1.1±0.6). These findings indicated that whole blood is a suitable source for quantification of both gene expressions, especially of LDLR. The high variation of LDLR expression detected in ear tissues possibly explain the previous quantification results for pig #72 indicating a misleadingly ∼0.5-fold decrease in LDLR expression after birth and ∼7 month and thus a heterozygous LDLR knockout at phenotypic level.

In order to validate a direct correlation between CX3CR1 expression and plasma LDL in the pig, already shown in CAD patients [320], blood cholesterol concentrations were determined and compared to respective CX3CR1 expression levels possibly indicating inflammation during an early atherosclerosis. Finally, atherosclerosis should be verified by plaques within the porcine abdominal aortas.

To induce an atherosclerotic phenotype, female pigs #206, #207, #208, #209, #210, #211, #212 and #213 at an age of 96 days and a weight of ∼40kg received a high-fat diet for 150 days. For this, the chow diet was supplemented with refined cocos oil featuring the most unbalanced ratio of hypo- and hypercholesterolemic fatty acids compared to the important edible oils and fats. Cocos oil exhibit 69.4–84.4% (w/w) of lauric, myristic and palmitic acids [611] shown to be responsible for plasma cholesterol and triglyceride elevation [612]. Blood cholesterol concentrations were measured eleven and 13 days before and 86 days after induction and compared to each other. Within this period, the pigs reached a weight of ∼110kg. Values of total cholesterol and respective fractions (VLDL, HDL, LDL) are referred for each pig initially receiving chow diet (see figure 4.28) followed by high-fat diet (see figure 4.29). For chow diet, the average value of total cholesterol was $71.4\pm6.6\frac{mg}{dL}$ increasing to $96.1\pm14.1\frac{mg}{dL}$ after high-fat diet.

Before feeding study, total cholesterol values at chow diet were determined from nine female and two male pigs. While females exhibited an almost identical average of $70.4\pm6.9\frac{mg}{dL}$, total cholesterol of males gained $87.0\pm5.7\frac{mg}{dL}$ (see table 5.1) according to measurements reported for castrated male German Landrace pigs [4, 613].

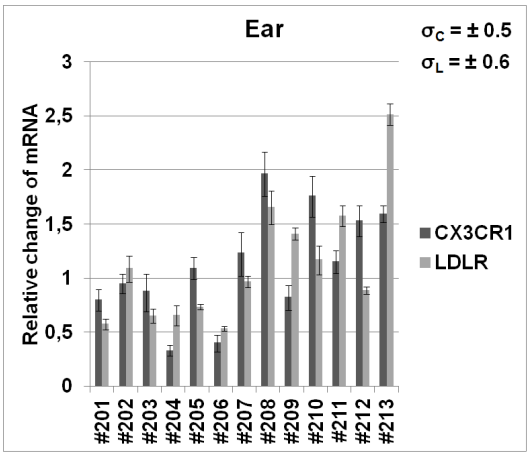

Figure 4.26: CX3CR1 and LDLR expression determined from ear tissue: Relative change of CX3CR1 and LDLR mRNA of piglets #201–#213 directly after birth. Data were normalised to TBP expression. Standard deviations are indicated for respective piglets and for whole litter (σ).

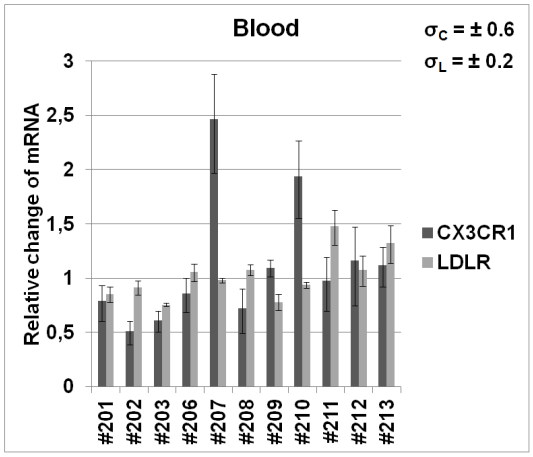

Figure 4.27: CX3CR1 and LDLR expression determined from whole blood: Relative change of CX3CR1 and LDLR mRNA of pigs #201–#213 (without #204 and #205) 85 and 90 days after birth. Data were normalised to TBP expression. Standard deviations are indicated for respective piglets and for whole litter (σ).

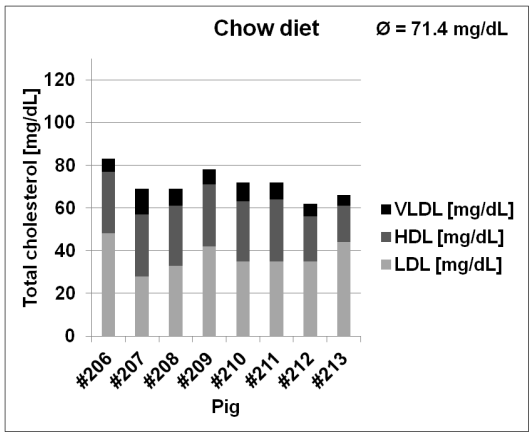

Figure 4.28: Blood cholesterol concentrations of pigs #206–#213 at chow diet: Total cholesterol, respective fractions of VLDL, HDL and LDL and total cholesterol average for all animals (Ø) in $\frac{mg}{dL}$.

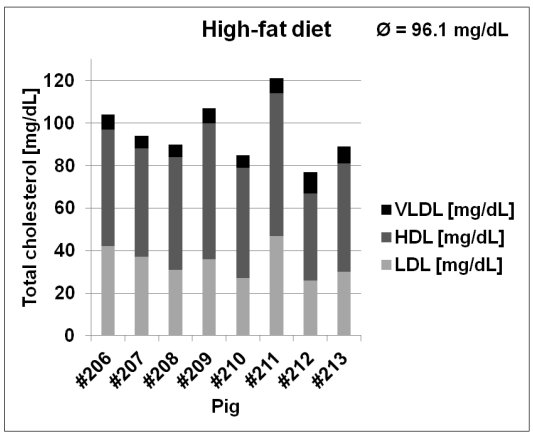

Figure 4.29: Blood cholesterol concentrations of pigs #206–#213 at high-fat diet: Total cholesterol, respective fractions of VLDL, HDL and LDL and total cholesterol average for all animals (Ø) in $\frac{mg}{dL}$.

During feeding study, the determined increase in total cholesterol for female pigs seemed to contribute solely to HDL fraction amounting $26.3 \pm 4.6 \frac{mg}{dL}$ at chow diet and $54.3 \pm 8.1 \frac{mg}{dL}$ at high-fat diet (see table 5.2). Differing thereof, male juvenile domestic crossbred pigs [517] and female cloned, genetically-defined ApoE4 Duroc pigs (see table 5.3) [5] on hyperlipidemic diet (2% cholesterol and 17% coconut fat) exhibited also highly increased LDL cholesterol.

For quantification of CX3CR1 gene expression, RNAs of pigs #206–#213 (without #210) were isolated from whole blood six and eleven days before and 86 days after high-fat diet. Subsequent qRT-PCR was performed as already described above. Relative expression levels for chow and high-fat diet relating to every single pig are referred in figure 4.30. Every pig exhibited an increase in CX3CR1 expression reaching statistical significance in paired two-sample t-test at a confidence interval of 95% ($p = 0.026$).

To validate an atherosclerotic phenotype, Sudan IV staining of abdominal aortas of pigs #206, #209, #212 and #213 was conducted after 150 days of high-fat diet. After 86 days of high-fat diet, pig #206 and #209 featured both the highest absolute expression of CX3CR1 and the greatest increase in expression, whereas pig #212 and #213 the lowest absolute expression. Before high-fat diet, all absolute expressions were almost identical for each pig, merely pig #207 exhibited a ∼2-fold increased CX3CR1 expression. However, this pig revealed one of the lowest increase of expression after high-fat diet. By Sudan IV staining of lipoproteins within the arterial wall (tunica media), atherosclerosis was only detected in pig #206 and #209 showing early atherosclerotic plaques (see figure 4.31) at bifurcations. Remarkably, pig #206 and #209 were wild-type animals and

pig #212 and #213 genetically modified animals (see table 4.5) indicating no potentiating effect of the confirmed incorrect LDL receptor gene targeting (see section 4.2.9) on an atherosclerotic phenotype. Bifurcations exhibit specific shear stress conditions contributing to endothelial dysfunction and eccentric plaque development and finally to their transformation into rupture-prone vulnerable plaques (reviewed in [109] and confirmed in the pig [525, 614]). At these sites, pig #206 revealed more advanced plaques also exhibiting the greatest increase in CX3CR1 expression. Furthermore, the arterial endothelium of pig #206 revealed pathological elevated structures dislocated of bifurcations possibly also atherosclerotic plaques or early aneurysms and tumors. Moreover, these pathological structures were also stained by Sudan IV (see * in figure 4.31). Altogether, these data indicated a direct correlation between plasma cholesterol level, CX3CR1 expression and coronary artery disease in pigs.

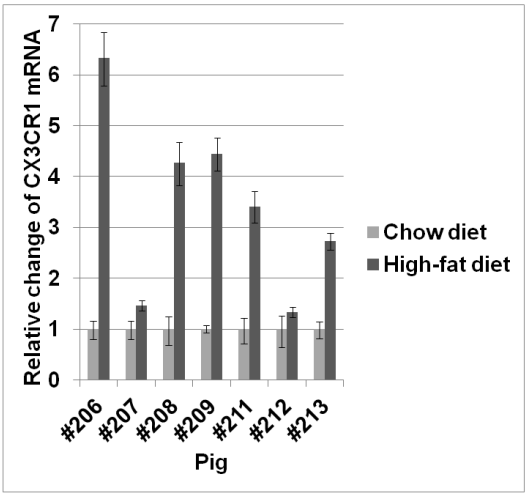

Figure 4.30: CX3CR1 expression determined from whole blood at chow and high-fat diet: Relative change of CX3CR1 mRNA for piglets #206–#213 relating to every single pig. Data were normalised to TBP expression. Relative standard deviations are indicated.

4.3 Fractalkine receptor project

Fractalkine receptor (CX3CR1) is a cell surface receptor involved in vascular inflammation during atherosclerosis. Inflamed endothelium activates platelets via CX3CR1 [126, 383] contributing to sub-endothelial recruitment of monocytes [127]. In addition, CX3CR1 supports adhesion and migration of monocytes [379] and accumulation of monocytes/macrophages [414, 393] important for formation [424], maintenance [425], neovascularisation [420] and instability of atherosclerotic plaques [100]. In coronary artery disease (CAD) patients, CX3CR1 expression was shown to be upregulated in peripheral blood mononuclear cells (PBMCs) [320], especially in the monocyte subpopulation [319] and was detected in both early and advanced stages of atherosclerotic plaques [322].

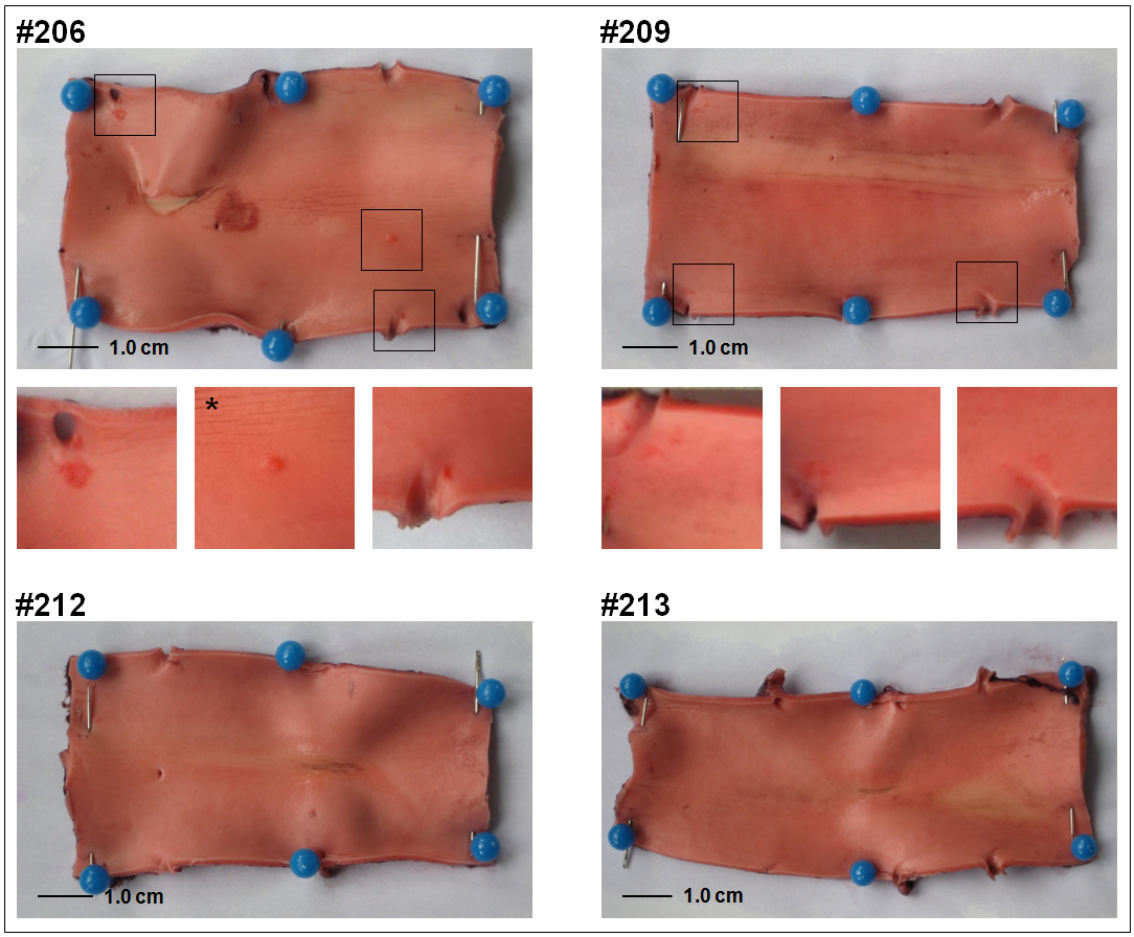

Figure 4.31: Sudan IV staining of porcine abdominal aortas: In pigs #206 and #209 red coloured areas indicated accumulation of lipoproteins, thus development of early atherosclerotic plaques. Pigs #212 and #213 showed no pathological indication. *: Pathological elevated structure, possibly atherosclerotic plaque, early aneurysm or tumor.

For cell imaging during atherogenesis, the reporter gene enhanced green fluorescent protein (EGFP) directed by porcine CX3CR1 promoter should be placed at ROSA26 genomic locus by gene targeting.

4.3.1 Genotyping of fractalkine receptor in German Landrace pigs

In the coding region of the human CX3CR1 gene two disease-related single nucleotide polymorphisms (SNPs) V249I and T280M were discovered [428], which are highly linked to each other [351]. The haplotype $I_{249}M_{280}$ is associated with a reduced risk of atherosclerosis and coronary artery disease (CAD) already at heterozygosity [351, 366], but with elevated risk of ischemic cerebrovascular disease at homozygosity [351, 353]. Independent of M_{280} allele, the I_{249} allele in the heterozygous state also decreases risk of atherosclerosis and CAD [351] and without the protective effect of M_{280} allele it is additionally associated with elevated risk of acute coronary syndrome (ACS) during CAD [431] and restenosis after stent implantation [355]. However, the I_{249} allele in both the homozygous and the heterozygous state promotes survival of acute myocardial infarction and decreases T-cell recruitment into infarct related artery [432].

The haplotype $I_{249}M_{280}$ revealed both a decreased binding affinity to labeled and soluble fractalkine (FKN) and density of FKN receptors compared to wild-type (WT) haplotype $V_{249}T_{280}$ with I_{249}-mediated reduced receptor expression [428]. In contrast, the haplotype $I_{249}M_{280}$ showed an I_{249}-mediated increased cell adhesion to membrane-bound FKN [430]. However, both SNPs are related to abnormal receptor functionality. For a I_{249} allele in the heterozygous state, the total number of fractalkine binding sites was decreased about $\sim$40% with reduced receptor expression and ligand binding affinity [427], for a M_{280} allele in the homozygous state, about $\sim$85% [428]. Furthermore, the M_{280} allele is associated with reduced cell-cell adhesion, FKN binding kinetics and FKN-induced chemotaxis [429].

For genotyping of analogue porcine SNPs V250I and T281M in pig #72, sows #175 and #178 and porcine adipose tissue-derived mesenchymal stem cells (pADMSCs) 110111, a PCR product of 554bp was amplified by PCR with the primers CX3CR1_poly_F1 and CX3CR1_poly_R1. The PCR products covering nucleotides for respective codons were sequenced and revealed a homozygous ATT coding for Isoleucine (I) at codon 250 and ACA for Threonine (T) at codon 281. Figures 4.32 and 4.33 display chromatograms of pig #72 with blue labeled nucleotides at codons 250 and 281 coding for Isoleucine and Threonine. All screened animals and pADMSCs 110111 revealed the haplotype $I_{250}T_{281}$. The frequency of the analogue human haplotype only ranges from $\sim$8–16% in different studies [366].

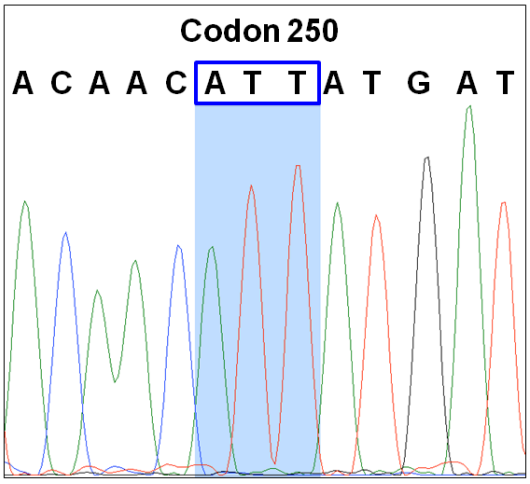

Figure 4.32: CX3CR1 genotyping by sequencing covering codon 250 of pig #72 (blue labeled): Nucleotides ATT coding for Isoleucine at respective site.

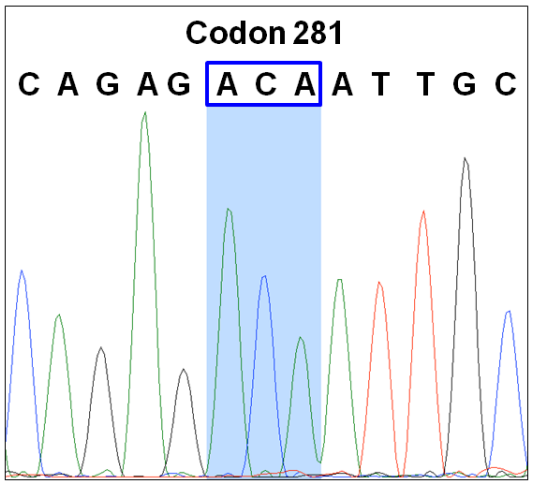

Figure 4.33: CX3CR1 genotyping by sequencing covering codon 281 of pig #72 (blue labeled): Nucleotides ACA coding for Threonine at respective site.

4.3.2 Fractalkine receptor expression analysis in different porcine cell types and tissues

In human, fractalkine receptor (CX3CR1) transcription was detected in natural killer (NK) cells, T-cells, monocytes, granulocytes [379], dendritic cells [380], mast cells [381] and platelets [383] from peripheral blood, also in endothelial cells [377] and in neurons, microglial cells and astrocytes from brain tissue [384, 385]. In mouse, CX3CR1 expression was also observed in peripheral blood monocytes, natural killer and dendritic cells and the brain microglia [615].

For validation of a specific expression of CX3CR1 in pig, semi-quantitative one-step RT-PCR was performed for different porcine cell types and tissues. Here, the primer pairs CX3CR1_RT_F1/CX3CR1_RT_R1 and GAPDH_F/GAPDH_R amplified products of 541bp and 536bp. Primer pairs were designed over exon junctions. Total RNA was isolated from pADMSCs, pKDNFs, pEFs and brain, kidney, lung and ear tissue. GAPDH RT-PCR revealed the expected product size for all samples (see figures 4.34 and 4.35), whereas CX3CX1 RT-PCR for brain, kidney, lung and ear tissue (see figures 4.36 and 4.37). For both, water control was negative. Although RT-PCR is only a semi-quantitative method of analysis, the results reflect the normalised CX3CR1 expression in human main tissues, whereas brain reveals stronger expression than kidney and lung (compare www.genecards.org). However, CX3CR1 expression was also detected in ear tissues of pigs #72 and #74. Compared to all analysed tissues, ear of pig #72 showed the strongest expression possibly indicating an upregulation in residual blood cells due to inflammation during an early atherosclerosis. In coronary artery disease (CAD) patients,

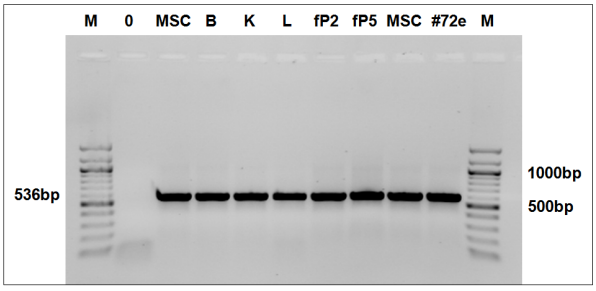

Figure 4.34: GAPDH RT-PCR: 536bp product amplified from pADMSCs (MSC), porcine brain (B), kidney (K) and lung tissue (L), pKDNFs of passage 2 and 5 (fP2, fP5) and ear tissue of pig #72 (#72e). 0: Water negative control; M: 100bp ladder.

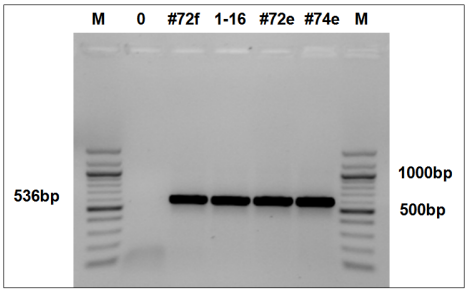

Figure 4.35: GAPDH RT-PCR: 536bp product amplified from pEFs of pig #72 (#72f), pADMSC cell clone 1-16 (1-16) and ear tissue of pigs #72 and #74 (#72e, #72e). 0: Water negative control; M: 100bp ladder.

upregulation of CX3CR1 expression was detected in peripheral blood mononuclear cells (PBMCs) [320], especially in the monocyte subpopulation [319]. Consistently, pEFs of pig #72, pADMSC cell clone 1-16, pADMSCs and pKDNFs revealed no expression of CX3CR1. For all cell types, only weak bands of unspecific products could be detected. These data verified a cell-specific expression of CX3CR1 in porcine tissues.

4.3.3 Transgene placement strategy and targeting vector

Targeted transgene placement was conducted by conventional homologous recombination into ROSA26 genomic locus. The promoter-trap vector comprised a promoter-less selectable cassette (SA BS) of 1.2kb and EGFP cDNA of 0.7kb under the control of porcine CX3CR1 promoter region of 4.9kb flanked by a 2.1kb short and 4.6kb long homology arm (HA) including exon 2 of ROSA26. After placement downstream of exon 1, the endogenous ROSA26 promoter would direct expression of the positive selectable marker BS, whereas inserted CX3CR1 promoter region would drive the expression of the reporter protein EGFP (see figure 4.38). ROSA26 locus was shown to be ubiquitously active in Cre reporter mouse strains utilising LacZ [616] or fluorescent proteins [617]. Furthermore, murine ROSA26 locus has adequate activity for live cell imaging within deep tissue layers revealing no toxicity of reporter proteins [618] and a homozygous disruption was demonstrated to be not lethal [619]. Recently, also the porcine ROSA26 locus was targeted showing ubiquitous expression of an inserted transgene in the pig [588, 620].

In human peripheral blood mononuclear cells (PBMCs), alternative splicing generates four transcript variants of CX3CR1 differing in their 5'-untranslated regions (UTR) and their expression levels. Each transcript features an universal exon coding a full open reading frame (ORF) and an additional exon containing a distinct functional promoter

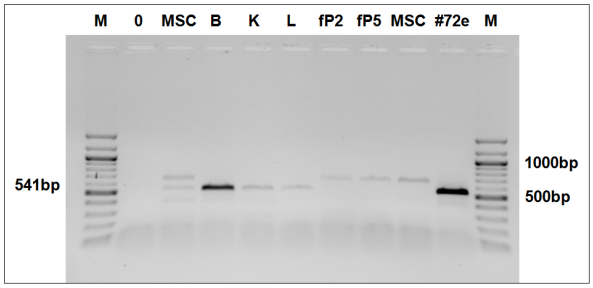

Figure 4.36: CX3CR1 RT-PCR: 541bp product amplified from porcine brain (B), kidney (K), lung (L) and ear tissue of pig #72 (#72e). MSC: pADMSCs; fP2, fP5: pKD-NFs of passage 2 and 5; 0: Water negative control; M: 100bp ladder.

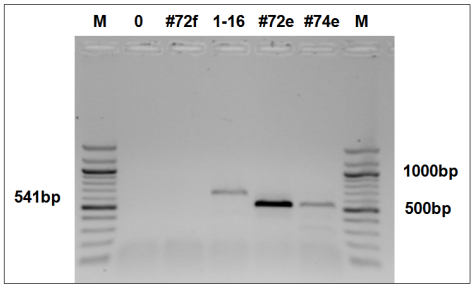

Figure 4.37: CX3CR1 RT-PCR: 541bp product amplified from ear tissue of pigs #72 and #74 (#72e, #72e). #72f: pEFs of pig #72; 1-16: pADMSC cell clone 1-16; 0: Water negative control; M: 100bp ladder.

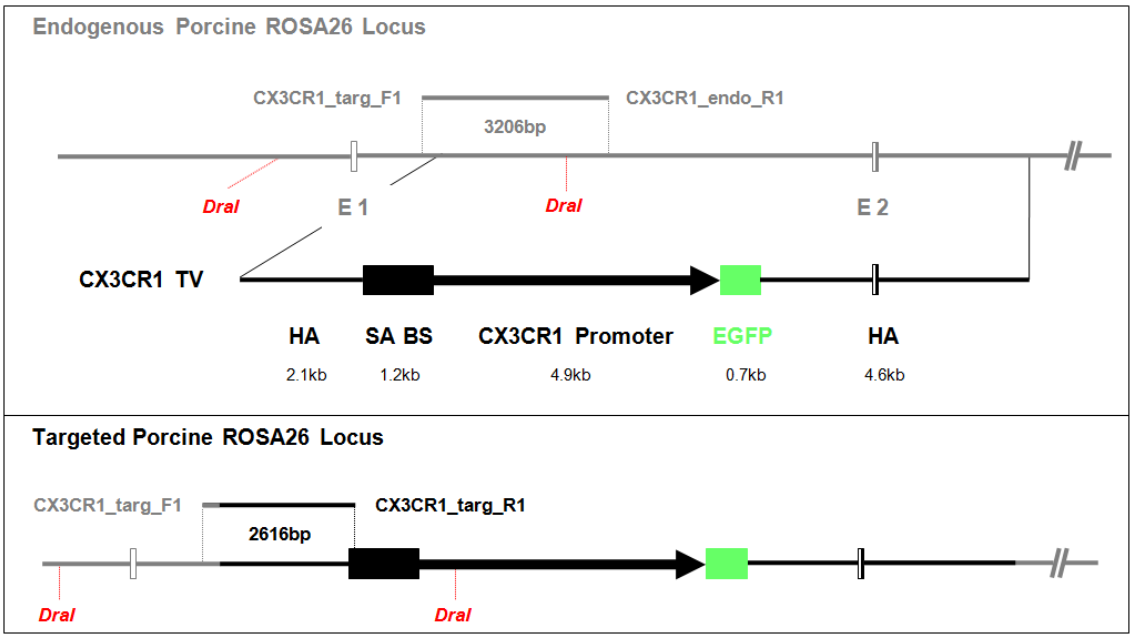

Figure 4.38: Gene targeting strategy and primer binding sites of endogenous and targeted porcine ROSA26 locus with respective PCR products: Endogenous ROSA26 locus with the first two exons (E1, E2) (gray labeled), CX3CR1 TV featuring promoter-less selectable cassette (SA BS) of 1.2kb, EGFP cDNA of 0.7kb driven by CX3CR1 promoter region of 4.9kb flanked by short and long homology arm of 2.1kb and 4.6kb (black/green labeled). Untranslated regions are labeled in white, coding regions in gray/black. Integration site, respective primers, primer binding sites and PCR product sizes are indicated. *DraI*: Restriction site for Southern blot (red indicated).

region. Two promoters reveal constitutive activities in a cell-specific manner [375, 376]. Thus, for directing EGFP expression the analogue porcine promoter region of the main human CX3CR1 transcript "V28" was used [375, 376]. The respective porcine promoter region was identified by 85% sequence homology of both the ORFs and 5'-UTRs.

As mentioned before, monocytes play a decisive role in atherogenesis differentiating into macrophages [128]. CX3CR1 expression was shown to be upregulated in monocytes of coronary artery disease (CAD) patients [319] and present in early and advanced stages of atherosclerotic plaques [322]. In contrast, in normal coronary arteries CX3CR1 expression could not be detected [323]. Within atherosclerotic plaques, hypoxia, low oxygen tension, was detected [621] promoting pro-atherosclerotic processes (reviewed in [622]). These progression of atherosclerosis is triggered by hypoxia-inducible factor 1 (HIF-1) (reviewed in [623]). However, in human atherosclerotic plaques hypoxia was detected in correlation with the presence of macrophages and the expression of HIF and vascular endothelial growth factor (VEGF). Both expressions were associated with plaque progression and intra-plaque angiogenesis [624]. HIF-1 was shown to recognise hypoxia-response elements (HREs) featuring a transcription factor binding site within the consensus sequence 5'-RCGTG-3' and a functionally essential sequence 5'-CACAG-3' [625]. The previously identified porcine promoter region also featured two of these HREs confirmed by sequencing of CX3CR1 targeting vectors utilising the primers CX3CR1_seq_F1 and CX3CR1_seq_R1. Since cell-specific expression CX3CR1 (see section 4.3.2) and also direct correlation between plasma cholesterol level, expression of analogue CX3CR1 transcript "V28" and coronary artery disease was demonstrated in pigs (see section 4.2.10), the used porcine promoter region was assumed to be functional.

4.3.4 Generation and genotype analysis of heterozygous targeted porcine cells

For targeted transgene placement of EGFP driven by CX3CR1 promoter region into ROSA26 genomic locus, pADMSCs 110111 P4 were transfected with linearised targeting vector CX3CR1 TV. After selection, single cell clones were analysed for CX3CR1 TV placement. Therefore, screening PCR (endogenous PCR and targeting PCR) was conducted with the primers CX3CR1_targ_F1 and CX3CR1_endo_R1, CX3CR1_targ_F1 and CX3CR1_targ_R1 amplifying PCR products of 3206bp and 2616bp, respectively. The forward primer CX3CR1_targ_F1 annealed to an intron-sequence downstream of exon 1, the reverse primer CX3CR1_endo_R1 to an intron-sequence between exon 1 and 2 substituted after CX3CR1 TV placement. The reverse primer CX3CR1_targ_R1 bound to the selectable cassette SA BS. All sequences, appropriate primers with their binding sites and expected PCR product sizes are indicated in figure 4.38.

The first transfection resulted in 58 single cell clones, of which seven (10, 16, 17, 43, 46, 48, 53) were positive for CX3CR1 TV placement, which was further confirmed by sequencing of correct targeting PCR products of cell clones 16 and 17. All cell clones could be expanded for nuclear transfer. Sufficient amounts of genomic DNA for further

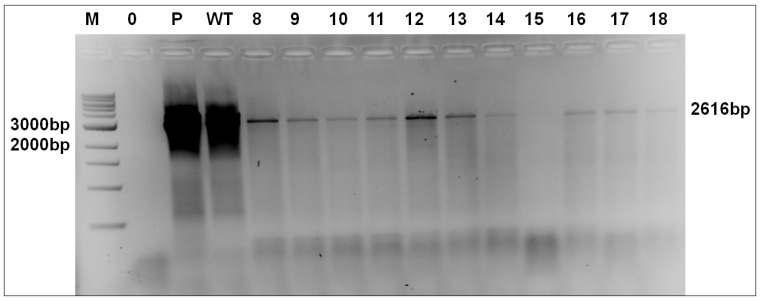

Figure 4.39: CX3CR1 endogenous PCR: 3206bp product amplified from heterozygous fetus #4 (P), wild-type positive control (WT) and single cell clones 8–14 and 16–18. 15: Single cell clone 15; 0: Water negative control; M: 1kb ladder.

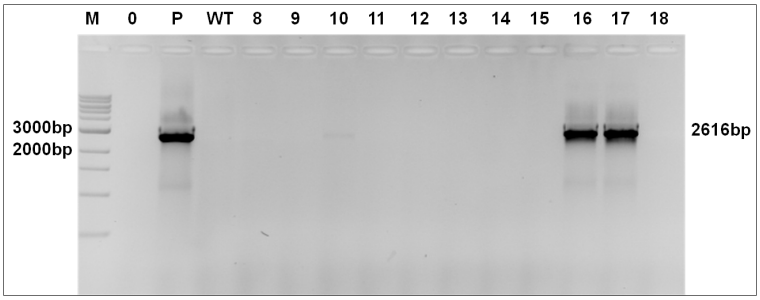

Figure 4.40: CX3CR1 targeting PCR: 2616bp product amplified from targeting positive control (P: heterozygous fetus #4) and single cell clones 10, 16, 17. 8, 9, 11–15, 18: Single cell clones; WT: Wild-type negative control; 0: Water negative control; M: 1kp ladder.

analysis like Southern blot could not be generated. Figures 4.39 and 4.40 show endogenous and targeting PCR with the expected PCR products indicating heterozygosity of ROSA26 alleles for the positively screened cell clones. Wild-type (WT) control was positive in endogenous PCR. For both PCRs, targeting control was positive and water control negative. For targeting positive control, gDNA of heterozygous fetus #4 was used, which had a dual fluorochrome cassette placed at the porcine ROSA26 locus [588].

4.3.5 Nuclear transfers, pregnancies and born animals

Generation of gene targeted animals was conducted by nuclear transfer followed by embryo transfer. For nuclear transfer, single cell clones 10, 16, 17, 43, 46 were pooled with a cell clone type from an unrelated experiment. Reconstituted embryos were transferred into a total of four sows establishing three pregnancies. Table 4.6 refers all trials of animal cloning with the used CX3CR1 cell clones, established pregnancies and offspring with respective genotypes and identities (#). In total, one healthy piglet (#260) and one stillborn piglet (#215*) were generated. The rather was used for pKDNFs isolation.

CX3CR1 cell clones	Pregnancy	Animal (genotypes, piglet ID)
10, 16, 17	+	1 piglet (ROSA26-EGFP$^{+/-}$, #260)
10, 16, 17	+	1 stillborn piglet (ROSA26-EGFP$^{+/-}$, #215*)
10, 17, 43, 46	-	0
10, 17, 43, 46	+	0

Table 4.6: Nuclear transfers of CX3CR1 project: Combinations of CX3CR1 cell clones (10, 16, 17, 43, 46), establishment of pregnancy and generated animals with their genotypes and identities (ID in #). -: No pregnancy; +: Pregnancy; $^{+/-}$: Heterozygosity.

4.3.6 Genotype analysis of nuclear transfer animals

Both the healthy piglet #260 and the stillborn piglet #215* were analysed genotypically by PCR and Southern blot. Screening PCR was performed as referred in section 4.3.4. Figures 4.41 and 4.42 show the endogenous PCR and targeting PCR with the expected product sizes for the screened piglets. Here, stillborn piglet #215* served as positive control for ROSA26 wild-type (WT) allele and CX3CR1 TV placement, piglet #269 as positive control for ROSA26 WT allele. In the endogenous PCR, all piglets (#215*, #260, #269) revealed the 3206bp product for WT allele. Targeting PCR amplified the 2616bp product for piglet #215* and #260. For both PCRs, water control was negative.

Since screening PCR confirmed CX3CR1 TV placement to the ROSA26 locus, but not the presence of EGFP cDNA within the CX3CR1 TV, a further PCR was conducted with the primer pair CX3CR1_LR_F1/EGFP_qPCR_R1 amplifying a PCR product of 664bp. The forward primer bound to CX3CR1 promoter region, the reverse primer to EGFP cDNA. In compliance with the previous screening PCR (see figures 4.41 and 4.42), piglet #215* and #260 showed the expected PCR product confirming the ROSA26-EGFP$^{+/-}$ genotype (see figure 4.43). Water control was negative.

Consistently, these data indicated both gene targeting of genomic ROSA26 locus and simultaneous presence of EGFP cDNA due to CX3CR1 TV placement in piglets #215* and #260.

Since EGFP expression in CX3CR1 cell clones, monocytes/macrophages isolated from whole blood of pig #260 and KDNFs of stillborn piglet #215* (ROSA26-EGFP$^{+/-}$ genotypes) could not be induced by hypoxia and validated visually under fluorescence microscope (see section 4.3.7), the respective cDNA sequence was analysed. Therefore, a PCR product of 1210bp was amplified with the primer pair CX3CR1_LR_F1/CMVpA_R. The correctness of EGFP cDNA sequence could be confirmed by sequencing.

To check the 5'-end structure of the CX3CR1 TV placement, Southern blot was performed. For detection of the promoter-less selectable cassette, the same BS probe was used as for LDLR Southern blot in section 4.2.9. Therefore, genomic DNA of pig #260 and stillborn piglet #215* was digested by restriction enzyme *DraI*. The utilised restriction sites within heterozygous targeted ROSA26 locus were located 1127bp upstream of

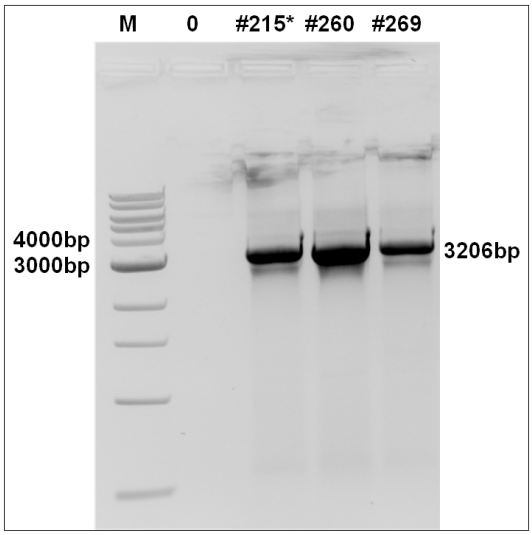

Figure 4.41: CX3CR1 endogenous PCR: 3206bp product amplified from piglets #215*, #260 and #269. Stillborn piglet #215* (ROSA26-EGFP$^{+/-}$) and piglet #269 served as positive controls. 0: Water negative control; M: 1kb ladder.

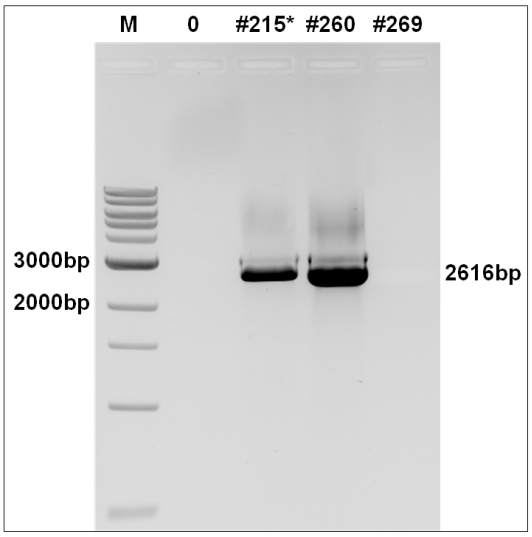

Figure 4.42: CX3CR1 targeting PCR: 2616bp product amplified from piglets #215* and #260. Stillborn piglet #215* (ROSA26-EGFP$^{+/-}$) served as positive control and piglet #269 as negative control. 0: Water negative control; M: 1kb ladder.

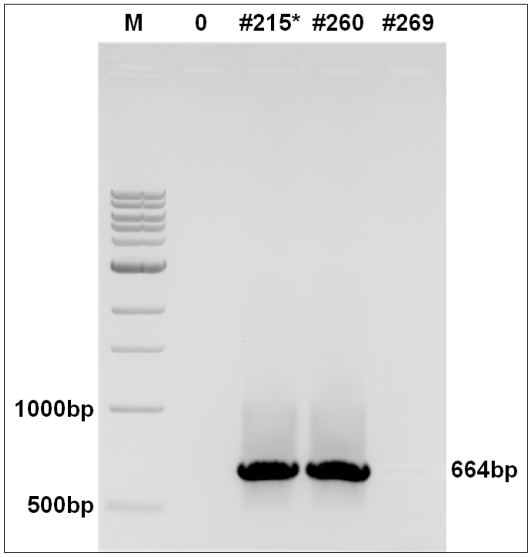

Figure 4.43: EGFP PCR: 664bp product amplified from piglets #215* and #260. Stillborn piglet #215* (ROSA26-EGFP$^{+/-}$) served as positive control and piglet #269 as negative control. 0: Water negative control; M: 100bp ladder.

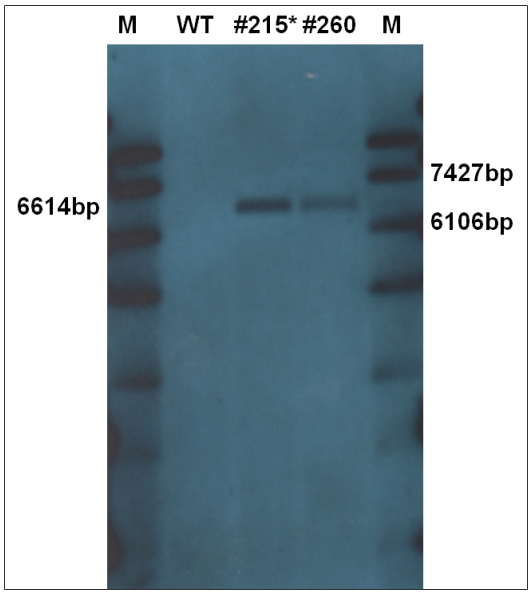

Figure 4.44: CX3CR1 Southern blot utilising BS probe: 6614bp fragment for CX3CR1 TV placement derived from *DraI* restriction enzyme digestion of genomic DNA of pig #260 and stillborn piglet #215*. Genomic DNA of pig #271 (WT) served as negative control. M: Southern blot ladder.

exon 1, 125bp downstream of short homology arm sequence substituted after CX3CR1 TV placement and 587bp downstream of 5'-end of CX3CR1 promoter region. Respective *DraI* restriction sites are indicated in figure 4.38. For CX3CR1 TV placement, a single fragment of 6614bp was expected. The endogenous fragment for WT allele was 4888bp. Genomic DNA of WT pig #271 served as negative control. Southern blot for both animals #260 and #215* revealed a single band of the expected 6614bp fragment. The control was negative (see figure 4.44). These data also indicated CX3CR1 TV placement.

4.3.7 Phenotype analysis of nuclear transfer animals

To prove functionality of the placed reporter gene EGFP driven by CX3CR1 promoter region, hypoxia assay was performed. Hereby, EGFP expression should be upregulated and validated visually under fluorescence microscope. Induction of CX3CR1 promoter, thus expression upregulation of CX3CR1 was demonstrated in human mesenchymal stem cells (MSCs isolated from bone marrow) cultured in 1% O_2 [626]. Moreover, CX3CR1 upregulation was also verified in peripheral blood mononuclear cells (PBMCs) of coronary artery disease (CAD) patients [320], especially in the monocyte subpopulation [319] differentiating into macrophages during atherogenesis [128]. CX3CR1 expression was detected in early and advanced stages of human atherosclerotic plaques [322], where hypoxia is correlating to the presence of macrophages and the expression of hypoxia-inducible factor (HIF) [624]. HIFs recognise hypoxia-response elements (HREs) [625], which were also identified in the porcine CX3CR1 promoter region. Therefore, hypoxia assay was performed with

CX3CR1 cell clones (pMSCs isolated from adipose tissue) and monocytes/macrophages isolated from whole blood of pig #260. Also KDNFs of stillborn piglet #215* were used. All cells featured the ROSA26-EGFP$^{+/-}$ genotype. Wild-type (WT) pADMSCs and WT monocytes/macrophages served as negative controls. However, EGFP expression could not be detected by fluorescence microscope (data not shown).

Since EGFP expression could not be validated by fluorescence microscopy, more sensitive analysis such as real time quantitative polymerase chain reaction (qRT-PCR) was performed for further characterisation. Therefore, RNA was isolated from CX3CR1 cell clones 16 and 17 (pADMSCs), monocytes/macrophages of pig #260 and KDNFs of stillborn piglet #215* featuring the ROSA26-EGFP$^{+/-}$ genotype. RNA isolated from WT pADMSCs and WT monocytes/macrophages were used as negative controls. To confirm specific isolation of monocytes/macrophages from porcine whole blood, the cell-surface marker CD14 was quantified and compared to cell types pKDNFs and pADMSCs. In human, the CD14 marker is expressed in all main blood monocyte populations (classical, intermediate and non-classical) [410]. Differing from section 3.4.5, only 100ng of RNA were transcribed and quantified using 2μl cDNA dilutions. Here, the primer pairs CD14_F1/CD14_R1, CX3CR1_RT_F1/CX3CR1_qPCR_R1, EGFP_qPCR_F1/EGFP_qPCR_R1 and TBP_F/ TBP_R amplified qRT-PCR products of 156bp, 160bp, 150bp and 153bp. Also differing, the annealing and elongation temperature was 62°C. All primer sets except the EGFP primer pair annealing to cDNA were designed over exon junctions. To exclude false positive detection of EGFP expression due to genomic DNA contamination of RNA isolations, one-step RT-PCR was conducted. The primer pair CD14_F1/CD14_R1 allowed for sensitive amplification of the expected RT-PCR product of 156bp and an additional product of 236bp at possible genomic DNA contamination. However, all RNA isolations finally revealed high quality additionally confirmed by melting curves after qRT-PCR.

In compliance with the proposed constitutive and cell-specific activity of CX3CR1 promoters [375, 376], low baseline EGFP expression was detected at varying levels within different cell types. Monocytes/macrophages of pig #260 exhibited 2-fold, whereas CX3CR1 cell clones 16 and 17 (pADMSCs) only 1.5-fold higher expression compared to pKDNFs of stillborn piglet #215*. Monocytes/macrophages derived from WT animal served as negative control (see figure 4.45).

Consistent with visual analysis by fluorescence microscopy the quantification of gene expression by qRT-PCR could detect neither CX3CR1 nor EGFP upregulation in monocytes/macrophages of pig #260 due to hypoxia (see figure 4.46).

However, specific cell isolation of monocytes/macrophages was verified by 170-fold and 200-fold higher expression of CD14 compared to negative control pKDNFs. The pADMSCs (WT and CX3CR1 cell clones 16 and 17) revealed a slightly higher 7-fold and 3-fold expression. Hypoxia even markedly increased the marker expression to 310-fold and 320-fold confirming cell response to hypoxic conditions (see figure 4.47). These data were consistent with the ∼100-fold expression level of CD14 above isotype control in flow cytometric

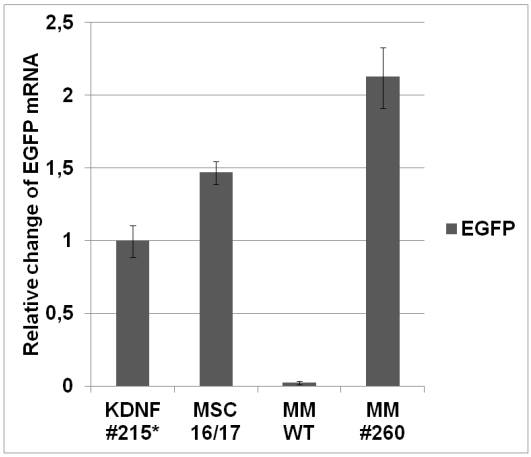

Figure 4.45: EGFP expression determined from different porcine cell types: Relative change of EGFP mRNA for pKDNFs of stillborn piglet #215* (KDNF #215*), CX3CR1 cell clones 16 and 17 (MSC 16/17) and monocytes/macrophages of wild-type animal (MM WT) and pig #260 (MM #260). Data were normalised to TBP expression. Relative standard deviations are indicated.

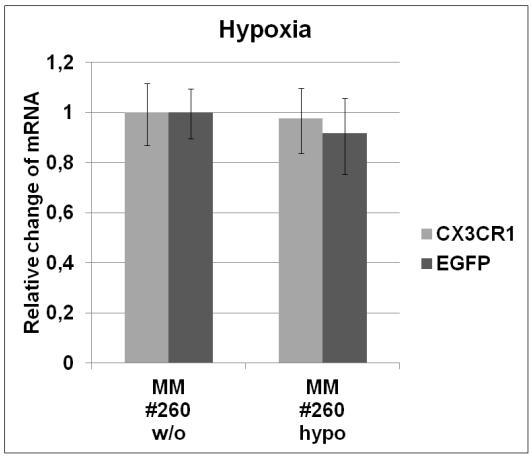

Figure 4.46: CX3CR1 and EGFP expression determined from monocytes/macrophages: Relative change of CX3CR1 and EGFP mRNA for monocytes/macrophages of pig #260 at normal (MM #260 w/o) and hypoxic conditions (MM #260 hypo). Data were normalised to TBP expression. Relative standard deviations are indicated.

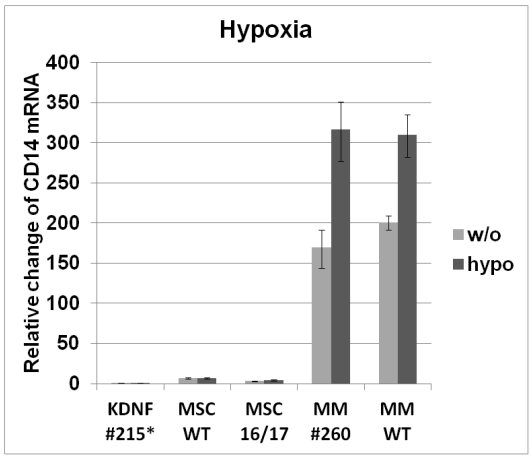

Figure 4.47: CD14 expression determined from different porcine cell isolations at normal and hypoxic conditions: Relative change of CD14 mRNA for pKDNFs of stillborn piglet #215* (KDNF #215*), wild-type pADMSCs (MSC WT), CX3CR1 cell clones 16 and 17 (MSC 16/17) and monocytes/macrophages of pig #260 (MM #260) and wild-type animal (MM WT). Data were normalised to TBP expression. Relative standard deviations are indicated.

analysis [410].

These data possibly indicate that the isolated monocytes seemed to be not responsible for an upregulation of CX3CR1 ascertained in CAD patients due to higher rates of CX3CR1 positive monocytes [319]. Compared to respective expression levels from whole blood of eleven pigs and ear tissue of 13 pigs, the CX3CR1 expression of the isolated monocytes/macrophages was low. They exhibited a 30-fold lower expression level compared to whole blood. Even ear tissue revealed a 4-fold higher expression (see figure 4.48).

Altogether, further analysis is needed for functional evidence of the reporter gene construct CX3CR1-EGFP placed by ROSA26 gene targeting. Since cell-specific expression of CX3CR1 and also direct correlation between plasma cholesterol level, CX3CR1 expression and coronary artery disease in pigs was demonstrated, a feeding study of pigs featuring ROSA26-EGFP$^{+/-}$ genotype is highly recommended.

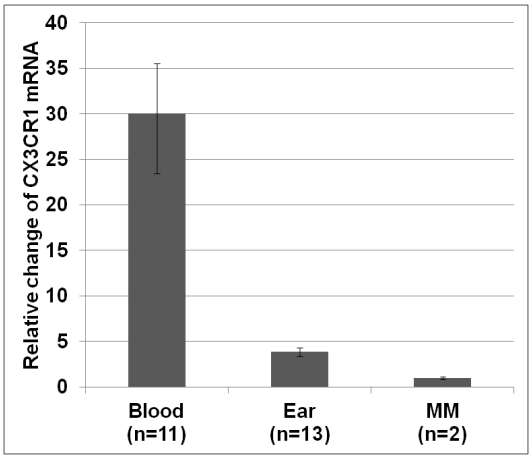

Figure 4.48: CX3CR1 expression determined from different tissues and cells: Relative change of CX3CR1 mRNA for eleven, 13 and two specimen of whole blood (Blood), ear tissue (Ear) and monocytes/macrophages (MM). Data were normalised to TBP expression. Relative standard deviations are indicated.

CHAPTER 5

Discussion

Cardiovascular diseases (CVDs) are the leading cause of death worldwide. The basic reason for this is the advanced atherosclerosis generating various life-threatening plaque classes in the arterial vasculature. Rupture-prone vulnerable plaques cause acute thromboses, which are responsible for about 60% of sudden coronary deaths. The most common animal models for atherosclerosis, the ApoE$^{-/-}$ and the LDLR$^{-/-}$ mice, do not resemble a human-like atherosclerosis with regard to susceptibility of coronary arteries and complications of plaque rupture and thrombosis. Overcoming these limitations, the pig is considered the most promising animal model bridging the gap between small animal models and human clinical trials.

The aim of this work was the generation of a porcine atherosclerosis model of vulnerable plaque. The two genes APOE and LDLR were to be disrupted and the reporter gene EGFP driven by the cell-specific porcine CX3CR1 promoter was to be placed at the endogenous ROSA26 locus.

5.1 Atherosclerosis at chow diet in the common mouse models and the LDLR$^{-/-}$ pig model

At regular chow diet (low fat, low cholesterol), the ApoE$^{-/-}$ mice exhibit plasma cholesterol level of 305–563$\frac{mg}{dL}$ and already spontaneously develop a reproducible pattern of complex and human-like lesions. In contrast, wild-type mice as well as heterozygous knockout mice reveal almost the same plasma cholesterol levels of 66–106$\frac{mg}{dL}$, 66–110$\frac{mg}{dL}$, respectively and show no pathology of the proximal aorta [444]. Within young mice at an age of 3–4 months, early lesions comprising deposits of foam cells and lipids initially occur at the aortic sinus. By 5–7 months of age, lesions increase their size, spread over proximal

ascending aorta and show deposits of multi-layered foam cells and occasionally intimal smooth muscle cells and cholesterol clefts. At an age of 8–10 months, some advanced lesions exhibit fibrous cap formation, smooth muscle cells covered necrotic cores, calcification and severely occlude the coronary ostium and even narrow the lumen of coronary arteries. Fibrous cap lesions are often present in abdominal aorta, aortic bifurcation, iliac arteries and carotid arteries and small vascular lesions also in pulmonary arteries [477]. However, high rates of luminal narrowing are exclusively detected in the peripheral arteries of 60 weeks aged homozygous mice [627]. In the brachiocephalic artery, stenotic lesions lack fibrous caps and necrotic cores and show extensive medial erosion, but thrombosis and platelet adhesion is always absent. Although high frequent and variable intra-plaque hemorrhage is detected in lesions of 30–60 weeks aged mice, the plaques show no evidence of fissure or rupture [475]. Even at an age of 60 weeks, the right and left coronary artery including the first level branches, the disease-prone sites in human, are still free of lesions. Early lesions only occur in smaller and intra-myocardial vessels, whose rare occlusions are not able to induce myocardial infarction [479].

For the LDLR$^{-/-}$ mice, there are no systemic studies of developmental lesional pathophysiology. At regular chow diet, the homozygous knockout mice exhibit plasma cholesterol levels of 226–242$\frac{mg}{dL}$, the heterozygous mice 142–150$\frac{mg}{dL}$ and the wild-type mice 104–112$\frac{mg}{dL}$ [447]. After 12 month, no grossly visible plaques arise in the aortic arch and only small infiltrations of intimal foam cells are present in the coronary sinuses [628].

Overcoming the disadvantages of the existing pig models for coronary atherosclerosis (see section 1.5.2), recently LDL receptor knockouts were generated in different breeds of miniature swine in Japan [579] and in the United States [523, 578], where they are even commercially available (www.exemplargenetics.com). At a standard chow diet (low fat, no cholesterol) for 26 weeks, both the homozygous (LDLR$^{-/-}$) and the heterozygous knockout pigs (LDLR$^{+/-}$) develop significantly elevated total cholesterol levels of 533–601$\frac{mg}{dL}$ and 95–101$\frac{mg}{dL}$ compared to 60–74$\frac{mg}{dL}$ of wild-type controls [523]. After six month, atherosclerotic lesions comprising foam cells, inflammatory cells and smooth muscle cells develop in the aorta, carotid, femoral and coronary arteries of LDLR$^{-/-}$ pigs [579]. After seven month, proximal and distal abdominal aortas are 45% covered with raised atherosclerotic lesions featuring areas of foam cells and necrosis. The coronary arteries show small foam cell lesions as well as intimal thickening predominantly in proximal portions [523] and even calcium deposits and a small mural thrombus [579].

5.2 Diet-induced atherosclerosis in the common mouse models and the LDLR$^{-/-}$ pig model

By feeding an atherogenic diet, the development of atherosclerosis can be considerably accelerated in ApoE$^{-/-}$ mice evolving dramatically increased plasma cholesterol levels [445, 478]. A detailed sequence of lesion development as well as the anatomic location

of arising lesions were analysed in homozygous mutants by feeding either a Western-type diet (high fat, low cholesterol) or regular chow diet for 40 weeks. Within this period, values of total plasma cholesterol range from 1085 to 4402$\frac{mg}{dL}$, 360 to 885$\frac{mg}{dL}$, respectively. Atherosclerotic lesions first develop in aortic root, the lesser curvature of the aortic arch, the branches of the brachiocephalic artery, the right common carotid artery, the branches of the superior mesenteric artery, both renal arteries, the aortic bifurcation, and the pulmonary artery and later in descending thoracic, lower abdominal, proximal coronary, common iliac, and femoral arteries. Generally, mice at Western-type diet exhibit wider lesion areas and develop more advanced lesions at each developmental stage than mice at regular chow diet. Advanced fibrous plaques narrow the arterial lumen up to 95%. However, in Western-type diet fed, six weeks old mice, adhesion of monocytes to endothelium and sub-endothelial foam cell accumulation is observed. Foam cell lesions arise at eight weeks of age and early fibrous plaques at 15 weeks of age. They feature extra-cellular matrix embedded smooth muscle cells covering a necrotic core with foam cells. At an age of 20–40 weeks, advanced fibrous plaques appear featuring calcification and protrusion into vessel media. In contrast, regular chow diet fed mice reveal delayed lesion formation. Here, monocytes first adhere at an age of eight weeks and foam cell lesions arise at an age of ten weeks still present at an age of 30 weeks. Early fibrous plaques develop at 20 weeks of age. The advanced fibrous plaques show less medial destruction and no calcification. Nevertheless, plaque rupture can not be observed for both feedings [476]. Corresponding to high rates of luminal narrowing in the peripheral arteries at regular chow diet, a highly consistent rate of stenotic lesions was also detected exclusively in peripheral arteries of 60 weeks aged homozygous mutants at a Western-type diet (high fat, low cholesterol). Here, the highest severity predominantly occurs in external carotid arteries. In contrast to human, especially the ascending aorta compensate lumen narrowing by dilation in response to lesion growth [627]. Interestingly, ApoE$^{-/-}$ mice with an unusual genetic background and fed a supplemented lard diet (high fat, low cholesterol) for up to 59 weeks develop acute atherosclerotic plaque rupture often accompanied with luminal thrombosis at the branches of brachiocephalic artery [629, 630]. However, plaque rupture and thrombosis is not associated to sudden death events [629].

When LDLR$^{-/-}$ mice are fed an atherogenic and pro-inflammatory modified Paigen diet (high fat, high cholesterol, cholic acid), the plasma cholesterol levels after two weeks rise to 1820–2006$\frac{mg}{dL}$, 220–328$\frac{mg}{dL}$ and 131–157$\frac{mg}{dL}$, respectively. After seven month, the homozygous knockout mice develop considerably xanthelasma, xanthomatous infiltration of the ears, ventral xanthomas and footpad thickening. Elevated lipid-rich plaques extend over the entire aortic arch and massive atheromas with advanced lipid-rich cores and infiltrated foam cells were detected in the aortic root, proximal aorta, coronary sinuses, proximal coronary arteries and occasionally in the main pulmonary trunk [628].

When homozygous (LDLR$^{-/-}$), heterozygous knockout pigs (LDLR$^{+/-}$) and wild-type pigs are fed a high fat, high cholesterol diet for 180 days, cholesterol levels successively

increase to 913–1007$\frac{mg}{dL}$, 232–416$\frac{mg}{dL}$ and 137–185$\frac{mg}{dL}$, respectively. After 90 days, the proximal and distal abdominal aorta of LDLR$^{-/-}$ pigs have significantly increased surface areas of raised lesions as well as intimal areas compared to LDLR$^{+/-}$ and wild-type pigs. Aortic lesions comprise foam cells, cholesterol clefts and calcification. After 180 days, also proximal and distal coronary arteries of LDLR$^{-/-}$ pigs show significantly larger areas of intimal thickening and percent stenosis. Arisen complex atherosclerotic lesions feature foam cells, fibrous caps, calcification and hemorrhage [523]. However, already after four month, LDLR$^{-/-}$ pigs develop complicated stenotic and human-like unstable atherosclerotic plaques in the coronary arteries featuring necrotic cores, fibrous caps, cholesterol clefts, calcium deposits, neovascularisation, plaque hemorrhage, media rupture, adventitia inflammation and expansive vascular remodeling [579].

5.3 Limitations of the ApoE$^{-/-}$ and LDLR$^{-/-}$ mouse models

Beside modulating the lipoprotein metabolism, especially ApoE has several additional anti-atherogenic functions (reviewed in [164, 170]). Since ApoE within the arterial wall decelerates atherosclerosis [212, 213, 214, 215, 216, 217] and regresses atherosclerosis [594] even at low expression [200, 201] and independently on lowering the plasma cholesterol levels [200], the ApoE$^{-/-}$ mice is not suitable for bone marrow transplantation.

Additionally, males of both ApoE$^{-/-}$ and LDLR$^{-/-}$ mice develop more frequently aortic lesions than females with correlating extend between the entire aorta and the aortic root [631]. In contrast, the females generate larger lesions at the aortic sinus than males [632].

Both the ApoE$^{-/-}$ and LDLR$^{-/-}$ mice have been extensively utilised for the reexamination of clinically relevant therapeutic modifiers against risk factors hypercholesterolemia, hypertriglyceridemia, hypertension, and inflammation and for their respective extend of anti-atherogenic effects. However, these mice respond differentially to specific experimental manipulations and also reveal paradoxical effects on atherosclerosis. For example in ApoE$^{-/-}$ mice, clinically established cholesterol-lowering drugs, statins (3-hydroxy-3-methylglutaryl coenzyme A reductase inhibitors), often do not decrease and even increase total plasma cholesterol, but still reduce the aortic lipid deposition (reviewed in [436]). Contrary, a statin-mediated lowering of total plasma cholesterol even with an additional elevation of athero-protective high-density lipoprotein (HDL) cholesterol was reported to have no effect on size and number of aortic lesions [633]. In LDLR$^{-/-}$ mice, statins were shown to reduce aortic atherosclerosis with or without lowering the plasma cholesterol levels. Thus, the choice of a mouse model is crucial for examining the mode of action of therapeutic drugs (reviewed in [436]). In contrast, translational utility of statins (Atorvastatin) was demonstrated in LDLR$^{+/-}$ pigs fed a high fat diet for six month. Here, drug administration significantly attenuate weight gain and reduce total cholesterol, HDL and low-density lipoprotein (LDL) without affecting very low-density lipoprotein (VLDL) levels. Adverse effects concerning liver function were not observed [634].

Furthermore, hemodynamic differences within the vasculature induce site-specific gene expression profiles of endothelial cells modulating different atherogenic responses to systemic risk factors such as hypercholesterolemia, oxidative stress, genetic background, gender and immune status. Thus, specific treatments can differentially affect lesion development at athero-susceptible sites (reviewed in [632]). For example, immune deficiency within male ApoE$^{-/-}$ mice reduce lesion area in the aortic root but not in the brachiocephalic artery [635]. There is a similar finding for male LDLR$^{-/-}$ mice featuring the same genetic background. Here, the immune deficiency reduce atherosclerosis in the aortic sinus but also not in the brachiocephalic artery [636]. Accordingly, for studying treatment-mediated effects on atherosclerosis, the susceptible vascular sites have to be chosen (reviewed in [632]). Introducing additional genetic manipulations can influence site-specificity of lesion development dependent of the diet. At regular chow diet, the knockout of recombinase activating gene 1 (RAG1) in the ApoE$^{-/-}$ Rag1$^{-/-}$ mouse account for ∼25% reduction of aortic root lesion area, whereas at Western-type diet (high fat, low cholesterol), no significant difference at this site is generated [637].

Murine models for atherosclerosis have their place in identification of therapeutic targets for preventive medicine. Although genetically modified mice develop atherosclerosis with human-like lesions, they markedly differ in distribution of lesions throughout vasculature and they fail to generate plaque rupture and thrombosis. Thus, other animal models have to be developed for investigating molecular and cellular mechanisms of these acute human complications, which will allow for the treatment of symptoms first appearing in late stage disease.

5.4 Polymorphisms associated with atherosclerotic diseases and complications

In this work, several pigs of various breeds were screened for common human single nucleotide polymorphims (SNPs) in the APOE and CX3CR1 gene and for a known porcine mutation of the LDL receptor gene. The ApoE4 isoform was detected in a homozygous phenotype for all 27 pigs of the three breeds German Landrace, Goettingen Minipig and Schwäbisch Hall Domestic (see section 4.1.1). In compliance, this finding was reported for a total of 128 pigs of eleven pig breeds [5]. In contrast, the human distribution of the homozygous ApoE4 phenotype ranges from ∼1–11% in different European Caucasian populations [233]. In humans, ApoE4 (genotypes $\epsilon 4/4$ and $\epsilon 2/4$) is associated with an up to 6.4 years shorter life expectancy [177] and a 42% higher risk of cardiovascular disease (CVD) [173]. In the pig, ApoE4 seems to be sufficient to trigger a high fat, high cholesterol diet (HFHC)-induced atherosclerosis with increased levels of total and low-density lipoprotein (LDL) cholesterol [5].

For CX3CR1, all screened pigs showed the haplotype $I_{250}T_{281}$ in a homozygous manner (see section 4.3.1). In human, the analogue haplotype $I_{249}T_{280}$ only ranges from ∼8–16%

in different studies [366]. Here, the I_{249} allele already in a heterozygous state promotes the survival after acute myocardial infarction and decreases T-cell recruitment into infarct related artery [432]. Without protective effect of the T_{280} allele, I_{249} elevates the risk of acute coronary syndrome (ACS) during coronary artery disease (CAD) [431] and restenosis after stent implantation [355].

In the LDL receptor gene, the missense mutation (C→T) causing amino acid substitution (Arg→Cys) at Arg_{115} and thus contributing to familial hypercholesterolemia in pigs [512, 513, 514] could not be detected in any of the 27 screened animals (see section 4.2.1). This finding was expected since substitution of Arg_{115} is not a common polymorphism.

Especially, the homozygous genetic background of ApoE4 isoform and CX3CR1 haplotype $I_{250}T_{281}$ make the pig an excellent model not only for atherosclerosis and CVD but also for disease- and treatment-related complications. Furthermore, it could be applied for the research of Alzheimer's disease (AD), other neuropathological disorders and traumatic brain injury [638]. ApoE4 is a major genetic risk factor for AD [174, 175] and enhances the production of the β-amyloid peptide (Aβ) [639], whose extra-cellular deposits in the brain are a hallmark pathology for disease diagnosis [640]. In neuronal cells, it potentiates Aβ-induced lysosomal leakage and apoptosis by destabilising cellular membranes [641, 642]. Furthermore, neuronal-synthesised ApoE4 is susceptible to proteolysis in the secretory pathway [643]. The fragments are translocated to the mitochondria and cause mitochondrial dysfunction and neurotoxicity [644] and decrease the density of dendritic spines [645]. They also contribute to the intra-neuronal formation of neuro-fibrillary tangles (NFTs) consisting of phosphorylated microtubule binding protein tau, a further AD hallmark [646].

5.5 The use of porcine adipose tissue-derived mesenchymal stem cells

The gene targeting experiments of all three projects (APOE knockout, LDLR knockout, CX3CR1-EGFP placement) were conducted in porcine mesenchymal stem cells (MSCs) derived from adipose tissue, which were proven to efficiently produce healthy offspring after somatic cell nuclear transfer (SCNT). These porcine adult pluripotent cells were also isolated specifically as adherent cells from bone marrow and were successfully differentiated *in vitro* into the lipogenic, chondrogenic and osteogenic mesodermal lineage [647] fulfilling important criteria for defining mesenchymal stem cells [648]. Their proliferation rate in the undifferentiated state could be significantly increased with increasing concentrations of foetal bovine serum (FBS) and low oxygen tension [647]. They could be proliferated extensively up to 30–40 cell doublings until senescence [647, 649] retaining a normal diploid karyotype [649]. Porcine MSCs were also shown to be suited for stable genetic modification and SCNT [647, 649]. Additional supplementation of fibroblast growth factor 2 (FGF-2) was demonstrated to extend the life span of human MSCs to about 70 doublings and retain

their differentiation potential for more than 50 doublings *in vitro* [650]. Studies in our lab confirmed these results with porcine MSCs allowing for 73 doublings and producing a more stable karyotype [651]. Their high plasticity and maintaining proliferation in tissue culture make them an excellent choice for gene targeting. Compared to the commonly used fibroblasts, these less differentiated porcine MSCs were hypothesised to increase cloning efficiency after SCNT and were already shown to double the embryo blastocyst development [584]. These porcine MSCs could be genetically modified *in vitro* and were capable to generate gene targeted live pigs with a latent mutant $p53^{R167H}$ [585] and a mutant APC^{1311} allele [587].

5.6 Conventional gene targeting and efficiencies

Gene targeting allows for any modification of a specific gene (e.g. introduction of mutations or disruptions). In this regard, homologous recombination (HR) facilitates the insertion of cloned DNA sequences into the chromosome resulting in insertion, deletion, or replacement. Typically, HR is a rare event in adult mammalian cells and occurs in only one cell per $10^5 - 10^7$ treated cells. In contrast, random integrations happen at a higher frequency of one cell per $10^2 - 10^5$ treated cells. Thus, random integrants overshadow the targeted recombinands more than 1000-fold [652]. Though, positive selection by a promoter-less resistance gene neomycin was shown to increase gene targeting in fibroblasts by the factor of 100 [653]. The advancement of positive negative selection (PNS) utilising a positive and an additional negative selectable marker produced further but limited 10-fold enrichment in fibroblasts and enabled for gene targeting frequency of 32% [596]. Contrary, in embryonic stem (ES) cells, solely the use of promoter-less neomycin as a positive selectable marker could generate a gene targeting frequency of 78% [654]. Within these cells, also PNS was more efficient and enriches gene targeting 2000-fold [597]. Although validated porcine embryonic cell lines have not been established to date [592], the available porcine mesenchymal stem cells (MSCs) were a promising alternative.

Beside cell choice, the targeting frequency is highly dependent of the extent of homology between targeting vector and target locus. In a range of 2–10kb vector homology, the targeting frequency was shown to enhance exponentially in ES cells and reach a 100-fold increase with saturation at 14kb. Here, the use of isogenic DNA was 4–5 times more efficient than non-isogenic DNA [655]. With the use of isogenic homology arms, even an up to 20-fold higher targeting frequency was demonstrated [654]. In this work, the cloning of targeting vectors from isogenic genomic DNA was not possible. The required sequences have to be amplified from bacterial artificial chromosomes (BACs) containing non-isogenic Duroc pig DNA and the targeting vectors comprised short and long homology arms of 1.6–2.5kb, 4.6–12.3kb, respectively.

As already mentioned, the promoter-trap strategy has emerged to be the most efficient targeting method for actively transcribed genes. This system provides a promoter-

less positive selectable marker (e.g. neomycin or blasticidin resistance gene) conditionally expressed from the endogenous promoter following homologous chromosomal insertion [654, 653, 656]. Since porcine adipose tissue-derived mesenchymal stem cells (pADMSCs) expressed the target genes APOE, LDL receptor and ROSA26, this strategy was conducted and achieved efficiencies of 0% (0/302), 25% (5/20) and 12% (7/58), respectively. Consistently, a promoter-trap strategy in porcine MSCs resulted in a gene targeting frequency of 9.3% [585]. However, for the ROSA26 locus in porcine MSCs derived from bone marrow and adipose tissue, others reported gene targeting frequencies of even 48% and 42% [588].

5.7 Optimisation of conventional APOE gene targeting

Gene targeting of APOE with the use of promoter-trap strategy even after optimising modifications of the targeting vector and upregulation of the target gene transcription was unsuccessful. For optimisation of the targeting vector, first the 5'-homology arm was screened for an enhancer element potentially driving positive selectable marker in random integrants [595]. In mammalian cells, such a transcriptional active instead of an inactive resistance gene was shown to enrich the number of random integrations detected and decrease the number of homologous recombinants by the factor of 100 [656]. However, depending on analysed cell type, a transcriptional regulatory region within APOE gene locus was identified to enhance gene expression ∼3–5-fold [595]. Therefore, a 0.9kb sequence within the first intron containing this region was removed from the 5'-homology arm of the initial targeting vector.

Second, targeting vectors containing repetitive sequence elements decrease the probability of homologous recombination (HR) at the specific gene locus [657]. Homologies of >10kb were shown to possibly reduce targeting efficiency [658]. Since minimal repetitive homologies were recommended [657], 4.5kb of repetitive sequences were excised from the 3'-homology arm of the targeting vector.

Third, positive negative selection (PNS) strategy was shown to enrich gene targeting 10-fold in fibroblasts [596] and even 2000-fold in ES (embryonic stem) cells [597]. For this strategy, the visual negative selectable marker CAGGS Cherry NLS (CCN) was cloned downstream of 3'-homology arm of the targeting vector. This allowed for negative selection against random, non-homologous integrants, which could be visually detected and omitted from screening revealing in an enrichment of targeted recombinands.

Since a direct enhancement of locus specific HR in mammalian cells was observed when transcription levels of the target gene were increased [598], this strategy was also tested for APOE. Cyclic AMP and retinoic acid were demonstrated to synergistically potentiate APOE expression 7.5-fold in a astrocytoma cell line (U87 cells) [599]. Although the stimulatory effect followed a cell-specific manner [598], an up to ∼5-fold increase in APOE transcription was stimulated in porcine adipose tissue-derived mesenchymal stem cells

(MSCs) after a treatment of 96h (see figure 4.5). But again, no positive targeted cell clones could be identified. Since it was found that a 64-fold and 14-fold increase in transcription only resulted in 22-fold and 4-fold enhancement of recombination [598], the achieved ∼5-fold transcription stimulation is assumed too low. The treatment with the morphogenetic and teratogenic retinoic acid was also too harmful for the cells resulting in only few growing single cell clones after transfection with the targeting vector.

5.8 Transcription activator-like effector nuclease-mediated APOE gene targeting

Since APOE could not be disrupted by a conventional promoter-trap strategy, gene targeting should be mediated by transcription activator-like effector nuclease (TALEN)-induced double strand break (DSB) stimulating subsequent introgression of donor plasmids by homology-directed repair (HDR) [602]. TALENs are site-specific nucleases consisting of modular and programmable DNA-binding domains and a coupled homo-dimer domain of FokI restriction endonuclease [578, 659]. The binding domain is arranged in nearly identical tandem repeats, the TALE repeats, which typically feature 34 amino acids. Hypervariable amino acids at position 12 and 13 determine recognition specificity of one DNA base-pair at the target site [660, 661]. This allows for a fast and cheap assembly of custom TALENs [606, 662, 663] featuring low specificity-related cytotoxicity [664]. Once a TALEN pair bound its recognition site, the two FokI catalytic domains dimerise and introduce a DSB in the DNA [600] dramatically enhancing homologous recombination (HR) in mammalian cells [601]. Beside HR, the DNA repair mechanisms also comprise non-homologous end joining (NHEJ) [665, 666], which often results in small deletions, insertions and even chromosomal translocations [667] and predominantly occurs in mammalian cells [668]. Thus, two-thirds of NHEJ cause frame shifts and disrupt encoded proteins [578].

TALENs were used for efficient gene knockouts in livestock including cattle, pig and goat [602, 578]. Here, the injection of TALEN mRNAs into zygote cytoplasma generated gene knockouts in up to 75% of analysed embryos, which also featured bi-allelic gene modifications. Mono- and bi-allelic modifications were observed in 54% and 17% of primary fibroblast colonies after a laborious transposon co-selection procedure [578]. Enabling a more comfortable selection and a precise gene editing (HR instead of NHEJ), primary fibroblasts were transfected with combined TALEN mRNAs and oligonucleotide templates. After TALEN-mediated allele introgression and drug-selection, gene targeting efficiencies of 10–50% were achieved [602]. Fibroblasts of both approaches were capable to generate Ossabaw pig clones with modified alleles of LDL receptor [578] and adenomatous polyposis coli (APC) [602]. Furthermore, the use of TALEN expression constructs (DNA) in combination with donor plasmids bearing either a promoter-less or a PGK-promoter driven selection cassette enabled targeting efficiencies of 50% in both embryonic stem (ES) cells and induced pluripotent stem cells (iPSCs). The received cell clones were targeted in a

single or both alleles and were negative for transgene random integration [603].

In this work, APOE was successfully inactivated *in vitro* utilising TALEN expression constructs and a PGK donor plasmid. With a targeting frequency of 13% in one experiment, in total four positive single cell clones were received, three of which were homozygous and one was heterozygous for the targeted allele (see section 4.1.5). However, including all transfection experiments, the efficiency decreased to only 3%, which is low compared to the reported targeting frequency range of 2–55% [602, 606, 578, 603]. Nevertheless, this approach successfully produced mono- and bi-allelic knockouts of the difficult target gene APOE, which were derived by TALEN-induced introgression of donor plasmids and additionally were deficient in NHEJ-induced target gene alterations and random integration of the TALEN expression construct. The high rate of homozygous compared to heterozygous modifications (3:1) mirrored the dynamic nature of gene targeting. Here, TALEN cleavage and re-cleavage were repeatedly repaired by HR with the sister chromatid till the donor plasmid lacking the TALEN recognition site introgressed [602]. With up to 50%, HR is the major repair mechanism in mammalian cells [669]. Although *in silico* analysis predicted no off-targets, the TALENs effected high cytotoxicity. Compared to the conventional gene targeting, fewer single cell clones with lower proliferation rates were received after drug-selection. For enrichment of targeting events against random integrations, also positive negative selection was conducted utilising the visual negative selectable marker CAGGS Cherry NLS (CCN).

To enhance the targeting frequency, a cold shock was performed. An incubation at 30°C for 72h after transfection was reported to increase cleavage efficiency in livestock fibroblasts [578, 604, 605]. Compared to standard incubation at 37°C, such a treatment could ∼2–5-fold enhance percentage of TALEN-induced and NHEJ-mediated minor insertions and deletions (indels) at an endogenous locus, but efficiencies highly depended on target gene and TALEN scaffold [578, 604].

Additionally, various truncations at the N- and C-terminus of the native TALE protein were shown to enhance TALEN activity [664, 604]. Nevertheless, the length of the N-terminus was found to inversely correlate with transcriptional activity of a TALE protein. While a deletion of 48 amino acids did not affect transcription activity, a deletion of 141 amino acids still maintained ∼80% of the activity [662]. Extended truncations resulted in high expression levels, whereas native TALE proteins were expressed only at low levels [664]. For an efficient DNA binding, 147 [662] and 153 [664] amino acid residues at the N-terminus were identified to be essential. In contrast, the C-terminal residue seemed to be less relevant for DNA interaction since a 17 amino acid residue still effected an efficient DNA binding [664]. Nevertheless, a DNA binding element was identified within the first 68 amino acids of the C-terminus. Since further truncation of 18 amino acids reduced TALE transcriptional activity by >50%, the preservation of this critical residue was recommended to receive full TALE activity [662]. A complete impairment was first observed at a C-terminal trimming to 23 residues. More importantly, the length of the C-

terminus linking the FokI cleavage domain with the TALE repeats highly determines the catalytic activity of TALENs. While 95 residues preserved full transcriptional activation, they completely disabled nuclease activity. An efficient DNA cleavage by interaction of FokI domains with DNA was provided by shorter C-terminal subregions of 28 and 63 amino acids [604]. In good agreement, the used TALENs had N- and C-terminal truncations of 177 (287 → 110) and 187 (231 → 44) amino acids, respectively.

Furthermore, the cleavage activity of TALENs depends on length adaptation of the C-terminal linker to the DNA spacer between two TALE recognition sites. While long native linkers of more than 200 amino acids worked with spacers of 14–40bp [670, 671], shorter truncated linkers of 17–63 amino acids were restricted to shorter spacers of 12–23bp [604, 664]. A spacer of 14–16bp was shown to be optimal for a 63-residue linker [604] and a spacer of 12–15bp for a 47-residue linker [664]. A prerequisite for identification of suitable TALE target sites is the presence of an invariant thymine in position -1 flanking the TALE repeat-defined nucleotides [660, 661] and contributing to TALE promoter activation [660]. In good compliance with this, the selected TALEN recognition site in exon 3 of APOE featured a 15bp spacer.

For minimisation of cytotoxicity, a number of 14–19 TALE repeat units was suggested. Although shorter TALENs with 8–10 repeats were found to be as efficient as the longer ones, they were more cytotoxic presumably due to their more frequent binding to genomic off-target sites [606]. An examination of 50 naturally occurring TALE proteins revealed a number of TALE repeats ranging from 9–29 with a maximum at 18 [604]. Consistently, ten and more repeats for artificial TALE effectors were shown to be essential for a strong gene activation [660]. The used TALENs featured 14 repeat units, but still mediated a high cytotoxicity characterised by low proliferation rates of only few arisen single cell clones.

The observed high cytotoxicity could be caused primarily by the transfected amounts of TALENs and to a lesser extend by their scaffold. Although increasing amounts of up to 600ng of each expression vector were demonstrated to efficiently enhance TALEN activity without significant increase in cytotoxicity [664], up to 2.5μg of each subunit were used. However, cold shock experiments increasing the cleavage efficiency of TALENs [578, 604] indicated their cytotoxicity. While 60 single cell clones could be picked after drug-selection at 37°C, this was reduced to 33 clones after incubation at 30°C. Cytotoxicity due to random integration of TALENs could be excluded since the only FokI-positive clone 1-5 presented the highest proliferation rate by far.

Since APOE in general emerged as difficult target gene, the low targeting efficiencies furthermore can be explained by inhibitory chromatin structure and DNA modification as well as low expression and misfolding of the used TALENs [606] or by low binding strength of their TALE repeats [662].

5.9 Incorrect LDL receptor gene targeting

Genotype analysis (PCR, RT-PCR, Southern blot) of F1 generation animals produced results, which were in contrast to previous repeated positive examinations of the paternal nuclear transfer animal #72 indicating a heterozygous LDLR knockout both at genotypic (screening PCR, RT-PCR in section 4.2.6) and phenotypic (qRT-PCR in section 4.2.7) level. Although homologous recombination (HR)-mediated LDLR TV integrations could be verified by PCR for ten out of 18 F1 animals, the corresponding RT-PCR was negative revealing an incorrect 5'-end of HR-mediated LDLR TV integration. Further RT-PCRs indicated the expression of IRES BS cassette and upstream exon clustering with at least a duplication of exon 4. However, targeting RT-PCR of the three cell clones (1-16, 2-2, 2-11) used for nuclear and embryo transfer and generating animal #72 was only reproducible for two of them (2-2, 2-11) (see figure 4.22). Moreover, Southern blot in combination with sequencing of high fidelity PCR product covering the utilised restriction sites could verify the 3'-end of HR-mediated LDLR TV integration including the ∼1kb downstream presence of exon 5. Additionally, it revealed a ∼2.8kb duplication of the IRES BS cassette and the short homology arm with an initial deletion of IRES (see figure 4.25). However, these results expulsed a simple random insertion of the LDLR TV.

A possible explanation could be a combination of bidirectional homology arm elongation following ectopic vector integration at an adjacent or random position [608] with additional complex partial duplication of the targeting vector [609]. Bidirectional elongations have been described in mammalian cells for both sequence insertion (ends-in) [672] and gene replacement (ends-out) targeting vectors [608]. In this work, LDL receptor gene targeting was performed using a conventional ends-out promoter-trap vector to replace the major coding region of exon 4 by a promoter-less selectable cassette (IRES BS) disrupting gene expression. Flanking homology arms of 12.3kb and 1.6kb should enable a site-specific homologous recombination (see figure 4.10). A report of ectopic gene targeting proposed the single-stranded 3'-end invasion of targeting vector into the endogenous wild-type locus following bidirectional extension using endogenous sequences and further vector integration at an adjacent or random position [608]. The described mechanism of homology arm elongation is compatible to the predominant homology-directed repair (HDR) pathway of two-ended double strand breaks (DSB), the synthesis-dependent strand annealing (SDSA) [673]. However, the suggested mechanism is affirmed by the expression of the IRES BS cassette in absence of the endogenous LDLR promoter in combination with additionally acquired sequences upstream (exon 4) and downstream (exon 5) of HR-mediated LDLR TV integration (see section 4.2.9). The presence of exon 4 upstream of exon 3 possibly originate from a targeting vector breakage upstream of exon 3 due to hydrodynamic shearing prior to invasion [674]. Moreover, LDLR expression levels of 13 pigs determined from whole blood did not indicate a gene disruption (see section 4.2.10). Gene targeting of a different LDL receptor family member could also be excluded since elongated sequences

emphasising exon 4 and 5 were exclusive for the porcine LDL receptor in a BLAST search.

A reason for the additional partial duplication of the IRES BS cassette and the short homology arm could be a secondary HR of another LDLR TV at the ectopic integration site. Either intra- or inter-chromosomal secondary recombinations between homologies of integrated plasmids and target sequences were supposed to generate partial deletions within mammalian cell clones [656]. Since intron sequences of the LDLR target locus were highly repetitive (∼40%), an unequal HR of repetitive transposable elements could also have contributed to genome instability. Such events in mammalian cells were described between long interspersed nuclear elements (LINEs) causing a deletion of ∼7.6kb [675] and a duplication of ∼5.5kb [676]. Additionally, deletions and duplications could also be produced by short interspersed nuclear elements (SINEs) [677]. An unequal crossing-over between these repetitive sequence elements during HR even introduced a duplication of 14kb within the LDL receptor gene comprising seven exons [678]. Furthermore, a proposed mechanism of partial HR resulting in a complex targeting vector duplication has been described formerly in mammalian cells. Here, the unusual structure might arise from 3'-end invasion of a second targeting vector, which annealed to the 5'-end of an already integrated vector resulting in partial vector deletion [609].

All these theoretical mechanisms are highly speculative and additionally require HR between repetitive sequence elements with regard to 3'-end invasions of long homology arms. The used LDLR TV featured 33 repetitive transposable elements making 5.6kb (∼40%) of intron sequence, which might have been responsible for the observed results.

5.10 Diet-induced atherosclerotic phenotype in F1 generation animals

Since both LDLR and CX3CR1 expression levels indicated a heterozygous LDLR knock-out at phenotypic level (see section 4.2.7), the nuclear transfer animal #72 was mated with two sows and a cocos oil feeding study was conducted with eight female pigs of one offspring. Gene expressions in pig #72 were repeatedly quantified from ear tissue. However, especially for LDLR expression levels a considerably higher variation was detected in ear tissues (1.1±0.6) than in whole blood (1.0±0.2) possibly explaining the misleadingly ∼0.5-fold decrease in LDLR expression and thus the assumed heterozygous LDLR knockout (see figures 4.26 and 4.27).

The high-fat diet (chow diet and $250 g/d/animal$ cocos oil) increased total cholesterol of the eight female German Landrace pigs from an average of $71.4 \pm 6.6 \frac{mg}{dL}$ to $96.1 \pm 14.1 \frac{mg}{dL}$ (see figures 4.28 and 4.29). Independent cholesterol measurements of two males at chow diet revealed almost identical average values as reported for castrated male German Landrace pigs confirming the correctness of measurement [4, 613]. Here, the determined values of $87.0 \pm 5.7 \frac{mg}{dL}$ total cholesterol, $54.0 \pm 4.2 \frac{mg}{dL}$ combined low-density lipoprotein (LDL) and very low-density lipoprotein (VLDL) cholesterol and $32.5 \pm 0.7 \frac{mg}{dL}$ high-density lipoprotein

Chow diet	TC $[\frac{mg}{dL}]$	LDL+VLDL $[\frac{mg}{dL}]$	HDL $[\frac{mg}{dL}]$
GL_m (n=2)	87.0±5.7	54.0±4.2	32.5±0.7
GL_m* (n=93)	86.1±13.7	53.8±12.0	32.3±8.1

Table 5.1: Average values of plasma cholesterol with respective standard deviations for two male German Landrace pigs (GL_m) compared to 93 castrated male German Landrace pigs (GL_m*) at chow diet in $\frac{mg}{dL}$. TC: total cholesterol; LDL+VLDL: combined LDL and VLDL cholesterol; HDL: HDL cholesterol. Values of GL_m* adopted from [4].

GL_f (n=8)	TC $[\frac{mg}{dL}]$	LDL $[\frac{mg}{dL}]$	HDL $[\frac{mg}{dL}]$	VLDL $[\frac{mg}{dL}]$	TG $[\frac{mg}{dL}]$
Chow diet	71.4±6.6	37.5±6.6	26.3±4.6	7.6±2.2	39.5±11.1
High-fat diet	96.1±14.1	34.5±7.4	54.3±8.1	7.1±1.4	36±6.0

Table 5.2: Average values of plasma cholesterol and triglycerides with respective standard deviations for eight female German Landrace pigs (GL_f) at chow and high-fat diet in $\frac{mg}{dL}$. TC: total cholesterol; LDL: LDL cholesterol; HDL: HDL cholesterol; VLDL: VLDL cholesterol; TG: triglycerides.

(HDL) cholesterol corresponded to the reported values of 86.1±13.7$\frac{mg}{dL}$, 53.8±12.0$\frac{mg}{dL}$ and 32.3±8.1$\frac{mg}{dL}$ [4] (see table 5.1).

The established increase in total cholesterol after high-fat diet of the female pigs (German Landrace) seemed to exclusively affect the HDL fraction. While average values of 37.5±6.6$\frac{mg}{dL}$ LDL cholesterol, 7.6±2.2$\frac{mg}{dL}$ VLDL cholesterol and 39.5±11.1$\frac{mg}{dL}$ triglycerides at chow diet remained constant to 34.5±7.4$\frac{mg}{dL}$, 7.1±1.4$\frac{mg}{dL}$ and 36±6.0$\frac{mg}{dL}$ at high-fat diet, the HDL cholesterol increased from 26.3±4.6$\frac{mg}{dL}$ to 54.3±8.1$\frac{mg}{dL}$ (see table 5.2).

However, male juvenile domestic crossbred pigs [517] and female cloned, genetically-defined ApoE4 Duroc pigs [5] were shown to also develop highly increased LDL cholesterol at a hyperlipidemic diet (2% cholesterol and 17% coconut fat). Here, the female Duroc pigs exhibited baseline values of 82.0±2.8$\frac{mg}{dL}$ total cholesterol, 37.0±2.8$\frac{mg}{dL}$ LDL cholesterol, 34.0±1.4$\frac{mg}{dL}$ HDL cholesterol, 11.0±1.4$\frac{mg}{dL}$ VLDL cholesterol and 52.0±12.7$\frac{mg}{dL}$ triglycerides, which increased to 470.5±17.7$\frac{mg}{dL}$, 404.0±24.0$\frac{mg}{dL}$, 55.5±4.9$\frac{mg}{dL}$, 25.5±9.2$\frac{mg}{dL}$ and 42.0±5.7$\frac{mg}{dL}$ after the high-fat, high-cholesterol (HFHC) diet [5] (see table 5.3).

Based on these HFHC diet-induced cholesterol values, the performed high-fat diet indeed

D_f (n=2)	TC $[\frac{mg}{dL}]$	LDL $[\frac{mg}{dL}]$	HDL $[\frac{mg}{dL}]$	VLDL $[\frac{mg}{dL}]$	TG $[\frac{mg}{dL}]$
Chow diet	82.0±2.8	37.0±2.8	34.0±1.4	11.0±1.4	52.0±12.7
HFHC diet	470.5±17.7	404.0±24.0	55.5±4.9	25.5±9.2	42.0±5.7

Table 5.3: Average values of plasma cholesterol and triglycerides with respective standard deviations for two female cloned, genetically-defined ApoE4 Duroc pigs (D_f) at chow and high-fat, high-cholesterol (HFHC) diet in $\frac{mg}{dL}$. TC: total cholesterol; LDL: LDL cholesterol; HDL: HDL cholesterol; VLDL: VLDL cholesterol; TG: triglycerides. Values adopted from [5].

was capable to generate a similar increase in HDL cholesterol ($54.3\pm8.1\frac{mg}{dL}$ compared to $56\pm5\frac{mg}{dL}$), but failed to dramatically increase the LDL cholesterol ($34.5\pm7.4\frac{mg}{dL}$ compared to $404\pm24\frac{mg}{dL}$) and thus total cholesterol ($96.1\pm14.1\frac{mg}{dL}$ compared to $471\pm18\frac{mg}{dL}$). Since both the measured total cholesterol of the female pigs was conform to the dynamic range of *Piccolo Xpress Chemistry Analyser (Abaxis)* (20–$520\frac{mg}{dL}$) and cholesterol fractions of the male pigs exactly resembled the reported values [4], the measurement could be assumed correct. However, continuative examinations should be conducted with a more defined hyperlipidemic diet as recently specified [5, 517].

Every female pig exhibited an increase in CX3CR1 expression probably indicating inflammation during an early atherosclerosis (see figure 4.30). Here, a paired two-sample t-test at a confidence interval of 95% reached statistical significance ($p = 0.026$). Additionally, the expression level of CX3CR1 seemed to directly correlate with the progress of plaque development. Compared to animal #209, pig #206 revealed both a higher absolute expression and a greater increase in expression and developed more advanced early atherosclerotic plaques at bifurcations (see figure 4.31). Especially, these sites are susceptible to atherosclerosis [524, 109] and were also validated in the pig [525, 526, 614], where atherosclerotic lesions developed in aorta, carotid, femoral and coronary arteries of a porcine atherosclerosis model for vulnerable plaque [523, 579]. In contrast to the wild-type pigs #206 and #209, the genetically modified pigs #212 and #213 (see table 4.5) developed no early atherosclerotic plaques indicating no potentiating effect of the confirmed incorrect LDL receptor gene targeting (see section 4.2.9) on an atherosclerotic phenotype.

Concluding, these data verified direct correlation between plasma cholesterol levels, CX3CR1 expression and coronary artery disease in pigs. Here, transformation of normal into dysfunctional HDL could have contributed to the atherosclerotic phenotype [84].

5.11 Phenotype of ROSA26-EGFP$^{+/-}$ nuclear transfer animals

To provide functional evidence of CX3CR1 promoter region-driven reporter gene EGFP placed at ROSA26 genomic locus, a hypoxia assay was performed (see section 4.3.7). Upregulation of CX3CR1 expression was detected in human bone marrow-derived mesenchymal stem cells (MSCs) cultured in 1% O_2 [626] and also in peripheral blood mononuclear cells (PBMCs) of coronary artery disease (CAD) patients [320], especially in the monocyte subpopulation [319]. For this reason, these two cell types featuring ROSA26-EGFP$^{+/-}$ genotype were used for hypoxia assay. In addition to CX3CR1 porcine adipose tissue-derived MSC clones, monocytes/macrophages were derived from pig #260 and their specific isolation from porcine whole blood was verified. Compared to the negative control kidney fibroblasts (KDNFs) of stillborn piglet #215*, the ROSA26-EGFP$^{+/-}$ and wild-type monocytes/macrophages featured 170-fold and 200-fold higher expression of their cell-surface marker CD14, which was in compliance with ∼100-fold expression level above

isotype control in flow cytometric analysis [410]. Moreover, their response to hypoxia was demonstrated by increasing the marker expression up to 310-fold and 320-fold under these conditions (see figure 4.47).

However, hypoxia-induced upregulation of EGFP could neither be detected in CX3CR1 porcine adipose tissue-derived MSC clones nor in monocytes/macrophages of pig #260, which were also negative for CX3CR1 upregulation (see figure 4.46). This could be an effect of species-related differences or cell population divergency. First, the porcine MSCs were derived from adipose tissue, but hypoxia-induced upregulation of CX3CR1 was reported in human MSCs derived from bone marrow [626]. In contrast to human bone marrow-derived MSCs, the adipose tissue-derived MSCs revealed an attenuated osteogenic and adipogenic differentiation under hypoxic conditions [679]. Second, the isolation of hypoxia susceptible monocytes/macrophages from porcine whole blood was demonstrably successful, but most likely lack the population responsible for CX3CR1 upregulation in CAD patients due to higher rates of CX3CR1 positive monocytes [319]. In general, human peripheral blood monocytes split into three subsets, a classical (90–95%: $CD14^{high}$ $CD16^{-}$ $CX3CR1^{low}$), intermediate ($CD14^{high}$ $CD16^{+}$ $CX3CR1^{high}$) and non-classical population (5–10%: $CD14^{low}$ $CD16^{high}$ $CX3CR1^{high}$) [409, 410] evolving gradually from classical via intermediate into non-classical monocytes [411]. The isolated porcine monocytes/macrophages indeed featured high expression of CD14 (see figure 4.47) but low expression of CX3CR1. They exhibited an expression level 30-fold lower than whole blood and even 4-fold lower than ear tissue (see figure 4.48). These expression data were in line with the classical monocyte population in human (90–95%) excluding isolation of both the CX3CR1 positive ($CX3CR1^{high}$) intermediate population and the non-classical population (9–10%) (reviewed in [409, 410]).

In this work, a significant *in vivo* upregulation of CX3CR1 was demonstrated in pigs with diet-induced atherosclerosis (see figure 4.30). Since the used promoter region featured two hypoxia-response elements (HREs) (see section 4.3.3) and additionally drove cell-specific porcine expression of the main and analogue human CX3CR1 transcript "V28" [375, 376] (see section 4.3.2), it could be regarded as functional. Affirming this assumption, varying levels of CX3CR1 promoter region-driven EGFP expression could be detected in different cell types confirming the proposed constitutive and cell-specific activity of CX3CR1 promoters [375, 376]. Compared to pKDNFs, isolated monocytes/macrophages exhibited a 2-fold and pADMSCs a 1.5-fold higher EGFP expression (see figure 4.45).

However, for definite functional evidence of the reporter gene construct CX3CR1-EGFP placed at ROSA26 locus, a feeding study of pigs featuring ROSA26-$EGFP^{+/-}$ genotype is highly recommended.

CHAPTER 6

Conclusion and Outlook

This work provides fundamental steps for both the generation and the analysis of a porcine atherosclerosis model of vulnerable plaque. Procedures for genetic modification, genotyping and phenotyping were established. Gene inactivation of apolipoprotein E (APOE) and LDL receptor (LDLR) as well as transgene placement of enhanced green fluorescent protein (EGFP) driven by the porcine fractalkine receptor (CX3CR1) promoter at the endogenous ROSA26 locus was accomplished in porcine mesenchymal stem cells (MSCs). Adipose tissue of German Landrace breed emerged as excellent cell source producing healthy offspring after somatic cell nuclear transfer (SCNT). The cloned pigs featured no gene knockout of APOE and LDLR, but placement of the reporter cassette CX3CR1-EGFP, whose first functional evidence was provided by cell-specific EGFP expression. Independent of this and for the first time in pigs, a feeding study verified direct correlation between plasma cholesterol levels, CX3CR1 expression and coronary artery disease. In addition, the genetic background of ApoE4 isoform and CX3CR1 haplotype $I_{250}T_{281}$ will allow not only for research of atherosclerosis and cardiovascular disease (CVD) but also for disease- and treatment-related complications. Nevertheless, gene inactivation of LDLR as well as APOE will enable a more cost-efficient and rapid preclinical validation of innovative diagnostic and therapeutic technologies for the treatment of human coronary artery disease (CAD) and bridge the gap between small animal models and human clinical trials.

In order to make a porcine model for accelerated and human-like atherosclerosis available, further work needs to be done. $ApoE^{-/-}$ and $LDLR^{-/-}$ pigs have to be generated and validated by a defined hyperlipidemic diet. For this purpose, the plasma level of cholesterol fractions and the histology of coronary plaques must be examined. Moreover, definite validation of the reporter cassette CX3CR1-EGFP requires upregulation of EGFP

expression during diet-induced atherosclerosis.

Bibliography

[1] Orth, Matthias ; Bellosta, Stefano: Cholesterol: its regulation and role in central nervous system disorders. In: *Cholesterol* 2012 (2012) 19, 30, 31

[2] Lusis, Aldons J. ; Fogelman, Alan M. ; Fonarow, Gregg C.: Genetic basis of atherosclerosis: part I new genes and pathways. In: *Circulation* 110 (2004), Nr. 13, S. 1868–1873 19, 33

[3] Virmani, Renu ; Kolodgie, Frank D. ; Burke, Allen P. ; Farb, Andrew ; Schwartz, Stephen M.: Lessons from sudden coronary death a comprehensive morphological classification scheme for atherosclerotic lesions. In: *Arteriosclerosis, thrombosis, and vascular biology* 20 (2000), Nr. 5, S. 1262–1275 20, 35, 37

[4] FALKENBERG, HEINZ ; KUHN, GERDA ; Hartung, M ; Langhammer, M ; Wolf, C: Verlauf von biochemischen Kennwerten im Blut von Schweinen mit unterschiedlicher Fettansatzleistung. In: *Arch. Tierz., Dummerstorf* 42 (1999), Nr. 2, S. 149–159 28, 116, 147, 148, 149

[5] Jensen, Tor W. ; Mazur, Meredith J. ; Pettigew, James E. ; Perez-Mendoza, Victor G. ; Zachary, James ; Schook, Lawrence B.: A cloned pig model for examining atherosclerosis induced by high fat, high cholesterol diets. In: *Animal biotechnology* 21 (2010), Nr. 3, S. 179–187 28, 54, 92, 118, 139, 148, 149

[6] Global status report on noncommunicable diseases 2010. (2011) 29

[7] Global atlas on cardiovascular disease prevention and control. (2011) 29

[8] Mathers, Colin D. ; Loncar, Dejan: Projections of global mortality and burden of disease from 2002 to 2030. In: *PLoS medicine* 3 (2006), Nr. 11, S. e442 29

[9] Heidenreich, Paul A. ; Trogdon, Justin G. ; Khavjou, Olga A. ; Butler, Javed ; Dracup, Kathleen ; Ezekowitz, Michael D. ; Finkelstein, Eric A. ;

Hong, Yuling ; Johnston, S C. ; Khera, Amit u. a.: Forecasting the future of cardiovascular disease in the United States a policy statement from the American heart association. In: *Circulation* 123 (2011), Nr. 8, S. 933–944 29

[10] Cooper, Richard A.: Influence of increased membrane cholesterol on membrane fluidity and cell function in human red blood cells. In: *Journal of supramolecular structure* 8 (1978), Nr. 4, S. 413–430 29

[11] Lingwood, Daniel ; Simons, Kai: Lipid rafts as a membrane-organizing principle. In: *science* 327 (2010), Nr. 5961, S. 46–50 29

[12] Saher, Gesine ; Brügger, Britta ; Lappe-Siefke, Corinna ; Möbius, Wiebke ; Tozawa, Ryu-ichi ; Wehr, Michael C. ; Wieland, Felix ; Ishibashi, Shun ; Nave, Klaus-Armin: High cholesterol level is essential for myelin membrane growth. In: *Nature neuroscience* 8 (2005), Nr. 4, S. 468–475 29

[13] Russell, David W.: The enzymes, regulation, and genetics of bile acid synthesis. In: *Annual review of biochemistry* 72 (2003), Nr. 1, S. 137–174 29

[14] Payne, Anita H. ; Hales, Dale B.: Overview of steroidogenic enzymes in the pathway from cholesterol to active steroid hormones. In: *Endocrine reviews* 25 (2004), Nr. 6, S. 947–970 29

[15] Vaya, Jacob ; Schipper, Hyman M.: Oxysterols, cholesterol homeostasis, and Alzheimer disease. In: *Journal of neurochemistry* 102 (2007), Nr. 6, S. 1727–1737 29

[16] DeLuca, Hector F.: Overview of general physiologic features and functions of vitamin D. In: *The American journal of clinical nutrition* 80 (2004), Nr. 6, S. 1689S–1696S 29

[17] Dietschy, John M. ; Turley, Stephen D.: Thematic review series: brain Lipids. Cholesterol metabolism in the central nervous system during early development and in the mature animal. In: *Journal of lipid research* 45 (2004), Nr. 8, S. 1375–1397 29, 30

[18] Angel, A ; Bray, GA: Synthesis of fatty acids and cholesterol by liver, adipose tissue and intestinal mucosa from obese and control patients. In: *European journal of clinical investigation* 9 (1979), Nr. 5, S. 355–362 29

[19] Waterham, Hans R.: Defects of cholesterol biosynthesis. In: *FEBS letters* 580 (2006), Nr. 23, S. 5442–5449 29, 45

[20] Grundy, Scott M.: Absorption and metabolism of dietary cholesterol. In: *Annual review of nutrition* 3 (1983), Nr. 1, S. 71–96 30

[21] Mahley, Robert W. ; Weisgraber, Karl H. ; Innerarity, Thomas L. ; Rall, Stanley C.: Genetic defects in lipoprotein metabolism: Elevation of atherogenic lipoproteins caused by impaired catabolism. In: *Jama* 265 (1991), Nr. 1, S. 78–83 30, 34

[22] Smith, Louis C. ; Pownall, Henry J. ; Gotto Jr, Antonio M.: The plasma lipoproteins: structure and metabolism. In: *Annual review of biochemistry* 47 (1978), Nr. 1, S. 751–777 30

[23] Eder, Howard A. ; Roheim, Paul S.: PLASMA LIPOPROTEINS AND APOLIPOPROTEINS*. In: *Annals of the New York Academy of Sciences* 275 (1976), Nr. 1, S. 169–179 30

[24] Björkhem, Ingemar ; Meaney, Steve: Brain cholesterol: long secret life behind a barrier. In: *Arteriosclerosis, thrombosis, and vascular biology* 24 (2004), Nr. 5, S. 806–815 30

[25] Pitas, RE ; Boyles, JK ; Lee, SH ; Hui, D ; Weisgraber, KH: Lipoproteins and their receptors in the central nervous system. Characterization of the lipoproteins in cerebrospinal fluid and identification of apolipoprotein B, E (LDL) receptors in the brain. In: *Journal of Biological Chemistry* 262 (1987), Nr. 29, S. 14352–14360 30

[26] Fünfschilling, Ursula ; Saher, Gesine ; Xiao, Le ; Möbius, Wiebke ; Nave, Klaus-Armin: Survival of adult neurons lacking cholesterol synthesis in vivo. In: *BMC neuroscience* 8 (2007), Nr. 1, S. 1 30

[27] Quan, Gang ; Xie, Chonglun ; Dietschy, John M. ; Turley, Stephen D.: Ontogenesis and regulation of cholesterol metabolism in the central nervous system of the mouse. In: *Developmental brain research* 146 (2003), Nr. 1, S. 87–98 30

[28] Suzuki, Shingo ; Kiyosue, Kazuyuki ; Hazama, Shunsuke ; Ogura, Akihiko ; Kashihara, Megumi ; Hara, Tomoko ; Koshimizu, Hisatsugu ; Kojima, Masami: Brain-derived neurotrophic factor regulates cholesterol metabolism for synapse development. In: *The Journal of neuroscience* 27 (2007), Nr. 24, S. 6417–6427 30

[29] Xu, Qin ; Bernardo, Aubrey ; Walker, David ; Kanegawa, Tiffany ; Mahley, Robert W. ; Huang, Yadong: Profile and regulation of apolipoprotein E (ApoE) expression in the CNS in mice with targeting of green fluorescent protein gene to the ApoE locus. In: *The Journal of neuroscience* 26 (2006), Nr. 19, S. 4985–4994 30

[30] Kim, Woojin S. ; Rahmanto, Aldwin S. ; Kamili, Alvin ; Rye, Kerry-Anne ; Guillemin, Gilles J. ; Gelissen, Ingrid C. ; Jessup, Wendy ; Hill, Andrew F. ; Garner, Brett: Role of ABCG1 and ABCA1 in regulation of neuronal cholesterol

efflux to apolipoprotein E discs and suppression of amyloid-β peptide generation. In: *Journal of Biological Chemistry* 282 (2007), Nr. 5, S. 2851–2861 30

[31] Björkhem, Ingemar ; Diczfalusy, Ulf: Oxysterols Friends, Foes, or Just Fellow Passengers? In: *Arteriosclerosis, thrombosis, and vascular biology* 22 (2002), Nr. 5, S. 734–742 30

[32] Lund, Erik G. ; Guileyardo, Joseph M. ; Russell, David W.: cDNA cloning of cholesterol 24-hydroxylase, a mediator of cholesterol homeostasis in the brain. In: *Proceedings of the National Academy of Sciences* 96 (1999), Nr. 13, S. 7238–7243 30

[33] Björkhem, Ingemar ; Lütjohann, Dieter ; Diczfalusy, Ulf ; Ståhle, Lars ; Ahlborg, Gunvor ; Wahren, John: Cholesterol homeostasis in human brain: turnover of 24S-hydroxycholesterol and evidence for a cerebral origin of most of this oxysterol in the circulation. In: *Journal of lipid research* 39 (1998), Nr. 8, S. 1594–1600 30

[34] Lütjohann, Dieter ; Breuer, Olof ; Ahlborg, Gunvor ; Nennesmo, Inger ; Siden, Ake ; Diczfalusy, Ulf ; Björkhem, Ingemar: Cholesterol homeostasis in human brain: evidence for an age-dependent flux of 24S-hydroxycholesterol from the brain into the circulation. In: *Proceedings of the National Academy of Sciences* 93 (1996), Nr. 18, S. 9799–9804 30

[35] Heverin, Maura ; Meaney, Steve ; Lütjohann, Dieter ; Diczfalusy, Ulf ; Wahren, John ; Björkhem, Ingemar: Crossing the barrier: net flux of 27-hydroxycholesterol into the human brain. In: *Journal of lipid research* 46 (2005), Nr. 5, S. 1047–1052 30

[36] Leoni, Valerio ; Masterman, Thomas ; Patel, Pria ; Meaney, Steve ; Diczfalusy, Ulf ; Björkhem, Ingemar: Side chain oxidized oxysterols in cerebrospinal fluid and the integrity of blood-brain and blood-cerebrospinal fluid barriers. In: *Journal of lipid research* 44 (2003), Nr. 4, S. 793–799 30

[37] Herz, Joachim: ApoE receptors in the nervous system. In: *Current opinion in lipidology* 20 (2009), Nr. 3, S. 190 30

[38] Sebastião, Ana M. ; Colino-Oliveira, Mariana ; Assaife-Lopes, Natália ; Dias, Raquel B. ; Ribeiro, Joaquim A.: Lipid rafts, synaptic transmission and plasticity: impact in age-related neurodegenerative diseases. In: *Neuropharmacology* 64 (2013), S. 97–107 30

[39] Porter, Jeffery A. ; Young, Keith E. ; Beachy, Philip A.: Cholesterol modification of hedgehog signaling proteins in animal development. In: *Science* 274 (1996), Nr. 5285, S. 255–259 30

[40] Stottmann, Rolf W. ; Turbe-Doan, Annick ; Tran, Pamela ; Kratz, Lisa E. ; Moran, Jennifer L. ; Kelley, Richard I. ; Beier, David R.: Cholesterol metabolism is required for intracellular hedgehog signal transduction in vivo. In: *PLoS genetics* 7 (2011), Nr. 9, S. e1002224 30

[41] Simons, Kai ; Ikonen, Elina: How cells handle cholesterol. In: *Science* 290 (2000), Nr. 5497, S. 1721–1726 31

[42] Goldstein, Joseph L. ; DeBose-Boyd, Russell A. ; Brown, Michael S.: Protein sensors for membrane sterols. In: *Cell* 124 (2006), Nr. 1, S. 35–46 31, 45

[43] Brown, Michael S. ; Goldstein, Joseph L.: A proteolytic pathway that controls the cholesterol content of membranes, cells, and blood. In: *Proceedings of the National Academy of Sciences* 96 (1999), Nr. 20, S. 11041–11048 31, 43, 44, 45, 102

[44] Horton, Jay D. ; Goldstein, Joseph L. ; Brown, Michael S. u. a.: SREBPs: activators of the complete program of cholesterol and fatty acid synthesis in the liver. In: *The Journal of clinical investigation* 109 (2002), Nr. 9, S. 1125–1131 31, 45

[45] Pai, Jih-tung ; Guryev, Oleg ; Brown, Michael S. ; Goldstein, Joseph L.: Differential stimulation of cholesterol and unsaturated fatty acid biosynthesis in cells expressing individual nuclear sterol regulatory element-binding proteins. In: *Journal of Biological Chemistry* 273 (1998), Nr. 40, S. 26138–26148 31, 45

[46] Nohturfft, Axel ; Yabe, Daisuke ; Goldstein, Joseph L. ; Brown, Michael S. ; Espenshade, Peter J.: Regulated step in cholesterol feedback localized to budding of SCAP from ER membranes. In: *Cell* 102 (2000), Nr. 3, S. 315–323 31, 43, 44, 45, 102

[47] Ehrlich, Marcelo ; Boll, Werner ; Oijen, Antoine van ; Hariharan, Ramesh ; Chandran, Kartik ; Nibert, Max L. ; Kirchhausen, Tomas: Endocytosis by random initiation and stabilization of clathrin-coated pits. In: *Cell* 118 (2004), Nr. 5, S. 591–605 31

[48] Dehouck, Bénédicte ; Fenart, Laurence ; Dehouck, Marie-Pierre ; Pierce, Annick ; Torpier, Gérard ; Cecchelli, Roméo: A new function for the LDL receptor: transcytosis of LDL across the blood–brain barrier. In: *The Journal of cell biology* 138 (1997), Nr. 4, S. 877–889 31

[49] Kruth, Howard S. ; Jones, Nancy L. ; Huang, Wei ; Zhao, Bin ; Ishii, Itsuko ; Chang, Janet ; Combs, Christian A. ; Malide, Daniela ; Zhang, Wei-Yang: Macropinocytosis is the endocytic pathway that mediates macrophage foam cell formation with native low density lipoprotein. In: *Journal of Biological Chemistry* 280 (2005), Nr. 3, S. 2352–2360 31

[50] Hoff, HF ; O'neil, J ; Pepin, JM ; Cole, TB: Macrophage uptake of cholesterol-containing particles derived from LDL and isolated from atherosclerotic lesions. In: *European heart journal* 11 (1990), Nr. suppl E, S. 105–115 31, 38

[51] Rothblat, George H. ; Phillips, Michael C.: High-density lipoprotein heterogeneity and function in reverse cholesterol transport. In: *Current opinion in lipidology* 21 (2010), Nr. 3, S. 229 31, 34

[52] Weingärtner, Oliver ; Laufs, Ulrich ; Böhm, Michael ; Lütjohann, Dieter: An alternative pathway of reverse cholesterol transport: the oxysterol 27-hydroxycholesterol. In: *Atherosclerosis* 209 (2010), Nr. 1, S. 39–41 31

[53] Cocucci, Emanuele ; Racchetti, Gabriella ; Meldolesi, Jacopo: Shedding microvesicles: artefacts no more. In: *Trends in cell biology* 19 (2009), Nr. 2, S. 43–51 31

[54] Nandi, Shilpi ; Ma, Loretta ; Denis, Maxime ; Karwatsky, Joel ; Li, Zhiqiang ; Jiang, Xian-Cheng ; Zha, Xiaohui: ABCA1-mediated cholesterol efflux generates microparticles in addition to HDL through processes governed by membrane rigidity. In: *Journal of lipid research* 50 (2009), Nr. 3, S. 456–466 31

[55] Ikonen, Elina: Cellular cholesterol trafficking and compartmentalization. In: *Nature Reviews Molecular Cell Biology* 9 (2008), Nr. 2, S. 125–138 32

[56] Soccio, Raymond E. ; Breslow, Jan L.: Intracellular cholesterol transport. In: *Arteriosclerosis, thrombosis, and vascular biology* 24 (2004), Nr. 7, S. 1150–1160 32

[57] Wang, Ming-Dong ; Kiss, Robert S. ; Franklin, Vivian ; McBride, Heidi M. ; Whitman, Stewart C. ; Marcel, Yves L.: Different cellular traffic of LDL-cholesterol and acetylated LDL-cholesterol leads to distinct reverse cholesterol transport pathways. In: *Journal of lipid research* 48 (2007), Nr. 3, S. 633–645 32

[58] Kwiterovich Jr, Peter O.: The metabolic pathways of high-density lipoprotein, low-density lipoprotein, and triglycerides: a current review. In: *The American journal of cardiology* 86 (2000), Nr. 12, S. 5–10 32, 34

[59] Otvos, James D.: Measurement of lipoprotein subclass profiles by nuclear magnetic resonance spectroscopy. In: *Clinical laboratory* 48 (2001), Nr. 3-4, S. 171–180 32

[60] Freedman, David S. ; Otvos, James D. ; Jeyarajah, Elias J. ; Barboriak, Joseph J. ; Anderson, Alfred J. ; Walker, John A.: Relation of lipoprotein subclasses as measured by proton nuclear magnetic resonance spectroscopy to coronary artery disease. In: *Arteriosclerosis, thrombosis, and vascular biology* 18 (1998), Nr. 7, S. 1046–1053 32, 34

[61] Brown, Michael S. ; Goldstein, Joseph L.: A receptor-mediated pathway for cholesterol homeostasis. In: *Science* 232 (1986), Nr. 4746, S. 34–47 32, 44, 46

[62] Young, SG: Recent progress in understanding apolipoprotein B. In: *Circulation* 82 (1990), Nr. 5, S. 1574–1594 32

[63] Mahley, Robert W. ; Ji, Zhong-Sheng: Remnant lipoprotein metabolism: key pathways involving cell-surface heparan sulfate proteoglycans and apolipoprotein E. In: *Journal of lipid research* 40 (1999), Nr. 1, S. 1–16 32, 43

[64] Rensen, PC ; Herijgers, N ; Netscher, MH ; Meskers, SC ; Van Eck, M ; Van Berkel, TJ: Particle size determines the specificity of apolipoprotein E-containing triglyceride-rich emulsions for the LDL receptor versus hepatic remnant receptor in vivo. In: *Journal of lipid research* 38 (1997), Nr. 6, S. 1070–1084 32

[65] Polonovski, J ; Beucler, I: [Structure and metabolism of plasma lipoproteins]. In: *Pathologie-biologie* 31 (1983), Nr. 4, S. 225–234 32

[66] Zambon, A ; Bertocco, S ; Vitturi, N ; Polentarutti, V ; Vianello, D ; Crepaldi, G: Relevance of hepatic lipase to the metabolism of triacylglycerol-rich lipoproteins. In: *Biochemical Society Transactions* 31 (2003), Nr. 5, S. 1070–1074 32

[67] Kesaniemi, Y A. ; Witztum, Joseph L. ; Steinbrecher, Urs P.: Receptor-mediated catabolism of low density lipoprotein in man. Quantitation using glucosylated low density lipoprotein. In: *Journal of Clinical Investigation* 71 (1983), Nr. 4, S. 950 32

[68] Steinberg, D: Lipoproteins and atherosclerosis. A look back and a look ahead. In: *Arteriosclerosis, Thrombosis, and Vascular Biology* 3 (1983), Nr. 4, S. 283–301 32

[69] Nordestgaard, Børge G ; Chapman, M J. ; Ray, Kausik ; Borén, Jan ; Andreotti, Felicita ; Watts, Gerald F. ; Ginsberg, Henry ; Amarenco, Pierre ; Catapano, Alberico ; Descamps, Olivier S. u. a.: Lipoprotein (a) as a cardiovascular risk factor: current status. In: *European heart journal* 31 (2010), Nr. 23, S. 2844–2853 32, 34

[70] Zannis, Vassilis I. ; Kardassis, Dimitris ; Cardot, Philippe ; Hadzopoulou-Cladaras, Margarita ; Zanni, Eleni E. ; Cladaras, Christos: Molecular biology of the human apolipoprotein genes: gene regulation and structure/function relationship. In: *Current Opinion in Lipidology* 3 (1992), Nr. 2, S. 96–113 34

[71] Kiss, Robert S. ; McManus, Dan C. ; Franklin, Vivian ; Tan, Wei L. ; McKenzie, Andrea ; Chimini, Giovanna ; Marcel, Yves L.: The lipidation by hepatocytes of human apolipoprotein AI occurs by both ABCA1-dependent and-independent

pathways. In: *Journal of Biological Chemistry* 278 (2003), Nr. 12, S. 10119–10127 34

[72] Lee, Ji-Young ; Parks, John S.: ATP-binding cassette transporter AI and its role in HDL formation. In: *Current opinion in lipidology* 16 (2005), Nr. 1, S. 19–25 34

[73] Barter, Philip J.: Hugh sinclair lecture: the regulation and remodelling of HDL by plasma factors. In: *Atherosclerosis Supplements* 3 (2002), Nr. 4, S. 39–47 34

[74] Koukos, Georgios ; Chroni, Angeliki ; Duka, Adelina ; Kardassis, Dimitris ; Zannis, V: Naturally occurring and bioengineered apoA-I mutations that inhibit the conversion of discoidal to spherical HDL: the abnormal HDL phenotypes can be corrected by treatment with LCAT. In: *Biochem. J* 406 (2007), S. 167–174 34

[75] Calabresi, Laura ; Franceschini, Guido: Lecithin: cholesterol acyltransferase, high-density lipoproteins, and atheroprotection in humans. In: *Trends in cardiovascular medicine* 20 (2010), Nr. 2, S. 50–53 34

[76] Asztalos, Bela F. ; Schaefer, Ernst J. ; Horvath, Katalin V. ; Yamashita, Shizuya ; Miller, Michael ; Franceschini, Guido ; Calabresi, Laura: Role of LCAT in HDL remodeling: investigation of LCAT deficiency states. In: *Journal of lipid research* 48 (2007), Nr. 3, S. 592–599 34

[77] Eisenberg, Shlomo: High density lipoprotein metabolism. In: *Journal of lipid research* 25 (1984), Nr. 10, S. 1017–1058 34

[78] Pownall, Henry J. ; Ehnholm, Christian: The unique role of apolipoprotein AI in HDL remodeling and metabolism. In: *Current opinion in lipidology* 17 (2006), Nr. 3, S. 209–213 34

[79] Zannis, Vassilis I. ; Chroni, Angeliki ; Krieger, Monty: Role of apoA-I, ABCA1, LCAT, and SR-BI in the biogenesis of HDL. In: *Journal of molecular medicine* 84 (2006), Nr. 4, S. 276–294 34, 42

[80] Cromwell, William C. ; Otvos, James D.: Low-density lipoprotein particle number and risk for cardiovascular disease. In: *Current atherosclerosis reports* 6 (2004), Nr. 5, S. 381–387 34, 52

[81] Campos, H ; Blijlevens, E ; McNamara, JR ; Ordovas, JM ; Posner, BM ; Wilson, PW ; Castelli, WP ; Schaefer, EJ: LDL particle size distribution. Results from the Framingham Offspring Study. In: *Arteriosclerosis, Thrombosis, and Vascular Biology* 12 (1992), Nr. 12, S. 1410–1419 34

[82] Chan, Hua-Chen ; Ke, Liang-Yin ; Chu, Chih-Sheng ; Lee, An-Sheng ; Shen, Ming-Yi ; Cruz, Miguel A. ; Hsu, Jing-Fang ; Cheng, Kai-Hung ; Chan, Hsiu-Chuan B. ; Lu, Jonathan u. a.: Highly electronegative LDL from patients with

ST-elevation myocardial infarction triggers platelet activation and aggregation. In: *Blood* 122 (2013), Nr. 22, S. 3632–3641 34

[83] Castelli, WP: Cholesterol and lipids in the risk of coronary artery disease–the Framingham Heart Study. In: *The Canadian journal of cardiology* 4 (1988), S. 5A–10A 34

[84] Otocka-Kmiecik, Aneta ; Mikhailidis, Dimitri P. ; Nicholls, Stephen J. ; Davidson, Michael ; Rysz, Jacek ; Banach, Maciej: Dysfunctional HDL: a novel important diagnostic and therapeutic target in cardiovascular disease? In: *Progress in lipid research* 51 (2012), Nr. 4, S. 314–324 35, 149

[85] Hafiane, Anouar ; Genest, Jacques: HDL, atherosclerosis, and emerging therapies. In: *Cholesterol* 2013 (2013) 35

[86] Kontush, Anatol ; Chantepie, Sandrine ; Chapman, M J.: Small, dense HDL particles exert potent protection of atherogenic LDL against oxidative stress. In: *Arteriosclerosis, thrombosis, and vascular biology* 23 (2003), Nr. 10, S. 1881–1888 35, 41, 42

[87] Itabe, Hiroyuki: Oxidative modification of LDL: its pathological role in atherosclerosis. In: *Clinical reviews in allergy & immunology* 37 (2009), Nr. 1, S. 4–11 35

[88] Ishigaki, Yasushi ; Katagiri, Hideki ; Gao, Junhong ; Yamada, Tetsuya ; Imai, Junta ; Uno, Kenji ; Hasegawa, Yutaka ; Kaneko, Keizo ; Ogihara, Takehide ; Ishihara, Hisamitsu u. a.: Impact of plasma oxidized low-density lipoprotein removal on atherosclerosis. In: *Circulation* 118 (2008), Nr. 1, S. 75–83 35

[89] Joshi, Parag H. ; Toth, Peter P. ; Lirette, Seth T. ; Griswold, Michael E. ; Massaro, Joseph M. ; Martin, Seth S. ; Blaha, Michael J. ; Kulkarni, Krishnaji R. ; Khokhar, Arif A. ; Correa, Adolfo u. a.: Association of high-density lipoprotein subclasses and incident coronary heart disease: The Jackson Heart and Framingham Offspring Cohort Studies. In: *European journal of preventive cardiology* (2014), S. 2047487314543890 35, 52

[90] Martin, Seth S. ; Khokhar, Arif A. ; May, Heidi T. ; Kulkarni, Krishnaji R. ; Blaha, Michael J. ; Joshi, Parag H. ; Toth, Peter P. ; Muhlestein, Joseph B. ; Anderson, Jeffrey L. ; Knight, Stacey u. a.: HDL cholesterol subclasses, myocardial infarction, and mortality in secondary prevention: the lipoprotein investigators collaborative. In: *European heart journal* (2014), S. ehu264 35, 52

[91] De Beer, MC ; Durbin, DM ; Cai, L ; Jonas, A ; De Beer, FC ; Westhuyzen, DR Van d.: Apolipoprotein AI conformation markedly influences HDL interaction with scavenger receptor BI. In: *Journal of lipid research* 42 (2001), Nr. 2, S. 309–313 35

[92] Thuahnai, Stephen T. ; Lund-Katz, Sissel ; Dhanasekaran, Padmaja ; Llera-Moya, Margarita de l. ; Connelly, Margery A. ; Williams, David L. ; Rothblat, George H. ; Phillips, Michael C.: Scavenger Receptor Class B Type I-mediated Cholesteryl Ester-selective Uptake and Efflux of Unesterified Cholesterol INFLUENCE OF HIGH DENSITY LIPOPROTEIN SIZE AND STRUCTURE. In: *Journal of Biological Chemistry* 279 (2004), Nr. 13, S. 12448–12455 35

[93] Zheng, Lemin ; Settle, Megan ; Brubaker, Gregory ; Schmitt, Dave ; Hazen, Stanley L. ; Smith, Jonathan D. ; Kinter, Michael: Localization of nitration and chlorination sites on apolipoprotein AI catalyzed by myeloperoxidase in human atheroma and associated oxidative impairment in ABCA1-dependent cholesterol efflux from macrophages. In: *Journal of Biological Chemistry* 280 (2005), Nr. 1, S. 38–47 35

[94] Jayaraman, Shobini ; Gantz, Donald L. ; Gursky, Olga: Effects of Protein Oxidation on the Structure and Stability of Model Discoidal High-Density Lipoproteins. In: *Biochemistry* 47 (2008), Nr. 12, S. 3875–3882 35

[95] Lamarche, Benoit ; Rashid, Shirya ; Lewis, Gary F.: HDL metabolism in hypertriglyceridemic states: an overview. In: *Clinica chimica acta* 286 (1999), Nr. 1, S. 145–161 35

[96] Greene, Diane J. ; Skeggs, Josephine W. ; Morton, Richard E.: Elevated triglyceride content diminishes the capacity of high density lipoprotein to deliver cholesteryl esters via the scavenger receptor class B type I (SR-BI). In: *Journal of Biological Chemistry* 276 (2001), Nr. 7, S. 4804–4811 35

[97] Mineo, Chieko ; Deguchi, Hiroshi ; Griffin, John H. ; Shaul, Philip W.: Endothelial and antithrombotic actions of HDL. In: *Circulation research* 98 (2006), Nr. 11, S. 1352–1364 35

[98] Libby, Peter: Inflammation in atherosclerosis. In: *Arteriosclerosis, thrombosis, and vascular biology* 32 (2012), Nr. 9, S. 2045–2051 35

[99] Wexler, Lewis ; Brundage, Bruce ; Crouse, John ; Detrano, Robert ; Fuster, Valentin ; Maddahi, Jamshid ; Rumberger, John ; Stanford, William ; White, Richard ; Taubert, Kathryn: Coronary Artery Calcification: Pathophysiology, Epidemiology, Imaging Methods, and Clinical Implications A Statement for Health Professionals From the American Heart Association. In: *Circulation* 94 (1996), Nr. 5, S. 1175–1192 35

[100] Virmani, Renu ; Burke, Allen P. ; Farb, Andrew ; Kolodgie, Frank D.: Pathology of the vulnerable plaque. In: *Journal of the American College of Cardiology* 47 (2006), Nr. 8s1, S. C13–C18 35, 36, 50, 119

[101] Kragel, Amy H. ; Gertz, S D. ; Roberts, William C.: Morphologic comparison of frequency and types of acute lesions in the major epicardial coronary arteries in unstable angina pectoris, sudden coronary death and acute myocardial infarction. In: *Journal of the American College of Cardiology* 18 (1991), Nr. 3, S. 801–808 35

[102] Moreno, Pedro R. ; Purushothaman, K-Raman ; Sirol, Marc ; Levy, Andrew P. ; Fuster, Valentin: Neovascularization in human atherosclerosis. In: *Circulation* 113 (2006), Nr. 18, S. 2245–2252 35

[103] Michel, Jean-Baptiste ; Virmani, Renu ; Arbustini, Eloïsa ; Pasterkamp, Gerard: Intraplaque haemorrhages as the trigger of plaque vulnerability. In: *European heart journal* 32 (2011), Nr. 16, S. 1977–1985 35

[104] Farb, Andrew ; Burke, Allen P. ; Tang, Anita L. ; Liang, Youhui ; Mannan, Poonam ; Smialek, John ; Virmani, Renu: Coronary plaque erosion without rupture into a lipid core A frequent cause of coronary thrombosis in sudden coronary death. In: *Circulation* 93 (1996), Nr. 7, S. 1354–1363 35, 36

[105] Burke, Allen P. ; Kolodgie, Frank D. ; Farb, Andrew ; Weber, Deena K. ; Malcom, Gray T. ; Smialek, John ; Virmani, Renu: Healed plaque ruptures and sudden coronary death evidence that subclinical rupture has a role in plaque progression. In: *Circulation* 103 (2001), Nr. 7, S. 934–940 35

[106] Napoli, C ; D'armiento, FP ; Mancini, FP ; Postiglione, A ; Witztum, JL ; Palumbo, G ; Palinski, W: Fatty streak formation occurs in human fetal aortas and is greatly enhanced by maternal hypercholesterolemia. Intimal accumulation of low density lipoprotein and its oxidation precede monocyte recruitment into early atherosclerotic lesions. In: *Journal of Clinical Investigation* 100 (1997), Nr. 11, S. 2680 36, 110, 116

[107] Strong, Jack P. ; Malcom, Gray T. ; McMahan, C A. ; Tracy, Richard E. ; Newman III, William P. ; Herderick, Edward E. ; Cornhill, J F. ; Youth Research Group, Pathobiological D. i. u. a.: Prevalence and extent of atherosclerosis in adolescents and young adults: implications for prevention from the Pathobiological Determinants of Atherosclerosis in Youth Study. In: *Jama* 281 (1999), Nr. 8, S. 727–735 36

[108] Velican, Doina ; Velican, C: Atherosclerotic involvement of the coronary arteries of adolescents and young adults. In: *Atherosclerosis* 36 (1980), Nr. 4, S. 449–460 36

[109] Slager, CJ ; Wentzel, JJ ; Gijsen, FJH ; Schuurbiers, JCH ; Der Wal, AC van ; Steen, AFW Van d. ; Serruys, PW: The role of shear stress in the generation of rupture-prone vulnerable plaques. In: *Nature clinical practice cardiovascular medicine* 2 (2005), Nr. 8, S. 401–407 36, 119, 149

[110] Cheruvu, Pavan K. ; Finn, Aloke V. ; Gardner, Craig ; Caplan, Jay ; Goldstein, James ; Stone, Gregg W. ; Virmani, Renu ; Muller, James E.: Frequency and Distribution of Thin-Cap Fibroatheroma and Ruptured Plaques in Human Coronary Arteries A Pathologic Study. In: *Journal of the American College of Cardiology* 50 (2007), Nr. 10, S. 940–949 36

[111] Arbustini, EDBB ; Dal Bello, B ; Morbini, P ; Burke, AP ; Bocciarelli, M ; Specchia, G ; Virmani, R: Plaque erosion is a major substrate for coronary thrombosis in acute myocardial infarction. In: *Heart* 82 (1999), Nr. 3, S. 269–272 36

[112] Strong, JP ; McGill Jr, HC: The pediatric aspects of atherosclerosis. In: *Journal of atherosclerosis research* 9 (1969), Nr. 3, S. 251–265 36

[113] Bild, Diane E. ; Detrano, Robert ; Peterson, DO ; Guerci, Alan ; Liu, Kiang ; Shahar, Eyal ; Ouyang, Pamela ; Jackson, Sharon ; Saad, Mohammed F.: Ethnic differences in coronary calcification the multi-ethnic study of atherosclerosis (MESA). In: *Circulation* 111 (2005), Nr. 10, S. 1313–1320 36

[114] Burke, Allen P. ; Virmani, Renu ; Galis, Zorina ; Haudenschild, Christian C. ; Muller, James E.: Task force #2–what is the pathologic basis for new atherosclerosis imaging techniques? In: *Journal of the American College of Cardiology* 41 (2003), Nr. 11, S. 1874–1886 36

[115] Kannel, William B. ; Schatzkin, Arthur: Sudden death: lessons from subsets in population studies. In: *Journal of the American College of Cardiology* 5 (1985), Nr. 6s1, S. 141B–149B 36

[116] Karim, Roksana ; Mack, Wendy J. ; Lobo, Roger A. ; Hwang, Juliana ; Liu, Chao-ran ; Liu, Ci-hua ; Sevanian, Alex ; Hodis, Howard N.: Determinants of the effect of estrogen on the progression of subclinical atherosclerosis: Estrogen in the Prevention of Atherosclerosis Trial. In: *Menopause* 12 (2005), Nr. 4, S. 366–373 36

[117] Tabas, Ira ; Williams, Kevin J. ; Borén, Jan: Subendothelial lipoprotein retention as the initiating process in atherosclerosis update and therapeutic implications. In: *Circulation* 116 (2007), Nr. 16, S. 1832–1844 38

[118] Nielsen, Lars B.: Transfer of low density lipoprotein into the arterial wall and risk of atherosclerosis. In: *Atherosclerosis* 123 (1996), Nr. 1, S. 1–15 38

[119] Skålén, Kristina ; Gustafsson, Maria ; Rydberg, Ellen K. ; Hultén, Lillemor M. ; Wiklund, Olov ; Innerarity, Thomas L. ; Borén, Jan: Subendothelial retention of atherogenic lipoproteins in early atherosclerosis. In: *Nature* 417 (2002), Nr. 6890, S. 750–754 38

[120] Borén, Jan ; Olin, Katherine ; Lee, Isabelle ; Chait, Alan ; Wight, Thomas N. ; Innerarity, Thomas L.: Identification of the principal proteoglycan-binding site in LDL. A single-point mutation in apo-B100 severely affects proteoglycan interaction without affecting LDL receptor binding. In: *Journal of Clinical Investigation* 101 (1998), Nr. 12, S. 2658 38

[121] Pentikäinen, MO ; Öörni, K ; Ala-Korpela, M ; Kovanen, PT: Modified LDL–trigger of atherosclerosis and inflammation in the arterial intima. In: *Journal of internal medicine* 247 (2000), Nr. 3, S. 359–370 38

[122] Leitinger, Norbert: Oxidized phospholipids as modulators of inflammation in atherosclerosis. In: *Current opinion in lipidology* 14 (2003), Nr. 5, S. 421–430 38

[123] Dai, Guohao ; Kaazempur-Mofrad, Mohammad R. ; Natarajan, Sripriya ; Zhang, Yuzhi ; Vaughn, Saran ; Blackman, Brett R. ; Kamm, Roger D. ; García-Cardeña, Guillermo ; Gimbrone, Michael A.: Distinct endothelial phenotypes evoked by arterial waveforms derived from atherosclerosis-susceptible and -resistant regions of human vasculature. In: *Proceedings of the National Academy of Sciences of the United States of America* 101 (2004), Nr. 41, S. 14871–14876 38

[124] Pirillo, Angela ; Norata, Giuseppe D. ; Catapano, Alberico L.: LOX-1, OxLDL, and atherosclerosis. In: *Mediators of inflammation* 2013 (2013) 38, 39

[125] Massberg, Steffen ; Brand, Korbinian ; Grüner, Sabine ; Page, Sharon ; Müller, Elke ; Müller, Iris ; Bergmeier, Wolfgang ; Richter, Thomas ; Lorenz, Michael ; Konrad, Ildiko u. a.: A critical role of platelet adhesion in the initiation of atherosclerotic lesion formation. In: *The Journal of experimental medicine* 196 (2002), Nr. 7, S. 887–896 38

[126] Santos, Sascha M. ; Klinkhardt, Ute ; Scholich, Klaus ; Nelson, Karen ; Monsefi, Nadejda ; Deckmyn, Hans ; Kuczka, Karina ; Zorn, Anita ; Harder, Sebastian: The CX3C chemokine fractalkine mediates platelet adhesion via the von Willebrand receptor glycoprotein Ib. In: *Blood* 117 (2011), Nr. 18, S. 4999–5008 38, 49, 119

[127] Lievens, Dirk ; Hundelshausen, Philipp von: Platelets in atherosclerosis. In: *Thrombosis and haemostasis* 106 (2011), Nr. 5, S. 827 38, 49, 119

[128] Johnson, Jason L. ; Newby, Andrew C.: Macrophage heterogeneity in atherosclerotic plaques. In: *Current opinion in lipidology* 20 (2009), Nr. 5, S. 370 38, 48, 125, 129

[129] Shashkin, Pavel ; Dragulev, Bojan ; Ley, Klaus: Macrophage differentiation to foam cells. In: *Current pharmaceutical design* 11 (2005), Nr. 23, S. 3061–3072 38, 43

[130] Peiser, Leanne ; Mukhopadhyay, Subhankar ; Gordon, Siamon: Scavenger receptors in innate immunity. In: *Current opinion in immunology* 14 (2002), Nr. 1, S. 123–128 38

[131] Krieger, Monty: The other side of scavenger receptors: pattern recognition for host defense. In: *Current opinion in lipidology* 8 (1997), Nr. 5, S. 275–280 38

[132] Paulson, Kim E. ; Zhu, Su-Ning ; Chen, Mian ; Nurmohamed, Sabrina ; Jongstra-Bilen, Jenny ; Cybulsky, Myron I.: Resident intimal dendritic cells accumulate lipid and contribute to the initiation of atherosclerosis. In: *Circulation research* 106 (2010), Nr. 2, S. 383–390 38

[133] Janeway Jr, Charles A. ; Medzhitov, Ruslan: Innate immune recognition. In: *Annual review of immunology* 20 (2002), Nr. 1, S. 197–216 38

[134] Edfeldt, Kristina ; Swedenborg, Jesper ; Hansson, Göran K ; Yan, Zhong-qun: Expression of toll-like receptors in human atherosclerotic lesions A possible pathway for plaque activation. In: *Circulation* 105 (2002), Nr. 10, S. 1158–1161 38

[135] Miller, Yury I. ; Chang, Mi-Kyung ; Binder, Christoph J. ; Shaw, Peter X. ; Witztum, Joseph L.: Oxidized low density lipoprotein and innate immune receptors. In: *Current opinion in lipidology* 14 (2003), Nr. 5, S. 437–445 38, 39

[136] Tedgui, Alain ; Mallat, Ziad: Cytokines in atherosclerosis: pathogenic and regulatory pathways. In: *Physiological reviews* 86 (2006), Nr. 2, S. 515–581 38

[137] Hansson, Göran K: Inflammation, atherosclerosis, and coronary artery disease. In: *New England Journal of Medicine* 352 (2005), Nr. 16, S. 1685–1695 38

[138] Newby, Andrew C.: Dual role of matrix metalloproteinases (matrixins) in intimal thickening and atherosclerotic plaque rupture. In: *Physiological reviews* 85 (2005), Nr. 1, S. 1–31 38, 39

[139] Hansson, Göran K: Immune mechanisms in atherosclerosis. In: *Arteriosclerosis, thrombosis, and vascular biology* 21 (2001), Nr. 12, S. 1876–1890 38

[140] Bot, Ilze ; Jager, Saskia C. ; Zernecke, Alma ; Lindstedt, Ken A. ; Berkel, Theo J. ; Weber, Christian ; Biessen, Erik A.: Perivascular mast cells promote atherogenesis and induce plaque destabilization in apolipoprotein E–deficient mice. In: *Circulation* 115 (2007), Nr. 19, S. 2516–2525 38

[141] Doran, Amanda C. ; Meller, Nahum ; McNamara, Coleen A.: Role of smooth muscle cells in the initiation and early progression of atherosclerosis. In: *Arteriosclerosis, thrombosis, and vascular biology* 28 (2008), Nr. 5, S. 812–819 39

[142] HEGYI, LASZLO ; SKEPPER, JEREMY N. ; CARY, NAT R. ; MITCHINSON, MALCOLM J.: Foam cell apoptosis and the development of the lipid core of human atherosclerosis. In: *The Journal of pathology* 180 (1996), Nr. 4, S. 423–429 39

[143] Tintut, Yin ; Patel, Jignesh ; Territo, Mary ; Saini, Trishal ; Parhami, Farhad ; Demer, Linda L.: Monocyte/macrophage regulation of vascular calcification in vitro. In: *Circulation* 105 (2002), Nr. 5, S. 650–655 39

[144] Moulton, Karen S. ; Vakili, Khashayar ; Zurakowski, David ; Soliman, Mohsin ; Butterfield, Catherine ; Sylvin, Erik ; Lo, Kin-Ming ; Gillies, Stephen ; Javaherian, Kashi ; Folkman, Judah: Inhibition of plaque neovascularization reduces macrophage accumulation and progression of advanced atherosclerosis. In: *Proceedings of the National Academy of Sciences* 100 (2003), Nr. 8, S. 4736–4741 39

[145] Trautwein, C ; Böker, K ; Manns, MP: Hepatocyte and immune system: acute phase reaction as a contribution to early defence mechanisms. In: *Gut* 35 (1994), Nr. 9, S. 1163–1166 39

[146] Gruys, E ; Toussaint, MJM ; Niewold, TA ; Koopmans, SJ: Review: Acute phase reaction and acute phase proteins. In: *Journal of Zhejiang University. Science. B* 6 (2005), Nr. 11, S. 1045 39

[147] Park, Hye S. ; Park, Jung Y. ; Yu, Rina: Relationship of obesity and visceral adiposity with serum concentrations of CRP, TNF-α and IL-6. In: *Diabetes research and clinical practice* 69 (2005), Nr. 1, S. 29–35 39

[148] Schuett, Harald ; Luchtefeld, Maren ; Grothusen, Christina ; Grote, Karsten ; Schieffer, Bernhard: How much is too much? Interleukin-6 and its signalling in atherosclerosis. In: *Thromb Haemost* 102 (2009), Nr. 2, S. 215–222 39

[149] Lutgens, Suzanne P. ; Cleutjens, Kitty B. ; Daemen, Mat J. ; Heeneman, Sylvia: Cathepsin cysteine proteases in cardiovascular disease. In: *The FASEB Journal* 21 (2007), Nr. 12, S. 3029–3041 39

[150] Badimon, Lina ; Storey, Robert F. ; Vilahur, Gemma: Update on lipids, inflammation and atherothrombosis. In: *Thrombosis and haemostasis* 105 (2011), Nr. 1, S. S34 39

[151] Zaman, AG ; Helft, G ; Worthley, SG ; Badimon, JJ: The role of plaque rupture and thrombosis in coronary artery disease. In: *Atherosclerosis* 149 (2000), Nr. 2, S. 251–266 39

[152] Yusuf, Salim ; Hawken, Steven ; Ôunpuu, Stephanie ; Dans, Tony ; Avezum, Alvaro ; Lanas, Fernando ; McQueen, Matthew ; Budaj, Andrzej ; Pais, Prem ; Varigos, John u. a.: Effect of potentially modifiable risk factors associated with

myocardial infarction in 52 countries (the INTERHEART study): case-control study. In: *The Lancet* 364 (2004), Nr. 9438, S. 937–952 40

[153] Fraser, Gary E. ; Shavlik, David J.: Ten years of life: Is it a matter of choice? In: *Archives of Internal Medicine* 161 (2001), Nr. 13, S. 1645–1652 40

[154] Yates, Laurel B. ; Djoussé, Luc ; Kurth, Tobias ; Buring, Julie E. ; Gaziano, J M.: Exceptional longevity in men: modifiable factors associated with survival and function to age 90 years. In: *Archives of Internal Medicine* 168 (2008), Nr. 3, S. 284–290 40

[155] Handschin, Christoph ; Spiegelman, Bruce M.: The role of exercise and PGC1α in inflammation and chronic disease. In: *Nature* 454 (2008), Nr. 7203, S. 463–469 40

[156] Wen, Chi P. ; Wai, Jackson Pui M. ; Tsai, Min K. ; Yang, Yi C. ; Cheng, Ting Yuan D. ; Lee, Meng-Chih ; Chan, Hui T. ; Tsao, Chwen K. ; Tsai, Shan P. ; Wu, Xifeng: Minimum amount of physical activity for reduced mortality and extended life expectancy: a prospective cohort study. In: *The Lancet* 378 (2011), Nr. 9798, S. 1244–1253 40

[157] Hambrecht, Rainer ; Walther, Claudia ; Möbius-Winkler, Sven ; Gielen, Stephan ; Linke, Axel ; Conradi, Katrin ; Erbs, Sandra ; Kluge, Regine ; Kendziorra, Kai ; Sabri, Osama u. a.: Percutaneous coronary angioplasty compared with exercise training in patients with stable coronary artery disease a randomized trial. In: *Circulation* 109 (2004), Nr. 11, S. 1371–1378 40

[158] Walther, Claudia ; Möbius-Winkler, Sven ; Linke, Axel ; Bruegel, Mathias ; Thiery, Joachim ; Schuler, Gerhard ; Halbrecht, Rainer: Regular exercise training compared with percutaneous intervention leads to a reduction of inflammatory markers and cardiovascular events in patients with coronary artery disease. In: *European Journal of Cardiovascular Prevention & Rehabilitation* 15 (2008), Nr. 1, S. 107–112 40

[159] Swain, David P. ; Franklin, Barry A.: Comparison of cardioprotective benefits of vigorous versus moderate intensity aerobic exercise. In: *The American journal of cardiology* 97 (2006), Nr. 1, S. 141–147 40

[160] Moholdt, Trine T. ; Amundsen, Brage H. ; Rustad, Lene A. ; Wahba, Alexander ; Løvø, Kjersti T. ; Gullikstad, Lisbeth R. ; Bye, Anja ; Skogvoll, Eirik ; Wisløff, Ulrik ; Slørdahl, Stig A.: Aerobic interval training versus continuous moderate exercise after coronary artery bypass surgery: a randomized study of cardiovascular effects and quality of life. In: *American heart journal* 158 (2009), Nr. 6, S. 1031–1037 40

[161] Keteyian, Steven J. ; Brawner, Clinton A. ; Savage, Patrick D. ; Ehrman, Jonathan K. ; Schairer, John ; Divine, George ; Aldred, Heather ; Ophaug, Kristin ; Ades, Philip A.: Peak aerobic capacity predicts prognosis in patients with coronary heart disease. In: *American heart journal* 156 (2008), Nr. 2, S. 292–300 40

[162] Munk, Peter S. ; Staal, Eva M. ; Butt, Noreen ; Isaksen, Kjetil ; Larsen, Alf I.: High-intensity interval training may reduce in-stent restenosis following percutaneous coronary intervention with stent implantation: a randomized controlled trial evaluating the relationship to endothelial function and inflammation. In: *American heart journal* 158 (2009), Nr. 5, S. 734–741 40

[163] Wald, Nicholas J. ; Law, Malcolm R.: A strategy to reduce cardiovascular disease by more than 80%. In: *Bmj* 326 (2003), Nr. 7404, S. 1419 40

[164] Getz, Godfrey S. ; Reardon, Catherine A.: Apoprotein E as a lipid transport and signaling protein in the blood, liver, and artery wall. In: *Journal of lipid research* 50 (2009), Nr. Supplement, S. S156–S161 40, 138

[165] Davignon, Jean: Apolipoprotein E and atherosclerosis beyond lipid effect. In: *Arteriosclerosis, thrombosis, and vascular biology* 25 (2005), Nr. 2, S. 267–269 40

[166] Shore, Virgie G. ; Shore, Bernard: Heterogeneity of human plasma very low density lipoproteins. Separation of species differing in protein components. In: *Biochemistry* 12 (1973), Nr. 3, S. 502–507 40

[167] Mahley, Robert W. ; Rall Jr, Stanley C.: Apolipoprotein E: far more than a lipid transport protein. In: *Annual review of genomics and human genetics* 1 (2000), Nr. 1, S. 507–537 40, 41, 43, 52, 91, 92

[168] Elshourbagy, Nabil A. ; Liao, Warren S. ; Mahley, Robert W. ; Taylor, John M.: Apolipoprotein E mRNA is abundant in the brain and adrenals, as well as in the liver, and is present in other peripheral tissues of rats and marmosets. In: *Proceedings of the National Academy of Sciences* 82 (1985), Nr. 1, S. 203–207 40

[169] Newman, Thomas C. ; Dawson, PA ; Rudel, LL ; Williams, DL: Quantitation of apolipoprotein E mRNA in the liver and peripheral tissues of nonhuman primates. In: *Journal of Biological Chemistry* 260 (1985), Nr. 4, S. 2452–2457 41, 91

[170] Greenow, Kirsty ; Pearce, Nigel J. ; Ramji, Dipak P.: The key role of apolipoprotein E in atherosclerosis. In: *Journal of Molecular Medicine* 83 (2005), Nr. 5, S. 329–342 41, 42, 91, 138

[171] Rall, SC ; Mahley, RW: The role of apolipoprotein E genetic variants in lipoprotein disorders. In: *Journal of internal medicine* 231 (1992), Nr. 6, S. 653–659 41, 42, 52, 54, 91

[172] Xue, Cheng ; Nie, Wei ; Tang, Dan ; Yi, Lujiang ; Mei, Changlin: Apolipoprotein E Gene Variants on the Risk of End Stage Renal Disease. In: *PloS one* 8 (2013), Nr. 12, S. e83367 41

[173] Song, Yiqing ; Stampfer, Meir J. ; Liu, Simin: Meta-analysis: apolipoprotein E genotypes and risk for coronary heart disease. In: *Annals of internal medicine* 141 (2004), Nr. 2, S. 137–147 41, 43, 52, 54, 92, 139

[174] Farrer, Lindsay A. ; Cupples, L A. ; Haines, Jonathan L. ; Hyman, Bradley ; Kukull, Walter A. ; Mayeux, Richard ; Myers, Richard H. ; Pericak-Vance, Margaret A. ; Risch, Neil ; Duijn, Cornelia M.: Effects of age, sex, and ethnicity on the association between apolipoprotein E genotype and Alzheimer disease: a meta-analysis. In: *Jama* 278 (1997), Nr. 16, S. 1349–1356 41, 140

[175] Corder, EH ; Saunders, AM ; Strittmatter, WJ ; Schmechel, DE ; Gaskell, PC ; Small, GWet ; Roses, AD ; Haines, JL ; Pericak-Vance, M A.: Gene dose of apolipoprotein E type 4 allele and the risk of Alzheimer's disease in late onset families. In: *Science* 261 (1993), Nr. 5123, S. 921–923 41, 140

[176] Kuhlmann, Inga ; Minihane, Anne M. ; Huebbe, Patricia ; Nebel, Almut ; Rimbach, Gerald: Apolipoprotein E genotype and hepatitis C, HIV and herpes simplex disease risk: a literature review. In: *Lipids in health and disease* 9 (2010), Nr. 1, S. 8 41

[177] Kulminski, Alexander M. ; Culminskaya, Irina ; Ukraintseva, Svetlana V. ; Arbeev, Konstantin G. ; Arbeeva, Liubov ; Wu, Deqing ; Akushevich, Igor ; Land, Kenneth C. ; Yashin, Anatoli I.: Trade-off in the effects of the apolipoprotein E polymorphism on the ages at onset of CVD and cancer influences human lifespan. In: *Aging cell* 10 (2011), Nr. 3, S. 533–541 41, 42, 139

[178] Horsburgh, Karen ; Graham, David I. ; Stewart, Janice ; Nicoll, JA: Influence of apolipoprotein E genotype on neuronal damage and apoE immunoreactivity in human hippocampus following global ischemia. In: *Journal of neuropathology and experimental neurology* 58 (1999), Nr. 3, S. 227–234 41

[179] Chamelian, Laury ; Reis, Marciano ; Feinstein, Anthony: Six-month recovery from mild to moderate traumatic brain injury: the role of APOE-ε4 allele. In: *Brain* 127 (2004), Nr. 12, S. 2621–2628 41

[180] Gottlieb, DJ ; DeStefano, AL ; Foley, DJ ; Mignot, E ; Redline, S ; Givelber, RJ ; Young, T: APOE ε4 is associated with obstructive sleep apnea/hypopnea The Sleep Heart Health Study. In: *Neurology* 63 (2004), Nr. 4, S. 664–668 41

[181] Zonouzi, Ahmad P. ; Farajzadeh, Davoud ; Bargahi, Nasrin ; Farajzadeh, Malak: Apolipoprotein E genotyping in women with recurrent pregnancy loss: An in silico and experimental hybrid study. In: *Gene* 549 (2014), Nr. 2, S. 209–213 41

[182] Yin, Yan-Wei ; Qiao, Li ; Sun, Qian-Qian ; Hu, Ai-Min ; Liu, Hong-Li ; Wang, Qi ; Hou, Zhi-Zhen: Influence of apolipoprotein E gene polymorphism on development of type 2 diabetes mellitus in Chinese Han population: A meta-analysis of 29 studies. In: *Metabolism* 63 (2014), Nr. 4, S. 532–541 41

[183] Allan, Charles M. ; Walker, David ; Segrest, Jere P. ; Taylor, John M.: Identification and characterization of a new human gene (APOC4) in the apolipoprotein E, CI, and C-II gene locus. In: *Genomics* 28 (1995), Nr. 2, S. 291–300 41

[184] Zannis, Vassilis I. ; McPherson, Joseph ; Goldberger, Gabriel ; Karathanasis, Sotirios K. ; Breslow, Jan L.: Synthesis, intracellular processing, and signal peptide of human apolipoprotein E. In: *Journal of Biological Chemistry* 259 (1984), Nr. 9, S. 5495–5499 41

[185] Mazzone, Theodore ; Papagiannes, Elaine ; Magner, James: Early kinetics of human macrophage apolipoprotein E synthesis and incorporation of carbohydrate precursors. In: *Biochimica et Biophysica Acta (BBA)-Lipids and Lipid Metabolism* 875 (1986), Nr. 2, S. 393–396 41

[186] Wetterau, JR ; Aggerbeck, LP ; Rall, SC ; Weisgraber, KH: Human apolipoprotein E3 in aqueous solution. I. Evidence for two structural domains. In: *Journal of Biological Chemistry* 263 (1988), Nr. 13, S. 6240–6248 41

[187] Aggerbeck, LP ; Wetterau, JR ; Weisgraber, KH ; Wu, CS ; Lindgren, FT: Human apolipoprotein E3 in aqueous solution. II. Properties of the amino-and carboxyl-terminal domains. In: *Journal of Biological Chemistry* 263 (1988), Nr. 13, S. 6249–6258 41

[188] Wilson, Charles ; Wardell, Mark R. ; Weisgraber, Karl H. ; Mahley, Robert W. ; Agard, David A.: Three-dimensional structure of the LDL receptor-binding domain of human apolipoprotein E. In: *Science* 252 (1991), Nr. 5014, S. 1817–1822 41, 43

[189] Saito, Hiroyuki ; Lund-Katz, Sissel ; Phillips, Michael C.: Contributions of domain structure and lipid interaction to the functionality of exchangeable human apolipoproteins. In: *Progress in lipid research* 43 (2004), Nr. 4, S. 350–380 41

[190] Thuahnai, Stephen T. ; Lund-Katz, Sissel ; Anantharamaiah, GM ; Williams, David L. ; Phillips, Michael C.: A quantitative analysis of apolipoprotein binding to SR-BI multiple binding sites for lipid-free and lipid-associated apolipoproteins. In: *Journal of lipid research* 44 (2003), Nr. 6, S. 1132–1142 41, 42

[191] Weisgraber, Karl H.: Apolipoprotein E: structure-function relationships. In: *Advances in protein chemistry* 45 (1994), S. 249–302 41

[192] Libeu, Clare P. ; Lund-Katz, Sissel ; Phillips, Michael C. ; Wehrli, Suzanne ; Hernáiz, Maria J. ; Capila, Ishan ; Linhardt, Robert J. ; Raffai, Robert L. ; Newhouse, Yvonne M. ; Zhou, Fanyu u. a.: New insights into the heparan sulfate proteoglycan-binding activity of apolipoprotein E. In: *Journal of Biological Chemistry* 276 (2001), Nr. 42, S. 39138–39144 41

[193] Choy, Nicole ; Raussens, Vincent ; Narayanaswami, Vasanthy: Inter-molecular coiled-coil formation in human apolipoprotein E C-terminal domain. In: *Journal of molecular biology* 334 (2003), Nr. 3, S. 527–539 41

[194] Dong, Li-Ming ; Wilson, Charles ; Wardell, Mark R. ; Simmons, Trey ; Mahley, Robert W. ; Weisgraber, Karl H. ; Agard, David A.: Human apolipoprotein E. Role of arginine 61 in mediating the lipoprotein preferences of the E3 and E4 isoforms. In: *Journal of Biological Chemistry* 269 (1994), Nr. 35, S. 22358–22365 41

[195] Weisgraber, KH ; Rall, SC ; Mahley, RW ; Milne, RW ; Marcel, YL ; Sparrow, JT: Human apolipoprotein E. Determination of the heparin binding sites of apolipoprotein E3. In: *Journal of Biological Chemistry* 261 (1986), Nr. 5, S. 2068–2076 41

[196] Kypreos, Kyriakos E. ; Dijk, Ko W. ; Havekes, Louis M. ; Zannis, Vassilis I.: Generation of a recombinant apolipoprotein E variant with improved biological functions: hydrophobic residues (L261, W264, F265, L268, V269) of apoE can account for the apoE-induced hypertriglyceridemia. In: *Journal of Biological Chemistry* (2004) 41, 42

[197] Pham, Thomas ; Kodvawala, Ahmer ; Hui, David Y.: The receptor binding domain of apolipoprotein E is responsible for its antioxidant activity. In: *Biochemistry* 44 (2005), Nr. 20, S. 7577–7582 41

[198] Miyata, Masaaki ; Smith, Jonathan D.: Apolipoprotein E allele–specific antioxidant activity and effects on cytotoxicity by oxidative insults and β–amyloid peptides. In: *Nature genetics* 14 (1996), Nr. 1, S. 55–61 41, 42

[199] Mahley, Robert W. ; Innerarity, Thomas L. ; Rall, Stanley C. ; Weisgraber, Karl H.: Plasma lipoproteins: apolipoprotein structure and function. In: *Journal of lipid research* 25 (1984), Nr. 12, S. 1277–1294 41

[200] Raffai, Robert L. ; Loeb, Samuel M. ; Weisgraber, Karl H.: Apolipoprotein E promotes the regression of atherosclerosis independently of lowering plasma choles-

terol levels. In: *Arteriosclerosis, thrombosis, and vascular biology* 25 (2005), Nr. 2, S. 436–441 41, 91, 138

[201] Thorngate, Fayanne E. ; Rudel, Lawrence L. ; Walzem, Rosemary L. ; Williams, David L.: Low levels of extrahepatic nonmacrophage ApoE inhibit atherosclerosis without correcting hypercholesterolemia in ApoE-deficient mice. In: *Arteriosclerosis, thrombosis, and vascular biology* 20 (2000), Nr. 8, S. 1939–1945 41, 91, 138

[202] Kuipers, Folkert ; Jong, Miek C. ; Lin, Yuguang ; Eck, M v. ; Havinga, Rick ; Bloks, Vincent ; Verkade, Henkjan J. ; Hofker, Marten H. ; Moshage, Han ; Berkel, TJ u. a.: Impaired secretion of very low density lipoprotein-triglycerides by apolipoprotein E-deficient mouse hepatocytes. In: *Journal of Clinical Investigation* 100 (1997), Nr. 11, S. 2915 42

[203] Fazio, S ; Yao, Z ; McCarthy, Brian J. ; Rall, SC: Synthesis and secretion of apolipoprotein E occur independently of synthesis and secretion of apolipoprotein B-containing lipoproteins in HepG2 cells. In: *Journal of Biological Chemistry* 267 (1992), Nr. 10, S. 6941–6945 42

[204] Huang, Yadong ; Ji, Zhong-Sheng ; Brecht, Walter J. ; Rall, Stanley C. ; Taylor, John M. ; Mahley, Robert W.: Overexpression of apolipoprotein E3 in transgenic rabbits causes combined hyperlipidemia by stimulating hepatic VLDL production and impairing VLDL lipolysis. In: *Arteriosclerosis, thrombosis, and vascular biology* 19 (1999), Nr. 12, S. 2952–2959 42

[205] Krimbou, Larbi ; Denis, Maxime ; Haidar, Bassam ; Carrier, Marilyn ; Marcil, Michel ; Genest, Jacques: Molecular interactions between apoE and ABCA1 impact on apoE lipidation. In: *Journal of lipid research* 45 (2004), Nr. 5, S. 839–848 42

[206] Hayek, Tony ; Oiknine, Judith ; Brook, J G. ; Aviram, Michael: Role of HDL apolipoprotein E in cellular cholesterol efflux: studies in apo E knockout transgenic mice. In: *Biochemical and biophysical research communications* 205 (1994), Nr. 2, S. 1072–1078 42

[207] Mazzone, Theodore ; Reardon, Catherine: Expression of heterologous human apolipoprotein E by J774 macrophages enhances cholesterol efflux to HDL3. In: *Journal of lipid research* 35 (1994), Nr. 8, S. 1345–1353 42

[208] Smith, Jonathan D. ; Miyata, Masaaki ; Ginsberg, Michael ; Grigaux, Claire ; Shmookler, Eric ; Plump, Andrew S.: Cyclic AMP induces apolipoprotein E binding activity and promotes cholesterol efflux from a macrophage cell line to

apolipoprotein acceptors. In: *Journal of Biological Chemistry* 271 (1996), Nr. 48, S. 30647–30655 42

[209] Kinoshita, Makoto ; Arai, Hiroyuki ; Fukasawa, M ; Watanabe, T ; Tsukamoto, K ; Hashimoto, Y ; Inoue, K ; Kurokawa, K ; Teramoto, T: Apolipoprotein E enhances lipid exchange between lipoproteins mediated by cholesteryl ester transfer protein. In: *Journal of lipid research* 34 (1993), Nr. 2, S. 261–268 42

[210] De Pauw, Martine ; Vanloo, Berlinda ; Weisgraber, Karl ; Rosseneu, Maryvonne: Comparison of lipid-binding and lecithin: cholesterol acyltransferase activation of the amino-and carboxyl-terminal domains of human apolipoprotein E3. In: *Biochemistry* 34 (1995), Nr. 34, S. 10953–10960 42

[211] Thuren, Tom ; Weisgraber, Karl H. ; Sisson, Patricia ; Waite, Moseley: Role of apolipoprotein E in hepatic lipase-catalyzed hydrolysis of phospholipid in high-density lipoproteins. In: *Biochemistry* 31 (1992), Nr. 8, S. 2332–2338 42

[212] Gough, Peter J. ; Raines, Elaine W.: Gene therapy of apolipoprotein E–deficient mice using a novel macrophage-specific retroviral vector. In: *Blood* 101 (2003), Nr. 2, S. 485–491 42, 91, 138

[213] Van Eck, Miranda ; Herijgers, Nicole ; Vidgeon-Hart, Martin ; Pearce, Nigel J. ; Hoogerbrugge, Peter M. ; Groot, Pieter H. ; Van Berkel, Theo J.: Accelerated atherosclerosis in C57Bl/6 mice transplanted with ApoE-deficient bone marrow. In: *Atherosclerosis* 150 (2000), Nr. 1, S. 71–80 42, 52, 91, 138

[214] Linton, MacRae F. ; Fazio, Sergio: Macrophages, lipoprotein metabolism, and atherosclerosis: insights from murine bone marrow transplantation studies. In: *Current opinion in lipidology* 10 (1999), Nr. 2, S. 97–106 42, 52, 91, 138

[215] Hasty, Alyssa H. ; Linton, MacRae F. ; Brandt, Stephen J. ; Babaev, Vladimir R. ; Gleaves, Linda A. ; Fazio, Sergio: Retroviral Gene Therapy in ApoE-Deficient Mice ApoE Expression in the Artery Wall Reduces Early Foam Cell Lesion Formation. In: *Circulation* 99 (1999), Nr. 19, S. 2571–2576 42, 91, 138

[216] Fazio, Sergio ; Babaev, Vladimir R. ; Murray, Alisa B. ; Hasty, Alyssa H. ; Carter, Kathy J. ; Gleaves, Linda A. ; Atkinson, James B. ; Linton, MacRae F.: Increased atherosclerosis in mice reconstituted with apolipoprotein E null macrophages. In: *Proceedings of the National Academy of Sciences* 94 (1997), Nr. 9, S. 4647–4652 42, 52, 91, 138

[217] Bellosta, S ; Mahley, RW ; Sanan, DA ; Murata, J ; Newland, DL ; Taylor, JM ; Pitas, RE: Macrophage-specific expression of human apolipoprotein E reduces

atherosclerosis in hypercholesterolemic apolipoprotein E-null mice. In: *Journal of Clinical Investigation* 96 (1995), Nr. 5, S. 2170 42, 91, 138

[218] Kawamura, Akira ; Baitsch, Daniel ; Telgmann, Ralph ; Feuerborn, Renata ; Weissen-Plenz, Gabriele ; Hagedorn, Claudia ; Saku, Keijiro ; Brand-Herrmann, Stefan-Martin ; Eckardstein, Arnold von ; Assmann, Gerd u. a.: Apolipoprotein E interrupts interleukin-1β signaling in vascular smooth muscle cells. In: *Arteriosclerosis, thrombosis, and vascular biology* 27 (2007), Nr. 7, S. 1610–1617 42

[219] Ali, Kamilah ; Middleton, Melissa ; Puré, Ellen ; Rader, Daniel J.: Apolipoprotein E suppresses the type I inflammatory response in vivo. In: *Circulation research* 97 (2005), Nr. 9, S. 922–927 42

[220] Vogel, Tikva ; Guo, Neng-Hua ; Guy, Rachel ; Drezlich, Nina ; Krutzsch, Henry C. ; Blake, Diane A. ; Panet, Amos ; Roberts, David D.: Apolipoprotein E: a potent inhibitor of endothelial and tumor cell proliferation. In: *Journal of cellular biochemistry* 54 (1994), Nr. 3, S. 299–308 42

[221] Riddell, David R. ; Vinogradov, Dimitri V. ; Stannard, Anita K. ; Chadwick, Nicholas ; Owen, James S.: Identification and characterization of LRP8 (apoER2) in human blood platelets. In: *Journal of lipid research* 40 (1999), Nr. 10, S. 1925–1930 42, 91

[222] Elzen, Peter van d. ; Garg, Salil ; León, Luis ; Brigl, Manfred ; Leadbetter, Elizabeth A. ; Gumperz, Jenny E. ; Dascher, Chris C. ; Cheng, Tan-Yun ; Sacks, Frank M. ; Illarionov, Petr A. u. a.: Apolipoprotein-mediated pathways of lipid antigen presentation. In: *Nature* 437 (2005), Nr. 7060, S. 906–910 42

[223] Tenger, Charlotta ; Zhou, Xinghua: Apolipoprotein E modulates immune activation by acting on the antigen-presenting cell. In: *Immunology* 109 (2003), Nr. 3, S. 392–397 42

[224] Hui, David Y. ; Harmony, JA: Inhibition of Ca2+ accumulation in mitogen-activated lymphocytes: role of membrane-bound plasma lipoproteins. In: *Proceedings of the National Academy of Sciences* 77 (1980), Nr. 8, S. 4764–4768 42

[225] Avila, EM ; Holdsworth, G ; Sasaki, N ; Jackson, RL ; Harmony, JA: Apoprotein E suppresses phytohemagglutinin-activated phospholipid turnover in peripheral blood mononuclear cells. In: *Journal of Biological Chemistry* 257 (1982), Nr. 10, S. 5900–5909 42

[226] Jofre-Monseny, Laia ; Minihane, Anne-Marie ; Rimbach, Gerald: Impact of apoE genotype on oxidative stress, inflammation and disease risk. In: *Molecular nutrition & food research* 52 (2008), Nr. 1, S. 131–145 42

[227] Kelly, Michael E. ; Clay, Moira A. ; Mistry, Meenakshi J. ; Hsieh-Li, Hsiu-Mei ; Harmony, Judith A.: Apolipoprotein E inhibition of proliferation of mitogen-activated T lymphocytes: production of interleukin 2 with reduced biological activity. In: *Cellular immunology* 159 (1994), Nr. 2, S. 124–139 42

[228] Hui, David Y. ; Basford, Joshua E.: Distinct signaling mechanisms for apoE inhibition of cell migration and proliferation. In: *Neurobiology of aging* 26 (2005), Nr. 3, S. 317–323 42

[229] Swertfeger, Debi K. ; Hui, David Y.: Apolipoprotein E Receptor Binding Versus Heparan Sulfate Proteoglycan Binding in Its Regulation of Smooth Muscle Cell Migration and Proliferation. In: *Journal of Biological Chemistry* 276 (2001), Nr. 27, S. 25043–25048 42

[230] Sacre, Sandra M. ; Stannard, Anita K. ; Owen, James S.: Apolipoprotein E (apoE) isoforms differentially induce nitric oxide production in endothelial cells. In: *FEBS letters* 540 (2003), Nr. 1, S. 181–187 42

[231] Napoli, Claudio ; Nigris, Filomena de ; Williams-Ignarro, Sharon ; Pignalosa, Orlando ; Sica, Vincenzo ; Ignarro, Louis J.: Nitric oxide and atherosclerosis: an update. In: *Nitric oxide* 15 (2006), Nr. 4, S. 265–279 42

[232] Knowles, Joshua W. ; Reddick, Robert L. ; Jennette, J C. ; Shesely, Edward G. ; Smithies, Oliver ; Maeda, Nobuyo u. a.: Enhanced atherosclerosis and kidney dysfunction in eNOS–/–Apoe–/–mice are ameliorated by enalapril treatment. In: *The Journal of clinical investigation* 105 (2000), Nr. 4, S. 451–458 42, 91

[233] Eichner, June E. ; Dunn, S T. ; Perveen, Ghazala ; Thompson, David M. ; Stewart, Kenneth E. ; Stroehla, Berrit C.: Apolipoprotein E polymorphism and cardiovascular disease: a HuGE review. In: *American journal of epidemiology* 155 (2002), Nr. 6, S. 487–495 42, 43, 91, 92, 139

[234] Zuo, Lingjun ; Van Dyck, Christopher H. ; Luo, Xingguang ; Kranzler, Henry R. ; Yang, Bao-zhu ; Gelernter, Joel: Variation at APOE and STH loci and Alzheimer's disease. In: *Behav Brain Funct* 2 (2006), S. 13 42, 91, 92

[235] Eisenberg, Dan T. ; Kuzawa, Christopher W. ; Hayes, M G.: Worldwide allele frequencies of the human apolipoprotein E gene: climate, local adaptations, and evolutionary history. In: *American journal of physical anthropology* 143 (2010), Nr. 1, S. 100–111 42

[236] Mahley, Robert W. ; Weisgraber, Karl H. ; Huang, Yadong: Apolipoprotein E: structure determines function, from atherosclerosis to Alzheimer's disease to AIDS. In: *Journal of lipid research* 50 (2009), Nr. Supplement, S. S183–S188 42, 43

[237] Hatters, Danny M. ; Peters-Libeu, Clare A. ; Weisgraber, Karl H.: Apolipoprotein E structure: insights into function. In: *Trends in biochemical sciences* 31 (2006), Nr. 8, S. 445–454 42, 43

[238] Acharya, Prathima ; Segall, Mark L. ; Zaiou, Mohamed ; Morrow, Julie ; Weisgraber, Karl H. ; Phillips, Michael C. ; Lund-Katz, Sissel ; Snow, Julian: Comparison of the stabilities and unfolding pathways of human apolipoprotein E isoforms by differential scanning calorimetry and circular dichroism. In: *Biochimica et Biophysica Acta (BBA)-Molecular and Cell Biology of Lipids* 1584 (2002), Nr. 1, S. 9–19 42

[239] Morrow, Julie A. ; Segall, Mark L. ; Lund-Katz, Sissel ; Phillips, Michael C. ; Knapp, Mark ; Rupp, Bernhard ; Weisgraber, Karl H.: Differences in stability among the human apolipoprotein E isoforms determined by the amino-terminal domain. In: *Biochemistry* 39 (2000), Nr. 38, S. 11657–11666 42

[240] Innerarity, TL ; Weisgraber, KH ; Arnold, KS ; Rall, SC ; Mahley, RW: Normalization of receptor binding of apolipoprotein E2. Evidence for modulation of the binding site conformation. In: *Journal of Biological Chemistry* 259 (1984), Nr. 11, S. 7261–7267 43, 92

[241] Lalazar, A ; Weisgraber, KH ; Rall, SC ; Giladi, H ; Innerarity, TL ; Levanon, AZ ; Boyles, JK ; Amit, B ; Gorecki, M ; Mahley, RW: Site-specific mutagenesis of human apolipoprotein E. Receptor binding activity of variants with single amino acid substitutions. In: *Journal of Biological Chemistry* 263 (1988), Nr. 8, S. 3542–3545 43

[242] Weintraub, Moshe S. ; Eisenberg, Shlomo ; Breslow, Jan L.: Dietary fat clearance in normal subjects is regulated by genetic variation in apolipoprotein E. In: *Journal of Clinical Investigation* 80 (1987), Nr. 6, S. 1571 43

[243] Mahley, Robert W. ; Huang, Yadong ; Rall, Stanley C.: Pathogenesis of type III hyperlipoproteinemia (dysbetalipoproteinemia): questions, quandaries, and paradoxes. In: *Journal of Lipid Research* 40 (1999), Nr. 11, S. 1933–1949 43

[244] Mahley, Robert W. ; Huang, Yadong u. a.: Atherogenic remnant lipoproteins: role for proteoglycans in trapping, transferring, and internalizing. In: *The Journal of clinical investigation* 117 (2007), Nr. 1, S. 94–98 43

[245] Hatters, Danny M. ; Budamagunta, Madhu S. ; Voss, John C. ; Weisgraber, Karl H.: Modulation of Apolipoprotein E Structure by Domain Interaction DIFFERENCES IN LIPID-BOUND AND LIPID-FREE FORMS. In: *Journal of Biological Chemistry* 280 (2005), Nr. 40, S. 34288–34295 43

[246] Dong, Li-Ming ; Weisgraber, Karl H.: Human apolipoprotein E4 domain interaction Arginine 61 and glutamic acid 255 interact to direct the preference for very low density lipoproteins. In: *Journal of Biological Chemistry* 271 (1996), Nr. 32, S. 19053–19057 43

[247] Saito, Hiroyuki ; Dhanasekaran, Padmaja ; Baldwin, Faye ; Weisgraber, Karl H. ; Phillips, Michael C. ; Lund-Katz, Sissel: Effects of polymorphism on the lipid interaction of human apolipoprotein E. In: *Journal of Biological Chemistry* 278 (2003), Nr. 42, S. 40723–40729 43

[248] Gregg, RE ; Zech, LA ; Schaefer, EJ ; Stark, D ; Wilson, D ; Brewer Jr, Hl B.: Abnormal in vivo metabolism of apolipoprotein E4 in humans. In: *Journal of Clinical Investigation* 78 (1986), Nr. 3, S. 815 43

[249] Cullen, Paul ; Cignarella, Andrea ; Brennhausen, Beate ; Mohr, Susanne ; Assmann, Gerd ; Eckardstein, Arnold von: Phenotype-dependent differences in apolipoprotein E metabolism and in cholesterol homeostasis in human monocyte-derived macrophages. In: *Journal of Clinical Investigation* 101 (1998), Nr. 8, S. 1670 43

[250] Heeren, Joerg ; Beisiegel, Ulrike ; Grewal, Thomas: Apolipoprotein E recycling implications for dyslipidemia and atherosclerosis. In: *Arteriosclerosis, thrombosis, and vascular biology* 26 (2006), Nr. 3, S. 442–448 43, 91

[251] Kesäniemi, YA ; Ehnholm, Christian ; Miettinen, Tatu A.: Intestinal cholesterol absorption efficiency in man is related to apoprotein E phenotype. In: *Journal of Clinical Investigation* 80 (1987), Nr. 2, S. 578 43

[252] Tammi, Anne ; Rönnemaa, Tapani ; Rask-Nissilä, Leena ; Miettinen, Tatu A. ; Gylling, Helena ; Valsta, Liisa ; Viikari, Jorma ; Välimäki, Ilkka ; Simell, Olli: Apolipoprotein E phenotype regulates cholesterol absorption in healthy 13-month-old children–The STRIP Study. In: *Pediatric research* 50 (2001), Nr. 6, S. 688–691 43

[253] Hanis, Craig L. ; Hewett-Emmett, David ; Douglas, Tommy C. ; Bertin, Terry K. ; Schull, William J.: Effects of the apolipoprotein E polymorphism on levels of lipids, lipoproteins, and apolipoproteins among Mexican-Americans in Starr County, Texas. In: *Arteriosclerosis, Thrombosis, and Vascular Biology* 11 (1991), Nr. 2, S. 362–370 43, 91, 92

[254] Huang, Yadong ; Liu, Xiao Q. ; Rall, Stanley C. ; Taylor, John M. ; Eckardstein, Arnold von ; Assmann, Gerd ; Mahley, Robert W.: Overexpression and accumulation of apolipoprotein E as a cause of hypertriglyceridemia. In: *Journal of Biological Chemistry* 273 (1998), Nr. 41, S. 26388–26393 44

[255] Brown, Michael S. ; Goldstein, Joseph L.: Receptor-mediated control of cholesterol metabolism. In: *Science* 191 (1976), Nr. 4223, S. 150–154 44, 46, 102

[256] Brown, Michael S. ; Anderson, Richard G. ; Goldstein, Joseph L.: Recycling receptors: the round-trip itinerary of migrant membrane proteins. In: *Cell* 32 (1983), Nr. 3, S. 663–667 44, 45, 102

[257] Basu, Sandip K. ; Goldstein, Joseph L. ; Anderson, Richard G. ; Brown, Michael S.: Monensin interrupts the recycling of low density lipoprotein receptors in human fibroblasts. In: *Cell* 24 (1981), Nr. 2, S. 493–502 44, 45, 102

[258] Soutar, AK ; Myant, NB ; Thompson, GR: Simultaneous measurement of apolipoprotein B turnover in very-low-and low-density lipoproteins in familial hypercholesterolaemia. In: *Atherosclerosis* 28 (1977), Nr. 3, S. 247–256 44, 46

[259] James, RW ; Martin, B ; Pometta, D ; Fruchart, JC ; Duriez, P ; Puchois, P ; Farriaux, JP ; Tacquet, A ; Demant, T ; Clegg, RJ: Apolipoprotein B metabolism in homozygous familial hypercholesterolemia. In: *Journal of lipid research* 30 (1989), Nr. 2, S. 159–169 44, 46

[260] Müller, Carl: Xanthomata, hypercholesterolemia, angina pectoris. In: *Acta Medica Scandinavica* 95 (1938), Nr. S89, S. 75–84 44, 46, 102

[261] Junyent, Mireia ; Gilabert, Rosa ; Jarauta, Estíbaliz ; Núñez, Isabel ; Cofán, Montserrat ; Civeira, Fernando ; Pocoví, Miguel ; Mallén, Miguel ; Zambón, Daniel ; Almagro, Fátima u. a.: Impact of low-density lipoprotein receptor mutational class on carotid atherosclerosis in patients with familial hypercholesterolemia. In: *Atherosclerosis* 208 (2010), Nr. 2, S. 437–441 44, 46, 102

[262] Goldstein, Joseph L. ; Brown, Michael S.: The LDL receptor. In: *Arteriosclerosis, thrombosis, and vascular biology* 29 (2009), Nr. 4, S. 431–438 44, 46, 102

[263] Goldstein, JL ; Hobbs, HH ; Brown, MS: The metabolic and molecular bases of inherited disease. In: *Familial hypercholesterolemia. New York: McGraw-Hill* (2001), S. 2863–913 44, 46, 102

[264] Mattevi, Vanessa S. ; Coimbra Jr, Carlos E. ; Santos, Ricardo V. ; Salzano, Francisco M. ; Hutz, Mara H.: Association of the low-density lipoprotein receptor gene with obesity in Native American populations. In: *Human genetics* 106 (2000), Nr. 5, S. 546–552 44

[265] Francke, Uta ; Brown, Michael S. ; Goldstein, Joseph L.: Assignment of the human gene for the low density lipoprotein receptor to chromosome 19: synteny of a receptor, a ligand, and a genetic disease. In: *Proceedings of the National Academy of Sciences* 81 (1984), Nr. 9, S. 2826–2830 44

[266] Sudhof, Thomas C. ; Goldstein, Joseph L. ; Brown, Michael S. ; Russell, David W.: The LDL receptor gene: a mosaic of exons shared with different proteins. In: *Science* 228 (1985), Nr. 4701, S. 815–822 44, 46

[267] Jansens, Annemieke ; Duijn, Esther van ; Braakman, Ineke: Coordinated nonvectorial folding in a newly synthesized multidomain protein. In: *Science* 298 (2002), Nr. 5602, S. 2401–2403 44

[268] Gent, J ; Braakman, I: Low-density lipoprotein receptor structure and folding. In: *Cellular and Molecular Life Sciences CMLS* 61 (2004), Nr. 19-20, S. 2461–2470 44, 45

[269] Cummings, Richard D. ; Kornfeld, S ; Schneider, WJ ; Hobgood, KK ; Tolleshaug, H ; Brown, MS ; Goldstein, JL: Biosynthesis of N-and O-linked oligosaccharides of the low density lipoprotein receptor. In: *Journal of Biological Chemistry* 258 (1983), Nr. 24, S. 15261–15273 44

[270] Pathak, Ravindra K. ; Merkle, Roberta K. ; Cummings, Richard D. ; Goldstein, Joseph L. ; Brown, Michael S. ; Anderson, RG: Immunocytochemical localization of mutant low density lipoprotein receptors that fail to reach the Golgi complex. In: *The Journal of cell biology* 106 (1988), Nr. 6, S. 1831–1841 44

[271] Hobbs, Helen H. ; Russell, David W. ; Brown, Michael S. ; Goldstein, Joseph L.: The LDL receptor locus in familial hypercholesterolemia: mutational analysis of a membrane protein. In: *Annual review of genetics* 24 (1990), Nr. 1, S. 133–170 44, 46

[272] Bieri, Stephan ; Djordjevic, Julianne T. ; Daly, Norelle L. ; Smith, Ross ; Kroon, Paulus A.: Disulfide bridges of a cysteine-rich repeat of the LDL receptor ligand-binding domain. In: *Biochemistry* 34 (1995), Nr. 40, S. 13059–13065 44

[273] Bieri, Stephan ; Djordjevic, Julianne T. ; Jamshidi, Negar ; Smith, Ross ; Kroon, Paulus A.: Expression and disulfide-bond connectivity of the second ligand-binding repeat of the human LDL receptor. In: *FEBS letters* 371 (1995), Nr. 3, S. 341–344 44

[274] Blacklow, Stephen C. ; Kim, Peter S.: Protein folding and calcium binding defects arising from familial hypercholesterolemia mutations of the LDL receptor. In: *Nature Structural & Molecular Biology* 3 (1996), Nr. 9, S. 758–762 44

[275] Daly, Norelle L. ; Scanlon, Martin J. ; Djordjevic, Julianne T. ; Kroon, Paulus A. ; Smith, Ross: Three-dimensional structure of a cysteine-rich repeat from the low-density lipoprotein receptor. In: *Proceedings of the National Academy of Sciences* 92 (1995), Nr. 14, S. 6334–6338 45

[276] Daly, Norelle L. ; Djordjevic, Julianne T. ; Kroon, Paulus A. ; Smith, Ross: Three-dimensional structure of the second cysteine-rich repeat from the human low-density lipoprotein receptor. In: *Biochemistry* 34 (1995), Nr. 44, S. 14474–14481 45

[277] Clayton, Daniel ; Brereton, Ian M. ; Kroon, Paulus A. ; Smith, Ross: Three-dimensional NMR structure of the sixth ligand-binding module of the human LDL receptor: comparison of two adjacent modules with different ligand binding specificities. In: *FEBS letters* 479 (2000), Nr. 3, S. 118–122 45

[278] North, Christopher L. ; Blacklow, Stephen C.: Solution structure of the sixth LDL-A module of the LDL receptor. In: *Biochemistry* 39 (2000), Nr. 10, S. 2564–2571 45

[279] Fass, Deborah ; Blacklow, Stephen ; Kim, Peter S. ; Berger, James M.: Molecular basis of familial hypercholesterolaemia from structure of LDL receptor module. In: *Nature* 388 (1997), Nr. 6643, S. 691–693 45

[280] Jeon, Hyesung ; Blacklow, Stephen C.: Structure and physiologic function of the low-density lipoprotein receptor. In: *Annual review of biochemistry* 74 (2005), S. 535–562 45

[281] Esser, Victoria ; Limbird, LE ; Brown, Michael S. ; Goldstein, Joseph L. ; Russell, David W.: Mutational analysis of the ligand binding domain of the low density lipoprotein receptor. In: *Journal of Biological Chemistry* 263 (1988), Nr. 26, S. 13282–13290 45, 46

[282] Russell, David W. ; Brown, Michael S. ; Goldstein, Joseph L.: Different combinations of cysteine-rich repeats mediate binding of low density lipoprotein receptor to two different proteins. In: *Journal of Biological Chemistry* 264 (1989), Nr. 36, S. 21682–21688 45, 46

[283] Daniel, Th O. ; Schneider, WJ ; Goldstein, JL ; Brown, MS: Visualization of lipoprotein receptors by ligand blotting. In: *Journal of Biological Chemistry* 258 (1983), Nr. 7, S. 4606–4611 45

[284] Jeon, Hyesung ; Meng, Wuyi ; Takagi, Junichi ; Eck, Michael J. ; Springer, Timothy A. ; Blacklow, Stephen C.: Implications for familial hypercholesterolemia from the structure of the LDL receptor YWTD-EGF domain pair. In: *Nature Structural & Molecular Biology* 8 (2001), Nr. 6, S. 499–504 45

[285] Springer, Timothy A.: An extracellular β-propeller module predicted in lipoprotein and scavenger receptors, tyrosine kinases, epidermal growth factor precursor, and extracellular matrix components. In: *Journal of molecular biology* 283 (1998), Nr. 4, S. 837–862 45

[286] Rudenko, Gabby ; Henry, Lisa ; Henderson, Keith ; Ichtchenko, Konstantin ; Brown, Michael S. ; Goldstein, Joseph L. ; Deisenhofer, Johann: Structure of the LDL receptor extracellular domain at endosomal pH. In: *Science* 298 (2002), Nr. 5602, S. 2353–2358 45

[287] Davis, C G. ; Goldstein, Joseph L. ; Südhof, Thomas C. ; Anderson, RG ; Russell, David W. ; Brown, Michael S.: Acid-dependent ligand dissociation and recycling of LDL receptor mediated by growth factor homology region. In: *Nature* 326 (1986), Nr. 6115, S. 760–765 45

[288] Davis, C G. ; Elhammer, A ; Russell, DW ; Schneider, WJ ; Kornfeld, S ; Brown, MS ; Goldstein, JL: Deletion of clustered O-linked carbohydrates does not impair function of low density lipoprotein receptor in transfected fibroblasts. In: *Journal of Biological Chemistry* 261 (1986), Nr. 6, S. 2828–2838 45

[289] Kuwano, M ; Seguchi, T ; Ono, M: Glycosylation mutations of serine/threonine-linked oligosaccharides in low-density lipoprotein receptor: indispensable roles of O-glycosylation. In: *Journal of cell science* 98 (1991), Nr. 2, S. 131–134 45

[290] Magrané, Jordi ; Casaroli-Marano, Ricardo P. ; Reina, Manuel ; Gåfvels, Mats ; Vilaró, Senén: The role of O-linked sugars in determining the very low density lipoprotein receptor stability or release from the cell. In: *FEBS letters* 451 (1999), Nr. 1, S. 56–62 45

[291] May, Petra ; Bock, Hans H. ; Nimpf, Johannes ; Herz, Joachim: Differential glycosylation regulates processing of lipoprotein receptors by γ-secretase. In: *Journal of Biological Chemistry* 278 (2003), Nr. 39, S. 37386–37392 45

[292] Koivisto, Ulla-Maija ; Hubbard, Ann L. ; Mellman, Ira: A novel cellular phenotype for familial hypercholesterolemia due to a defect in polarized targeting of LDL receptor. In: *Cell* 105 (2001), Nr. 5, S. 575–585 45, 46

[293] Davis, C G. ; Van Driel, IR ; Russell, DW ; Brown, Michael S. ; Goldstein, Joseph L.: The low density lipoprotein receptor. Identification of amino acids in cytoplasmic domain required for rapid endocytosis. In: *Journal of Biological Chemistry* 262 (1987), Nr. 9, S. 4075–4082 45

[294] Maurer, Meghan E. ; Cooper, Jonathan A.: The adaptor protein Dab2 sorts LDL receptors into coated pits independently of AP-2 and ARH. In: *Journal of cell science* 119 (2006), Nr. 20, S. 4235–4246 45

[295] Garuti, Rita ; Jones, Christopher ; Li, Wei-Ping ; Michaely, Peter ; Herz, Joachim ; Gerard, Robert D. ; Cohen, Jonathan C. ; Hobbs, Helen H.: The modular adaptor protein autosomal recessive hypercholesterolemia (ARH) promotes

low density lipoprotein receptor clustering into clathrin-coated pits. In: *Journal of Biological Chemistry* 280 (2005), Nr. 49, S. 40996–41004 45

[296] Wu, Jiao-Hui ; Peppel, Karsten ; Nelson, Christopher D. ; Lin, Fang-Tsyr ; Kohout, Trudy A. ; Miller, William E. ; Exum, Sabrina T. ; Freedman, Neil J.: The adaptor protein β-arrestin2 enhances endocytosis of the low density lipoprotein receptor. In: *Journal of Biological Chemistry* 278 (2003), Nr. 45, S. 44238–44245 45

[297] Burden, Jemima J. ; Sun, Xi-Ming ; García, Ana Bárbara G. ; Soutar, Anne K.: Sorting motifs in the intracellular domain of the low density lipoprotein receptor interact with a novel domain of sorting nexin-17. In: *Journal of Biological Chemistry* 279 (2004), Nr. 16, S. 16237–16245 45

[298] Stockinger, Walter ; Sailler, Beate ; Strasser, Vera ; Recheis, Burgi ; Fasching, Daniela ; Kahr, Larissa ; Schneider, Wolfgang J. ; Nimpf, Johannes: The PX-domain protein SNX17 interacts with members of the LDL receptor family and modulates endocytosis of the LDL receptor. In: *The EMBO journal* 21 (2002), Nr. 16, S. 4259–4267 45

[299] Goldstein, Joseph L. ; Brown, Michael S.: Binding and Degradation of Low Density Lipoproteins by Cultured Human Fibroblasts COMPARISON OF CELLS FROM A NORMAL SUBJECT AND FROM A PATIENT WITH HOMOZYGOUS FAMILIAL HYPERCHOLESTEROLEMIA. In: *Journal of Biological Chemistry* 249 (1974), Nr. 16, S. 5153–5162 45

[300] Goldstein, Joseph L. ; Anderson, Richard G. ; Brown, Michael S.: Coated pits, coated vesicles, and receptor-mediated endocytosis. In: *Nature* 279 (1979), Nr. 5715, S. 679–685 45

[301] Goldstein, JL ; Brunschede, GY ; Brown, MS: Inhibition of proteolytic degradation of low density lipoprotein in human fibroblasts by chloroquine, concanavalin A, and Triton WR 1339. In: *Journal of Biological Chemistry* 250 (1975), Nr. 19, S. 7854–7862 45

[302] Goldstein, JL ; Dana, SE ; Faust, JR ; Beaudet, AL ; Brown, MS: Role of lysosomal acid lipase in the metabolism of plasma low density lipoprotein. Observations in cultured fibroblasts from a patient with cholesteryl ester storage disease. In: *Journal of Biological Chemistry* 250 (1975), Nr. 21, S. 8487–8495 45

[303] Brown, Michael S. ; Dana, Suzanna E. ; Goldstein, Joseph L.: Regulation of 3-hydroxy-3-methylglutaryl coenzyme A reductase activity in human fibroblasts by lipoproteins. In: *Proceedings of the National Academy of Sciences* 70 (1973), Nr. 7, S. 2162–2166 45, 46

[304] Goldstein, Joseph L. ; Brown, Michael S.: Familial hypercholesterolemia: identification of a defect in the regulation of 3-hydroxy-3-methylglutaryl coenzyme A reductase activity associated with overproduction of cholesterol. In: *Proceedings of the National Academy of Sciences* 70 (1973), Nr. 10, S. 2804–2808 45, 46

[305] Brown, Michael S. ; Dana, Suzanna E. ; Goldstein, Joseph L.: Regulation of 3-Hydroxy-3-methylglutaryl Coenzyme A Reductase Activity in Cultured Human Fibroblasts COMPARISON OF CELLS FROM A NORMAL SUBJECT AND FROM A PATIENT WITH HOMOZYGOUS FAMILIAL HYPERCHOLESTEROLEMIA. In: *Journal of Biological Chemistry* 249 (1974), Nr. 3, S. 789–796 45, 46

[306] Gil, Gregorio ; Faust, Jerry R. ; Chin, Daniel J. ; Goldstein, Joseph L. ; Brown, Michael S.: Membrane-bound domain of HMG CoA reductase is required for sterol-enhanced degradation of the enzyme. In: *Cell* 41 (1985), Nr. 1, S. 249–258 45

[307] Brown, Michael S. ; Dana, Suzanna E. ; Goldstein, Joseph L.: Receptor-dependent hydrolysis of cholesteryl esters contained in plasma low density lipoprotein. In: *Proceedings of the National Academy of Sciences* 72 (1975), Nr. 8, S. 2925–2929 45

[308] Brown, MS ; Dana, SE ; Goldstein, JL: Cholesterol ester formation in cultured human fibroblasts. Stimulation by oxygenated sterols. In: *Journal of Biological Chemistry* 250 (1975), Nr. 10, S. 4025–4027 45

[309] Brown, Michael S. ; Goldstein, Joseph L.: Regulation of the activity of the low density lipoprotein receptor in human fibroblasts. In: *Cell* 6 (1975), Nr. 3, S. 307–316 46

[310] Usifo, Ebele ; Leigh, Sarah E. ; Whittall, Ros A. ; Lench, Nicholas ; Taylor, Alison ; Yeats, Corin ; Orengo, Christine A. ; Martin, Andrew C. ; Celli, Jacopo ; Humphries, Steve E.: Low-Density Lipoprotein Receptor Gene Familial Hypercholesterolemia Variant Database: Update and Pathological Assessment. In: *Annals of human genetics* 76 (2012), Nr. 5, S. 387–401 46, 102

[311] Khachadurian, Avedis K.: The inheritance of essential familial hypercholesterolemia. In: *The American journal of medicine* 37 (1964), Nr. 3, S. 402–407 46

[312] Hobbs, Helen H. ; Brown, Michael S. ; Goldstein, Joseph L.: Molecular genetics of the LDL receptor gene in familial hypercholesterolemia. In: *Human mutation* 1 (1992), Nr. 6, S. 445–466 46

[313] Bazan, J F. ; Bacon, Kevin B. ; Hardiman, Gary ; Wang, Wei ; Soo, Ken ; Rossi, Devora ; Greaves, David R. ; Zlotnik, Albert ; Schall, Thomas J.: A

new class of membrane-bound chemokine with a CX3C motif. In: *Nature* 385 (1997), Nr. 6617, S. 640–644 47, 48

[314] Zabel, Matthew K. ; Kirsch, Wolff M.: From development to dysfunction: Microglia and the complement cascade in CNS homeostasis. In: *Ageing research reviews* 12 (2013), Nr. 3, S. 749–756 47

[315] Gemma, Carmelina ; Bachstetter, Adam D.: The role of microglia in adult hippocampal neurogenesis. In: *Frontiers in cellular neuroscience* 7 (2013) 47

[316] Lee, Yun S. ; Morinaga, Hidetaka ; Kim, Jane J. ; Lagakos, William ; Taylor, Susan ; Keshwani, Malik ; Perkins, Guy ; Dong, Hui ; Kayali, Ayse G. ; Sweet, Ian R. u. a.: The fractalkine/CX3CR1 system regulates β cell function and insulin secretion. In: *Cell* 153 (2013), Nr. 2, S. 413–425 47

[317] Ruchaya, PJ ; Paton, JFR ; Murphy, D ; Yao, ST: A cardiovascular role for fractalkine and its cognate receptor, CX3CR1, in the rat nucleus of the solitary tract. In: *Neuroscience* 209 (2012), S. 119–127 47

[318] Krishnan, Sonya ; Wilson, Eleanor M. ; Sheikh, Virginia ; Rupert, Adam ; Mendoza, Daniel ; Yang, Jun ; Lempicki, Richard ; Migueles, Stephen A. ; Sereti, Irini: Evidence for Innate Immune System Activation in HIV Type 1–Infected Elite Controllers. In: *Journal of Infectious Diseases* 209 (2014), Nr. 6, S. 931–939 47

[319] Apostolakis, Stavros ; Krambovitis, Elias ; Vlata, Zaharenia ; Kochiadakis, Georgios E. ; Baritaki, Stavroula ; Spandidos, Demetrios A.: CX3CR1 receptor is up-regulated in monocytes of coronary artery diseased patients: impact of pre-inflammatory stimuli and renin–angiotensin system modulators. In: *Thrombosis research* 121 (2007), Nr. 3, S. 387–395 47, 48, 110, 115, 119, 123, 125, 129, 132, 149, 150

[320] Damås, Jan K. ; Boullier, Agnes ; Wæhre, Torgun ; Smith, Camilla ; Sandberg, Wiggo J. ; Green, Simone ; Aukrust, Pål ; Quehenberger, Oswald: Expression of fractalkine (CX3CL1) and its receptor, CX3CR1, is elevated in coronary artery disease and is reduced during statin therapy. In: *Arteriosclerosis, thrombosis, and vascular biology* 25 (2005), Nr. 12, S. 2567–2572 47, 48, 49, 110, 115, 116, 119, 123, 129, 149

[321] Foussat, Arnaud ; Coulomb-L'Hermine, Aurore ; Gosling, Jennifa ; Krzysiek, Roman ; Durand-Gasselin, Ingrid ; Schall, Thomas ; Balian, Axel ; Richard, Yolande ; Galanaud, Pierre ; Emilie, Dominique: Fractalkine receptor expression by T lymphocyte subpopulations and in vivo production of fractalkine in human. In: *European journal of immunology* 30 (2000), Nr. 1, S. 87–97 47, 48, 50

[322] Stolla, Moritz ; Pelisek, Jaroslav ; Von Brühl, Marie-Luise ; Schäfer, Andreas ; Barocke, Verena ; Heider, Peter ; Lorenz, Michael ; Tirniceriu, Anca ; Steinhart, Alexander ; Bauersachs, Johann u. a.: Fractalkine is expressed in early and advanced atherosclerotic lesions and supports monocyte recruitment via CX3CR1. In: *PloS one* 7 (2012), Nr. 8, S. e43572 47, 48, 119, 125, 129

[323] Wong, Brian W. ; Wong, Donald ; McManus, Bruce M.: Characterization of fractalkine (CX3CL1) and CX3CR1 in human coronary arteries with native atherosclerosis, diabetes mellitus, and transplant vascular disease. In: *Cardiovascular pathology* 11 (2002), Nr. 6, S. 332–338 47, 48, 125

[324] Kasama, Tsuyoshi ; Wakabayashi, Kuninobu ; Sato, Michihito ; Takahashi, Ryo ; Isozaki, Takeo: Relevance of the CX3CL1/fractalkine-CX3CR1 pathway in vasculitis and vasculopathy. In: *Translational Research* 155 (2010), Nr. 1, S. 20–26 47

[325] Robinson, Lisa A. ; Nataraj, Chandra ; Thomas, Dennis W. ; Howell, David N. ; Griffiths, Robert ; Bautch, Victoria ; Patel, Dhavalkumar D. ; Feng, Lili ; Coffman, Thomas M.: A role for fractalkine and its receptor (CX3CR1) in cardiac allograft rejection. In: *The Journal of Immunology* 165 (2000), Nr. 11, S. 6067–6072 47

[326] Zhang, Jianliang ; Patel, Jawaharlal M.: Role of the CX3CL1-CX3CR1 axis in chronic inflammatory lung diseases. In: *International journal of clinical and experimental medicine* 3 (2010), Nr. 3, S. 233 47

[327] Efsen, Eva ; Grappone, Cecilia ; DeFranco, Raffaella ; Milani, Stefano ; Romanelli, Roberto G. ; Bonacchi, Andrea ; Caligiuri, Alessandra ; Failli, Paola ; Annunziato, Francesco ; Pagliai, Gabriella u. a.: Up-regulated expression of fractalkine and its receptor CX3CR1 during liver injury in humans. In: *Journal of hepatology* 37 (2002), Nr. 1, S. 39–47 47

[328] Shimizu, Kazuaki ; Furuichi, Kengo ; Sakai, Norihiko ; Kitagawa, Kiyoki ; Matsushima, Kouji ; Mukaida, Naofumi ; Kaneko, Shuichi ; Wada, Takashi: Fractalkine and its receptor, CX3CR1, promote hypertensive interstitial fibrosis in the kidney. In: *Hypertension Research* 34 (2011), Nr. 6, S. 747–752 47

[329] Yadav, Ashok K. ; Lal, Anupam ; Jha, Vivekanand: Association of circulating fractalkine (CX3CL1) and CX3CR1 (+) CD4 (+) T cells with common carotid artery intima-media thickness in patients with chronic kidney disease. In: *Journal of atherosclerosis and thrombosis* 18 (2010), Nr. 11, S. 958–965 47

[330] TANG, Ke-jing ; LI, You-ji ; XIE, Can-mao ; ZHU, Sheng-lang ; CHEN, Wen-fang ; YU, Xue-qing: Expression of fractalkine and CX3CR1 in renal tissues of patients

with WHO class IV lupus nephritis [J]. In: *Chinese Journal of Pathophysiology* 5 (2007), S. 017 47

[331] Segerer, Stephan ; Hughes, Erik ; Hudkins, Kelly L. ; Mack, Matthias ; Goodpaster, Tracy ; Alpers, Charles E.: Expression of the fractalkine receptor (CX3CR1) in human kidney diseases. In: *Kidney international* 62 (2002), Nr. 2, S. 488–495 47

[332] Li, Li ; Huang, Liping ; Sung, Sun-Sang J. ; Vergis, Amy L. ; Rosin, Diane L. ; Rose, C E. ; Lobo, Peter I. ; Okusa, Mark D.: The chemokine receptors CCR2 and CX3CR1 mediate monocyte/macrophage trafficking in kidney ischemia–reperfusion injury. In: *Kidney international* 74 (2008), Nr. 12, S. 1526–1537 47

[333] Furuichi, Kengo ; Gao, Ji-Liang ; Murphy, Philip M.: Chemokine receptor CX3CR1 regulates renal interstitial fibrosis after ischemia-reperfusion injury. In: *The American journal of pathology* 169 (2006), Nr. 2, S. 372–387 47

[334] Raspé, C ; Höcherl, K ; Rath, S ; Sauvant, C ; Bucher, M: NF-κB-mediated inverse regulation of fractalkine and CX3CR1 during CLP-induced sepsis. In: *Cytokine* 61 (2013), Nr. 1, S. 97–103 47

[335] Xu, Xianhui ; Wang, Yang ; Chen, Jinshui ; Ma, Hongyun ; Shao, Zhuo ; Chen, Haitao ; Jin, Gang: High expression of CX3CL1/CX3CR1 axis predicts a poor prognosis of pancreatic ductal adenocarcinoma. In: *Journal of gastrointestinal surgery* 16 (2012), Nr. 8, S. 1493–1498 47

[336] Marchesi, Federica ; Locatelli, Marco ; Solinas, Graziella ; Erreni, Marco ; Allavena, Paola ; Mantovani, Alberto: Role of CX3CR1/CX3CL1 axis in primary and secondary involvement of the nervous system by cancer. In: *Journal of neuroimmunology* 224 (2010), Nr. 1, S. 39–44 47

[337] Marchesi, Federica ; Piemonti, Lorenzo ; Fedele, Giuseppe ; Destro, Annarita ; Roncalli, Massimo ; Albarello, Luca ; Doglioni, Claudio ; Anselmo, Achille ; Doni, Andrea ; Bianchi, Paolo u. a.: The chemokine receptor CX3CR1 is involved in the neural tropism and malignant behavior of pancreatic ductal adenocarcinoma. In: *Cancer research* 68 (2008), Nr. 21, S. 9060–9069 47

[338] Matsubara, Takeshi ; Ono, Takashi ; Yamanoi, Akira ; Tachibana, Mitsuo ; Nagasue, Naofumi: Fractalkine-CX3CR1 axis regulates tumor cell cycle and deteriorates prognosis after radical resection for hepatocellular carcinoma. In: *Journal of surgical oncology* 95 (2007), Nr. 3, S. 241–249 47

[339] Garcia, Jenny A. ; Pino, Paula A. ; Mizutani, Makiko ; Cardona, Sandra M. ; Charo, Israel F. ; Ransohoff, Richard M. ; Forsthuber, Thomas G. ; Cardona,

Astrid E.: Regulation of adaptive immunity by the fractalkine receptor during autoimmune inflammation. In: *The Journal of Immunology* 191 (2013), Nr. 3, S. 1063–1072 47

[340] K Clark, Anna ; A Staniland, Amelia ; Malcangio, Marzia: Fractalkine/CX3CR1 signalling in chronic pain and inflammation. In: *Current pharmaceutical biotechnology* 12 (2011), Nr. 10, S. 1707–1714 47

[341] Fevang, Børre ; Yndestad, Arne ; Damås, Jan K. ; Bjerkeli, Vigdis ; Ueland, Thor ; Holm, Are M. ; Beiske, Klaus ; Aukrust, Pål ; Frøland, Stig S.: Chemokines and common variable immunodeficiency; possible contribution of the fractalkine system (CX3CL1/CX3CR1) to chronic inflammation. In: *Clinical Immunology* 130 (2009), Nr. 2, S. 151–161 47

[342] Lamb, Bruce: The roles of fractalkine signaling in neurodegenerative disease. In: *Molecular neurodegeneration* 7 (2012), Nr. Suppl 1, S. L21 47

[343] Rezai-Zadeh, Kavon ; Gate, David ; Gowing, Genvève ; Town, Terrence: How to get from here to there: macrophage recruitment in Alzheimer's disease. In: *Current Alzheimer Research* 8 (2011), Nr. 2, S. 156 47

[344] Staumont-Sallé, Delphine ; Fleury, Sébastien ; Lazzari, Anne ; Molendi-Coste, Olivier ; Hornez, Nicolas ; Lavogiez, Céline ; Kanda, Akira ; Wartelle, Julien ; Fries, Anissa ; Pennino, Davide u. a.: CX3CL1 (fractalkine) and its receptor CX3CR1 regulate atopic dermatitis by controlling effector T cell retention in inflamed skin. In: *The Journal of experimental medicine* (2014), S. jem–20121350 47

[345] Stojković, Ljiljana ; Djurić, Tamara ; Stanković, Aleksandra ; Dinčić, Evica ; Stančić, Olja ; Veljković, Nevena ; Alavantić, Dragan ; Živković, Maja: The association of V249I and T280M fractalkine receptor haplotypes with disease course of multiple sclerosis. In: *Journal of neuroimmunology* 245 (2012), Nr. 1, S. 87–92 47

[346] Pingiotti, Elisa ; Cipriani, Paola ; Marrelli, Alessandra ; Liakouli, Vasiliki ; Fratini, Simona ; Penco, Maria ; Giacomelli, Roberto: Surface expression of fractalkine receptor (CX3CR1) on CD4+/CD28- T cells in RA patients and correlation with atherosclerotic damage. In: *Annals of the New York Academy of Sciences* 1107 (2007), Nr. 1, S. 32–41 47

[347] Yano, Ryusuke ; Yamamura, Masahiro ; Sunahori, Katsue ; Takasugi, Kouji ; Yamana, Jiro ; Kawashima, Masanori ; Makino, Hirofumi: Recruitment of CD16+ monocytes into synovial tissues is mediated by fractalkine and CX3CR1 in rheumatoid arthritis patients. In: *Acta medica Okayama* 61 (2007), Nr. 2, S. 89 47

[348] Hasegawa, M ; Sato, S ; Echigo, T ; Hamaguchi, Y ; Yasui, M ; Takehara, K: Up regulated expression of fractalkine/CX3CL1 and CX3CR1 in patients with systemic sclerosis. In: *Annals of the rheumatic diseases* 64 (2005), Nr. 1, S. 21–28 47

[349] Wojdasiewicz, Piotr ; Poniatowski, Łukasz A ; Kotela, Andrzej ; Deszczyński, Jarosław ; Kotela, Ireneusz ; Szukiewicz, Dariusz: The Chemokine CX3CL1 (Fractalkine) and its Receptor CX3CR1: Occurrence and Potential Role in Osteoarthritis. In: *Archivum immunologiae et therapiae experimentalis* (2014), S. 1–9 47

[350] Bjerkeli, Vigdis ; Damås, Jan K. ; Fevang, Borre ; Holter, Jan C. ; Aukrust, Pal ; Frøland, Stig S.: Increased expression of fractalkine (CX3CL1) and its receptor, CX3CR1, in Wegener's granulomatosis-possible role in vascular inflammation. In: *Rheumatology* 46 (2007), Nr. 9, S. 1422–1427 47

[351] Wu, Jian ; Yin, Rui-Xing ; Lin, Quan-Zhen ; Guo, Tao ; Shi, Guang-Yuan ; Sun, Jia-Qi ; Shen, Shao-Wen ; Li, Qing: Two Polymorphisms in the Fractalkine Receptor CX3CR1 Gene Influence the Development of Atherosclerosis: A Meta-Analysis. In: *Disease markers* 2014 (2014) 47, 50, 51, 121

[352] ZHANG, Yun-li ; YU, Wei ; FANG, Boyan: Association study between the polymorphisms of fractalkine receptor CX3CR1 and cerebral infarction. In: *China Journal of Modern Medicine* 1 (2010), S. 003 47

[353] Lavergne, Elise ; Labreuche, Julien ; Daoudi, Mehdi ; Debré, Patrice ; Cambien, François ; Deterre, Philippe ; Amarenco, Pierre ; Combadière, Christophe u. a.: Adverse associations between CX3CR1 polymorphisms and risk of cardiovascular or cerebrovascular disease. In: *Arteriosclerosis, thrombosis, and vascular biology* 25 (2005), Nr. 4, S. 847–853 47, 50, 121

[354] Ghilardi, Giorgio ; Biondi, Maria L. ; Turri, Olivia ; Guagnellini, Emma ; Scorza, Roberto: Internal Carotid Artery Occlusive Disease and Polymorphisms of Fractalkine Receptor CX3CR1 A Genetic Risk Factor. In: *Stroke* 35 (2004), Nr. 6, S. 1276–1279 47

[355] Niessner, Alexander ; Marculescu, Rodrig ; Kvakan, Heda ; Haschemi, Arvand ; Endler, Georg ; Weyand, Cornelia M. ; Maurer, Gerald ; Mannhalter, Christine ; Wojta, Johann ; Wagner, Oswald u. a.: Fractalkine receptor polymorphisms V249I and T280M as genetic risk factors for restenosis. In: *THROMBOSIS AND HAEMOSTASIS-STUTTGART-* 94 (2005), Nr. 6, S. 1251 47, 51, 121, 140

[356] Marasini, Bianca ; Cossutta, Roberta ; Selmi, Carlo ; Pozzi, Maria R. ; Gardinali, Marco ; Massarotti, Marco ; Erario, Maddalena ; Battaglioli, Lodovica ;

Biondi, Maria L.: Polymorphism of the fractalkine receptor CX3CR1 and systemic sclerosis-associated pulmonary arterial hypertension. In: *Journal of Immunology Research* 12 (2005), Nr. 4, S. 275–279 47

[357] Sirois-Gagnon, Dave ; Chamberland, Annie ; Perron, Stéphanie ; Brisson, Diane ; Gaudet, Daniel ; Laprise, Catherine: Association of common polymorphisms in the fractalkine receptor (CX3CR1) with obesity. In: *Obesity* 19 (2011), Nr. 1, S. 222–227 47

[358] Wasmuth, Hermann E. ; Zaldivar, Mirko M. ; Berres, Marie-Luise ; Werth, Alexa ; Scholten, David ; Hillebrandt, Sonja ; Tacke, Frank ; Schmitz, Petra ; Dahl, Edgar ; Wiederholt, Tonio u. a.: The fractalkine receptor CX3CR1 is involved in liver fibrosis due to chronic hepatitis C infection. In: *Journal of hepatology* 48 (2008), Nr. 2, S. 208–215 47

[359] Iacob, Speranta ; Cicinnati, Vito R. ; Dechêne, Alexander ; Lindemann, Monika ; Heinemann, Falko M. ; Rebmann, Vera ; Ferencik, Stanislav ; Sotiropoulos, Georgios C. ; Popescu, Irinel ; Horn, Peter A. u. a.: Genetic, immunological and clinical risk factors for biliary strictures following liver transplantation. In: *Liver International* 32 (2012), Nr. 8, S. 1253–1261 47

[360] Borkar, Minal ; Tripathi, Gaurav ; Sharma, Raj K. ; Sankhwar, Satya N. ; Agrawal, Suraksha: Chemokine (CCR) and fractalkine (CX3CR) receptors and end stage renal disease. In: *Inflammation research* 60 (2011), Nr. 4, S. 399–407 47

[361] Plant, Darren ; Young, Helen S. ; Watson, Rachel E. ; Worthington, Jane ; Griffiths, Christopher E.: The CX3CL1–CX3CR1 system and psoriasis. In: *Experimental dermatology* 15 (2006), Nr. 11, S. 900–903 47

[362] Courivaud, Cécile ; Bamoulid, Jamal ; Loupy, Alexandre ; Deschamps, Marina ; Ferrand, Christophe ; Simula-Faivre, Dominique ; Tiberghien, Pierre ; Chalopin, Jean-Marc ; Legendre, Christophe ; Thervet, Eric u. a.: Influence of fractalkine receptor gene polymorphisms V249I-T280M on cancer occurrence after renal transplantation. In: *Transplantation* 95 (2013), Nr. 5, S. 728–732 47

[363] Dimberg, Jan ; Dienus, Olaf ; Löfgren, Sture ; Hugander, Anders ; Wågsäter, Dick: Polymorphisms of Fractalkine receptor CX3CR1 and plasma levels of its ligand CX3CL1 in colorectal cancer patients. In: *International journal of colorectal disease* 22 (2007), Nr. 10, S. 1195–1200 47

[364] Feldman, George J. ; Parvizi, Javad ; Levenstien, Mark ; Scott, Kathryn ; Erickson, Jill A. ; Fortina, Paolo ; Devoto, Marcella ; Peters, Christopher L.: Developmental Dysplasia of the Hip: Linkage Mapping and Whole Exome Sequencing Identify a Shared Variant in CX3CR1 in All Affected Members of a Large

Multigeneration Family. In: *Journal of Bone and Mineral Research* 28 (2013), Nr. 12, S. 2540–2549 47

[365] Amanatidou, Virginia ; Sourvinos, George ; Apostolakis, Stavros ; Tsilimigaki, Amalia ; Spandidos, Demetrios A.: T280M variation of the CX3C receptor gene is associated with increased risk for severe respiratory syncytial virus bronchiolitis. In: *The Pediatric infectious disease journal* 25 (2006), Nr. 5, S. 410–414 47

[366] Apostolakis, Stavros ; Amanatidou, Virginia ; Papadakis, Emmanouil G. ; Spandidos, Demetrios A.: Genetic diversity of CX3CR1 gene and coronary artery disease: new insights through a meta-analysis. In: *Atherosclerosis* 207 (2009), Nr. 1, S. 8–15 47, 50, 121, 140

[367] Kimouli, Maria ; Miyakis, Spiros ; Georgakopoulos, Petros ; Neofytou, Eirini ; Achimastos, Apostolos D. ; Spandidos, Demetrios A.: Polymorphisms of fractalkine receptor CX3CR1 gene in patients with symptomatic and asymptomatic carotid artery stenosis. In: *J Atheroscler Thromb* 16 (2009), Nr. 5, S. 604–10 47

[368] Nadif, Rachel ; Mintz, Margaret ; Rivas-Fuentes, Selma ; Jedlicka, Anne ; Lavergne, Elise ; Rodero, Mathieu ; Kauffmann, Francine ; Combadière, Christophe ; Kleeberger, Steven R.: Polymorphisms in chemokine and chemokine receptor genes and the development of coal workers' pneumoconiosis. In: *Cytokine* 33 (2006), Nr. 3, S. 171–178 47

[369] Rodero, Mathieu ; Marie, Yannick ; Coudert, Mathieu ; Blondet, Emmeline ; Mokhtari, Karima ; Rousseau, Audrey ; Raoul, William ; Carpentier, Catherine ; Sennlaub, Florian ; Deterre, Philippe u. a.: Polymorphism in the microglial cell-mobilizing CX3CR1 gene is associated with survival in patients with glioblastoma. In: *Journal of Clinical Oncology* 26 (2008), Nr. 36, S. 5957–5964 47

[370] Babakurban, Seda T. ; Erbek, Selim S. ; Terzi, Yunus K. ; Arslan, Fatih ; Sahin, Feride I.: Fractalkine receptor polymorphism and chronic tonsillitis. In: *European Archives of Oto-Rhino-Laryngology* 271 (2014), Nr. 7, S. 2045–2048 47

[371] Combadière, Christophe ; Godin, Ophelia ; Vidal, Cécile ; Cangialosi, Arnaud ; Proust, Carole ; Tzourio, Christophe: Common CX3CR1 alleles are associated with a reduced risk of headaches. In: *Headache: The Journal of Head and Face Pain* 48 (2008), Nr. 7, S. 1061–1066 47

[372] D'Haese, Jan G. ; Friess, Helmut ; Ceyhan, Güralp O: Therapeutic potential of the chemokine-receptor duo fractalkine/CX3CR1: an update. In: *Expert opinion on therapeutic targets* 16 (2012), Nr. 6, S. 613–618 47

[373] D'Haese, Jan G. ; Demir, Ihsan E. ; Friess, Helmut ; Ceyhan, Güralp O: Fractalkine/CX3CR1: why a single chemokine-receptor duo bears a major and unique therapeutic potential. In: *Expert opinion on therapeutic targets* 14 (2010), Nr. 2, S. 207–219 47

[374] Maho, Arielle ; Bensimon, A ; Vassart, Gilbert ; Parmentier, Marc: Mapping of the CCXCR1, CX3CR1, CCBP2 and CCR9 genes to the CCR cluster within the 3p21. 3 region of the human genome. In: *Cytogenetic and Genome Research* 87 (2000), Nr. 3-4, S. 265–268 47

[375] DeVries, Mark E. ; Cao, Henian ; Wang, Jian ; Xu, Luoling ; Kelvin, Alyson A. ; Ran, Longsi ; Chau, Luan A. ; Madrenas, Joaquin ; Hegele, Robert A. ; Kelvin, David J.: Genomic organization and evolution of the CX3CR1/CCR8 chemokine receptor locus. In: *Journal of Biological Chemistry* 278 (2003), Nr. 14, S. 11985–11994 48, 125, 130, 150

[376] Garin, Alexandre ; Pellet, Philippe ; Deterre, Philippe ; Debré, Patrice ; Combadière, Christophe: Cloning and functional characterization of the human fractalkine receptor promoter regions. In: *Biochem. J* 368 (2002), S. 753–760 48, 125, 130, 150

[377] Yang, Xiao P. ; Mattagajasingh, Subhendra ; Su, Shaobo ; Chen, Guibin ; Cai, Zheqing ; Fox-Talbot, Karen ; Irani, Kaikobad ; Becker, Lewis C.: Fractalkine Upregulates Intercellular Adhesion Molecule-1 in Endothelial Cells Through CX3CR1 and the Jak–Stat5 Pathway. In: *Circulation research* 101 (2007), Nr. 10, S. 1001–1008 48, 49, 50, 122

[378] Ancuta, Petronela ; Rao, Ravi ; Moses, Ashlee ; Mehle, Andrew ; Shaw, Sunil K. ; Luscinskas, F W. ; Gabuzda, Dana: Fractalkine preferentially mediates arrest and migration of CD16+ monocytes. In: *The Journal of experimental medicine* 197 (2003), Nr. 12, S. 1701–1707 48

[379] Imai, Toshio ; Hieshima, Kunio ; Haskell, Christopher ; Baba, Masataka ; Nagira, Morio ; Nishimura, Miyuki ; Kakizaki, Mayumi ; Takagi, Shin ; Nomiyama, Hisayuki ; Schall, Thomas J. u. a.: Identification and Molecular Characterization of Fractalkine Receptor CX3CR1, which Mediates Both Leukocyte Migration and Adhesion. In: *Cell* 91 (1997), Nr. 4, S. 521–530 48, 49, 119, 122

[380] Dichmann, S ; Herouy, Y ; Purlis, D ; Rheinen, H ; Gebicke-Härter, P ; Norgauer, J: Fractalkine induces chemotaxis and actin polymerization in human dendritic cells. In: *Inflammation research* 50 (2001), Nr. 11, S. 529–533 48, 122

[381] Papadopoulos, Elektra J. ; Fitzhugh, David J. ; Tkaczyk, Christine ; Gilfillan, Alasdair M. ; Sassetti, Christopher ; Metcalfe, Dean D. ; Hwang, Sam T.:

Mast cells migrate, but do not degranulate, in response to fractalkine, a membrane-bound chemokine expressed constitutively in diverse cells of the skin. In: *European journal of immunology* 30 (2000), Nr. 8, S. 2355–2361 48, 122

[382] Nishimura, Miyuki ; Umehara, Hisanori ; Nakayama, Takashi ; Yoneda, Osamu ; Hieshima, Kunio ; Kakizaki, Mayumi ; Dohmae, Naochika ; Yoshie, Osamu ; Imai, Toshio: Dual functions of fractalkine/CX3C ligand 1 in trafficking of perforin+/granzyme B+ cytotoxic effector lymphocytes that are defined by CX3CR1 expression. In: *The Journal of immunology* 168 (2002), Nr. 12, S. 6173–6180 48

[383] Schäfer, Andreas ; Schulz, Christian ; Eigenthaler, Martin ; Fraccarollo, Daniela ; Kobsar, Anna ; Gawaz, Meinrad ; Ertl, Georg ; Walter, Ulrich ; Bauersachs, Johann: Novel role of the membrane-bound chemokine fractalkine in platelet activation and adhesion. In: *Blood* 103 (2004), Nr. 2, S. 407–412 48, 49, 119, 122

[384] Hulshof, Sandra ; Haastert, Elise S. ; Kuipers, Hedwich F. ; Elsen, Peter J. d. ; De Groot, Corline J. ; Valk, Paul van d. ; Ravid, Rivka ; Biber, Knut: CX3CL1 and CX3CR1 expression in human brain tissue: noninflammatory control versus multiple sclerosis. In: *Journal of Neuropathology & Experimental Neurology* 62 (2003), Nr. 9, S. 899–907 48, 122

[385] Hatori, Kozo ; Nagai, Atsushi ; Heisel, Rochelle ; Ryu, Jae K. ; Kim, Seung U.: Fractalkine and fractalkine receptors in human neurons and glial cells. In: *Journal of neuroscience research* 69 (2002), Nr. 3, S. 418–426 48, 122

[386] Mizoue, Laura S. ; Bazan, J F. ; Johnson, Eric C. ; Handel, Tracy M.: Solution structure and dynamics of the CX3C chemokine domain of fractalkine and its interaction with an N-terminal fragment of CX3CR1. In: *Biochemistry* 38 (1999), Nr. 5, S. 1402–1414 48

[387] Haskell, Christopher A. ; Cleary, Michael D. ; Charo, Israel F.: Molecular uncoupling of fractalkine-mediated cell adhesion and signal transduction Rapid flow arrest of CX3CR1-expressing cells is independent of G-protein activation. In: *Journal of Biological Chemistry* 274 (1999), Nr. 15, S. 10053–10058 48

[388] Ikejima, Hideyuki ; Imanishi, Toshio ; Tsujioka, Hiroto ; Kashiwagi, Manabu ; Kuroi, Akio ; Tanimoto, Takashi ; Kitabata, Hironori ; Ishibashi, Kohei ; Komukai, Kenichi ; Takeshita, Tatsuya u. a.: Upregulation of fractalkine and its receptor, CX3CR1, is associated with coronary plaque rupture in patients with unstable angina pectoris. In: *Circulation journal: official journal of the Japanese Circulation Society* 74 (2010), Nr. 2, S. 337–345 48

[389] Zhang, Huili ; Guo, Changfa ; Wu, Duojiao ; Zhang, Alian ; Gu, Ting ; Wang, Liansheng ; Wang, Changqian: Hydrogen sulfide inhibits the development of atherosclerosis with suppressing CX3CR1 and CX3CL1 expression. In: *PloS one* 7 (2012), Nr. 7, S. e41147 48

[390] Poupel, Lucie ; Boissonnas, Alexandre ; Hermand, Patricia ; Dorgham, Karim ; Guyon, Elodie ; Auvynet, Constance ; Saint Charles, Flora ; Lesnik, Philippe ; Deterre, Philippe ; Combadiere, Christophe: Pharmacological inhibition of the chemokine receptor, CX3CR1, reduces atherosclerosis in mice. In: *Arteriosclerosis, thrombosis, and vascular biology* 33 (2013), Nr. 10, S. 2297–2305 48

[391] Combadière, Christophe ; Potteaux, Stéphane ; Gao, Ji-Liang ; Esposito, Bruno ; Casanova, Saveria ; Lee, Eric J. ; Debré, Patrice ; Tedgui, Alain ; Murphy, Philip M. ; Mallat, Ziad: Decreased atherosclerotic lesion formation in CX3CR1/apolipoprotein E double knockout mice. In: *Circulation* 107 (2003), Nr. 7, S. 1009–1016 48

[392] Lesnik, Philippe ; Haskell, Christopher A. ; Charo, Israel F. u. a.: Decreased atherosclerosis in CX3CR1–/–mice reveals a role for fractalkine in atherogenesis. In: *The Journal of clinical investigation* 111 (2003), Nr. 3, S. 333–340 48

[393] Barlic, Jana ; Zhang, Yuan ; Foley, John F. ; Murphy, Philip M.: Oxidized Lipid-Driven Chemokine Receptor Switch, CCR2 to CX3CR1, Mediates Adhesion of Human Macrophages to Coronary Artery Smooth Muscle Cells Through a Peroxisome Proliferator-Activated Receptor γ–Dependent Pathway. In: *Circulation* 114 (2006), Nr. 8, S. 807–819 48, 49, 119

[394] Lucas, Andrew D. ; Bursill, Christina ; Guzik, Tomasz J. ; Sadowski, Jerzy ; Channon, Keith M. ; Greaves, David R.: Smooth muscle cells in human atherosclerotic plaques express the fractalkine receptor CX3CR1 and undergo chemotaxis to the CX3C chemokine fractalkine (CX3CL1). In: *Circulation* 108 (2003), Nr. 20, S. 2498–2504 48, 49

[395] Liu, Hong ; Jiang, Deqian: Fractalkine/CX3CR1 and atherosclerosis. In: *Clinica chimica acta* 412 (2011), Nr. 13, S. 1180–1186 48, 49

[396] Ludwig, Andreas ; Berkhout, Theo ; Moores, Kitty ; Groot, Pieter ; Chapman, Gayle: Fractalkine is expressed by smooth muscle cells in response to IFN-γ and TNF-α and is modulated by metalloproteinase activity. In: *The Journal of immunology* 168 (2002), Nr. 2, S. 604–612 48, 50

[397] Garton, Kyle J. ; Gough, Peter J. ; Blobel, Carl P. ; Murphy, Gillian ; Greaves, David R. ; Dempsey, Peter J. ; Raines, Elaine W.: Tumor necrosis factor-α-converting enzyme (ADAM17) mediates the cleavage and shedding of

fractalkine (CX3CL1). In: *Journal of Biological Chemistry* 276 (2001), Nr. 41, S. 37993–38001 48

[398] Tsou, Chia-Lin ; Haskell, Christopher A. ; Charo, Israel F.: Tumor necrosis factor-α-converting enzyme mediates the inducible cleavage of fractalkine. In: *Journal of Biological Chemistry* 276 (2001), Nr. 48, S. 44622–44626 48

[399] Umehara, Hisanori ; Goda, Seiji ; Imai, Toshio ; Nagano, Yutaka ; Minami, Yasuhiro ; Tanaka, Yoshiya ; Okazaki, Toshiro ; Bloom, Eda T. ; Domae, Naochika: Fractalkine, a CX3C-chemokine, functions predominantly as an adhesion molecule in monocytic cell line THP-1. In: *Immunology and cell biology* 79 (2001), Nr. 3, S. 298–302 49

[400] Goda, Seiji ; Imai, Toshio ; Yoshie, Osamu ; Yoneda, Osamu ; Inoue, Hiroshi ; Nagano, Yutaka ; Okazaki, Toshiro ; Imai, Hisao ; Bloom, Eda T. ; Domae, Naochika u. a.: CX3C-chemokine, fractalkine-enhanced adhesion of THP-1 cells to endothelial cells through integrin-dependent and-independent mechanisms. In: *The Journal of immunology* 164 (2000), Nr. 8, S. 4313–4320 49

[401] Volin, Michael V. ; Huynh, Nha ; Klosowska, Karolina ; Reyes, Rosemary D. ; Woods, James M.: Fractalkine-induced endothelial cell migration requires MAP kinase signaling. In: *Pathobiology* 77 (2010), Nr. 1, S. 7–16 49

[402] Green, Simone R. ; Han, Ki H. ; Chen, Yiming ; Almazan, Felicidad ; Charo, Israel F. ; Miller, Yury I. ; Quehenberger, Oswald: The CC chemokine MCP-1 stimulates surface expression of CX3CR1 and enhances the adhesion of monocytes to fractalkine/CX3CL1 via p38 MAPK. In: *The Journal of Immunology* 176 (2006), Nr. 12, S. 7412–7420 49

[403] Apostolakis, Stavros ; Vlata, Zacharenia ; Vogiatzi, Konstantina ; Krambovitis, Elias ; Spandidos, Demetrios A.: Angiotensin II up-regulates CX3CR1 expression in THP-1 monocytes: impact on vascular inflammation and atherogenesis. In: *Journal of thrombosis and thrombolysis* 29 (2010), Nr. 4, S. 443–448 49

[404] Weiss, Daiana ; Sorescu, Dan ; Taylor, W R.: Angiotensin II and atherosclerosis. In: *The American journal of cardiology* 87 (2001), Nr. 8, S. 25–32 49

[405] Vitale, Sébastien ; Schmid-Alliana, Annie ; Breuil, Véronique ; Pomeranz, Manuel ; Millet, Marie-Ange ; Rossi, Bernard ; Schmid-Antomarchi, Heidy: Soluble fractalkine prevents monocyte chemoattractant protein-1-induced monocyte migration via inhibition of stress-activated protein kinase 2/p38 and matrix metalloproteinase activities. In: *The Journal of immunology* 172 (2004), Nr. 1, S. 585–592 49, 50

[406] Kerfoot, Steven M. ; Lord, Sarah E. ; Bell, Robert B. ; Gill, Varinder ; Robbins, Stephen M. ; Kubes, Paul: Human fractalkine mediates leukocyte adhesion but not capture under physiological shear conditions; a mechanism for selective monocyte recruitment. In: *European journal of immunology* 33 (2003), Nr. 3, S. 729–739 49

[407] Fong, Alan M. ; Robinson, Lisa A. ; Steeber, Douglas A. ; Tedder, Thomas F. ; Yoshie, Osamu ; Imai, Toshio ; Patel, Dhavalkumar D.: Fractalkine and CX3CR1 mediate a novel mechanism of leukocyte capture, firm adhesion, and activation under physiologic flow. In: *The Journal of experimental medicine* 188 (1998), Nr. 8, S. 1413–1419 49

[408] Schulz, Christian ; Schäfer, Andreas ; Stolla, Moritz ; Kerstan, Sandra ; Lorenz, Michael ; Brühl, Marie-Luise von ; Schiemann, Matthias ; Bauersachs, Johann ; Gloe, Torsten ; Busch, Dirk H. u. a.: Chemokine Fractalkine Mediates Leukocyte Recruitment to Inflammatory Endothelial Cells in Flowing Whole Blood A Critical Role for P-Selectin Expressed on Activated Platelets. In: *Circulation* 116 (2007), Nr. 7, S. 764–773 49

[409] Shi, Chao ; Pamer, Eric G.: Monocyte recruitment during infection and inflammation. In: *Nature Reviews Immunology* 11 (2011), Nr. 11, S. 762–774 49, 150

[410] Ziegler-Heitbrock, Loems ; Ancuta, Petronela ; Crowe, Suzanne ; Dalod, Marc ; Grau, Veronika ; Hart, Derek N. ; Leenen, Pieter J. ; Liu, Yong-Jun ; MacPherson, Gordon ; Randolph, Gwendalyn J. u. a.: Nomenclature of monocytes and dendritic cells in blood. In: *Blood* 116 (2010), Nr. 16, S. e74–e80 49, 130, 132, 150

[411] Weiner, Louis M. ; Li, Wei ; Holmes, Michele ; Catalano, Robert B. ; Dovnarsky, Monica ; Padavic, Kristin ; Alpaugh, R K.: Phase I trial of recombinant macrophage colony-stimulating factor and recombinant γ-interferon: toxicity, monocytosis, and clinical effects. In: *Cancer research* 54 (1994), Nr. 15, S. 4084–4090 49, 150

[412] Geissmann, Frederic ; Jung, Steffen ; Littman, Dan R.: Blood monocytes consist of two principal subsets with distinct migratory properties. In: *Immunity* 19 (2003), Nr. 1, S. 71–82 49

[413] Landsman, Limor ; Bar-On, Liat ; Zernecke, Alma ; Kim, Ki-Wook ; Krauthgamer, Rita ; Shagdarsuren, Erdenechimeg ; Lira, Sergio A. ; Weissman, Irving L. ; Weber, Christian ; Jung, Steffen: CX3CR1 is required for monocyte homeostasis and atherogenesis by promoting cell survival. In: *Blood* 113 (2009), Nr. 4, S. 963–972 49

[414] Tacke, Frank ; Alvarez, David ; Kaplan, Theodore J. ; Jakubzick, Claudia ; Spanbroek, Rainer ; Llodra, Jaime ; Garin, Alexandre ; Liu, Jianhua ; Mack, Matthias ; Rooijen, Nico van u. a.: Monocyte subsets differentially employ CCR2, CCR5, and CX3CR1 to accumulate within atherosclerotic plaques. In: *The Journal of clinical investigation* 117 (2007), Nr. 1, S. 185–194 49, 119

[415] Volger, Oscar L. ; Fledderus, Joost O. ; Kisters, Natasja ; Fontijn, Ruud D. ; Moerland, Perry D. ; Kuiper, Johan ; Berkel, Theo J. ; Bijnens, Ann-Pascale J. ; Daemen, Mat J. ; Pannekoek, Hans u. a.: Distinctive expression of chemokines and transforming growth factor-β signaling in human arterial endothelium during atherosclerosis. In: *The American journal of pathology* 171 (2007), Nr. 1, S. 326–337 49, 50

[416] Chandrasekar, Bysani ; Mummidi, Srinivas ; Perla, R ; Bysani, Sailaja ; DULIN, N ; Liu, Feng ; MELBY, P: Fractalkine (CX3CL1) stimulated by nuclear factor kappaB (NF-kappaB)-dependent inflammatory signals induces aortic smooth muscle cell proliferation through an autocrine pathway. In: *Biochem. J* 373 (2003), S. 547–558 49, 50

[417] Butoi, Elena D. ; Gan, Ana M. ; Manduteanu, Ileana ; Stan, Daniela ; Calin, Manuela ; Pirvulescu, Monica ; Koenen, Rory R. ; Weber, Christian ; Simionescu, Maya: Cross talk between smooth muscle cells and monocytes/activated monocytes via CX3CL1/CX3CR1 axis augments expression of pro-atherogenic molecules. In: *Biochimica et Biophysica Acta (BBA)-Molecular Cell Research* 1813 (2011), Nr. 12, S. 2026–2035 50

[418] White, Gemma E. ; Tan, Thomas C. ; John, Alison E. ; Whatling, Carl ; McPheat, William L. ; Greaves, David R.: Fractalkine has anti-apoptotic and proliferative effects on human vascular smooth muscle cells via epidermal growth factor receptor signalling. In: *Cardiovascular research* 85 (2010), Nr. 4, S. 825–835 50

[419] Kumar, Arun H. ; Metharom, Pat ; Schmeckpeper, Jeff ; Weiss, Sharon ; Martin, Kenneth ; Caplice, Noel M.: Bone marrow-derived CX3CR1 progenitors contribute to neointimal smooth muscle cells via fractalkine CX3CR1 interaction. In: *The FASEB Journal* 24 (2010), Nr. 1, S. 81–92 50

[420] Kumar, Arun H. ; Martin, Kenneth ; Turner, Elizebeth C. ; Buneker, Chirlei K. ; Dorgham, Karim ; Deterre, Philippe ; Caplice, Noel M.: Role of CX3CR1 receptor in monocyte/macrophage driven neovascularization. In: *PloS one* 8 (2013), Nr. 2, S. e57230 50, 119

[421] Cambien, Bèatrice ; Pomeranz, Manuel ; Schmid-Antomarchi, Heidy ; Millet, Marie-Ange ; Breittmayer, Violette ; Rossi, Bernard ; Schmid-Alliana, Annie:

Signal transduction pathways involved in soluble fractalkine–induced monocytic cell adhesion. In: *Blood* 97 (2001), Nr. 7, S. 2031–2037 50

[422] Kansra, Vikram ; Groves, Christopher ; Gutierrez-Ramos, Jose C. ; Polakiewicz, Roberto D.: Phosphatidylinositol 3-kinase-dependent extracellular calcium influx is essential for CX3CR1-mediated activation of the mitogen-activated protein kinase cascade. In: *Journal of Biological Chemistry* 276 (2001), Nr. 34, S. 31831–31838 50

[423] Yoneda, Osamu ; Imai, Toshio ; Goda, Seiji ; Inoue, Hiroshi ; Yamauchi, Akira ; Okazaki, Toshio ; Imai, Hisao ; Yoshie, Osamu ; Bloom, Eda T. ; Domae, Naochika u. a.: Fractalkine-mediated endothelial cell injury by NK cells. In: *The Journal of immunology* 164 (2000), Nr. 8, S. 4055–4062 50

[424] Moore, Kathryn J. ; Tabas, Ira: Macrophages in the pathogenesis of atherosclerosis. In: *Cell* 145 (2011), Nr. 3, S. 341–355 50, 119

[425] Potteaux, Stephane ; Gautier, Emmanuel L. ; Hutchison, Susan B. ; Rooijen, Nico van ; Rader, Daniel J. ; Thomas, Michael J. ; Sorci-Thomas, Mary G. ; Randolph, Gwendalyn J. u. a.: Suppressed monocyte recruitment drives macrophage removal from atherosclerotic plaques of Apoe–/–mice during disease regression. In: *The Journal of clinical investigation* 121 (2011), Nr. 121 (5), S. 2025–2036 50, 52, 119

[426] Ryu, Jewon ; Lee, Cheol-Whan ; Hong, Kyung-Hee ; Shin, Jin-Ae ; Lim, Sun-Hee ; Park, Chan-Sik ; Shim, Jiyeon ; Nam, Ki B. ; Choi, Kee-Joon ; Kim, You-Ho u. a.: Activation of fractalkine/CX3CR1 by vascular endothelial cells induces angiogenesis through VEGF-A/KDR and reverses hindlimb ischaemia. In: *Cardiovascular research* 78 (2008), Nr. 2, S. 333–340 50

[427] Moatti, Didier ; Faure, Sophie ; Fumeron, Frédéric ; Amara, Mohamed El W. ; Seknadji, Patrick ; McDermott, David H. ; Debré, Patrice ; Aumont, Marie C. ; Murphy, Philip M. ; Prost, Dominique de u. a.: Polymorphism in the fractalkine receptor CX3CR1 as a genetic risk factor for coronary artery disease. In: *Blood* 97 (2001), Nr. 7, S. 1925–1928 50, 51, 121

[428] Faure, Sophie ; Meyer, Laurence ; Costagliola, Dominique ; Vaneensberghe, Céline ; Genin, Emmanuelle ; Autran, Brigitte ; French, ALT ; Delfraissy, Jean-François ; McDermott, David H. ; Murphy, Philip M. u. a.: Rapid progression to AIDS in HIV+ individuals with a structural variant of the chemokine receptor CX3CR1. In: *Science* 287 (2000), Nr. 5461, S. 2274–2277 50, 51, 121

[429] McDermott, David H. ; Fong, Alan M. ; Yang, Qiong ; Sechler, Joan M. ; Cupples, L A. ; Merrell, Maya N. ; Wilson, Peter W. ; D'Agostino, Ralph B.

; O'Donnell, Christopher J. ; Patel, Dhavalkumar D. u. a.: Chemokine receptor mutant CX3CR1-M280 has impaired adhesive function and correlates with protection from cardiovascular disease in humans. In: *Journal of Clinical Investigation* 111 (2003), Nr. 8, S. 1241–1250 50, 51, 121

[430] Daoudi, Mehdi ; Lavergne, Elise ; Garin, Alexandre ; Tarantino, Nadine ; Debré, Patrice ; Pincet, Frédéric ; Combadière, Christophe ; Deterre, Philippe: Enhanced adhesive capacities of the naturally occurring Ile249–Met280 variant of the chemokine receptor CX3CR1. In: *Journal of Biological Chemistry* 279 (2004), Nr. 19, S. 19649–19657 50, 121

[431] Niessner, Alexander ; Marculescu, Rodrig ; Haschemi, Arvand ; Endler, Georg ; Zorn, Gerlinde ; Weyand, Cornelia M. ; Maurer, Gerald ; Mannhalter, Christine ; Wojta, Johann ; Wagner, Oswald u. a.: Opposite effects of CX3CR1 receptor polymorphisms V249I and T280M on the development of acute coronary syndrome. A possible implication of fractalkine in inflammatory activation. In: *Thrombosis and haemostasis* 93 (2005), Nr. 5, S. 949–954 51, 121, 140

[432] Pucci, S ; Mazzarelli, P ; Zonetti, MJ ; Fisco, T ; Bonanno, E ; Spagnoli, LG ; Mauriello, A: CX3CR1 Receptor Polymorphisms, Th1 Cell Recruitment, and Acute Myocardial Infarction Outcome: Looking for a Link. In: *BioMed research international* 2013 (2013) 51, 121, 140

[433] Getz, Godfrey S. ; Reardon, Catherine A.: Animal models of atherosclerosis. In: *Arteriosclerosis, thrombosis, and vascular biology* 32 (2012), Nr. 5, S. 1104–1115 51, 52, 53

[434] Xiangdong, Li ; Yuanwu, Liu ; Hua, Zhang ; Liming, Ren ; Qiuyan, Li ; Ning, Li: Animal models for the atherosclerosis research: a review. In: *Protein & cell* 2 (2011), Nr. 3, S. 189–201 51, 52, 54

[435] Zaragoza, Carlos ; Gomez-Guerrero, Carmen ; Martin-Ventura, Jose L. ; Blanco-Colio, Luis ; Lavin, Begona ; Mallavia, Benat ; Tarin, Carlos ; Mas, Sebastian ; Ortiz, Alberto ; Egido, Jesus: Animal models of cardiovascular diseases. In: *BioMed Research International* 2011 (2011) 51, 52

[436] Zadelaar, Susanne ; Kleemann, Robert ; Verschuren, Lars ; Weij, Jitske de Vries-Van d. ; Hoorn, José van der ; Princen, Hans M. ; Kooistra, Teake: Mouse models for atherosclerosis and pharmaceutical modifiers. In: *Arteriosclerosis, thrombosis, and vascular biology* 27 (2007), Nr. 8, S. 1706–1721 51, 138

[437] Pendse, Avani A. ; Arbones-Mainar, Jose M. ; Johnson, Lance A. ; Altenburg, Michael K. ; Maeda, Nobuyo: Apolipoprotein E knock-out and knock-in

mice: atherosclerosis, metabolic syndrome, and beyond. In: *Journal of lipid research* 50 (2009), Nr. Supplement, S. S178–S182 52

[438] Van Vlijmen, BJ ; Maagdenberg, AM Van d. ; Gijbels, MJ ; Boom, H Van d. ; HogenEsch, H ; Frants, RR ; Hofker, MH ; Havekes, LM: Diet-induced hyperlipoproteinemia and atherosclerosis in apolipoprotein E3-Leiden transgenic mice. In: *Journal of Clinical Investigation* 93 (1994), Nr. 4, S. 1403 52

[439] Maagdenberg, AM Van d. ; Hofker, MH ; Krimpenfort, PJ ; De Bruijn, I ; Van Vlijmen, B ; Boom, H Van d. ; Havekes, LM ; Frants, RR: Transgenic mice carrying the apolipoprotein E3-Leiden gene exhibit hyperlipoproteinemia. In: *Journal of Biological Chemistry* 268 (1993), Nr. 14, S. 10540–10545 52

[440] Marotti, Keith R. ; Castle, Christine K. ; Boyle, Timothy P. ; Lin, Alice H. ; Murray, Robert W. ; Melchior, George W.: Severe atherosclerosis in transgenic mice expressing simian cholesteryl ester transfer protein. In: *Nature* 364 (1993), Nr. 6432, S. 73–75 52

[441] Plump, Andrew S. ; Scott, Christopher J. ; Breslow, Jan L.: Human apolipoprotein AI gene expression increases high density lipoprotein and suppresses atherosclerosis in the apolipoprotein E-deficient mouse. In: *Proceedings of the National Academy of Sciences* 91 (1994), Nr. 20, S. 9607–9611 52

[442] Purcell-Huynh, DA ; Farese Jr, RV ; Johnson, DF ; Flynn, LM ; Pierotti, V ; Newland, DL ; Linton, MF ; Sanan, DA ; Young, SG: Transgenic mice expressing high levels of human apolipoprotein B develop severe atherosclerotic lesions in response to a high-fat diet. In: *Journal of Clinical Investigation* 95 (1995), Nr. 5, S. 2246 52

[443] Boisvert, William A. ; Black, Audrey S. ; Curtiss, Linda K.: ApoA1 Reduces Free Cholesterol Accumulation in Atherosclerotic Lesions of ApoE–Deficient Mice Transplanted With ApoE–Expressing Macrophages. In: *Arteriosclerosis, thrombosis, and vascular biology* 19 (1999), Nr. 3, S. 525–530 52

[444] Zhang, Sunny H. ; Reddick, Robert L. ; Piedrahita, Jorge A. ; Maeda, Nobuyo: Spontaneous hypercholesterolemia and arterial lesions in mice lacking apolipoprotein E. In: *Science* 258 (1992), Nr. 5081, S. 468–471 52, 53, 135

[445] Plump, Andrew S. ; Smith, Jonathan D. ; Hayek, Tony ; Aalto-Setälä, Katriina ; Walsh, Annemarie ; Verstuyft, Judy G. ; Rubin, Edward M. ; Breslow, Jan L.: Severe hypercholesterolemia and atherosclerosis in apolipoprotein E-deficient mice created by homologous recombination in ES cells. In: *Cell* 71 (1992), Nr. 2, S. 343–353 52, 136

[446] Véniant, Murielle M. ; Zlot, Constance H. ; Walzem, Rosemary L. ; Pierotti, Vincenzo ; Driscoll, Robert ; Dichek, David ; Herz, Joachim ; Young, Stephen G.: Lipoprotein clearance mechanisms in LDL receptor-deficient "Apo-B48-only" and "Apo-B100-only" mice. In: *Journal of Clinical Investigation* 102 (1998), Nr. 8, S. 1559 52, 53

[447] Ishibashi, Shun ; Brown, Michael S. ; Goldstein, Joseph L. ; Gerard, Robert D. ; Hammer, Robert E. ; Herz, Joachim: Hypercholesterolemia in low density lipoprotein receptor knockout mice and its reversal by adenovirus-mediated gene delivery. In: *Journal of Clinical Investigation* 92 (1993), Nr. 2, S. 883 52, 136

[448] Jawien, J ; Nastalek, P ; Korbut, R: Mouse models of experimental atherosclerosis. In: *Journal of Physiology and Pharmacology* 55 (2004), Nr. 3, S. 503–517 52

[449] Bonthu, Srinivas ; Heistad, Donald D. ; Chappell, David A. ; Lamping, Kathryn G. ; Faraci, Frank M.: Atherosclerosis, vascular remodeling, and impairment of endothelium-dependent relaxation in genetically altered hyperlipidemic mice. In: *Arteriosclerosis, Thrombosis, and Vascular Biology* 17 (1997), Nr. 11, S. 2333–2340 52

[450] Paigen, Beverly ; Morrow, Arlene ; Brandon, Catherine ; Mitchell, Diane ; Holmes, Patricia: Variation in susceptibility to atherosclerosis among inbred strains of mice. In: *Atherosclerosis* 57 (1985), Nr. 1, S. 65–73 52, 53

[451] Shi, Weibin ; Wang, Nicholas J. ; Shih, Diana M. ; Sun, Victor Z. ; Wang, Xuping ; Lusis, Aldons J.: Determinants of Atherosclerosis Susceptibility in the C3H and C57BL/6 Mouse Model Evidence for Involvement of Endothelial Cells but Not Blood Cells or Cholesterol Metabolism. In: *Circulation research* 86 (2000), Nr. 10, S. 1078–1084 52

[452] Shim, Jeong ; Handberg, Aase ; Östergren, Caroline ; Falk, Erling ; Bentzon, Jacob F.: Genetic susceptibility of the arterial wall is an important determinant of atherosclerosis in C57BL/6 and FVB/N mouse strains. In: *Arteriosclerosis, thrombosis, and vascular biology* 31 (2011), Nr. 8, S. 1814–1820 52

[453] Tomita, Hirofumi ; Zhilicheva, Svetlana ; Kim, Shinja ; Maeda, Nobuyo: Aortic Arch Curvature and Atherosclerosis Have Overlapping Quantitative Trait Loci in a Cross Between 129S6/SvEvTac and C57BL/6J Apolipoprotein E–Null Mice. In: *Circulation research* 106 (2010), Nr. 6, S. 1052–1060 52

[454] Yang, Xia ; Peterson, Larry ; Thieringer, Rolf ; Deignan, Joshua L. ; Wang, Xuping ; Zhu, Jun ; Wang, Susanna ; Zhong, Hua ; Stepaniants, Serguei ; Beaulaurier, John u. a.: Identification and validation of genes affecting aortic

lesions in mice. In: *The Journal of clinical investigation* 120 (2010), Nr. 7, S. 2414–2422 52

[455] Teupser, Daniel ; Tan, Marietta ; Persky, Adam D. ; Breslow, Jan L.: Atherosclerosis quantitative trait loci are sex-and lineage-dependent in an intercross of C57BL/6 and FVB/N low-density lipoprotein receptor–/–mice. In: *Proceedings of the National Academy of Sciences of the United States of America* 103 (2006), Nr. 1, S. 123–128 52

[456] Smith, Jonathan D. ; James, Daylon ; Dansky, Hayes M. ; Wittkowski, Knut M. ; Moore, Karen J. ; Breslow, Jan L.: In Silico Quantitative Trait Locus Map for Atherosclerosis Susceptibility in Apolipoprotein E–Deficient Mice. In: *Arteriosclerosis, thrombosis, and vascular biology* 23 (2003), Nr. 1, S. 117–122 52

[457] Allayee, Hooman ; Ghazalpour, Anatole ; Lusis, Aldons J.: Using mice to dissect genetic factors in atherosclerosis. In: *Arteriosclerosis, thrombosis, and vascular biology* 23 (2003), Nr. 9, S. 1501–1509 52

[458] Berisha, Stela Z. ; Smith, Jonathan D.: Combining genome-wide data from humans and animal models of dyslipidemia and atherosclerosis. In: *Current opinion in lipidology* 22 (2011), Nr. 2, S. 100 52

[459] Weinreb, David B. ; Aguinaldo, Juan Gilberto S. ; Feig, Jonathan E. ; Fisher, Edward A. ; Fayad, Zahi A.: Non-invasive MRI of mouse models of atherosclerosis. In: *NMR in Biomedicine* 20 (2007), Nr. 3, S. 256–264 52

[460] VanderLaan, Paul A. ; Reardon, Catherine A. ; Sagiv, Yuval ; Blachowicz, Lydia ; Lukens, John ; Nissenbaum, Michael ; Wang, Chyung-Ru ; Getz, Godfrey S.: Characterization of the natural killer T-cell response in an adoptive transfer model of atherosclerosis. In: *The American journal of pathology* 170 (2007), Nr. 3, S. 1100–1107 52

[461] Subramanian, Venkateswaran ; Golledge, Jonathan ; Ijaz, Talha ; Bruemmer, Dennis ; Daugherty, Alan: Pioglitazone-Induced Reductions in Atherosclerosis Occur via Smooth Muscle Cell–Specific Interaction With PPARγ. In: *Circulation research* 107 (2010), Nr. 8, S. 953–958 52

[462] Billon-Galés, Audrey ; Fontaine, Coralie ; Douin-Echinard, Victorine ; Delpy, Laurent ; Berges, Hortense ; Calippe, Bertrand ; Lenfant, Françoise ; Laurell, Henrik ; Guéry, Jean-Charles ; Gourdy, Pierre u. a.: Endothelial estrogen receptor-α plays a crucial role in the atheroprotective action of 17β-estradiol in low-density lipoprotein receptor–deficient mice. In: *Circulation* 120 (2009), Nr. 25, S. 2567–2576 52

[463] Rohlmann, Astrid ; Gotthardt, Michael ; Hammer, Robert E. ; Herz, Joachim: Inducible inactivation of hepatic LRP gene by cre-mediated recombination confirms role of LRP in clearance of chylomicron remnants. In: *Journal of Clinical Investigation* 101 (1998), Nr. 3, S. 689 52

[464] Zeng, Hongkui ; Horie, Kyoji ; Madisen, Linda ; Pavlova, Maria N. ; Gragerova, Galina ; Rohde, Alex D. ; Schimpf, Brian A. ; Liang, Yuqiong ; Ojala, Ethan ; Kramer, Farah u. a.: An inducible and reversible mouse genetic rescue system. In: *PLoS genetics* 4 (2008), Nr. 5, S. e1000069 52

[465] Tsukamoto, Kazuhisa ; Tangirala, Rajendra ; Chun, Sam H. ; Puré, Ellen ; Rader, Daniel J.: Rapid regression of atherosclerosis induced by liver-directed gene transfer of ApoE in ApoE-deficient mice. In: *Arteriosclerosis, thrombosis, and vascular biology* 19 (1999), Nr. 9, S. 2162–2170 52

[466] Mestas, Javier ; Hughes, Christopher C.: Of mice and not men: differences between mouse and human immunology. In: *The Journal of Immunology* 172 (2004), Nr. 5, S. 2731–2738 52

[467] Fernandez, Maria L. ; Volek, Jeff S.: Guinea pigs: a suitable animal model to study lipoprotein metabolism, atherosclerosis and inflammation. In: *Nutr Metab (Lond)* 3 (2006), S. 17 52

[468] Rader, Daniel J. u. a.: Beyond high-density lipoprotein cholesterol levelsevaluating high-density lipoprotein function as influenced by novel therapeutic approaches. In: *Journal of the American College of Cardiology* 51 (2008), Nr. 23, S. 2199–2211 52

[469] Davidson, Michael H.: Update on CETP inhibition. In: *Journal of clinical lipidology* 4 (2010), Nr. 5, S. 394–398 52

[470] Higuchi, Keiichi ; Kitagawa, Kaori ; Kogishi, Kumiko ; Takeda, Toehio: Developmental and age-related changes in apolipoprotein B mRNA editing in mice. In: *Journal of lipid research* 33 (1992), Nr. 12, S. 1753–1764 53

[471] Chan, L: Apolipoprotein B, the major protein component of triglyceride-rich and low density lipoproteins. In: *Journal of Biological Chemistry* 267 (1992), S. 25621–25621 53

[472] Carter, Christopher P. ; Howles, Philip N. ; Hui, David Y.: Genetic variation in cholesterol absorption efficiency among inbred strains of mice. In: *The Journal of nutrition* 127 (1997), Nr. 7, S. 1344–1348 53

[473] Nishina, Patsy M. ; Verstuyft, J ; Paigen, B: Synthetic low and high fat diets for the study of atherosclerosis in the mouse. In: *Journal of lipid research* 31 (1990), Nr. 5, S. 859–869 53

[474] Calara, Federico ; Silvestre, Mercedes ; Casanada, Florencia ; Yuan, Natalie ; Napoli, Claudio ; Palinski, Wulf: Spontaneous plaque rupture and secondary thrombosis in apolipoprotein E-deficient and LDL receptor-deficient mice. In: *The Journal of pathology* 195 (2001), Nr. 2, S. 257–263 53

[475] Rosenfeld, Michael E. ; Polinsky, Patti ; Virmani, Renu ; Kauser, Katalin ; Rubanyi, Gabor ; Schwartz, Stephen M.: Advanced atherosclerotic lesions in the innominate artery of the ApoE knockout mouse. In: *Arteriosclerosis, thrombosis, and vascular biology* 20 (2000), Nr. 12, S. 2587–2592 53, 136

[476] Nakashima, Yutaka ; Plump, Andrew S. ; Raines, Elaine W. ; Breslow, Jan L. ; Ross, Russell: ApoE-deficient mice develop lesions of all phases of atherosclerosis throughout the arterial tree. In: *Arteriosclerosis, thrombosis, and vascular biology* 14 (1994), Nr. 1, S. 133–140 53, 137

[477] Reddick, Robert L. ; Zhang, Sunny H. ; Maeda, Nobuyo: Atherosclerosis in mice lacking apo E. Evaluation of lesional development and progression. In: *Arteriosclerosis, Thrombosis, and Vascular Biology* 14 (1994), Nr. 1, S. 141–147 53, 136

[478] Zhang, Sunny H. ; Reddick, Robert L. ; Burkey, Bryan ; Maeda, Nobuyo: Diet-induced atherosclerosis in mice heterozygous and homozygous for apolipoprotein E gene disruption. In: *Journal of Clinical Investigation* 94 (1994), Nr. 3, S. 937 53, 136

[479] Hu, Weicheng ; Polinsky, Patti ; Sadoun, Eman ; Rosenfeld, Michael E. ; Schwartz, Stephen M.: Atherosclerotic lesions in the common coronary arteries of ApoE knockout mice. In: *Cardiovascular Pathology* 14 (2005), Nr. 3, S. 120–125 53, 136

[480] Bentzon, Jacob F. ; Falk, Erling: Atherosclerotic lesions in mouse and man: is it the same disease? In: *Current opinion in lipidology* 21 (2010), Nr. 5, S. 434–440 53

[481] Lunney, Joan K.: Advances in swine biomedical model genomics. In: *International journal of biological sciences* 3 (2007), Nr. 3, S. 179 53

[482] Schwartz, Robert S. ; Murphy, Joseph G. ; Edwards, William D. ; Camrud, AR ; Vliestra, RE ; Holmes, DR: Restenosis after balloon angioplasty. A practical proliferative model in porcine coronary arteries. In: *Circulation* 82 (1990), Nr. 6, S. 2190–2200 53

[483] Schwartz, Robert S. ; Huber, Kenneth C. ; Murphy, Joseph G. ; Edwards, William D. ; Camrud, Allan R. ; Vlietstra, Ronald E. ; Holmes, David R.:

Restenosis and the proportional neointimal response to coronary artery injury: results in a porcine model. In: *Journal of the American College of Cardiology* 19 (1992), Nr. 2, S. 267–274 53

[484] Nobuyoshi, Masakiyo ; Kimura, Takeshi ; Nosaka, Hideyuki ; Mioka, Sokei ; Ueno, Katsumi ; Yokoi, Hiroatsu ; Hamasaki, Naoya ; Horiuchi, Hisanori ; Ohishi, Hiroto: Restenosis after successful percutaneous transluminal coronary angioplasty: serial angiographic follow-up of 229 patients. In: *Journal of the American College of Cardiology* 12 (1988), Nr. 3, S. 616–623 54

[485] Austin, Garth E. ; Ratliff, Norman B. ; Hollman, Jay ; Tabei, Seyed ; Phillips, Daniel F.: Intimal proliferation of smooth muscle cells as an explanation for recurrent coronary artery stenosis after percutaneous transluminal coronary angioplasty. In: *Journal of the American College of Cardiology* 6 (1985), Nr. 2, S. 369–375 54

[486] Gallo, Richard ; Padurean, Adrian ; Jayaraman, Thottala ; Marx, Steven ; Roque, Merce ; Adelman, Steven ; Chesebro, James ; Fallon, John ; Fuster, Valentin ; Marks, Andrew u. a.: Inhibition of intimal thickening after balloon angioplasty in porcine coronary arteries by targeting regulators of the cell cycle. In: *Circulation* 99 (1999), Nr. 16, S. 2164–2170 54

[487] Schwartz, Robert S. ; Holder, Daniel J. ; Holmes, David R. ; Veinot, John P. ; Camrud, Allan R. ; Jorgenson, Michael A. ; Johnson, Robert G.: Neointimal Thickening After Severe Coronary Artery Injury Is Limited by Short-term Administration of a Factor Xa Inhibitor Results in a Porcine Model. In: *Circulation* 93 (1996), Nr. 8, S. 1542–1548 54

[488] Wiedermann, Joseph G. ; Marboe, Charles ; Amols, Howard ; Schwartz, Allan ; Weinberger, Judah: Intracoronary irradiation markedly reduces restenosis after balloon angioplasty in a porcine model. In: *Journal of the American College of Cardiology* 23 (1994), Nr. 6, S. 1491–1498 54

[489] Huber, Kenneth C. ; Schwartz, Robert S. ; Edwards, William D. ; Camrud, Allan R. ; Bailey, Kent R. ; Jorgenson, Michael A. ; Holmes Jr, David R.: Effects of angiotensin converting enzyme inhibition on neointimal proliferation in a porcine coronary injury model. In: *American heart journal* 125 (1993), Nr. 3, S. 695–701 54

[490] Suzuki, Takeshi ; Kopia, Greg ; Hayashi, Shin-ichiro ; Bailey, Lynn R. ; Llanos, Gerard ; Wilensky, Robert ; Klugherz, Bruce D. ; Papandreou, George ; Narayan, Pallassana ; Leon, Martin B. u. a.: Stent-based delivery of sirolimus reduces neointimal formation in a porcine coronary model. In: *Circulation* 104 (2001), Nr. 10, S. 1188–1193 54

[491] Joner, Michael ; Finn, Aloke V. ; Farb, Andrew ; Mont, Erik K. ; Kolodgie, Frank D. ; Ladich, Elena ; Kutys, Robert ; Skorija, Kristi ; Gold, Herman K. ; Virmani, Renu: Pathology of drug-eluting stents in humans: delayed healing and late thrombotic risk. In: *Journal of the American College of Cardiology* 48 (2006), Nr. 1, S. 193–202 54

[492] Finn, Aloke V. ; Joner, Michael ; Nakazawa, Gaku ; Kolodgie, Frank ; Newell, John ; John, Mike C. ; Gold, Herman K. ; Virmani, Renu: Pathological correlates of late drug-eluting stent thrombosis strut coverage as a marker of endothelialization. In: *Circulation* 115 (2007), Nr. 18, S. 2435–2441 54

[493] Schwartz, Robert S. ; Edelman, Elazer ; Virmani, Renu ; Carter, Andrew ; Granada, Juan F. ; Kaluza, Greg L. ; Chronos, Nicolas A. ; Robinson, Keith A. ; Waksman, Ron ; Weinberger, Judah u. a.: Drug-Eluting Stents in Preclinical Studies Updated Consensus Recommendations for Preclinical Evaluation. In: *Circulation: Cardiovascular Interventions* 1 (2008), Nr. 2, S. 143–153 54

[494] Schwartz, Robert S. ; Edelman, Elazer R. ; Carter, Andrew ; Chronos, Nicolas ; Rogers, Campbell ; Robinson, Keith A. ; Waksman, Ron ; Weinberger, Judah ; Wilensky, Robert L. ; Jensen, Donald N. u. a.: Drug-eluting stents in preclinical studies recommended evaluation from a consensus group. In: *Circulation* 106 (2002), Nr. 14, S. 1867–1873 54

[495] Suzuki, Yoriyasu ; Lyons, Jennifer K. ; Yeung, Alan C. ; Ikeno, Fumiaki: The porcine restenosis model using thermal balloon injury: comparison with the model by coronary stenting. In: *Journal of Invasive Cardiology* 20 (2008), Nr. 3, S. 142 54

[496] Staab, Michael E. ; Srivatsa, Sanjay S. ; Lerman, Amir ; Sangiorgi, Giuseppe ; Jeong, Myung H. ; Edwards, William D. ; Holmes Jr, David R. ; Schwartz, Robert S.: Arterial remodeling after experimental percutaneous injury is highly dependent on adventitial injury and histopathology. In: *International journal of cardiology* 58 (1997), Nr. 1, S. 31–40 54

[497] Suzuki, Yoriyasu ; Yeung, Alan C. ; Ikeno, Fumiaki: The representative porcine model for human cardiovascular disease. In: *BioMed Research International* 2011 (2010) 54

[498] Prosser, LaVerne ; Agrawal, C ; Polan, Jodie ; Elliott, James ; Adams, Daniel G. ; Bailey, Steven R.: Implantation of oxygen enhanced, three-dimensional microporous L-PLA polymers: A reproducible porcine model of chronic total coronary occlusion. In: *Catheterization and cardiovascular interventions* 67 (2006), Nr. 3, S. 412–416 54

[499] McKenzie, Jack E. ; Scandling, Debbie M. ; Ahle, Neil W. ; Bryant, Howard J. ; Kyle, Richard R. ; Abbrecht, Peter H.: Effects of soman (pinacolyl methylphosphonofluoridate) on coronary blood flow and cardiac function in swine. In: *Fundamental and Applied Toxicology* 29 (1996), Nr. 1, S. 140–146 54

[500] Hughes, HC: Swine in cardiovascular research. In: *Laboratory animal science* 36 (1986), Nr. 4, S. 348–350 54

[501] WEAVER, MORRIS E. ; PANTELY, GEORGE A. ; BRISTOW, J D. ; D LADLEY, HERBERT: A quantitative study of the anatomy and distribution of coronary arteries in swine in comparison with other animals and man. In: *Cardiovascular research* 20 (1986), Nr. 12, S. 907–917 54

[502] Shimokawa, Hiroaki ; Tomoike, Hitonobu ; Nabeyama, Shozo ; Yamamoto, Hideo ; Araki, Haruo ; Nakamura, Motoomi ; Ishii, Y ; Tanaka, Kenzo: Coronary artery spasm induced in atherosclerotic miniature swine. In: *Science* 221 (1983), Nr. 4610, S. 560–562 54

[503] Liedtke, AJ ; Hughes, HC ; Neely, JR: An experimental model for studying myocardial ischemia. Correlation of hemodynamic performance and metabolism in the working swine heart. In: *The Journal of thoracic and cardiovascular surgery* 69 (1975), Nr. 2, S. 203–211 54

[504] Lam, JY ; Lacoste, Lucie ; Bourassa, Martial G.: Cilazapril and early atherosclerotic changes after balloon injury of porcine carotid arteries. In: *Circulation* 85 (1992), Nr. 4, S. 1542–1547 54

[505] Buschmann, Ivo R. ; Voskuil, Michiel ; Royen, Niels van ; Hoefer, Imo E. ; Scheffler, Klaus ; Grundmann, Sebastian ; Hennig, Jürgen ; Schaper, Wolfgang ; Bode, Christoph ; Piek, Jan J.: Invasive and non-invasive evaluation of spontaneous arteriogenesis in a novel porcine model for peripheral arterial obstructive disease. In: *Atherosclerosis* 167 (2003), Nr. 1, S. 33–43 54

[506] White, FC ; Carroll, SM ; Magnet, A ; Bloor, CM: Coronary collateral development in swine after coronary artery occlusion. In: *Circulation research* 71 (1992), Nr. 6, S. 1490–1500 54

[507] Mahley, Robert W. ; Weisgraber, Karl H. ; Innerarity, Thomas ; Brewer Jr, H B. ; Assmann, Gerd: Swine lipoproteins and atherosclerosis. Changes in the plasma lipoproteins and apoproteins induced by cholesterol feeding. In: *Biochemistry* 14 (1975), Nr. 13, S. 2817–2823 54

[508] Mahley, Robert ; Weisgraber, Karl: An electrophoretic method for the quantitative isolation of human and swine plasma lipoproteins. In: *Biochemistry* 13 (1974), Nr. 9, S. 1964–1968 54

[509] Prescott, Margaret F. ; HASLER-RAPACZ, JUDITH ; LINDEN-REED, JEAN ; Rapacz, Jan: Familial hypercholesterolemia associated with coronary atherosclerosis in swine bearing different alleles for apolipoprotein B. In: *Annals of the New York Academy of Sciences* 748 (1994), Nr. 1, S. 283–292 54, 55

[510] Prescott, Margaret F. ; McBride, CH ; Hasler-Rapacz, J ; Von Linden, J ; Rapacz, J: Development of complex atherosclerotic lesions in pigs with inherited hyper-LDL cholesterolemia bearing mutant alleles for apolipoprotein B. In: *The American journal of pathology* 139 (1991), Nr. 1, S. 139 54, 55

[511] Rapacz, Jan ; Hasler-Rapacz, JUDITH ; Taylor, KATHERINE M. ; Checovich, William J. ; Attie, Alan D.: Lipoprotein mutations in pigs are associated with elevated plasma cholesterol and atherosclerosis. In: *Science* 234 (1986), Nr. 4783, S. 1573–1577 54, 55

[512] Thim, Troels: Human-like atherosclerosis in minipigs: a new model for detection and treatment of vulnerable plaques. In: *Danish medical bulletin* 57 (2010), Nr. 7, S. B4161–B4161 54, 55, 102, 140

[513] Grunwald, Kurt A. ; Schueler, Kathryn ; Uelmen, Patricia J. ; Lipton, Beth A. ; Kaiser, Mary ; Buhman, Kimberly ; Attie, Alan D.: Identification of a novel Arg–Cys mutation in the LDL receptor that contributes to spontaneous hypercholesterolemia in pigs. In: *Journal of lipid research* 40 (1999), Nr. 3, S. 475–485 54, 55, 56, 102, 140

[514] Hasler-Rapacz, Judith ; Ellegren, Hans ; Fridolfsson, Anna-Karin ; Kirkpatrick, Brian ; Kirk, Scott ; Andersson, Leif ; Rapacz, Jan: Identification of a mutation in the low density lipoprotein receptor gene associated with recessive familial hypercholesterolemia in swine. In: *American journal of medical genetics* 76 (1998), Nr. 5, S. 379–386 54, 55, 102, 140

[515] Skold, BH ; Getty, R ; Ramsey, FK: Spontaneous atherosclerosis in the arterial system of aging swine. In: *American journal of veterinary research* 27 (1966), Nr. 116, S. 257 54

[516] French, JE ; Jennings, MA ; Florey, HW: MORPHOLOGICAL STUDIES ON ATHEROSCLEROSIS IN SWINE*. In: *Annals of the New York Academy of Sciences* 127 (1965), Nr. 1, S. 780–799 54

[517] Artinger, Sandra ; Deiner, Carolin ; Loddenkemper, Christoph ; Schwimmbeck, Peter L. ; Schultheiss, Heinz-Peter ; Pels, Klaus: Complex porcine model of atherosclerosis: Induction of early coronary lesions after long-term hyperlipidemia without sustained hyperglycemia. In: *Canadian Journal of Cardiology* 25 (2009), Nr. 4, S. e109–e114 54, 118, 148, 149

[518] Turk, James R. ; Henderson, Kyle K. ; Vanvickle, Gregory D. ; Watkins, Justin ; Laughlin, M H.: Arterial endothelial function in a porcine model of early stage atherosclerotic vascular disease. In: *International journal of experimental pathology* 86 (2005), Nr. 5, S. 335–345 54

[519] Gerrity, Ross G. ; Naito, Herbert K. ; Richardson, Mary ; Schwartz, Colin J.: Dietary induced atherogenesis in swine: morphology of the intima in prelesion stages. In: *The American journal of pathology* 95 (1979), Nr. 3, S. 775 54

[520] REISER, RAYMOND ; SORRELS, MARY F. ; WILLIAMS, MARY C.: Influence of high levels of dietary fats and cholesterol on atherosclerosis and lipid distribution in swine. In: *Circulation research* 7 (1959), Nr. 6, S. 833–846 54

[521] Downie, HG ; Mustard, JF ; Rowsell, HC: SWINE ATHEROSCLEROSIS: THE RELATIONSHIP OF LIPIDS AND BLOOD COAGULATION TO ITS DEVELOPMENT*. In: *Annals of the New York Academy of Sciences* 104 (1963), Nr. 2, S. 539–562 54

[522] Badimon, Lina: Atherosclerosis and thrombosis: lessons from animal models. In: *THROMBOSIS AND HAEMOSTASIS-STUTTGART-* 86 (2001), Nr. 1, S. 356–365 54

[523] Davis, Bryan T. ; Wang, Xiao-Jun ; Rohret, Judy A. ; Struzynski, Jason T. ; Merricks, Elizabeth P. ; Bellinger, Dwight A. ; Rohret, Frank A. ; Nichols, Timothy C. ; Rogers, Christopher S.: Targeted Disruption of LDLR Causes Hypercholesterolemia and Atherosclerosis in Yucatan Miniature Pigs. In: *PloS one* 9 (2014), Nr. 4, S. e93457 54, 55, 56, 57, 136, 138, 149

[524] Davies, Peter F.: Hemodynamic shear stress and the endothelium in cardiovascular pathophysiology. In: *Nature Clinical Practice Cardiovascular Medicine* 6 (2008), Nr. 1, S. 16–26 55, 149

[525] Koskinas, Konstantinos C. ; Feldman, Charles L. ; Chatzizisis, Yiannis S. ; Coskun, Ahmet U. ; Jonas, Michael ; Maynard, Charles ; Baker, Aaron B. ; Papafaklis, Michail I. ; Edelman, Elazer R. ; Stone, Peter H.: Natural History of Experimental Coronary Atherosclerosis and Vascular Remodeling in Relation to Endothelial Shear Stress A Serial, In Vivo Intravascular Ultrasound Study. In: *Circulation* 121 (2010), Nr. 19, S. 2092–2101 55, 119, 149

[526] Alviar, Carlos L. ; Tellez, Armando ; Wallace-Bradley, David ; Lopez-Berestein, Gabriel ; Sanguino, Angela ; Schulz, Daryl G. ; Builes, Angela ; Ballantyne, Christie M. ; Yang, Chao-Yuh ; Kaluza, Greg L. u. a.: Impact of adventitial neovascularisation on atherosclerotic plaque composition and vascular remodelling in a porcine model of coronary atherosclerosis. In: *EuroIntervention:*

journal of EuroPCR in collaboration with the Working Group on Interventional Cardiology of the European Society of Cardiology 5 (2010), Nr. 8, S. 981–988 55, 149

[527] Gerrity, RG ; Richardson, Mary ; Somer, JB ; Bell, FP ; Schwartz, CJ: Endothelial cell morphology in areas of in vivo Evans blue uptake in the aorta of young pigs: II. Ultrastructure of the intima in areas of differing permeability to proteins. In: *The American journal of pathology* 89 (1977), Nr. 2, S. 313 55

[528] Civelek, Mete ; Manduchi, Elisabetta ; Riley, Rebecca J. ; Stoeckert, Christian J. ; Davies, Peter F.: Coronary Artery Endothelial Transcriptome In Vivo Identification of Endoplasmic Reticulum Stress and Enhanced Reactive Oxygen Species by Gene Connectivity Network Analysis. In: *Circulation: Cardiovascular Genetics* 4 (2011), Nr. 3, S. 243–252 55

[529] Bell, Frank P. ; Gerrity, Ross G.: Evidence for an altered lipid metabolic state in circulating blood monocytes under conditions of hyperlipemia in swine and its implications in arterial lipid metabolism. In: *Arteriosclerosis, Thrombosis, and Vascular Biology* 12 (1992), Nr. 2, S. 155–162 55

[530] Gerrity, Ross G. ; Goss, Jennifer A. ; Soby, Lynn: Control of monocyte recruitment by chemotactic factor(s) in lesion-prone areas of swine aorta. In: *Arteriosclerosis, Thrombosis, and Vascular Biology* 5 (1985), Nr. 1, S. 55–66 55

[531] Gerrity, RG: The role of the monocyte in atherogenesis: I. Transition of bloodborne monocytes into foam cells in fatty lesions. In: *The American journal of pathology* 103 (1981), Nr. 2, S. 181 55

[532] Gerrity, ROSS G.: The role of the monocyte in atherogenesis: II. Migration of foam cells from atherosclerotic lesions. In: *The American journal of pathology* 103 (1981), Nr. 2, S. 191 55

[533] Kim, DN ; Lee, KT ; Schmee, J ; Thomas, WA: Quantification of intimal cell masses and atherosclerotic lesions in coronary arteries of control and hyperlipidemic swine. In: *Atherosclerosis* 52 (1984), Nr. 1, S. 115–122 55

[534] Mohler, Emile R. ; Sarov-Blat, Lea ; Shi, Yi ; Hamamdzic, Damir ; Zalewski, Andrew ; MacPhee, Colin ; Llano, Raul ; Pelchovitz, Dan ; Mainigi, Sumeet K. ; Osman, Hashim u. a.: Site-specific atherogenic gene expression correlates with subsequent variable lesion development in coronary and peripheral vasculature. In: *Arteriosclerosis, thrombosis, and vascular biology* 28 (2008), Nr. 5, S. 850–855 55

[535] Shi, Z-S ; Feng, L ; He, X ; Ishii, A ; Goldstine, J ; Vinters, HV ; Viñuela, F: Vulnerable plaque in a Swine model of carotid atherosclerosis. In: *American Journal of Neuroradiology* 30 (2009), Nr. 3, S. 469–472 55

[536] Granada, Juan F. ; Kaluza, Greg L. ; Wilensky, Robert L. ; Biedermann, Barbara C. ; Schwartz, Robert S. ; Falk, Erling: Porcine models of coronary atherosclerosis and vulnerable plaque for imaging and interventional research. In: *EuroIntervention: journal of EuroPCR in collaboration with the Working Group on Interventional Cardiology of the European Society of Cardiology* 5 (2009), Nr. 1, S. 140–148 55

[537] Lichtman, Andrew H. ; Clinton, Steven K. ; Iiyama, Kaeko ; Connelly, Philip W. ; Libby, Peter ; Cybulsky, Myron I.: Hyperlipidemia and atherosclerotic lesion development in LDL receptor–deficient mice fed defined semipurified diets with and without cholate. In: *Arteriosclerosis, thrombosis, and vascular biology* 19 (1999), Nr. 8, S. 1938–1944 55

[538] Hamamdzic, Damir ; Wilensky, Robert L.: Porcine models of accelerated coronary atherosclerosis: role of diabetes mellitus and hypercholesterolemia. In: *Journal of diabetes research* 2013 (2013) 55, 56

[539] Gerrity, Ross G. ; Natarajan, Rama ; Nadler, Jerry L. ; Kimsey, Troy: Diabetes-induced accelerated atherosclerosis in swine. In: *Diabetes* 50 (2001), Nr. 7, S. 1654–1665 55

[540] Thim, Troels ; Hagensen, Mette K. ; Drouet, Ludovic ; Bal, Dit Sollier C. ; Bonneau, Michel ; Granada, Juan F. ; Nielsen, Lars B. ; Paaske, William P. ; Bøtker, Hans E. ; Falk, Erling: Familial hypercholesterolaemic downsized pig with human-like coronary atherosclerosis: a model for preclinical studies. In: *EuroIntervention: journal of EuroPCR in collaboration with the Working Group on Interventional Cardiology of the European Society of Cardiology* 6 (2010), Nr. 2, S. 261–268 55, 56

[541] Hasler-Rapacz, Judith ; Prescott, Margaret F. ; Von Linden-Reed, Jean ; Rapacz, Jan M. ; Hu, Zhiliang ; Rapacz, Jan: Elevated concentrations of plasma lipids and apolipoproteins B, C-III, and E are associated with the progression of coronary artery disease in familial hypercholesterolemic swine. In: *Arteriosclerosis, thrombosis, and vascular biology* 15 (1995), Nr. 5, S. 583–592 55

[542] Al-Mashhadi, Rozh H. ; Sørensen, Charlotte B. ; Kragh, Peter M. ; Christoffersen, Christina ; Mortensen, Martin B. ; Tolbod, Lars P. ; Thim, Troels ; Du, Yutao ; Li, Juan ; Liu, Ying u. a.: Familial hypercholesterolemia and atherosclerosis in cloned minipigs created by DNA transposition of a human PCSK9 gain-of-function mutant. In: *Science translational medicine* 5 (2013), Nr. 166, S. 166ra1–166ra1 55, 56

[543] Sturek, M ; Alloosh, M ; Wenzel, J ; Byrd, JP ; Edwards, JM ; Lloyd, PG ; Tune, JD ; March, KL ; Miller, MA ; Mokelke, EA u. a.: Ossabaw

Island miniature swine: cardiometabolic syndrome assessment. In: *Swine in the Laboratory: Surgery, Anesthesia, Imaging, and Experimental Techniques* 2 (2007), S. 397–402 55

[544] Dyson, Melissa C. ; Alloosh, Mouhamad ; Vuchetich, James P. ; Mokelke, Eric A. ; Sturek, Michael: Components of metabolic syndrome and coronary artery disease in female Ossabaw swine fed excess atherogenic diet. In: *Comparative medicine* 56 (2006), Nr. 1, S. 35–45 55

[545] Neeb, Zachary P. ; Edwards, Jason M. ; Alloosh, Mouhamad ; Long, Xin ; Mokelke, Eric A. ; Sturek, Michael: Metabolic syndrome and coronary artery disease in Ossabaw compared with Yucatan swine. In: *Comparative medicine* 60 (2010), Nr. 4, S. 300 56

[546] Neeb, Zachary P. ; Edwards, Jason M. ; Bratz, Ian N. ; Alloosh, M ; Schultz, Carrie ; Thompson, Kristi ; Cunha, Timothy ; Sturek, Michael: Occlusive, diffuse coronary artery disease in Ossabaw miniature swine with metabolic syndrome. In: *FASEB J* 22 (2008), S. 1152–10 56

[547] Whitworth, Kristin M. ; Prather, Randall S.: Somatic cell nuclear transfer efficiency: how can it be improved through nuclear remodeling and reprogramming? In: *Molecular reproduction and development* 77 (2010), Nr. 12, S. 1001–1015 56

[548] Suemizu, Hiroshi ; Aiba, Kazuhiro ; Yoshikawa, Toshiyuki ; Sharov, Alexei A. ; Shimozawa, Nobuhiro ; Tamaoki, Norikazu ; Ko, Minoru S.: Expression profiling of placentomegaly associated with nuclear transplantation of mouse ES cells. In: *Developmental biology* 253 (2003), Nr. 1, S. 36–53 56

[549] Tanaka, Satoshi ; Oda, Mayumi ; Toyoshima, Yasushi ; Wakayama, Teruhiko ; Tanaka, Mika ; Yoshida, Naoko ; Hattori, Naka ; Ohgane, Jun ; Yanagimachi, Ryuzo ; Shiota, Kunio: Placentomegaly in cloned mouse concepti caused by expansion of the spongiotrophoblast layer. In: *Biology of Reproduction* 65 (2001), Nr. 6, S. 1813–1821 56

[550] Cassar-Malek, Isabelle ; Picard, Brigitte ; Jurie, Catherine ; Listrat, Anne ; Guillomot, Michel ; Chavatte-Palmer, Pascale ; Heyman, Yvan: Myogenesis is delayed in bovine fetal clones. In: *Cellular Reprogramming (Formerly "Cloning and Stem Cells")* 12 (2010), Nr. 2, S. 191–201 56

[551] Estrada, Jose ; Sommer, Jeffrey ; Collins, Bruce ; Mir, Bashir ; Martin, Amy ; York, Abby ; Petters, Robert M. ; Piedrahita, Jorge A.: Swine generated by somatic cell nuclear transfer have increased incidence of intrauterine growth restriction (IUGR). In: *Cloning and stem cells* 9 (2007), Nr. 2, S. 229–236 56

[552] Lai, Liangxue ; Prather, Randall S.: Production of cloned pigs by using somatic cells as donors. In: *Cloning & Stem Cells* 5 (2003), Nr. 4, S. 233–241 56

[553] Boquest, Andrew C. ; Grupen, Christopher G. ; Harrison, Sharon J. ; McIlfatrick, Stephen M. ; Ashman, Rodney J. ; d'Apice, Anthony J. ; Nottle, Mark B.: Production of cloned pigs from cultured fetal fibroblast cells. In: *Biology of reproduction* 66 (2002), Nr. 5, S. 1283–1287 56

[554] Bondioli, Kenneth ; Ramsoondar, Jagdeece ; Williams, Barry ; Costa, Cristina ; Fodor, William: Cloned pigs generated from cultured skin fibroblasts derived from a H-transferase transgenic boar. In: *Molecular reproduction and development* 60 (2001), Nr. 2, S. 189–195 56

[555] Polejaeva, Irina A. ; Chen, Shu-Hung ; Vaught, Todd D. ; Page, Raymond L. ; Mullins, June ; Ball, Suyapa ; Dai, Yifan ; Boone, Jeremy ; Walker, Shawn ; Ayares, David L. u. a.: Cloned pigs produced by nuclear transfer from adult somatic cells. In: *Nature* 407 (2000), Nr. 6800, S. 86–90 56

[556] Onishi, Akira ; Iwamoto, Masaki ; Akita, Tomiji ; Mikawa, Satoshi ; Takeda, Kumiko ; Awata, Takashi ; Hanada, Hirohumi ; Perry, Anthony C.: Pig cloning by microinjection of fetal fibroblast nuclei. In: *Science* 289 (2000), Nr. 5482, S. 1188–1190 56

[557] Betthauser, Jeff ; Forsberg, Erik ; Augenstein, Monica ; Childs, Lynette ; Eilertsen, Kenneth ; Enos, Joellyn ; Forsythe, Todd ; Golueke, Paul ; Jurgella, Gail ; Koppang, Richard u. a.: Production of cloned pigs from in vitro systems. In: *Nature biotechnology* 18 (2000), Nr. 10, S. 1055–1059 56

[558] Li, Ping ; Estrada, Jose L. ; Burlak, Christopher ; Tector, A J.: Biallelic knockout of the α-1, 3 galactosyltransferase gene in porcine liver-derived cells using zinc finger nucleases. In: *journal of surgical research* 181 (2013), Nr. 1, S. e39–e45 56, 57

[559] Park, Jong-Yi ; Park, Mi-Ryung ; Bui, Hong-Thuy ; Kwon, Deug-Nam ; Kang, Min-Hui ; Oh, Mihye ; Han, Jae-Woong ; Cho, Ssang-Goo ; Park, Chankyu ; Shim, Hosup u. a.: α1, 3-Galactosyltransferase Deficiency in Germ-Free Miniature Pigs Increases N-Glycolylneuraminic Acids As the Xenoantigenic Determinant in Pig–Human Xenotransplantation. In: *Cellular Reprogramming (Formerly" Cloning and Stem Cells")* 14 (2012), Nr. 4, S. 353–363 56

[560] Hauschild, Janet ; Petersen, Bjoern ; Santiago, Yolanda ; Queisser, Anna-Lisa ; Carnwath, Joseph W. ; Lucas-Hahn, Andrea ; Zhang, Lei ; Meng, Xiangdong ; Gregory, Philip D. ; Schwinzer, Reinhard u. a.: Efficient generation of a

biallelic knockout in pigs using zinc-finger nucleases. In: *Proceedings of the National Academy of Sciences* 108 (2011), Nr. 29, S. 12013–12017 56

[561] Takahagi, Yoichi ; Fujimura, Tatsuya ; Miyagawa, Shuji ; Nagashima, Hiroshi ; Shigehisa, Tamotsu ; Shirakura, Ryota ; Murakami, Hiroshi: Production of α1, 3-galactosyltransferase gene knockout pigs expressing both human decay-accelerating factor and N-acetylglucosaminyltransferase III. In: *Molecular reproduction and development* 71 (2005), Nr. 3, S. 331–338 56

[562] Harrison, Sharon ; Boquest, Andrew ; Grupen, Christopher ; Faast, Renate ; Guildolin, Angelo ; Giannakis, Christopher ; Crocker, Lesley ; McIlfatrick, Stephen ; Ashman, Rodney ; Wengle, James u. a.: An efficient method for producing α (1, 3)-galactosyltransferase gene knockout pigs. In: *Cloning and stem cells* 6 (2004), Nr. 4, S. 327–331 56

[563] Kolber-Simonds, Donna ; Lai, Liangxue ; Watt, Steven R. ; Denaro, Maria ; Arn, Scott ; Augenstein, Monica L. ; Betthauser, Jeffery ; Carter, David B. ; Greenstein, Julia L. ; Hao, Yanhong u. a.: Production of α-1, 3-galactosyltransferase null pigs by means of nuclear transfer with fibroblasts bearing loss of heterozygosity mutations. In: *Proceedings of the National Academy of Sciences of the United States of America* 101 (2004), Nr. 19, S. 7335–7340 56

[564] Phelps, Carol J. ; Koike, Chihiro ; Vaught, Todd D. ; Boone, Jeremy ; Wells, Kevin D. ; Chen, Shu-Hung ; Ball, Suyapa ; Specht, Susan M. ; Polejaeva, Irina A. ; Monahan, Jeff A. u. a.: Production of α1, 3-galactosyltransferase-deficient pigs. In: *Science* 299 (2003), Nr. 5605, S. 411–414 56

[565] Ramsoondar, Jagdeece J. ; Macháty, Zoltán ; Costa, Cristina ; Williams, Barry L. ; Fodor, William L. ; Bondioli, Kenneth R.: Production of α1, 3-galactosyltransferase-knockout cloned pigs expressing human α1, 2-fucosylosyltransferase. In: *Biology of reproduction* 69 (2003), Nr. 2, S. 437–445 56

[566] Dai, Yifan ; Vaught, Todd D. ; Boone, Jeremy ; Chen, Shu-Hung ; Phelps, Carol J. ; Ball, Suyapa ; Monahan, Jeff A. ; Jobst, Peter M. ; McCreath, Kenneth J. ; Lamborn, Ashley E. u. a.: Targeted disruption of the α1, 3-galactosyltransferase gene in cloned pigs. In: *Nature biotechnology* 20 (2002), Nr. 3, S. 251–255 56

[567] Lai, Liangxue ; Kolber-Simonds, Donna ; Park, Kwang-Wook ; Cheong, Hee-Tae ; Greenstein, Julia L. ; Im, Gi-Sun ; Samuel, Melissa ; Bonk, Aaron ; Rieke, August ; Day, Billy N. u. a.: Production of α-1, 3-galactosyltransferase knockout pigs by nuclear transfer cloning. In: *Science* 295 (2002), Nr. 5557, S. 1089–1092 56

[568] Luo, Yonglun ; Kofod-Olsen, Emil ; Christensen, Rikke ; Sørensen, Charlotte B. ; Bolund, Lars: Targeted genome editing by recombinant adeno-associated virus (rAAV) vectors for generating genetically modified pigs. In: *Journal of Genetics and Genomics* 39 (2012), Nr. 6, S. 269–274 56

[569] Klymiuk, N ; Mundhenk, L ; Kraehe, K ; Wuensch, A ; Plog, S ; Emrich, D ; Langenmayer, MC ; Stehr, M ; Holzinger, A ; Kröner, C u. a.: Sequential targeting of CFTR by BAC vectors generates a novel pig model of cystic fibrosis. In: *Journal of molecular medicine* 90 (2012), Nr. 5, S. 597–608 56

[570] Welsh, Michael J. ; Rogers, Christopher S. ; Stoltz, David A. ; Meyerholz, David K. ; Prather, Randall S.: Development of a porcine model of cystic fibrosis. In: *Transactions of the American Clinical and Climatological Association* 120 (2009), S. 149 56

[571] Rogers, Christopher S. ; Hao, Yanhong ; Rokhlina, Tatiana ; Samuel, Melissa ; Stoltz, David A. ; Li, Yuhong ; Petroff, Elena ; Vermeer, Daniel W. ; Kabel, Amanda C. ; Yan, Ziying u. a.: Production of CFTR-null and CFTR-ΔF508 heterozygous pigs by adeno-associated virus–mediated gene targeting and somatic cell nuclear transfer. In: *The Journal of clinical investigation* 118 (2008), Nr. 4, S. 1571–1577 56

[572] Rogers, Christopher S. ; Stoltz, David A. ; Meyerholz, David K. ; Ostedgaard, Lynda S. ; Rokhlina, Tatiana ; Taft, Peter J. ; Rogan, Mark P. ; Pezzulo, Alejandro A. ; Karp, Philip H. ; Itani, Omar A. u. a.: Disruption of the CFTR gene produces a model of cystic fibrosis in newborn pigs. In: *Science* 321 (2008), Nr. 5897, S. 1837–1841 56

[573] Mendicino, M ; Ramsoondar, J ; Phelps, C ; Vaught, T ; Ball, S ; LeRoith, T ; Monahan, J ; Chen, S ; Dandro, A ; Boone, J u. a.: Generation of antibody- and B cell-deficient pigs by targeted disruption of the J-region gene segment of the heavy chain locus. In: *Transgenic research* 20 (2011), Nr. 3, S. 625–641 56

[574] Ramsoondar, J ; Mendicino, M ; Phelps, C ; Vaught, T ; Ball, S ; Monahan, J ; Chen, S ; Dandro, A ; Boone, J ; Jobst, P u. a.: Targeted disruption of the porcine immunoglobulin kappa light chain locus. In: *Transgenic research* 20 (2011), Nr. 3, S. 643–653 57

[575] Luo, Yonglun ; Bolund, Lars ; Sørensen, Charlotte B.: Pig gene knockout by rAAV-mediated homologous recombination: comparison of BRCA1 gene knockout efficiency in Yucatan and Göttingen fibroblasts with slightly different target sequences. In: *Transgenic research* 21 (2012), Nr. 3, S. 671–676 57

[576] Luo, Yonglun ; Li, Juan ; Liu, Ying ; Lin, Lin ; Du, Yutao ; Li, Shengting ; Yang, Huanming ; Vajta, Gábor ; Callesen, Henrik ; Bolund, Lars u. a.: High efficiency of BRCA1 knockout using rAAV-mediated gene targeting: developing a pig model for breast cancer. In: *Transgenic research* 20 (2011), Nr. 5, S. 975–988 57

[577] Suzuki, Shunichi ; Iwamoto, Masaki ; Saito, Yoriko ; Fuchimoto, Daiichiro ; Sembon, Shoichiro ; Suzuki, Misae ; Mikawa, Satoshi ; Hashimoto, Michiko ; Aoki, Yuki ; Najima, Yuho u. a.: Il2rg Gene-Targeted Severe Combined Immunodeficiency Pigs. In: *Cell stem cell* 10 (2012), Nr. 6, S. 753–758 57

[578] Carlson, Daniel F. ; Tan, Wenfang ; Lillico, Simon G. ; Stverakova, Dana ; Proudfoot, Chris ; Christian, Michelle ; Voytas, Daniel F. ; Long, Charles R. ; Whitelaw, C Bruce A. ; Fahrenkrug, Scott C.: Efficient TALEN-mediated gene knockout in livestock. In: *Proceedings of the National Academy of Sciences* 109 (2012), Nr. 43, S. 17382–17387 57, 95, 97, 136, 143, 144, 145

[579] Sudo, Mitsumasa ; Li, Yuxin ; Onishi, Akira ; Fukushima, Seiji ; Suzuki, Shunichi ; Fuchimoto, Daiichiro ; Sembon, Shoichiro ; Iwamato, Masaki ; Hashimoto, Michiko ; Haruta, Hironori u. a.: Development of Hypercholesterolemia-Induced Complex Unstable Atherosclerotic Lesions in a Novel Low Density Lipoprotein Receptor Knockout Pig. In: *CIRCULATION* Bd. 126 LIPPINCOTT WILLIAMS & WILKINS 530 WALNUT ST, PHILADELPHIA, PA 19106-3621 USA, 2012 57, 136, 138, 149

[580] Prather, Randall S. ; Rowland, Raymond R. ; Ewen, Catherine ; Trible, Benjamin ; Kerrigan, Maureen ; Bawa, Bhupinder ; Teson, Jennifer M. ; Mao, Jiude ; Lee, Kiho ; Samuel, Melissa S. u. a.: An intact sialoadhesin (Sn/SIGLEC1/CD169) is not required for attachment/internalization of the porcine reproductive and respiratory syndrome virus. In: *Journal of virology* 87 (2013), Nr. 17, S. 9538–9546 57

[581] Kwon, Deug-Nam ; Lee, Kiho ; Kang, Man-Jong ; Choi, Yun-Jung ; Park, Chankyu ; Whyte, Jeffrey J. ; Brown, Alana N. ; Kim, Jae-Hwan ; Samuel, Melissa ; Mao, Jiude u. a.: Production of biallelic CMP-Neu5Ac hydroxylase knockout pigs. In: *Scientific reports* 3 (2013) 57

[582] Huang, Jiao ; Guo, Xiaogang ; Fan, Nana ; Song, Jun ; Zhao, Bentian ; Ouyang, Zhen ; Liu, Zhaoming ; Zhao, Yu ; Yan, Quanmei ; Yi, Xiaoling u. a.: RAG1/2 Knockout pigs with severe combined immunodeficiency. In: *The Journal of Immunology* 193 (2014), Nr. 3, S. 1496–1503 57

[583] Li, FD ; Li, Y ; Liu, H ; Zhang, HH ; Liu, CX ; Zhang, XJ ; Dou, HW ; Yang, WX ; Du, YT: Production of GHR double-allelic knockout Bama pig by TALENs

and handmade cloning. In: *Yi chuan= Hereditas/Zhongguo yi chuan xue hui bian ji* 36 (2014), Nr. 9, S. 903–911 57

[584] Faast, Renate ; Harrison, Sharon J. ; Beebe, Luke F. ; Mcilfatrick, Stephen M. ; Ashman, Rodney J. ; Nottle, Mark B.: Use of adult mesenchymal stem cells isolated from bone marrow and blood for somatic cell nuclear transfer in pigs. In: *Cloning and stem cells* 8 (2006), Nr. 3, S. 166–173 57, 141

[585] Leuchs, Simon ; Saalfrank, Anja ; Merkl, Claudia ; Flisikowska, Tatiana ; Edlinger, Marlene ; Durkovic, Marina ; Rezaei, Nousin ; Kurome, Mayuko ; Zakhartchenko, Valeri ; Kessler, Barbara u. a.: Inactivation and inducible oncogenic mutation of p53 in gene targeted pigs. In: *PloS one* 7 (2012), Nr. 10, S. e43323 57, 141, 142

[586] Li, Shun ; Edlinger, Marlene ; Saalfrank, Anja ; Flisikowski, Krzysztof ; Tschukes, Alexander ; Kurome, Mayuko ; Zakhartchenko, Valeri ; Kessler, Barbara ; Saur, Dieter ; Kind, Alexander u. a.: Viable pigs with a conditionally-activated oncogenic KRAS mutation. In: *Transgenic research* (2015), S. 1–9 57

[587] Flisikowska, Tatiana ; Merkl, Claudia ; Landmann, Martina ; Eser, Stefan ; Rezaei, Nousin ; Cui, Xinxin ; Kurome, Mayuko ; Zakhartchenko, Valeri ; Kessler, Barbara ; Wieland, Hagen u. a.: A porcine model of familial adenomatous polyposis. In: *Gastroenterology* 143 (2012), Nr. 5, S. 1173–1175 57, 141

[588] Li, Shun ; Flisikowska, Tatiana ; Kurome, Mayuko ; Zakhartchenko, Valeri ; Kessler, Barbara ; Saur, Dieter ; Kind, Alexander ; Wolf, Eckhard ; Flisikowski, Krzysztof ; Schnieke, Angelika: Dual Fluorescent Reporter Pig for Cre Recombination: Transgene Placement at the ROSA26 Locus. In: *PloS one* 9 (2014), Nr. 7, S. e102455 57, 123, 126, 142

[589] Richter, Anne ; Kurome, Mayuko ; Kessler, Barbara ; Zakhartchenko, Valeri ; Klymiuk, Nikolai ; Nagashima, Hiroshi ; Wolf, Eckhard ; Wuensch, Annegret: Potential of primary kidney cells for somatic cell nuclear transfer mediated transgenesis in pig. In: *BMC biotechnology* 12 (2012), Nr. 1, S. 84 57

[590] Li, Ping ; Estrada, Jose L. ; Burlak, Christopher ; Montgomery, Jessica ; Butler, James R. ; Santos, Rafael M. ; Wang, Zheng-Yu ; Paris, Leela L. ; Blankenship, Ross L. ; Downey, Susan M. u. a.: Efficient generation of genetically distinct pigs in a single pregnancy using multiplexed single-guide RNA and carbohydrate selection. In: *Xenotransplantation* (2014) 57

[591] Fan, Nana ; Chen, Jijun ; Shang, Zhouchun ; Dou, Hongwei ; Ji, Guangzhen ; Zou, Qingjian ; Wu, Lu ; He, Lixiazi ; Wang, Fang ; Liu, Kai u. a.: Piglets cloned

from induced pluripotent stem cells. In: *Cell research* 23 (2012), Nr. 1, S. 162–166 57

[592] Wu, Zhao ; Chen, Jijun ; Ren, Jiangtao ; Bao, Lei ; Liao, Jing ; Cui, Chun ; Rao, Linjun ; Li, Hui ; Gu, Yijun ; Dai, Huiming u. a.: Generation of pig induced pluripotent stem cells with a drug-inducible system. In: *Journal of molecular cell biology* 1 (2009), Nr. 1, S. 46–54 57, 141

[593] Farkas, Monica H. ; Weisgraber, Karl H. ; Shepherd, Virginia L. ; Linton, MacRae F. ; Fazio, Sergio ; Swift, Larry L.: The recycling of apolipoprotein E and its amino-terminal 22 kDa fragment evidence for multiple redundant pathways. In: *Journal of lipid research* 45 (2004), Nr. 8, S. 1546–1554 91

[594] Tangirala, Rajendra K. ; Praticó, Domenico ; FitzGerald, Garret A. ; Chun, Sam ; Tsukamoto, Kazuhisa ; Maugeais, Cyrille ; Usher, David C. ; Puré, Ellen ; Rader, Daniel J.: Reduction of isoprostanes and regression of advanced atherosclerosis by apolipoprotein E. In: *Journal of Biological Chemistry* 276 (2001), Nr. 1, S. 261–266 91, 138

[595] Paik, YK ; Chang, DJ ; Reardon, CA ; Walker, MD ; Taxman, E ; Taylor, JM: Identification and characterization of transcriptional regulatory regions associated with expression of the human apolipoprotein E gene. In: *Journal of Biological Chemistry* 263 (1988), Nr. 26, S. 13340–13349 94, 142

[596] Hanson, Keith D. ; Sedivy, John M.: Analysis of biological selections for high-efficiency gene targeting. In: *Molecular and cellular biology* 15 (1995), Nr. 1, S. 45–51 94, 97, 141, 142

[597] Mansour, Suzanne L. ; Thomas, Kirk R. ; Capecchi, Mario R.: Disruption of the proto-oncogene int-2 in mouse embryo-derived stem cells: a general strategy for targeting mutations to non-selectable genes. In: *Nature* 336 (1988), Nr. 6197, S. 348–352 94, 97, 141, 142

[598] Gottipati, Ponnari ; Cassel, Tobias N. ; Savolainen, Linda ; Helleday, Thomas: Transcription-associated recombination is dependent on replication in Mammalian cells. In: *Molecular and cellular biology* 28 (2008), Nr. 1, S. 154–164 95, 142, 143

[599] Garciá, Miguel A. ; Vázquez, Jesús ; Giménez, Cecilio ; Valdivieso, Fernando ; Zafra, Francisco: Transcription factor AP-2 regulates human apolipoprotein E gene expression in astrocytoma cells. In: *The Journal of neuroscience* 16 (1996), Nr. 23, S. 7550–7556 95, 142

[600] Bitinaite, Jurate ; Wah, David A. ; Aggarwal, Aneel K. ; Schildkraut, Ira: FokI dimerization is required for DNA cleavage. In: *Proceedings of the national academy of sciences* 95 (1998), Nr. 18, S. 10570–10575 95, 143

[601] Rouet, Philippe ; Smih, Fatima ; Jasin, Maria: Expression of a site-specific endonuclease stimulates homologous recombination in mammalian cells. In: *Proceedings of the National Academy of Sciences* 91 (1994), Nr. 13, S. 6064–6068 95, 143

[602] Tan, Wenfang ; Carlson, Daniel F. ; Lancto, Cheryl A. ; Garbe, John R. ; Webster, Dennis A. ; Hackett, Perry B. ; Fahrenkrug, Scott C.: Efficient non-meiotic allele introgression in livestock using custom endonucleases. In: *Proceedings of the National Academy of Sciences* 110 (2013), Nr. 41, S. 16526–16531 95, 143, 144

[603] Hockemeyer, Dirk ; Wang, Haoyi ; Kiani, Samira ; Lai, Christine S. ; Gao, Qing ; Cassady, John P. ; Cost, Gregory J. ; Zhang, Lei ; Santiago, Yolanda ; Miller, Jeffrey C. u. a.: Genetic engineering of human pluripotent cells using TALE nucleases. In: *Nature biotechnology* 29 (2011), Nr. 8, S. 731–734 95, 144

[604] Miller, Jeffrey C. ; Tan, Siyuan ; Qiao, Guijuan ; Barlow, Kyle A. ; Wang, Jianbin ; Xia, Danny F. ; Meng, Xiangdong ; Paschon, David E. ; Leung, Elo ; Hinkley, Sarah J. u. a.: A TALE nuclease architecture for efficient genome editing. In: *Nature biotechnology* 29 (2011), Nr. 2, S. 143–148 97, 144, 145

[605] Doyon, Yannick ; Choi, Vivian M. ; Xia, Danny F. ; Vo, Thuy D. ; Gregory, Philip D. ; Holmes, Michael C.: Transient cold shock enhances zinc-finger nuclease–mediated gene disruption. In: *Nature methods* 7 (2010), Nr. 6, S. 459–460 97, 144

[606] Reyon, Deepak ; Tsai, Shengdar Q. ; Khayter, Cyd ; Foden, Jennifer A. ; Sander, Jeffry D. ; Joung, J K.: FLASH assembly of TALENs for high-throughput genome editing. In: *Nature biotechnology* 30 (2012), Nr. 5, S. 460–465 101, 143, 144, 145

[607] Fouchier, Sigrid W. ; Kastelein, John J. ; Defesche, Joep C.: Update of the molecular basis of familial hypercholesterolemia in The Netherlands. In: *Human mutation* 26 (2005), Nr. 6, S. 550–556 102

[608] Mangerich, Aswin ; Scherthan, Harry ; Diefenbach, Jörg ; Kloz, Ulrich ; Hoeven, Franciscus van d. ; Beneke, Sascha ; Bürkle, Alexander: A caveat in mouse genetic engineering: ectopic gene targeting in ES cells by bidirectional extension of the homology arms of a gene replacement vector carrying human PARP-1. In: *Transgenic research* 18 (2009), Nr. 2, S. 261–279 115, 146

[609] Reed, Michael R. ; Huang, Chiung-Fang ; Riggs, Arthur D. ; Mann, Jeffrey R.: A Complex Duplication Created by Gene Targeting at the Imprinted H19 Locus Results in Two Classes of Methylation and Correlated Igf2 Expression Phenotypes. In: *Genomics* 74 (2001), Nr. 2, S. 186–196 115, 146, 147

[610] Powell, Elizabeth E. ; Kroon, Paulus A.: Low density lipoprotein receptor and 3-hydroxy-3-methylglutaryl coenzyme A reductase gene expression in human mononuclear leukocytes is regulated coordinately and parallels gene expression in human liver. In: *Journal of Clinical Investigation* 93 (1994), Nr. 5, S. 2168 115

[611] Fiebig, HJ: Fettsäurezusammensetzung wichtiger pflanzlicher und tierischer Speiseöle und -fette. In: *Deutsches Lebensmittelbuch* (2011) 116

[612] Kris-Etherton, Penny M. ; Yu, Shaomei: Individual fatty acid effects on plasma lipids and lipoproteins: human studies. In: *The American journal of clinical nutrition* 65 (1997), Nr. 5, S. 1628S–1644S 116

[613] Falkenberg, HEINZ ; Kuhn, GERDA ; Langhammer, MARTINA ; Renne, U ; Redel, H: Vergleich von Cholesterinparametern im Blut von Schweinen, Kaninchen und Mäusen. In: *Arch. Tierz* 42 (1999), S. 365–376 116, 147

[614] Huo, Yunlong ; Wischgoll, Thomas ; Kassab, Ghassan S.: Flow patterns in three-dimensional porcine epicardial coronary arterial tree. In: *American Journal of Physiology-Heart and Circulatory Physiology* 293 (2007), Nr. 5, S. H2959–H2970 119, 149

[615] Jung, Steffen ; Aliberti, Julio ; Graemmel, Petra ; Sunshine, Mary J. ; Kreutzberg, Georg W. ; Sher, Alan ; Littman, Dan R.: Analysis of fractalkine receptor CX3CR1 function by targeted deletion and green fluorescent protein reporter gene insertion. In: *Molecular and cellular biology* 20 (2000), Nr. 11, S. 4106–4114 122

[616] Soriano, Philippe: Generalized lacZ expression with the ROSA26 Cre reporter strain. In: *Nature genetics* 21 (1999), Nr. 1, S. 70–71 123

[617] Srinivas, Shankar ; Watanabe, Tomoko ; Lin, Chyuan-Sheng ; William, Chris M. ; Tanabe, Yasuto ; Jessell, Thomas M. ; Costantini, Frank: Cre reporter strains produced by targeted insertion of EYFP and ECFP into the ROSA26 locus. In: *BMC developmental biology* 1 (2001), Nr. 1, S. 4 123

[618] Abe, Takaya ; Kiyonari, Hiroshi ; Shioi, Go ; Inoue, Ken-Ichi ; Nakao, Kazuki ; Aizawa, Shinichi ; Fujimori, Toshihiko: Establishment of conditional reporter mouse lines at ROSA26 locus for live cell imaging. In: *Genesis* 49 (2011), Nr. 7, S. 579–590 123

[619] Zambrowicz, Brian P. ; Imamoto, Akira ; Fiering, Steve ; Herzenberg, Leonard A. ; Kerr, William G. ; Soriano, Philippe: Disruption of overlapping transcripts in the ROSA βgeo 26 gene trap strain leads to widespread expression of β-galactosidase in mouse embryos and hematopoietic cells. In: *Proceedings of the National Academy of Sciences* 94 (1997), Nr. 8, S. 3789–3794 123

[620] Li, Xiaoping ; Yang, Yi ; Bu, Lei ; Guo, Xiaogang ; Tang, Chengcheng ; Song, Jun ; Fan, Nana ; Zhao, Bentian ; Ouyang, Zhen ; Liu, Zhaoming u. a.: Rosa26-targeted swine models for stable gene over-expression and Cre-mediated lineage tracing. In: *Cell research* 24 (2014), Nr. 4, S. 501–504 123

[621] Björnheden, T ; Levin, M ; Evaldsson, M ; Wiklund, O: Evidence of hypoxic areas within the arterial wall in vivo. In: *Arteriosclerosis, Thrombosis, and Vascular Biology* 19 (1999), Nr. 4, S. 870–876 125

[622] Marsch, Elke ; Sluimer, Judith C. ; Daemen, Mat J.: Hypoxia in atherosclerosis and inflammation. In: *Current opinion in lipidology* 24 (2013), Nr. 5, S. 393–400 125

[623] Gao, Linggen ; Chen, Qian ; Zhou, Xianliang ; Fan, Li: The role of hypoxia-inducible factor 1 in atherosclerosis. In: *Journal of clinical pathology* (2012), S. jclinpath–2012 125

[624] Sluimer, Judith C. ; Gasc, Jean-Marie ; Wanroij, Job L. ; Kisters, Natasja ; Groeneweg, Mathijs ; Gelpke, Maarten D S. ; Cleutjens, Jack P. ; Akker, Luc H. d. ; Corvol, Pierre ; Wouters, Bradly G. u. a.: Hypoxia, hypoxia-inducible transcription factor, and macrophages in human atherosclerotic plaques are correlated with intraplaque angiogenesis. In: *Journal of the American College of Cardiology* 51 (2008), Nr. 13, S. 1258–1265 125, 129

[625] Semenza, Gregg L. ; Jiang, Bing-Hua ; Leung, Sandra W. ; Passantino, Rosa ; Concordet, Jean-Paul ; Maire, Pascal ; Giallongo, Agata: Hypoxia response elements in the aldolase A, enolase 1, and lactate dehydrogenase A gene promoters contain essential binding sites for hypoxia-inducible factor 1. In: *Journal of Biological Chemistry* 271 (1996), Nr. 51, S. 32529–32537 125, 129

[626] Hung, Shih-Chieh ; Pochampally, Radhika R. ; Hsu, Shu-Ching ; Sanchez, Cecelia ; Chen, Sy-Chi ; Spees, Jeffrey ; Prockop, Darwin J.: Short-term exposure of multipotent stromal cells to low oxygen increases their expression of CX3CR1 and CXCR4 and their engraftment in vivo. In: *PloS one* 2 (2007), Nr. 5, S. e416 129, 149, 150

[627] Seo, Hong S. ; Lombardi, Donna M. ; Polinsky, Patti ; Powell-Braxton, Lyn ; Bunting, Stuart ; Schwartz, Stephen M. ; Rosenfeld, Michael E.: Peri-

pheral Vascular Stenosis in Apolipoprotein E-Deficient Mice Potential Roles of Lipid Deposition, Medial Atrophy, and Adventitial Inflammation. In: *Arteriosclerosis, thrombosis, and vascular biology* 17 (1997), Nr. 12, S. 3593–3601 136, 137

[628] Ishibashi, S ; Goldstein, JL ; Brown, MS ; Herz, J ; Burns, DK: Massive xanthomatosis and atherosclerosis in cholesterol-fed low density lipoprotein receptor-negative mice. In: *Journal of Clinical Investigation* 93 (1994), Nr. 5, S. 1885 136, 137

[629] Williams, Helen ; Johnson, Jason L. ; Carson, Kevin George S. ; Jackson, Christopher L.: Characteristics of intact and ruptured atherosclerotic plaques in brachiocephalic arteries of apolipoprotein E knockout mice. In: *Arteriosclerosis, thrombosis, and vascular biology* 22 (2002), Nr. 5, S. 788–792 137

[630] Johnson, Jason L. ; Jackson, Christopher L.: Atherosclerotic plaque rupture in the apolipoprotein E knockout mouse. In: *Atherosclerosis* 154 (2001), Nr. 2, S. 399–406 137

[631] Tangirala, Rajendra K. ; Rubin, Edward M. ; Palinski, W: Quantitation of atherosclerosis in murine models: correlation between lesions in the aortic origin and in the entire aorta, and differences in the extent of lesions between sexes in LDL receptor-deficient and apolipoprotein E-deficient mice. In: *Journal of lipid research* 36 (1995), Nr. 11, S. 2320–2328 138

[632] VanderLaan, Paul A. ; Reardon, Catherine A. ; Getz, Godfrey S.: Site specificity of atherosclerosis site-selective responses to atherosclerotic modulators. In: *Arteriosclerosis, thrombosis, and vascular biology* 24 (2004), Nr. 1, S. 12–22 138, 139

[633] Gervais, Marianne ; Pons, Sandrine ; Nicoletti, Antonino ; Cosson, Claudine ; Giudicelli, Jean-François ; Richer, Christine: Fluvastatin prevents renal dysfunction and vascular NO deficit in apolipoprotein E-deficient mice. In: *Arteriosclerosis, thrombosis, and vascular biology* 23 (2003), Nr. 2, S. 183–189 138

[634] Mais, Dale E. ; Vihtelic, Thomas ; Amuzie, Chidozie ; Denham, Steven ; Swart, John R. ; Rogers, Christopher S.: A New Translational Model of Hypercholesterolemia and Atherosclerosis: Effect of Statins on LDLR KO Miniature Swine. In: *Arteriosclerosis, Thrombosis, and Vascular Biology* 34 (2014), Nr. Suppl 1, S. A657–A657 138

[635] Reardon, Catherine A. ; Blachowicz, Lydia ; White, Traci ; Cabana, Veneracion ; Wang, Yougen ; Lukens, John ; Bluestone, Jeffrey ; Getz, Godfrey S.:

Effect of immune deficiency on lipoproteins and atherosclerosis in male apolipoprotein E–deficient mice. In: *Arteriosclerosis, thrombosis, and vascular biology* 21 (2001), Nr. 6, S. 1011–1016 139

[636] Reardon, Catherine A. ; Blachowicz, Lydia ; Lukens, John ; Nissenbaum, Michael ; Getz, Godfrey S.: Genetic Background Selectively Influences Innominate Artery Atherosclerosis Immune System Deficiency as a Probe. In: *Arteriosclerosis, thrombosis, and vascular biology* 23 (2003), Nr. 8, S. 1449–1454 139

[637] Dansky, Hayes M. ; Charlton, Sherri A. ; Harper, Monnie M. ; Smith, Jonathan D.: T and B lymphocytes play a minor role in atherosclerotic plaque formation in the apolipoprotein E-deficient mouse. In: *Proceedings of the National Academy of Sciences* 94 (1997), Nr. 9, S. 4642–4646 139

[638] Mahley, Robert W. ; Weisgraber, Karl H. ; Huang, Yadong: Apolipoprotein E4: a causative factor and therapeutic target in neuropathology, including Alzheimer's disease. In: *Proceedings of the National Academy of Sciences* 103 (2006), Nr. 15, S. 5644–5651 140

[639] Ye, Shiming ; Huang, Yadong ; Müllendorff, Karin ; Dong, Liming ; Giedt, Gretchen ; Meng, Elaine C. ; Cohen, Fred E. ; Kuntz, Irwin D. ; Weisgraber, Karl H. ; Mahley, Robert W.: Apolipoprotein (apo) E4 enhances amyloid β peptide production in cultured neuronal cells: ApoE structure as a potential therapeutic target. In: *Proceedings of the National Academy of Sciences of the United States of America* 102 (2005), Nr. 51, S. 18700–18705 140

[640] Murphy, M P. ; LeVine, Harry III: Alzheimer's Disease and the Amyloid-β Peptide. In: *Journal of Alzheimer's Disease* 19 (2010), Nr. 1, S. 311–323 140

[641] Ji, Zhong-Sheng ; Müllendorff, Karin ; Cheng, Irene H. ; Miranda, R D. ; Huang, Yadong ; Mahley, Robert W.: Reactivity of Apolipoprotein E4 and Amyloid β Peptide Lysosomal stability and neurodegeneration. In: *Journal of Biological Chemistry* 281 (2006), Nr. 5, S. 2683–2692 140

[642] Ji, Zhong-Sheng ; Miranda, R D. ; Newhouse, Yvonne M. ; Weisgraber, Karl H. ; Huang, Yadong ; Mahley, Robert W.: Apolipoprotein E4 potentiates amyloid β peptide-induced lysosomal leakage and apoptosis in neuronal cells. In: *Journal of Biological Chemistry* 277 (2002), Nr. 24, S. 21821–21828 140

[643] Harris, Faith M. ; Brecht, Walter J. ; Xu, Qin ; Tesseur, Ina ; Kekonius, Lisa ; Wyss-Coray, Tony ; Fish, Jo D. ; Masliah, Eliezer ; Hopkins, Paul C. ; Scearce-Levie, Kimberly u. a.: Carboxyl-terminal-truncated apolipoprotein E4

causes Alzheimer's disease-like neurodegeneration and behavioral deficits in transgenic mice. In: *Proceedings of the National Academy of Sciences* 100 (2003), Nr. 19, S. 10966–10971 140

[644] Chang, Shengjun ; Ma, Tian ran ; Miranda, R D. ; Balestra, Maureen E. ; Mahley, Robert W. ; Huang, Yadong: Lipid-and receptor-binding regions of apolipoprotein E4 fragments act in concert to cause mitochondrial dysfunction and neurotoxicity. In: *Proceedings of the National Academy of Sciences of the United States of America* 102 (2005), Nr. 51, S. 18694–18699 140

[645] Brodbeck, Jens ; Balestra, Maureen E. ; Saunders, Ann M. ; Roses, Allen D. ; Mahley, Robert W. ; Huang, Yadong: Rosiglitazone increases dendritic spine density and rescues spine loss caused by apolipoprotein E4 in primary cortical neurons. In: *Proceedings of the National Academy of Sciences* 105 (2008), Nr. 4, S. 1343–1346 140

[646] Brecht, Walter J. ; Harris, Faith M. ; Chang, Shengjun ; Tesseur, Ina ; Yu, Gui-Qiu ; Xu, Qin ; Fish, Jo D. ; Wyss-Coray, Tony ; Buttini, Manuel ; Mucke, Lennart u. a.: Neuron-specific apolipoprotein e4 proteolysis is associated with increased tau phosphorylation in brains of transgenic mice. In: *The Journal of neuroscience* 24 (2004), Nr. 10, S. 2527–2534 140

[647] Bosch, Pablo ; Pratt, Scott L. ; Stice, Steven L.: Isolation, characterization, gene modification, and nuclear reprogramming of porcine mesenchymal stem cells. In: *Biology of reproduction* 74 (2006), Nr. 1, S. 46–57 140

[648] Dominici, M ; Le Blanc, K ; Mueller, I ; Slaper-Cortenbach, I ; Marini, FC ; Krause, DS ; Deans, RJ ; Keating, A ; Prockop, DJ ; Horwitz, EM: Minimal criteria for defining multipotent mesenchymal stromal cells. The International Society for Cellular Therapy position statement. In: *Cytotherapy* 8 (2006), Nr. 4, S. 315–317 140

[649] Colleoni, S ; Donofrio, G ; Lagutina, I ; Duchi, R ; Galli, C ; Lazzari, G: Establishment, differentiation, electroporation, viral transduction, and nuclear transfer of bovine and porcine mesenchymal stem cells. In: *Cloning and stem cells* 7 (2005), Nr. 3, S. 154–166 140

[650] Bianchi, Giordano ; Banfi, Andrea ; Mastrogiacomo, Maddalena ; Notaro, Rosario ; Luzzatto, Lucio ; Cancedda, Ranieri ; Quarto, Rodolfo: Ex vivo enrichment of mesenchymal cell progenitors by fibroblast growth factor 2. In: *Experimental cell research* 287 (2003), Nr. 1, S. 98–105 141

[651] Landmann, Martina: *Gene-targeted pigs predisposed to colorectal cancer*. Technische Universität München, Lehrstuhl für Biotechnologie der Nutztiere, 2010 141

[652] Kandavelou, Karthikeyan ; Ramalingam, Sivaprakash ; London, Viktoriya ; Mani, Mala ; Wu, Joy ; Alexeev, Vitali ; Civin, Curt I. ; Chandrasegaran, Srinivasan: Targeted manipulation of mammalian genomes using designed zinc finger nucleases. In: *Biochemical and biophysical research communications* 388 (2009), Nr. 1, S. 56–61 141

[653] Sedivy, John M. ; Sharp, Phillip A.: Positive genetic selection for gene disruption in mammalian cells by homologous recombination. In: *Proceedings of the National Academy of Sciences* 86 (1989), Nr. 1, S. 227–231 141, 142

[654] Te Riele, Hein ; Maandag, E R. ; Berns, Anton: Highly efficient gene targeting in embryonic stem cells through homologous recombination with isogenic DNA constructs. In: *Proceedings of the National Academy of Sciences* 89 (1992), Nr. 11, S. 5128–5132 141, 142

[655] Deng, Chuxia ; Capecchi, MARIO R.: Reexamination of gene targeting frequency as a function of the extent of homology between the targeting vector and the target locus. In: *Molecular and cellular biology* 12 (1992), Nr. 8, S. 3365–3371 141

[656] Jasin, Maria ; Berg, Paul: Homologous integration in mammalian cells without target gene selection. In: *Genes & development* 2 (1988), Nr. 11, S. 1353–1363 142, 147

[657] Sanford, L. P. ; Doetschman, Tom: *Gene transfer in embryonic stem cells, I: History and methodology. In transgenic animal technology: a laboratory handbook. Edited by Pinkert, Carl A.* Newnes, 2014. – 109–140 S. 142

[658] Doetschman, Thomas: *Gene transfer in embryonic stem cells. In transgenic animal technology: a laboratory handbook. Edited by Pinkert, Carl A.* Academic Press, San Diego, 1994. – 115–146 S. 142

[659] Bogdanove, Adam J. ; Voytas, Daniel F.: TAL effectors: customizable proteins for DNA targeting. In: *Science* 333 (2011), Nr. 6051, S. 1843–1846 143

[660] Boch, Jens ; Scholze, Heidi ; Schornack, Sebastian ; Landgraf, Angelika ; Hahn, Simone ; Kay, Sabine ; Lahaye, Thomas ; Nickstadt, Anja ; Bonas, Ulla: Breaking the code of DNA binding specificity of TAL-type III effectors. In: *Science* 326 (2009), Nr. 5959, S. 1509–1512 143, 145

[661] Moscou, Matthew J. ; Bogdanove, Adam J.: A simple cipher governs DNA recognition by TAL effectors. In: *Science* 326 (2009), Nr. 5959, S. 1501–1501 143, 145

[662] Zhang, Feng ; Cong, Le ; Lodato, Simona ; Kosuri, Sriram ; Church, George M. ; Arlotta, Paola: Efficient construction of sequence-specific TAL effectors for

modulating mammalian transcription. In: *Nature biotechnology* 29 (2011), Nr. 2, S. 149–153 143, 144, 145

[663] Cermak, Tomas ; Doyle, Erin L. ; Christian, Michelle ; Wang, Li ; Zhang, Yong ; Schmidt, Clarice ; Baller, Joshua A. ; Somia, Nikunj V. ; Bogdanove, Adam J. ; Voytas, Daniel F.: Efficient design and assembly of custom TALEN and other TAL effector-based constructs for DNA targeting. In: *Nucleic acids research* (2011), S. gkr218 143

[664] Mussolino, Claudio ; Morbitzer, Robert ; Lütge, Fabienne ; Dannemann, Nadine ; Lahaye, Thomas ; Cathomen, Toni: A novel TALE nuclease scaffold enables high genome editing activity in combination with low toxicity. In: *Nucleic acids research* 39 (2011), Nr. 21, S. 9283–9293 143, 144, 145

[665] Perez-Pinera, Pablo ; Ousterout, David G. ; Gersbach, Charles A.: Advances in targeted genome editing. In: *Current opinion in chemical biology* 16 (2012), Nr. 3, S. 268–277 143

[666] Sun, Ning ; Abil, Zhanar ; Zhao, Huimin: Recent advances in targeted genome engineering in mammalian systems. In: *Biotechnology journal* 7 (2012), Nr. 9, S. 1074–1087 143

[667] Porteus, Matthew H. ; Carroll, Dana: Gene targeting using zinc finger nucleases. In: *Nature biotechnology* 23 (2005), Nr. 8, S. 967–973 143

[668] Valerie, Kristoffer ; Povirk, Lawrence F.: Regulation and mechanisms of mammalian double-strand break repair. In: *Oncogene* 22 (2003), Nr. 37, S. 5792–5812 143

[669] Liang, Feng ; Han, Mingguang ; Romanienko, Peter J. ; Jasin, Maria: Homology-directed repair is a major double-strand break repair pathway in mammalian cells. In: *Proceedings of the National Academy of Sciences* 95 (1998), Nr. 9, S. 5172–5177 144

[670] Christian, Michelle ; Cermak, Tomas ; Doyle, Erin L. ; Schmidt, Clarice ; Zhang, Feng ; Hummel, Aaron ; Bogdanove, Adam J. ; Voytas, Daniel F.: TAL effector nucleases create targeted DNA double-strand breaks. In: *Genetics* 186 (2010), Nr. 2, S. 757–61 145

[671] Li, Ting ; Huang, Sheng ; Jiang, Wen Z. ; Wright, David ; Spalding, Martin H. ; Weeks, Donald P. ; Yang, Bing: TAL nucleases (TALNs): hybrid proteins composed of TAL effectors and FokI DNA-cleavage domain. In: *Nucleic acids research* 39 (2011), Nr. 1, S. 359–372 145

[672] McCulloch, Richard D. ; Read, Leah R. ; Baker, Mark D.: Strand invasion and DNA synthesis from the two 3' ends of a double-strand break in mammalian cells. In: *Genetics* 163 (2003), Nr. 4, S. 1439–1447 146

[673] Helleday, Thomas ; Lo, Justin ; Gent, Dik C. ; Engelward, Bevin P.: DNA double-strand break repair: from mechanistic understanding to cancer treatment. In: *DNA repair* 6 (2007), Nr. 7, S. 923–935 146

[674] Yang, Yi ; Seed, Brian: Site-specific gene targeting in mouse embryonic stem cells with intact bacterial artificial chromosomes. In: *Nature biotechnology* 21 (2003), Nr. 4, S. 447–451 146

[675] Burwinkel, Barbara ; Kilimann, Manfred W.: Unequal homologous recombination between LINE-1 elements as a mutational mechanism in human genetic disease. In: *Journal of molecular biology* 277 (1998), Nr. 3, S. 513–517 147

[676] Fitch, DH ; Bailey, Wendy J. ; Tagle, Danilo A. ; Goodman, Morris ; Sieu, Leang ; Slightom, Jerry L.: Duplication of the gamma-globin gene mediated by L1 long interspersed repetitive elements in an early ancestor of simian primates. In: *Proceedings of the National Academy of Sciences* 88 (1991), Nr. 16, S. 7396–7400 147

[677] Jurka, Jerzy: Evolutionary impact of human Alu repetitive elements. In: *Current opinion in genetics & development* 14 (2004), Nr. 6, S. 603–608 147

[678] Lehrman, Mark A. ; Goldstein, Joseph L. ; Russell, David W. ; Brown, Michael S.: Duplication of seven exons in LDL receptor gene caused by Alu-Alu recombination in a subject with familial hypercholesterolemia. In: *Cell* 48 (1987), Nr. 5, S. 827–835 147

[679] Lee, Jee-Hyung ; Kemp, Daniel M.: Human adipose-derived stem cells display myogenic potential and perturbed function in hypoxic conditions. In: *Biochemical and biophysical research communications* 341 (2006), Nr. 3, S. 882–888 150